Université Fédérale
Toulouse Midi-Pyrénées

THÈSE

En vue de l'obtention du

DOCTORAT DE L'UNIVERSITÉ DE TOULOUSE

Délivré par :

Université Toulouse 3 Paul Sabatier (UT3 Paul Sabatier)

Présentée et soutenue par :
Weili Wang

le jeudi 17 septembre 2015

Titre :

De la catalyse homogène vers la catalyse hétérogène
pour l'époxydation sans solvant à partir de (pré)catalyseurs du molybdène

From homogeneous to heterogeneous catalysis
for solvent-free olefin epoxidation using molybdenum pre-catalysts

---

École doctorale et discipline ou spécialité :

ED SDM : Chimie organométallique de coordination - CO 043

Unité de recherche :

Laboratoire de Chimie de Coordination UPR 8241 - Toulouse

Directeur/trice(s) de Thèse :

M. Rinaldo Poli (Professeur INP Toulouse)
M. Dominique Agustin (Maître de Conferénces Université Toulouse 3)

Jury :

M. Eric Benoist (Professeur Université Toulouse 3) Président du Jury
Mme Véronique Nardello-Rataj (Professeur Université de Lille) Rapportrice
M. André Vioux (Professeur Université de Montpellier) Rapporteur
Mme Alessandra Elsje Quadrelli (Chargée de Recherches CNRS, CPE Lyon) Examinatrice

UNIVERSITE TOULOUSE III – PAUL SABATIER

THESIS in CHEMISTRY
Speciality: Organometallic and coordination chemisstry

Weili WANG

From homogeneous to heterogeneous catalysis for solvent-free olefin epoxidation using molybdenum pre-catalysts

De la catalyse homogène vers la catalyse hétérogène pour l'époxydation sans solvant à partir de (pré)catalyseurs du molybdène

Defended on September 17th of 2015
At University Paul Sabatier
(IUT Paul Sabatier, Castres)

Committee

Eric Benoist, Full Professor, University Paul Sabatier (Toulouse) Committee President

Véronique Nardello-Rataj, Full Professor, University ofLille (Lille) Referee
André Vioux, Full Professor, University of Montpellier (Montpellier) Referee
Alessandra Elsje Quadrelli, CNRS Researcher, CPE (Lyon) CNRS, Examiner
Rinaldo POLI, Full Professor, INP Toulouse (Toulouse), Supervisor
Dominique AGUSTIN, Assoc.Professor, University Paul Sabatier (Toulouse), co-Supervisor

Foreword

The experimental work has been realized as member of the Laboratoire de Coordination (LCC) at the IUT of Castres. I would like to express my gratitude to Doctors Azzedine Bousseksou and Denis Neibecker, directors of LCC, to have welcomed me in LCC. I would like to thank the IUT Castres to have given me the opportunity to develop this research along the three years within the research laboratory.

I thank the China Scholarship Council (CSC) to have given me a Fellowship for my PhD. Without this financial support, this fantastic life experience in France (my first time abroad China) could not have been possible.

I would like to strongly acknowledge Professor Véronique Nardello-Rataj from University of Lille and Professor André Vioux from University of Montpellier to have accepted to referee my work.

I am grateful to Dr Alessandra Elsje Quadrelli from CPE-Lyon and Professor Eric Benoist from University of Toulouse to take part at this commission as examiners.

I wish to express my gratitude to all those who helped me during the writing of this thesis. Many people have made invaluable contributions, both directly and indirectly to my research.

I would like to express my warmest gratitude to Professor Rinaldo Poli and Doctor Dominique Agustin, to have supervised this thesis all along these three years. Their advices were great helpful during the experimental work. Their instructive suggestions and valuable comments helped me lot for the writing of the thesis. Without their invaluable helps and generous encouragements, the present thesis would not have been accomplished. To work under their direction makes me work more precise in research and have more creative thoughts in science.

I am also greatly indebted to the professors, teachers and technical staff at the Chemistry Departement of the IUT at Castres (Dr. Eric Deydier, Dr. Pascal Guillo, Sébastien Bernard, Professor Patrick Sharrock, Thierry Scandella and Laurence Orts) who have instructed and helped me a lot in the past three years with the analytical equipments.

Obviously, I do not forget to be thankful to Doctor Jean-Claude Daran, who has been of inestimable help for the determination of the X-ray structures presented in this manuscript.

Besides, I wish to thank my colleagues Dr. Azzam Faour and Dr. Jana Pisk in Castres, who helped me solve the problems in life and academics. I particularly owe my sincere gratitude to my friends and my fellow classmates who shared with me the laboratory and office in Castres (Audric Michelot, Tomas Guerrero Briseno, Mohamed Loubidi, Béatrice Guérin, Robert Katava, Louay Al-Husseini), giving me their time, listening to me and helping me to solve problems encountered during the difficult course of the thesis. Finally, I would like to thank all other permanents members and students from the Research Group in Castres and Toulouse encountered during my stay.

The lovely friends in France should not be forgotten, such as Guanhua Jin, Yandi Lan, Jing Guo, Marine Benezech and so on, they help me and share their time with me, these make my life here much easier.

Lastly, my thanks would give to my beloved family for their loving considerations and great confidence in me all through these years. Especially, my father and brother do their best to help. Also, without my wife's encouragement, I would not have thought about doing a PhD abroad China. Her full support and dedication, give me a great of help and courage.

As Chinese say

天下无不撒之宴席，

No feast in the world can last forever.

此地一为别，孤蓬万里征,

Today we have to say goodbye since then, thousands of miles apart,

But there is also a poetry:

莫愁前路无知己，天下谁人不识君,

(Don't worry about that there is no friend close, everyone knows you in the world, your friend is all over the world).

Abstract in English

The work of this PhD thesis deals with the study of molybdenum complexes of general formula $[MoO_2L]_n$ (L being a tridentate Schiff base ligand with an ONO or ONS coordination sphere around the molybdenum) as catalysts for the organic solvent-free epoxidation of olefins. Within the spirit of Green Chemistry, the work has focused on four of the twelve Green Chemistry principles: the use of catalysis rather than stoichiometric transformations, the use of organic solvent-free procedures rather than operating in solution of organic solvents, the use of renewable substrates and the grafting of catalysts for their recovery.

The first part of the manuscript presents a concise state of the art on the chemistry of molybdenum complexes with ligands similar to those used within the thesis. Specific aspects such as the effect of ligand substituents and the different activities – mainly catalytic – observed in organic media are reviewed. A section of this chapter is dedicated to the different strategies employed for the grafting of molybdenum complexes to solid supports as well as to the use of the resulting supported complexes in heterogenized homogeneous catalysis.

The next chapter details the synthesis and characterization of all the molecular complexes used as catalysts. This chapter shows the different substitutions operated on the ligands, i.e. changing the *ONO* coordination sphere to *ONS* and adding different substituents on the ligands, i.e. OH free functions or additional donor (diethylamino) and/or withdrawing (nitro) substituents at different positions on the tridentate ligand in order to modify the catalytic activity. Six of the synthesized complexes could be characterized by X-ray crystallography.

The third chapter reports the results obtained for the catalyzed organic solvent-free epoxidation of cyclooctene as a model substrate using all the molybdenum complexes presented in the previous chapter. It is shown that the nature of the coordination sphere around the molybdenum (ONO vs ONS) is in favour of the latter in terms of catalytic activity towards the formation of the desired epoxide. The catalyzed reactions with complexes containing an OH substituent at different positions on the aromatic ring have shown more significant effects in the case of the ONO coordination sphere than in the corresponding ONS case. The epoxidation performed in the presence of a dimethylamino and/or a nitro substituent on the ONO ligand revealed that the catalytic activity is enhanced by the electron withdrawing group.

The catalytic investigations were pursued by the epoxidation of cyclohexene and of one natural substrate, limonene. This study has shown that limonene oxides and/or limonene diols are generated, depending on the nature of the catalyst. The ONS complexes are very reactive and quickly lead to the limonene diols. The effect of different parameters has been studied with particular attention to the reaction temperature.

Finally, one stable molybdenum complex with an ONO coordination sphere has been grafted onto a commercial Merrifield resin. Different grafting strategies are presented. The isolated objects have been tested as catalysts under organic solvent-free conditions for the epoxidation of cyclooctene. The catalytic results are promising in terms of activity and the recovery/recycling tests have shown that the catalysts could be used three times without significant decrease of conversion and selectivity, but some metal leaching was observed.

Résumé en français

Le sujet de cette thèse concerne l'étude de complexes du molybdène de formule $[MoO_2L]_n$ (L étant un ligand base de Schiff tridente ayant une coordination ONO ou ONS autour du molybdène) en tant que catalyseurs d'époxydation d'oléfines sans solvant organique ajouté.

Le travail s'est concentré sur quatre des douze principes de la chimie verte: l'utilisation de la catalyse plutôt que des transformations stœchiométriques, l'utilisation de procédures sans solvant organique ajouté plutôt que des procédures opérant dans des solvants organiques, l'utilisation de substrats renouvelables et le greffage de catalyseurs pour leur récupération.

La première partie du manuscrit présente un état de l'art concis de la chimie des complexes du molybdène à ligands similaires de ceux utilisés dans cette thèse. Des aspects spécifiques comme l'effet des substituants sur les ligands et les différentes activités – essentiellement catalytiques – observées en milieu organique ont été recensées. Un partie de ce chapitre est aussi dédiée aux différentes stratégies employées pour le greffage de complexes du molybdène sur des supports solides ainsi que l'utilisation des complexes supportés résultants en catalyse homogène hétérogénéisée.

Cette partie bibliographique est suivie d'un chapitre détaillant la synthèse et la caractérisation de tous les complexes moléculaires utilisés comme catalyseurs. Ce chapitre montre les différentes substitutions opérées sur les ligands, c.-à-d. remplaçant la sphère de coordination ONO par ONS et ajoutant différents substituants sur les ligands, telles des fonctions OH libres ou des substituants donneurs (diéthylamino) et/ou attracteurs (nitro) à différentes positions sur le ligand tridente afin de modifier l'activité catalytique. Six des complexes ont pu être caractérisés par diffraction des rayons X.

Le troisième chapitre reporte les résultats obtenus pour l'époxydation catalysée sans solvant organique ajouté du cyclooctène (substrat modèle) utilisant tous les complexes du molybdène présentés dans le chapitre précédent. Il est montré que la nature de la sphère de coordination autour le molybdène (ONO vs ONS) est en faveur de la deuxième en terme d'activité catalytique en faveur de l'époxyde désiré.

Les réactions catalysées par les complexes contenant des OH libres ont montré des effets plus significatifs dans le cas de la sphère de coordination ONO que dans le cas des ONS correspondants. L'époxydation en présence de substituants diéthylamino et/ou nitro sur le ligand ONO ont révélé que l'activité catalytique était améliorée par le groupement attracteur d'électrons.

Les recherches catalytiques ont été poursuivies par l'époxydation du cyclohexène et d'un substrat naturel, le limonène. Cette étude a montré que des oxydes de limonène et/ou des limonènes diols étaient générés, en fonction de la nature du catalyseur. Les complexes ONS sont très réactifs et conduisent rapidement aux limonènes diols. L'effet de différents paramètres a été étudié avec une attention particulière à la température de réaction.

Enfin, un complexe stable ONO du molybdène a été greffé sur une résine de Merrifield commerciale. De différentes stratégies de greffage sont présentées. Les objets isolés ont été testés comme catalyseurs en condition sans solvant organique ajouté pour l'époxydation du cyclooctène. Les résultats catalytiques sont prometteurs en termes d'activité et des tests de récupération/recyclage ont montré que les catalyseurs pouvaient être utilisés trois fois sans perte significative de conversion et de sélectivité. Toutefois, un peu de relargage du métal a été observé.

Table of contents

Résumé détaillé de la thèse en français

Introduction

Dans le contexte d'une prise de conscience de l'effet néfaste des procédés et produits chimiques pour l'environnement, les chimistes essaient de développer depuis quelques années des procédés plus propres, plus sûrs et qui tiennent compte du développement de l'utilisation de ressources renouvelables. Ces différents principes ont été rassemblés sous la notion de « chimie verte ». Ce concept énoncé en 1995 se décline en douze principes.

Le travail effectué dans ce mémoire s'inscrit dans le respect de certains de ces principes :

- L'utilisation de la catalyse a pour but de diminuer la quantité de réactifs dangereux en rendant les procédés plus efficaces.
- Les réactions sans solvant organique diminuent la quantité de composés toxiques utilisés, limitant à la source le nombre de produits polluants.
- Un des substrats étudié dans ce mémoire étant un composé naturel, ce travail essaie de commencer à étudier la transformation de produits organiques naturels, ressources issues de la biomasse au cycle de carbone court comparé aux ressources fossiles.
- Enfin, en plus des avantages précédemment cités, il a été étudié une méthode de récupération et recyclage des catalyseurs par le greffage des catalyseurs sur des polymères organiques.

Ce mémoire s'inscrit dans le respect des principes énoncés précédemment. Le travail se décline au long de cinq chapitres, en utilisant des complexes moléculaires du molybdène dans des réactions d'époxydation sans solvant organique. Trois substrats ont été étudiés, le cyclooctène et le cyclohéxène et le limonène, substrat naturel. Enfin, en plus de l'étude catalytique effectuée en présence de catalyseurs moléculaires en conditions homogènes, des catalyseurs greffés sur des résines polymères commerciales ont été testés et ont montré la possibilité de recyclage et de récupération des catalyseurs.

CHAPITRE 1 – Mise au point bibliographique

Le premier chapitre est un état de l'art sur la thématique développée dans cette thèse. Cette revue bibliographique concerne notamment les différents complexes tridentates du molybdène synthétisés, en insistant sur la nature des substituants attachés au squelette des ligands et l'effet de ces substituants sur les propriétés électrochimiques des complexes du molybdène associés.

Les différentes activités catalytiques de ces complexes ont été montrées avec diverses réactions (oxydation de sulfures, oxydation d'alcools, …)

En fin du chapitre, un effort a été porté sur la présentation des différentes méthodes de greffage de complexes du molybdène sue différents supports (polymères, silices et composés mésoporeux, supports inorganiques, nanotubes de carbones) et des différentes applications catalytiques testées.

Pour la plupart de ces composés, les applications catalytiques ont lieu en présence de solvant organique. Ce point étant important pour comprendre la suite du travail de cette thèse puisque le part pris a été d'effectuer les réactions d'époxydation sans solvant organique, afin de satisfaire aux différents principes de la chimie verte énoncés dans l'introduction.

CHAPITRE 2 – Synthèse et caractérisation des complexes moléculaires du molybdène

Ce chapitre présente les différents complexes synthétisés et caractérisés par différentes méthodes (IR, RMN, ATG, diffraction RX). Les complexes, de formule générale $[MoO_2L^n]_2$ et $[MoO_2L^n(D)]$, présentent une caractéristique commune en ce qui concerne les ligands L^n. Ceux-ci sont dérivés d'un squelette de base, appelé salicylidène aminophénol (H_2SAP).

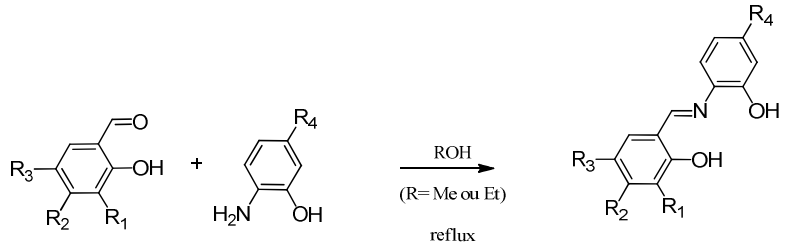

H_2SAP
$H_2L^{a\text{-}f}$

	Substituants			
	R_1	**R_2**	**R_3**	**R_4**
H_2SAP	H	H	H	H
H_2L^a	OH	H	H	H
H_2L^b	H	OH	H	H
H_2L^c	H	H	OH	H
H_2L^d	H	H	H	NO_2
H_2L^e	H	NEt_2	H	H
H_2L^f	H	NEt_2	H	NO_2

Schéma 1 - Synthèse des tridentate ligands *ONO*

Les variations opérées sur les ligands *ONO* sont de deux types (Schéma 1).

La première variation concerne la présence de groupements libres OH sur les ligands a été effectuée avec des ligands à sphère de coordination.($H_2L^{a\text{-}c}$)

La deuxième concerne l'ajout de groupement à effet donneur (NEt_2) et/ou attracteur (NO_2) d'électrons de part et d'autre du ligand ($H_2L^{d\text{-}g}$).

Les complexes à sphère de coordination *ONO* de formule $[MoO_2(SAP)]_2$ et $[MoO_2L^n]_2$ (n=a-f) ont été synthétisés à partir des précurseurs H_2SAP et $H_2L^{a\text{-}f}$ isolés et du complexe $[MoO_2(acac)_2]$ en milieu alcoolique (éthanol ou méthanol) en fonction des différents ligands. (Schéma 2)

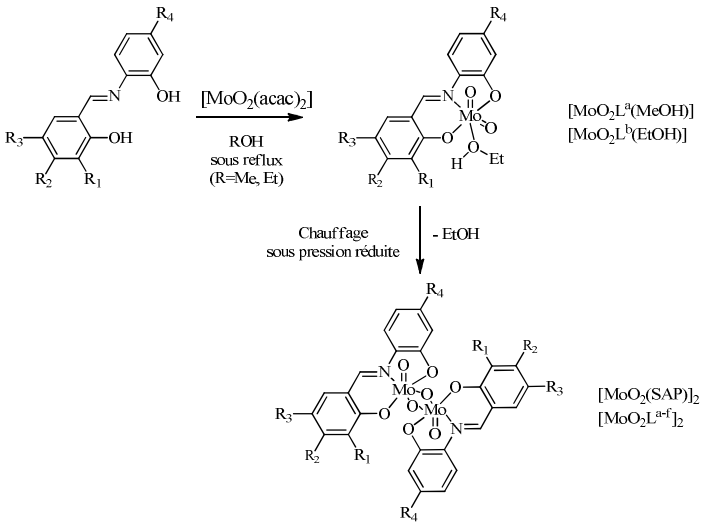

Schéma 2 - Synthèse des complexes du molybdène *ONO*

Les complexes à sphère de coordination *ONS* de formule générale $[MoO_2L^{h\text{-}k}]_2$ n'ont pas pu être synthétisés en utilisant la même méthode que les complexes *ONO* car les précurseurs des ligands *ONS* $H_2L^{h\text{-}k}$ n'ont pu être isolés de façon satisfaisante. La synthèse s'est donc faite en « one-pot », créant le ligand en solution alcoolique et faisant réagir le complexe $[MoO_2(acac)_2]$ directement dans la solution alcoolique. (Schéma 3) Comme dans le cas des complexes *ONO*, il a été aussi ici possible de modifier les « ligands » *ONS* par ajout de groupements OH sur les squelettes des ligands.

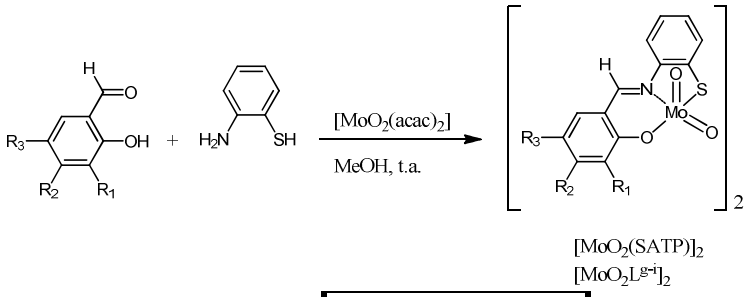

	Substituants		
	R_1	**R_2**	**R_3**
$[MoO_2(SATP)]_2$	H	H	H
$[MoO_2L^g]_2$	OH	H	H
$[MoO_2L^h]_2$	H	OH	H
$[MoO_2L^i]_2$	H	H	OH

Schéma 3 - Synthèse des complexes du molybdène *ONS*

Les ligands H_2SAP et H_2L^{a-f} ont pu être authentifiés par différentes méthodes spectroscopiques. (Table 1) L'analyse IR a montré la présence de la liaison imine vers 1600 cm^{-1}. La RMN du ^1H a permis de confirmer la formation des ligands, notamment par la présence d'un proton correspondant à la liaison imine CH=N entre 8.6 et 9 ppm et la présence de signaux attribués aux OH libres et au groupement NEt_2.

Table 1- Données IR et RMN ^1H des ligands *ONO* .

Formule	IR (ν en cm^{-1})	RMN ^1H (δ en ppm) dans d^6-DMSO				
	C=N	ArH	CH=N	OH	CH_2	CH_3
H_2SAP	1633	6.86-7.66	8.99	9.79, 13.78	-	-
H_2L^a	1618	6.69-7.42	8.93	9.05, 9.83, 14.21	-	-
H_2L^b	1603	6.24-7.38	8.78	9.66, 10.17, 14.24	-	-
H_2L^c	1600	6.75-7.34	8.84	9.04, 9.64, 12.88	-	-
H_2L^d	1603	6.97-7.80	8.99	10.72, 13.02	-	-
H_2L^e	1606	6.24-7.26	8.61	9.57, 14.26	3.35	1.09
H_2L^f	1608	6.00-7.77	8.74	10.57, 13.83	3.42	1.13

Les complexes du molybdène $[MoO_2(SAP)]_2$, $[MoO_2(SATP)]_2$ et $[MoO_2L^{a-i}]_2$ ont été caractérisés par spectroscopie IR, RMN ^1H et ATG. Six complexes ont peu être caractérisés par diffraction des rayons X.

Analyse Infrarouge (IR)

L'analyse des spectres IR (Table 2) montre différentes informations. La présence d'une vibration vers entre 1598 et 1615 cm^{-1} est attribuée à la présence de la fonction imine C=N. Celle-ci possède une valeur différente de celle observée pour les ligands libres dans le cas des ligands *ONO* (L^a à L^f), indiquant bien la fixation du ligand sur le groupement molybdènyle.

L'information la plus importante provient de l'observation de vibrations entre 760 et 945 cm^{-1} attribuées au groupement MoO_2. La valeur des vibrations indique la formation des composés monomères stabilisés (présence de deux vibrations proches correspondants aux Mo=O entre 908 et 935 cm^{-1}) ou oligomères (une vibration apparaissant entre 900 et 935 cm^{-1} pour les Mo=O terminaux et entre 780 et 844 cm^{-1} pour les vibrations correspondants au Mo-O-Mo pontants).

Table 2- Données IR importantes (cm^{-1}) des complexes du molybdène.

Type	Formule	ν (cm^{-1})		
		C=N	Mo=O	Mo-O-Mo
ONO	$[MoO_2(SAP)]_2$	1608	935	808
	$[MoO_2L^a(MeOH)]$	1612	908, 933	-
	$[MoO_2L^a]_2$	1612	919	780
	$[MoO_2L^b(EtOH)]$	1600	908, 945	-
	$[MoO_2L^b]_2$	1598	904	821
	$[MoO_2L^c]_2$	1613	912	804
	$[MoO_2L^d]_2$	1603	922	798
	$[MoO_2L^e]_2$	1615	927	844
	$[MoO_2L^f]_2$	1614	934	809
ONS	$[MoO_2(SATP)]_2$	1602	920	781
	$[MoO_2L^g]_2$	1605	935	770
	$[MoO_2L^h]_2$	1600	871	760
	$[MoO_2L^i]_2$	1603	901	772

Analyses RMN ^1H

La RMN ^1H permet d'observer les différents protons des ligands et notamment celui correspondant au proton imine CH=N (entre 8.89 et 9.23 ppm). Les déplacements différents de ceux des H_2L correspondants dans les cas des ligands *ONO* (n = a-f) permet d'attester de la fixation du ligand sur le fragment MoO_2. (Table 3)

Table 3- Données RMN ^1H importantes des complexes du molybdène.

Type	Formule	RMN ^1H (δ en ppm) dans d^6-DMSO		
		ArH	CH=N	OH
ONO	$[MoO_2(SAP)]_2$	6.83-7.81	9.23	-
	$[MoO_2L^a(MeOH)]$	6.82-7.82	9.20	9.36
	$[MoO_2L^a]_2$	6.82-7.82	9.20	9.36
	$[MoO_2L^b(EtOH)]$	6.32-7.82	9.03	10.6
	$[MoO_2L^b]_2$	6.32-7.82	9.03	10.6
	$[MoO_2L^c]_2$	6.76-7.83	9.16	9.43
	$[MoO_2L^d]_2$	6.97-8.07	9.43	-
	$[MoO_2L^e]_2$	6.15-7.69	8.89	-
	$[MoO_2L^f]_2$	6.16-7.83	9.01	-
ONS	$[MoO_2(SATP)]_2$	6.89-7.81	9.06	-
	$[MoO_2L^g]_2$	6.61-8.06	8.89	9.61
	$[MoO_2L^h]_2$	6.25-7.70	8.83	10.7
	$[MoO_2L^i]_2$	6.68-7.72	8.91	9.41

Analyses thermogravimétriques (ATG)

L'analyse thermogravimétrique des différents complexes a permis de montrer que les complexes se présentent sous forme de $[MoO_2L]_2$, la perte de masse unique correspondant à la destruction du ligand (entre 200 et 600°C) ou $[MoO_2L(D)]_2$ (avec une perte de masse avant 200°C correspondant au départ de D). La proportion du résidu final obtenu MoO_3 permet de confirmer les complexes. (Table 4) Le comportement des complexes correspond à l'équation 1

$$[\boldsymbol{MoO_2L(D)}] \xrightarrow{\Delta m_1\,(-D)} [\boldsymbol{MoO_2L}] \xrightarrow{\Delta m_2\,(-L+O)} \boldsymbol{MoO_3}$$

Equation 1

Table 4- Données ATG pour les complexes du molybdène.

Type	Formule	Δm_1 (< 250°C)		Δm_2 (250°C ~ 700°C)	
		Exp	Théo	Exp	Théo
ONO	$[MoO_2(SAP)]_2$	-	-	58.5	57.6
	$[MoO_2L^a(MeOH)]$	8.3	9.8	62.8	63.4
	$[MoO_2L^a]_2$	-	-	59.1	59.5
	$[MoO_2L^b(EtOH)]$	11.6	11.5	65.0	64.1
	$[MoO_2L^b]_2$	-	-	59.2	59.5
	$[MoO_2L^c]_2$	-	-	58.7	59.5
	$[MoO_2L^d]_2$	-	-	62.6	62.9
	$[MoO_2L^e]_2$	-	-	64.9	64.4
	$[MoO_2L^i]_2$	-	-	68.4	69.2
ONS	$[MoO_2(SATP)]_2$	-	-	58.5	59.5
	$[MoO_2L^g]_2$	-	-	61.1	61.2
	$[MoO_2L^h]_2$	-	-	60.1	61.2
	$[MoO_2L^i]_2$	-	-	61.8	61.2

Analyse par diffraction des rayons X (RX)

Six structures de complexes $[MoO_2L(D)]$ ont pu être isolées et caractérisées. De façon générale, les deux liaisons Mo=O bonds sont positionnées en conformation *cis*, le ligand L occupant trois positions dans un arrangement de type mer une molécule de solvant occupe le sixième site de coordination (le DMSO pour cinq complexes, l'eau pour le sixième) en position *trans* d'un ligand oxido avec une géométrie pseudo-octaédrique autour du métal, en accord avec des structures similaires.

Le complexe [MoO_2(SAP)(DMSO)] (Figure 1) présente un désordre cristallin dû à la symétrie du ligand L^a.

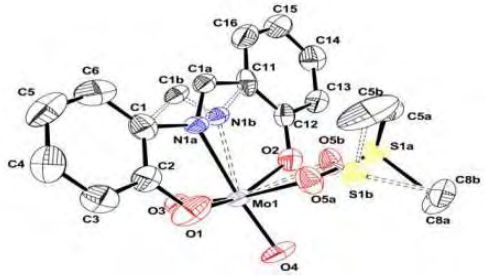

Fig. 1. Vue ORTEP de [MoO_2(SAP)(DMSO)]. La deuxième forme est représentée en pointillés.

La caractérisation complète de la série des complexes [MoO_2L(D)] à ligands contenant des OH libres $L^{b\text{-}d}$ a permis de prouver la nature des complexes (Figures 2 à 4).

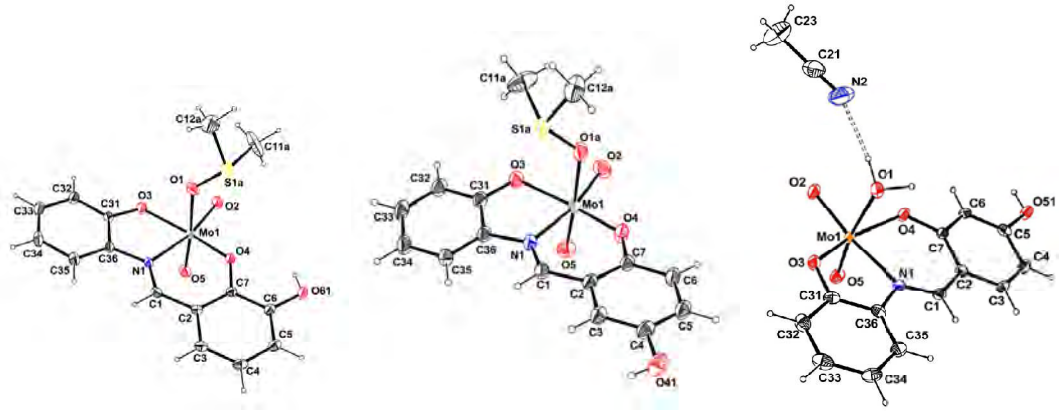

Fig. 2. Vues ORTEP des composés [MoO_2L^a(DMSO)] (gauche), [MoO_2L^c(DMSO)] (milieu) et [$MoO_2L^b(H_2O)$]·CH_3CN.(droite)

Dans le cas de [MoO_2L^a(DMSO)] (Figure 3) et [$MoO_2L^b(H_2O)$] (Figure 4), la distance entre le OH libre et les groupements oxido du molybdène sont favorables à la formation de dimères de coordination entre deux molécules via des liaisons hydrogènes.

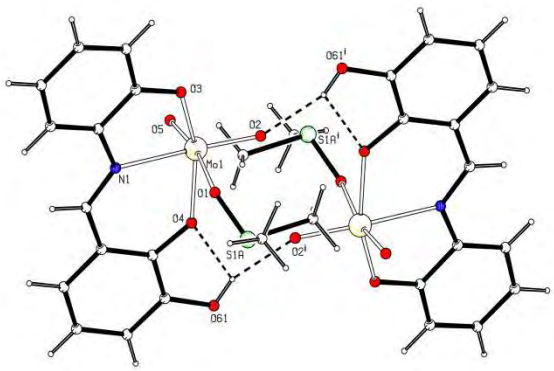

Figure 3 : Vue de l'unité dinucléaire formée par liaisons hydrogènes entre deux unités de [MoO_2L^a(DMSO)].

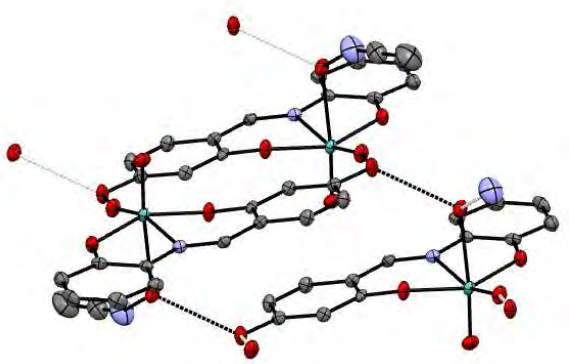

Fig. 4 Vue de l'unité dinucléaire formée par liaisons hydrogènes entre deux unités de $[MoO_2L^b(H_2O)]\cdot CH_3CN$.

Les structures des complexes $[MoO_2L^e(DMSO)]$ et $[MoO_2L^f(DMSO)]$ ont permis d'observer la planéarité des groupements NEt_2 et NO_2.(Figure 5)

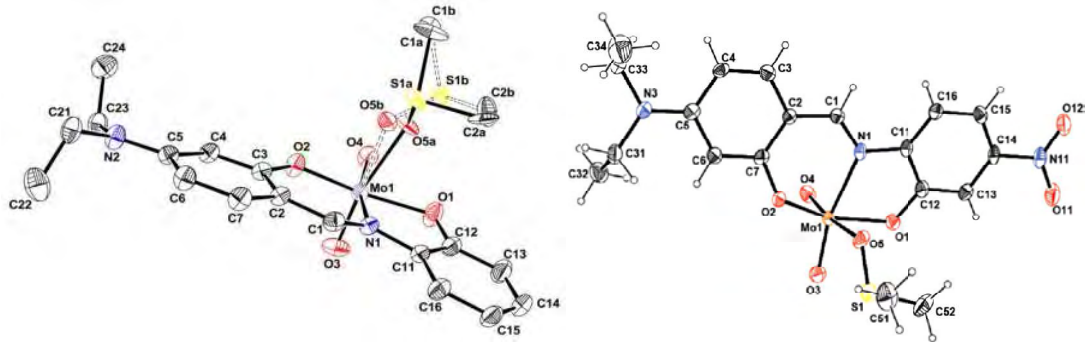

Fig. 5- Vues ORTEP de $[MoO_2L^e(DMSO)]$ (gauche) and $[MoO_2L^f(DMSO)]$ (droite). La deuxième position du DMSO est représentée en pointillés.

Ces complexes ont été utilisés dans l'étude catalytique de différents substrats, le cyclooctène dans le chapitre 3 et le limonène et le cyclohéxène dans le chapitre 4.

CHAPITRE 3 – Epoxydation du cyclooctène sans solvant organique catalysée par des complexes moléculaires du molybdène.

Ce chapitre s'attache à étudier les propriétés catalytiques des complexes $[MoO_2L]_2$ et $[MoO_2L(D)]$ présentés dans le chapitre 2 lors de l'époxydation du cyclooctène en absence de solvant organique et en utilisant TBHP dans l'eau comme oxydant.

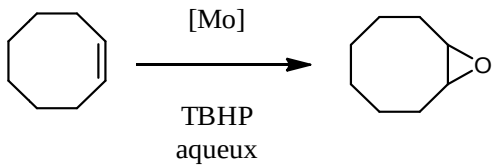

Schéma 4- Réaction d'époxydation du cyclooctène

Tous les complexes présentés dans le chapitre 2 ont été testés dans des conditions identiques. Les résultats comparatifs ont été rassemblés dans le tableau 5

Table 5– Epoxydation sans solvant organique du cyclooctène avec différents complexes du molybdène *ONO* and *ONS*.

Catalyseur	Conversion [%]	Sélectivité [%]	TOF [h^{-1}]	TON
$[MoO_2(SAP)]_2$	74	93	70	153
$[MoO_2L^a]_2$	92	93	251	184
$[MoO_2L^b]_2$	73	85	71	146
$[MoO_2L^b(EtOH)]$	74	90	68	148
$[MoO_2L^c]_2$	81	91	127	163
$[MoO_2(SATP)]_2$	90	94	253	180
$[MoO_2L^g]_2$	95	88	267	195
$[MoO_2L^h]_2$	98	82	298	196
$[MoO_2L^i]_2$	96	87	303	193
Conditions : Mo/TBHP/cyclooctene = 0.5/200/100; T= 80°C; t = 4h. Le TOF est calculé dans l'intervalle de temps à conversion maximale.				

Influence de la sphère de coordination ONO vs. ONS

L'influence de la sphère de coordination *ONO vs. ONS* a été montrée. Dans tous les cas, Les complexes du molybdène à ligands ONS réagissent mieux (90-96% de conversion) que les complexes à ligands *ONO* (73-92%). (Figure 6) L'introduction du soufre apporte donc un effet supplémentaire dans la vitesse de conversion. La sélectivité est équivalente pour les composés $[MoO_2(SAP)]_2$ et $[MoO_2(SATP)]_2$. (Table 5)

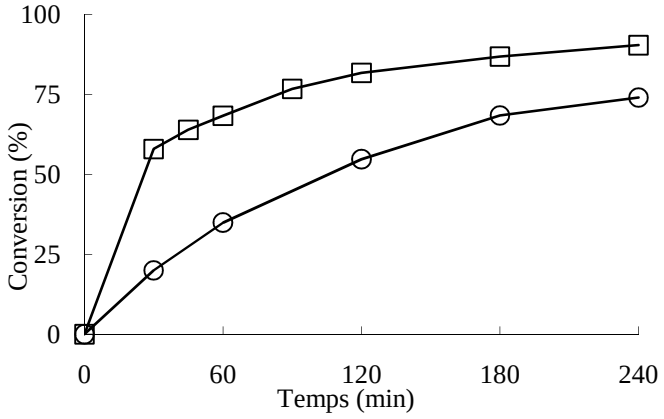

Fig. 6 Conversion du cyclooctène en fonction du temps catalysée par $[MoO_2(SAP)]_2$ (○) et $[MoO_2(SATP)]_2$ (□). Conditions expérimentales: Mo/TBHP/cyclooctène= 0.5/200/100; T = 80 °C.

Influence des groupements OH

L'effet des groupements OH sur les ligands *ONO* est notable avec des conversions allant entre 73 et 92% après 4 heures de réaction selon position du groupement OH (Table 5 et Figure 7). Le complexe $[MoO_2L^a]_2$ étant plus actif (conversion de 92%) que le composé de référence $[MoO_2(SAP)]_2$ (conversion de 74 %)

Pour les complexes à ligands *ONS*, les groupements OH permettent une meilleure conversion (95-98%) que le complexe sans groupement OH $[MoO_2(SATP)]_2$ (90%), mais la position du groupement OH ne modifie pas sensiblement les conversions. (Table 5)

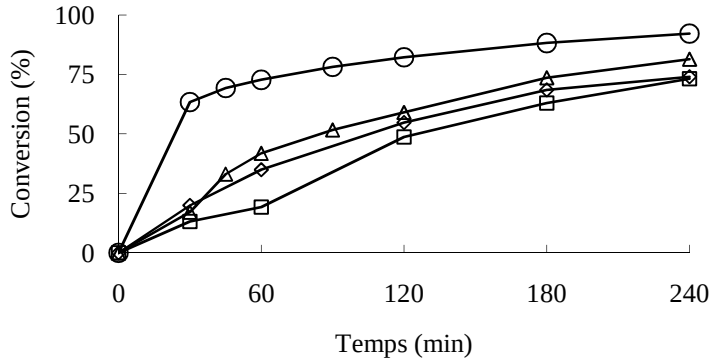

Fig. 7 - Conversion du cyclooctène en fonction du temps avec différents (pré)catalyseurs de type *ONO* $[MoO_2(SAP)]_2$ (◊), $[MoO_2L^a]_2$ (○), $[MoO_2L^b(EtOH)]$ (□) and $[MoO_2L^c]_2$ (Δ). Conditions expérimentales: Mo/TBHP/cyclooctène= 0.5/200/100; T = 80 °C.

Influence des groupements NEt_2 et NO_2

L'effet des groupements NEt_2 et NO_2 a été aussi observé avec des conversions entre 62 et 86%. (Table 6) Alors que la présence du groupement attracteur NO_2 dans $[MoO_2L^d]_2$ accélère la réaction (conversion de 86% de conversion et TOF de 344 h^{-1}), la présence du groupement NEt_2 dans $[MoO_2L^e]_2$ la ralentit sensiblement (62% et TOF de 167 h^{-1}). Le composé possédant les deux groupements NEt_2 et NO_2 $[MoO_2L^f]_2$ réagit de façon similaire au composé de référence $[MoO_2(SAP)]_2$. (Figure 8) Ces effets électroniques ont été reliés à un mécanisme théorique précédemment établi dans le groupe.

Table 6- Epoxidation du cyclooctène avec les complexes $[MoO_2L^a]_2$ et $[MoO_2L^{f-g}]_2$

Catalyseur	Conversion (%)[a]	Sélectivité (%)[a]	TON	TOF/h^{-1}
$[MoO_2(SAP)]_2$	71	94	286	195
$[MoO_2L^e]_2$	62	93	252	167
$[MoO_2L^d]_2$	86	96	346	344
$[MoO_2L^f]_2$	73	91	293	192

[a] après 4 h de réaction.

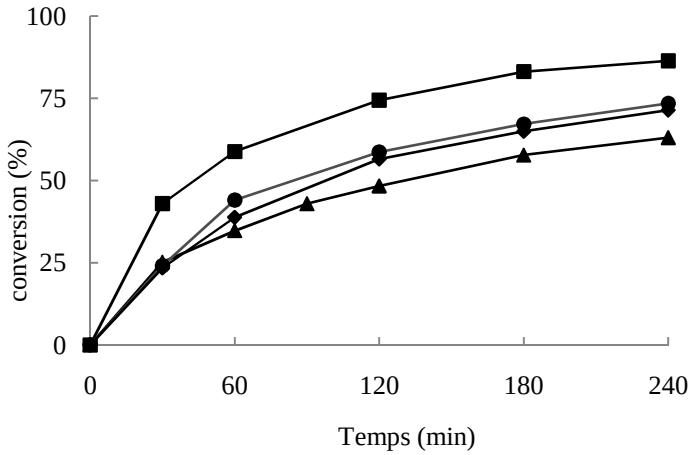

Fig. 8 - Conversion du cyclooctène en fonction du temps avec différents (pré)catalyseurs $[MoO_2(SAP)]_2$ (◆), $[MoO_2L^d]_2$ (■), $[MoO_2L^e]_2$ (▲), $[MoO_2L^f]_2$(●). Conditions: TBHP/substrat/[Mo] = 800:400:1; T = 80°C.

Divers autres paramètres ont été étudiés.

L'effet de la charge de catalyseur a été testé avec différents complexes. Une très faible charge (0.025%) du complexe ONS $[MoO_2(SATP)]_2$ a montré d'excellents résultats de conversion, (68%) avec une sélectivité de 93%. Le complexe $[MoO_2(SAP)]_2$ à 0.1% présentait 50% de conversion avec une sélectivité de 73%. Le complexe avec un groupement OH le plus actif à 1%, $[MoO_2L^a]_2$ se montrait plus actif à 0.1% (conversion 88% et 93% de sélectivité)

L'influence de l'eau dans le milieu réactionnel a aussi été testée avec ces trois mêmes complexes. Alors que l'ajout d'eau ralentit la réaction pour les trois complexes, certainement du au transfert plus lent du TBHP en phase organique, la sélectivité reste quasiment inchangée avec les complexes *ONO* alors que la sélectivité semble supérieure en présence d'eau avec le complexe *ONS* étudié.

Il a été aussi montré que l'augmentation du ratio TBHP/substrat améliorait la conversion de réaction.

Un essai de recyclage du complexe $[MoO_2(SATP)]_2$ a été fait. Durant six expériences consécutives, des résultats de conversion et sélectivité comparables ont pu être obtenus.

CHAPITRE 4 - Epoxydation du limonène et du cyclohéxène sans solvant organique catalysée par des complexes moléculaires du molybdène

Les catalyseurs présentés précédemment $[MoO_2L]_2$ ont été testés pour l'époxydation du limonène et du cyclohéxène. L'effet de la sphère de coordination autour du métal (*ONO vs*. *ONS*) et de l'introduction des groupements OH sur les ligands ont été mis en exergue.

Epoxydation du Limonène sans solvant organique

L'oxydation du limonène en présence de complexes du molybdène $[MoO_2L]_2$ conduit aux deux époxydes *cis* (cis-LO) et *trans* (trans-LO) ainsi qu'à l'ouverture des deux époxydes et la formation des diols correspondants (ax-LD et eq-LD) a été observée. (Schema 5)

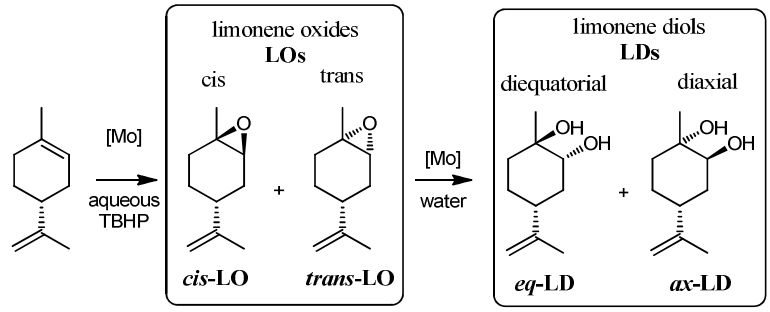

Schéma 5 – Epoxydation du limonène

Tous les complexes testés sont actifs à 80°C. Alors que le complexe *ONO* équivalent $[MoO_2(SAP)]_2$ présente une conversion plus modérée (Figure 9) et montre la formation des quatre produits précédemment cités, le complexe *ONS* $[MoO_2(SATP)]_2$ conduit rapidement et directement à la formation des LDs.

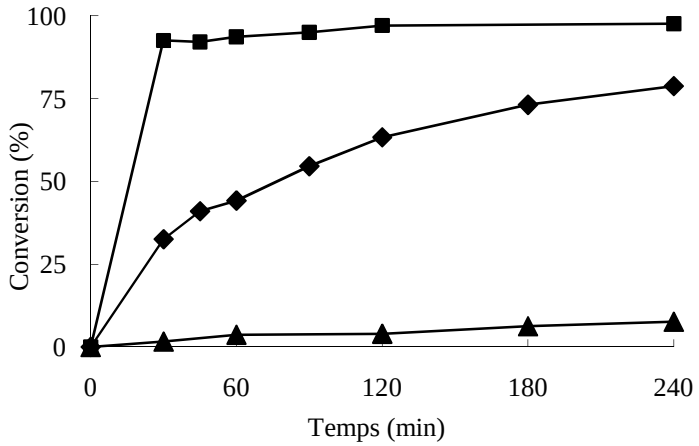

Figure 9 - Influence de la sphère de coordination (O *vs*. S) dans l'oxydation du limonène sans solvant organique: sans catalyseur (▲), $[MoO_2(SAP)]_2$ (◆), $[MoO_2(SATP)]_2$ (■). Conditions: [Mo]/limonène/TBHP = 0.5/100/200; T = 80°C.

La présence de groupement OH sur les complexes à ligands *ONO* et *ONS* a été étudiée et un comportement similaire à celui du cyclooctène a été observé. La conversion du limonène en présence du complexe $[MoO_2L^a]_2$ est plus rapide alors que les complexes à ligands *ONS* possédant des OH libres présentent peu de différence de réactivité. (Figure 10)

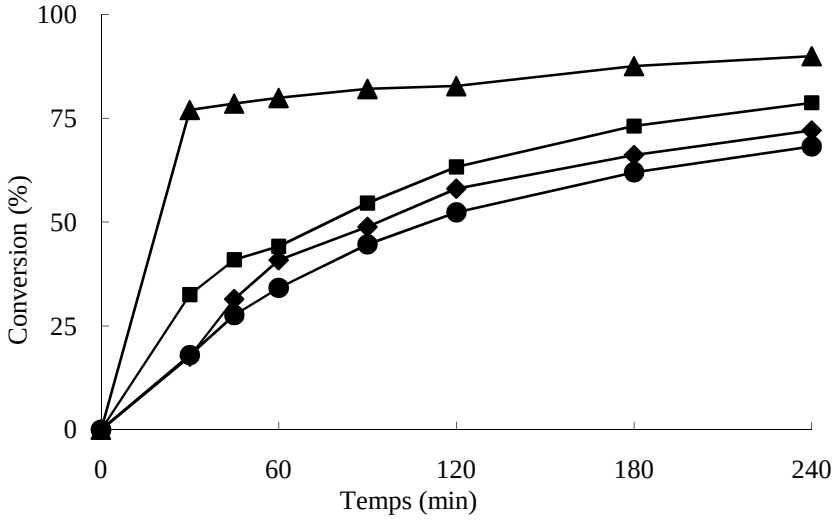

Figure 10 - Oxydation du limonène sans solvant organique catalysée par les complexes du molybdène *ONO* à 80°C: [Mo]/limonène/TBHP = 0.5/100/200 TBHP. Temps de réaction = 4 h, $[MoO_2(SAP)]_2$ (■), $[MoO_2L^a]_2$(▲), $[MoO_2L^b]_2$ (●), $[MoO_2L^c]_2$(◆).

Influence de la température

La température de réaction est un facteur clé dans la réactivité du complexe $[MoO_2(SATP)]_2$ En effet, ce dernier réagit à 30 et 50°C de façon similaire aux complexes à ligands *ONO* à 80°C (Figure 11) et il est possible d'observer des LOs en solution, quelle que soit la charge de catalyseur.

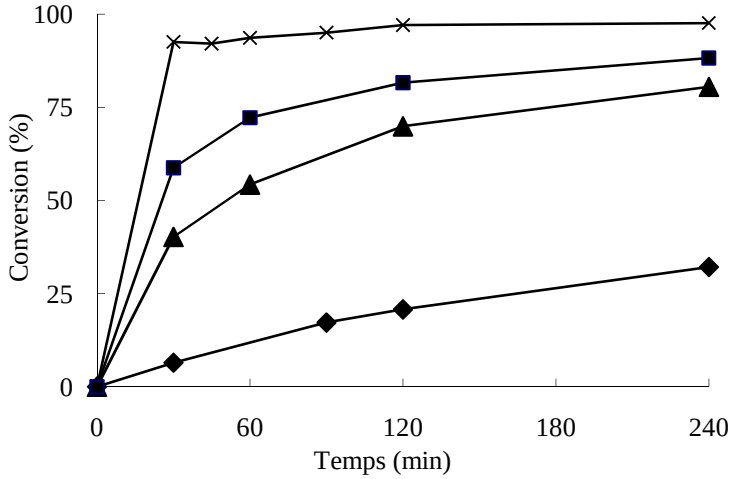

Figure 11 – Influence de la température pour l'oxydation sans solvant organique du limonène catalysé par $[MoO_2(SATP)]_2$: 30°C (◆), 50°C (▲) , 60°C (■), 80°C (×). Conditions: [Mo]/limonene/TBHP = 0.5/100/200

Néanmoins, les deux époxydes présentent des vitesses d'hydrolyse différentes, et des ratios différents entre eq-LD et ax-LD ont été observés, comme observé par ailleurs dans la littérature. Nous avons pu observer en présence des catalyseurs $[MoO_2(SATP)]_2$ et avec des conditions précises (entre 0,25 et 0.5% de catalyseur, 80°C) que la formation du diol diéquatorial, non préférentiel car moins stable, pouvait être formé jusqu'à 20% de la fraction de diol en fin de réaction.

Epoxydation sans solvant organique du cyclohexène

L'oxydation du cyclohexène (Schéma 6) a été réalisée avec les complexes du molybdène à ligands *ONO* possédant des groupements OH.

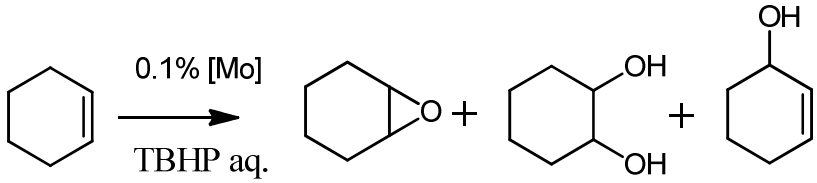

Schéma 6 - Epoxydation du cyclooctène

L'influence du groupement OH a pu être aussi ici être mise en avant avec une meilleure conversion du substrat en présence du complexe $[MoO_2L^a]_2$. (Figure 12) Cependant, la réactivité est sensiblement différente car ce catalyseur à ligand *ONO* conduit à une sélectivité plus faible en époxyde et une formation plus importante de diol.

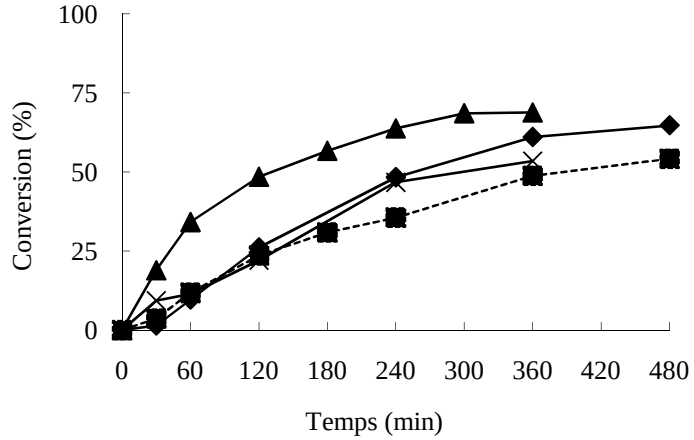

Figure 12 - Conversion du cyclohexène en fonction du temps avec différents (pré)catalyseurs de type *ONO*: $[MoO_2(SAP)]_2$ (■), $[MoO_2L^a]_2$ (▲), $[MoO_2L^b]_2$ (×), $[MoO_2L^c]_2$(◆). Conditions: substrat/[Mo] = 400:1; T = 80°C.

CHAPITRE 5 – Greffage de complexe du molybdène *ONO* sur résine Merrifield et époxydation du cyclooctène sans solvant organique

Ce chapitre concerne le greffage de complexes du molybdène à ligand tridentate de type *ONO* sur des résines polymères Merrifield. Les résines polymères commerciales choisies sont compatibles avec le milieu réactionnel. Deux méthodes de greffage ont conduit à deux types de résines.

Modèles moléculaires

Un travail préliminaire de synthèse d'analogues moléculaires a été effectué afin de valider au niveau moléculaire les différentes réactions de greffages sur résines.

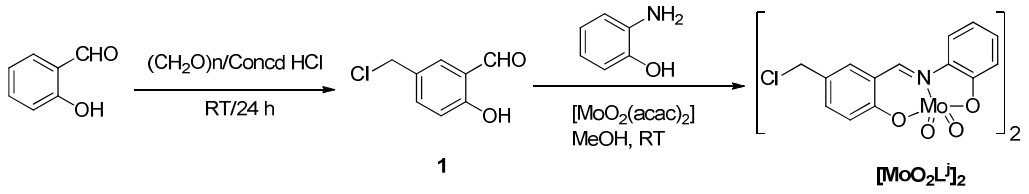

Schéma 7 - synthèse de l'analogue moléculaire

Ainsi, en utilisant des ligands à fonctions chlorométhyl pendantes, fonctions analogues à celles présentes sur le polymère, il a été formellement greffé un complexe du molybdène à ligands tridentate *ONO* pouvant utiliser comme linker la pipérazine (Schéma 7). Il a été montré au niveau moléculaire la difficulté de greffer sélectivement un seul groupement aldéhyde sur une pipérazine libre (ROUTE A Schéma 8). Par contre en greffant un côté de la pipérazine avec un groupement benzyl (ROUTE B Schéma 9), un complexe modèle de la résine a pu être synthétisé. Cependant, deux voies de synthèse de la résine ont été envisagées.

Les différents complexes moléculaires ont été caractérisés par différentes techniques spectroscopiques et ont été validés.

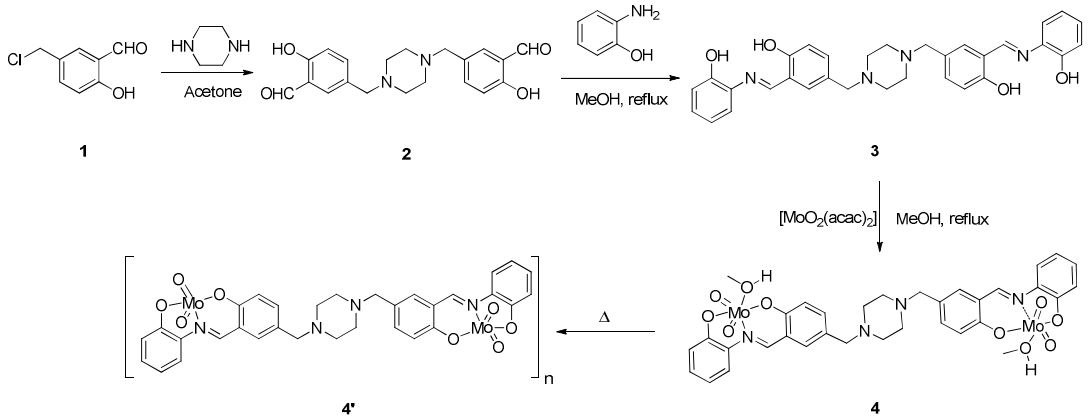

Schéma 8 - Synthèse « route A » sans protection de la pipérazine

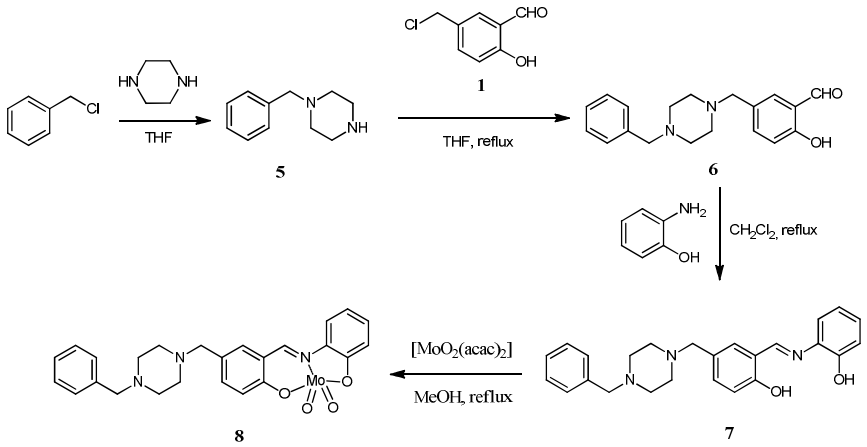

Schéma 9 - synthèse « route B » avec greffage de benzylamine

Greffage sur résine

Une méthode « pas à pas » (méthode A) et une méthode démarrant d'un fragment plus élaboré (méthode B) ont été présentées. (Schéma 10) Les différentes analyses (analyses élémentaires, IR et ATG) ont permis d'évaluer la résine à chaque étape et ainsi d'évaluer le pourcentage de molybdène présent sur les résines en fin de synthèse.

Les deux résines ont présentés des données spectroscopiques similaires, bien que les produits finaux n'aient pas la même couleur. La voie B présente moins de réactions parasites possibles et semble être la plus prometteuse.

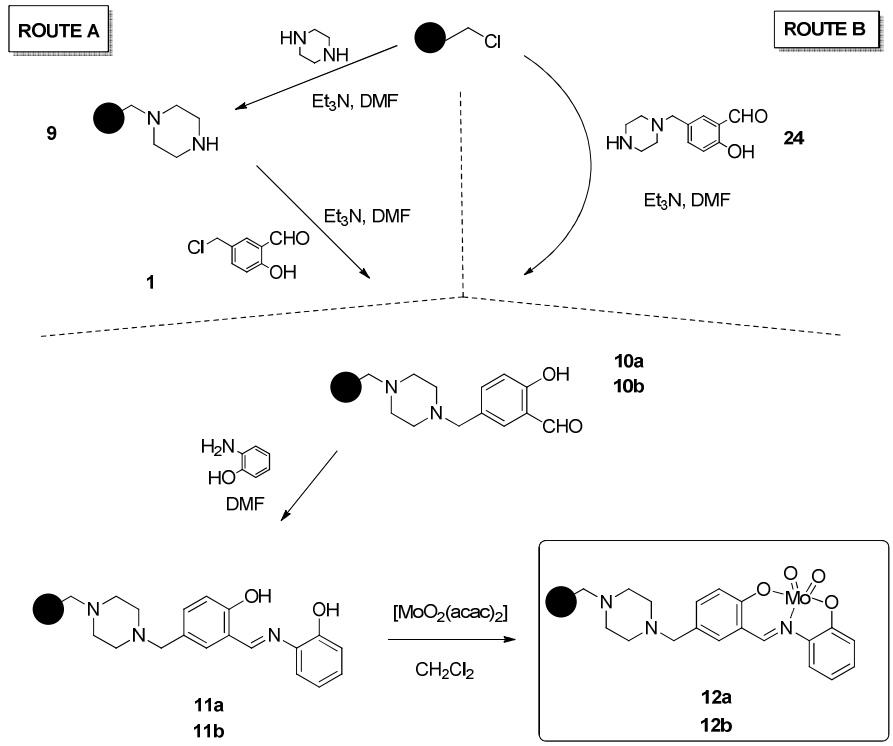

Schéma 10- Greffages sur la résine.

Les différentes routes ont permis de conduire à deux résines. Les différentes mesures sur les résines **12a** et **12b** ont permis de quantifier le nombre de moles de molybdène par g de polymère à une valeur de 2.22 mmoles Mo / g polymère

Epoxydation du cyclooctène avec les resins

A partir de ces résines, des réactions d'époxydation du cyclooctène sans solvant organique (Schéma 11) ajouté et en utilisant le TBHP en solution aqueuse comme oxydant ont permis d'évaluer la réactivité des résines vis-à-vis des analogues moléculaires.

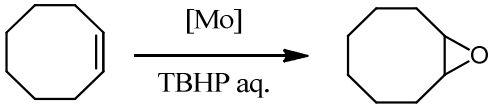

Schéma 11 – Epoxydation du cyclooctène

Table 7 – Epoxydation du cyclooctène catalysée par des complexes du molybdène et des résines sans solvant organique .

complexe	Conversion/%	Sélectivité/%	TOF_{init} [h^{-1}]	TON
$[MoO_2(SAP)]_2$[a]	74	93	70	153
$[MoO_2L^j]_2$[a]	88	93	193	175
12a[b] (Run 1)	51	72	28	102
12a'[b] (Run 2)	70	72	18	142
12a"[b] (Run 3)	79	68	93	159
12b[b] (Run 1)	63	64	15	127
12b'[b] (Run 2)	64	78	15	129
12b"[b] (Run 3)	54	59	18	107

[a] Conditions: Mo/TBHP/cyclooctene = 0.5/200/100; T = 80°C; t = 4 h. Le TOF initial est calculé après 30 min.

[b]Mo/TBHP/cyclooctene = 0.5 /200/100; T = 80°C; t = 8 h.

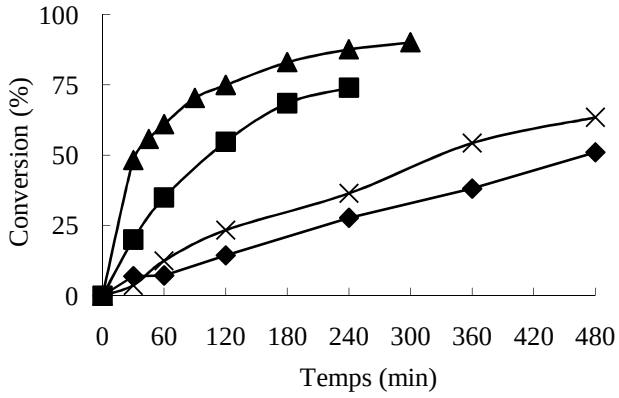

Figure 13 - Conversion du cyclooctène sans solvant organique en fonction du temps Conditions: Mo/TBHP/cyclooctene = 0.5/200/100; T = 80°C, $[MoO_2(SAP)]_2$ (■), $[MoO_2L^j]_2$ (▲), **12b** (×), **12a** (◆).

La conversion et la sélectivité est plus faible en présence des résines greffées

qu’en présence des composés homogènes mais les résines greffées on pu être utilisées 4 fois sans perte d’efficacité. (Table 7 et figure 13) La résine greffée obtenue par la méthode A semble évoluer au cours du temps (un changement de couleur notable est observé après chaque réutilisation) alors que la résine B semble inchangée. Des analyses IR de chaque résine après chaque réaction catalysée a permis de voir que la structure du polymère est peu modifiée (Figures 14 et 15). Cependant, une analyse thermogravimétrique de la résine après quatre réactions a montré que du relargage était observé avec les deux résines

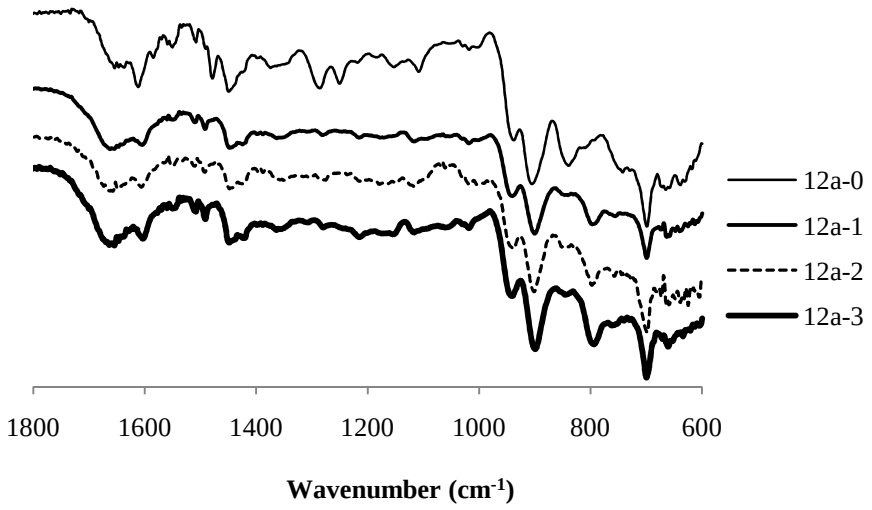

Figure 14 - IR des résines 12a-0 (avant la première expérience) et après chaque n-ième expérience (12a-n).

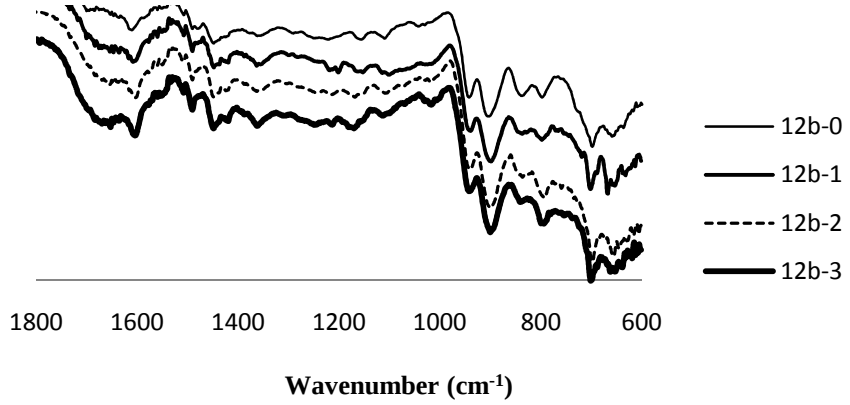

Figure 15 - IR des résines 12b-0 (avant la première expérience) et après chaque n-ième expérience (12b-n).

Conclusion et perspectives

Ce mémoire de thèse a montré différents résultats intéressants.

Différents complexes du molybdène $[MoO_2L]_2$ et $[MoO_2L(D)]$ (D = MeOH, EtOH) à ligand tridentates possédant des fonctions périphériques sur le ligand (OH, NEt_2 et NO_2) et une sphère de coordination différente (*ONO* et *ONS*) ont été synthétisés et caractérisés par différentes méthodes (IR, RMN ^1H, ATG). Six structures $[MoO_2L(D)]$ (D= DMSO ou H_2O) ont été caractérisées par diffraction des rayons X.

Les complexes du molybdène $[MoO_2L]_2$ ont été utilisés pour l'époxydation du cyclooctène, substrat modèle, sans solvant organique et en présence de TBHP aqueux. Il a été observé un effet notable sur la conversion et la sélectivité de la réaction en fonction de la nature des ligands.

Cet effet a été aussi observé sur deux autres substrats, le limonène et le cyclohexène,. Pour ces deux substrats, la réaction d'époxydation (dans les mêmes conditions que précédemment) conduit non seulement aux époxydes attendus mais aussi aux diols correspondant à l'ouverture de l'époxyde par l'eau. La nature de la sphère de coordination est primordiale pour la sélectivité des réactions. La nature des substituants libres sur les ligands intervient dans un second temps.

Il a été aussi possible de greffer des complexes tridentates du molybdène sur des résines Merrifield. Leur utilisation en tant que catalyseur pour l'époxydation du cyclooctène sans solvant organique a été mise en évidence. Bien que plus lent que les composés homogènes analogues, ces objets catalytiques semblent prometteurs.

Toutes les réactions catalytiques ont été effectuées sans solvant organique. Ce travail constitue une avancée notable dans le domaine de la chimie verte.

Les perspectives de ce travail concernent les différents aspects en rapport avec les développements de procédés verts. Il est planifié de continuer l'étude de l'oxydation de nombreux substrats modèles issus du pétrole afin de valider les oxydations de différentes fonctions simples.

Ces études seront suivies par l'oxydation de composés complexes issus de la biomasse. Par exemple, des terpènes accessibles en Europe sont intéressants par la diversité des composés d'oxydation qui peuvent être obtenus.

Enfin, des études d'optimisation de greffage sur d'autres supports, tels des silices greffées, d'autres polymères organique, ainsi que des macromolécules monodisperses tels les dendrimères semblent être un nouveau défi vers la synthèse de composés greffés récupérables. La diversité des supports existants devrait permettre de trouver des objets plus stables que ceux présentés (faible relargage de métal) dans le mémoire afin de pouvoir passer à des procédés en flux continu.

List of Abbreviations

Boc_2O	Di-tert-butyl dicarbonate
$CDCl_3$	Deuterated chloroform
CHP	cumene hydroperoxide
DCE	dichloroethane
DCM	dichloromethane
DMF	N,N-Dimethylformamide
DMSO	Dimethyl Sulfoxide
ee	Enantiomeric excess
ESI-MS	Electrospray Ionization mass spectrometry
FTIR	Fourier transform infrared spectroscopy
GC	Gas Chromatography
H_2SAE	salicylideneaminoethanol
H_2SAMP	salicylideneaminomethylpropanol
H_2SAN	N-(salicylidene)-2-aminobenzoic acid
H_2SAP	salicylideneaminophenol
H_2SATE	Salicylidene-2-aminoethanethiol
H_2SATP	salicylideneaminothiophenol
HMPA	hexamethylphosphoramide
HRMS	High resolution mass spectra
LCC	Laboratoire de Chimie de Coordination
LD	Limonene diol
lim	limonene
LO	Limonene oxide
MCM-41	Mobil Composition of Matter No. 41
MR	Merrifield Resin
MWCNT	Multiwall Carbon Nanotubes
NMR	Nuclear magnetic resonance
PS	Polystyrene
RT	Room temperature
SBA-15	spherical particles of mesoporous silicates
TBHP	tertiobutylhydroperoxide
TGA	Thermogravimetric Analysis

General Introduction

Within the research of cleaner and safer chemical processes, in which sustainable development of resources is a key point, chemists have in the 90s imagined different concepts that have been summarized by Anastas and Warner in the so-called 12 Principles of Green Chemistry.

The work developed in this manuscript tends to follow several of those 12 principles:

- The use of catalysis aims to diminish the quantity of hazardous reagents, doing the processes cleaner and more efficient.

- The organic solvent-free reactions diminish the quantity of toxic compounds used within a chemical process, limiting the number of potential pollutants from the beginning of the process.

- The use of renewables as substrates is also an interesting aspect. Renewable compounds issued from biomass are valuable ores of chemicals issued from short carbon cycle at the difference with fossil resources abundantly used and announced to deplete within some years.

- The recovery and recycling of catalysts is challenging aspect, since the metal-based catalysts can be toxic, depending on the metal center. Several regulations for production of chemical compounds in pharmaceutical and food industry require very low content of metals. The recovery is a method to diminish the quantity of metals in a process.

This manuscript is following those principles.

All along the manuscript, the use of molybdenum catalysts with very low metal content was used for the organic solvent-free epoxidation of different substrates (cyclooctene, cyclohexene and limonene). Limonene is issued from biomass, following the quest of new reactions with environment-friendly processes. In order to diminish the quantity of leached metal within the process, the catalyst was grafted on a polymer resin.

The first chapter presents a bibliographic state of the art within the topic, pointing out the different molybdenum complexes with Schiff base tridentate ligands close to those studied within the manuscript, their use in catalysis and different molybdenum-grafted catalysts.

The second chapter deals with the syntheses and characterizations of molybdenum complexes with Schiff base tridentate ligands. Those ligands possess two different coordination spheres around the metal (*ONO* and *ONS*) and different substitution on the ligand (OH, NEt_2, NO_2).

The third chapter describes the use of the catalysts from chapter two for the organic solvent-free epoxidation of cyclooctene, a model substrate. The effect of the different ligands is discussed.

The fourth chapter treats the organic solvent-free epoxidation of two other substrates, limonene and cyclohexene in presence of the molybdenum complexes. The effect of the different ligands is discussed.

The last chapter shows the grafting of one molybdenum complex within a Merrifield resin. The prepared heterogeneous catalyst is used for the organic solvent-free epoxidation of cyclooctene. Recovery and reuse of the grafted resins is presented.

I. Chapter I
Bibliographic background

I.1. Introduction

The imines, also called Schiff bases, since firstly reported by Ugo Schiff [1] are widely used organic compounds, because of different properties, as their biological activities,[2] their electrochemical behaviours,[3] and their water stability. [4]
The preparation of Schiff base is very easy. The reaction between a primary amine and an aldehyde or a ketone, with or without heating, lead very quickly to the formation of an imine bond (-CH=N-).

Schiff bases are used massively in coordination chemistry and several metal complexes can be obtained under very simple procedures.[5] Among all those complexes, molybdenum Schiff base complexes have been observed to be active as catalyst in several reactions, especially in oxidation of olefins,[6] sulfides,[7] or alcohols.[8]

Since the thesis present activities of those complexes, we have focused this bibliographic presentation on the molybdenum complexes with Schiff base ligands.

Since several ligands will be shown repeatedly all along the text, we will assign to each of them a unique symbol, as introduced in the various schemes. The most common ligands are shown in Scheme 1.1. H_2SAE stands for salicylidene-aminoethanol, H_2SAMP for salicylideneaminomethylpropanol, H_2SAP for salicylideneaminophenol, H_2SATP for salicylideneaminothiophenol, SATE for Salicylidene-2-aminoethanethiol and H_2SAN for N-(salicylidene)-2-aminobenzoic acid.

More elaborate ligands will be introduced further in the next sections and defined by an L^n symbol. All ligands result from the condensation between a (substituted) salicylaldehyde and a NH_2-(linker)-XH molecule (see the retrosynthetic pathway in Scheme 1.1), therefore forming a Schiff base where X is a third donor atom in addition to the salicylideneamino O and N atoms, typically separated from the N donor by a two-atom linker. The ligands can be classified into two main types, the *ONO*-type and *ONS*-type depending on the nature of the donor atom X. The NH_2-(linker)-XH part of the molecule is most typically an aminoalcohol, aminothiol, or amino(thio)phenol, but can also consist of a hydroxy- (or mercapto)-hydrazone, (thio)semicarbazone, *etc.* For all the structures in the thesis, the ligand modification will take place in the left aromatic part (salicyl ring) or on the aromatic linker in the right part of the ligand backbone for SAP/SATP type structures.

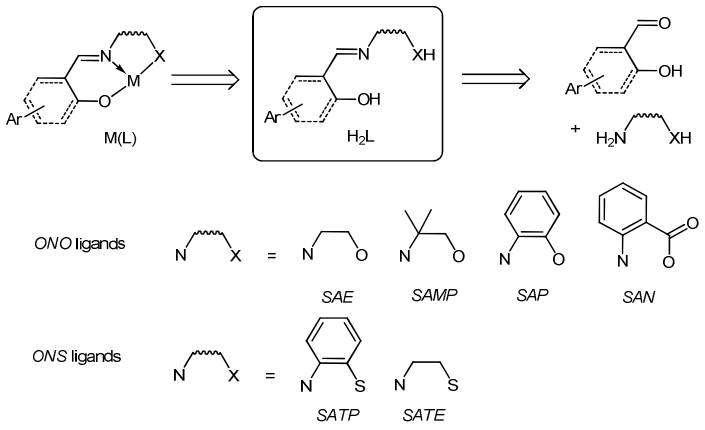

Scheme 1.1

I.2. Molybdenum complexes with tridentate Schiff base ligands

I.2.1. Monomer versus oligomer

One of the first reports concerning the $[MoO_2(SAP)(D)]$ (D = 2-electron donor ligand) family of complexes was published in 1973 by Chjo. The *cis*-dioxomolybdenum(VI) complex $[MoO_2(SAP)(H_2O)]$ (Scheme 1.2) was identified by infrared (IR) to have an octahedral geometry around the molybdenum atom.[9]

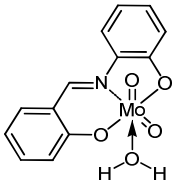

Scheme 1.2

These complexes have shown interesting reactivity especially on the *oxido* functions. As an example, Sharpless, Ibers and coworkers treated in 1978 the $[MoO_2(SAP)(HMPA)]$ complex (HMPA = hexamethylphosphoramide, $(Me_2N)_3P=O$) with N-substituted hydroxylamines producing the molybdooxaziridine [MoO(ONR')(SAP)(HMPA)] (see Scheme 1.3). One structure was identified by single crystal X-ray diffraction (Figure 1. 1). These products were used for the high yield amination of several olefins.[10]

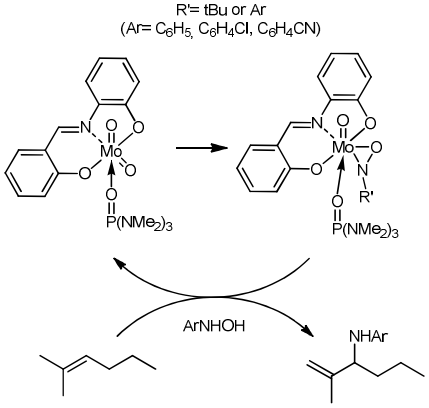

Scheme 1.3. Aminationof olefins and produced molybdooxaziridine

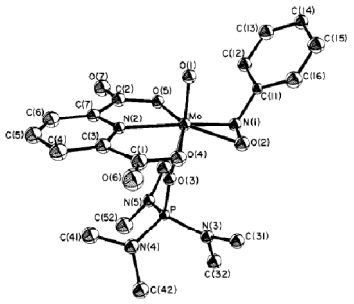

Figure 1. 1. A perspective drawing of one [MoO(ONR')(SAP)(HMPA)].Hydrogen atoms are not included, reproduced with permission from ref. 10. Copyright 1978 ACS

The easy coordination of different donors to the sixth position of the Mo center has been extensively studied. One relevant article was published in 1981 by Rajan and Chakravorty.[11] They reported different $[MoO_2L]$ complexes with *ONO*-type (SAP and SAE) and *ONS*-type (SATP) tridentate Schiff base ligands. IR measurements suggested that the compounds were monomeric $[MoO_2L(EtOH)]$ when prepared in ethanol but oligomerization via Mo=O-Mo bridge formation occurred upon heating with expulsion of the EtOH ligand. The oligomers featured pseudo-octahedral coordination around the molybdenum atom (see Scheme 1.4). Those complexes were converted to the monomeric form $[MoO_2L(D)]$ by addition of several donors D (aldehyde, amide, amine, N-oxide, sulfoxide, phosphine oxide, water, alcohol).

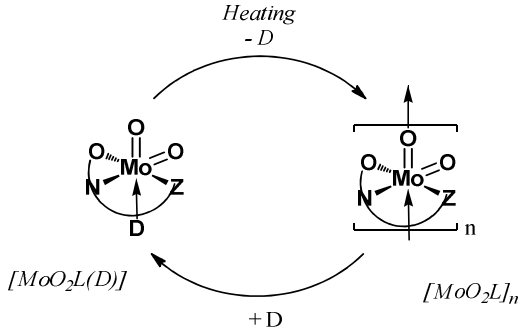

Scheme 1.4. Exchange between monomer and oligomer.

In 1990, Ziołkowski and coworkers reported several dimeric $[MoO_2L]_2$ and monomeric $[MoO_2L(D)]$ molybdenum complexes with dianionic *ONO* tridentate Schiff bases ligands,[12] *i.e.* H_2SAP, H_2SAE and H_2SAMP ligands, D being coordinating solvent. The structures were characterized by X-Ray diffraction (see Figure 1.2) and by IR spectroscopy, proving that the oligomeric $[MoO_2L]_n$ complexes obtained separately by Rajan[11] and Topich[13] were in fact dimeric complexes with an asymmetric $Mo_2(\mu\text{-}O)_2$ bridge.

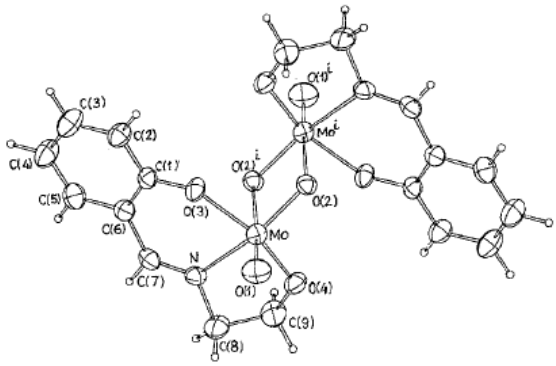

Figure 1.2. Structure of $[Mo(O)(\mu\text{-}O)(SAE)]_2$, reproduced with permission from ref. 12. Copyright 1990 Springer.

In 2000, Sobczak and coworkers reported the structure of a new molybdenum *ONO* complex [MoO_2L^1(EtOH)] with an SAP-type ligand (H_2L^1 = 3,5-di-*tert*-butyl-*N*-salicylidene-2-aminophenol, see Figure 1.3).[14] This complex can form the *oxo*-bridged oligomer or dimer by losing the ethanol ligand.

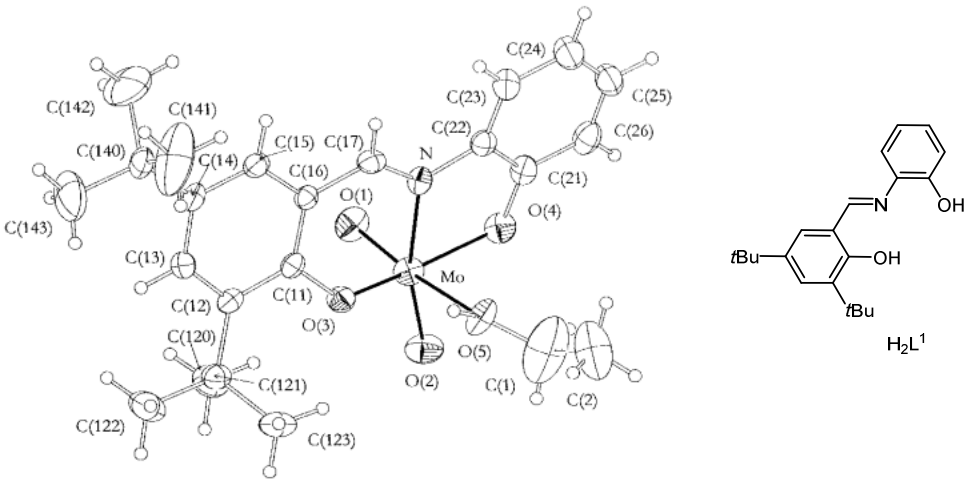

Figure 1.3. Structure of [MoO_2L^1(EtOH)] showing 30% probability ellipsoids and the atom-labelling scheme. Reproduced with permission from ref. 14. Copyright 2000 Royal Society of Chemistry.

I.2.2. Effect of the ligand substitution

In 1980 and 1981,[11] Topich synthesized [MoO_2L] complexes with functionalized SAP, SAE and SAN ligands (L = SAP, SAE and SAN and L^2-L^{12}, see Scheme 1.5) in dry tetrahydrofuran, ethanol, or ethyl acetate), the products being isolated recrystallized in DMSO by adding H_2O. The IR spectra revealed a mixture of monomer [$MoO_2L(D)$] and dimer [$MoO_2L]_2$ in the solid state while in solution (such as ethanol, DMSO, DMF, pyridine, *etc.*) the complexes are monomeric. The authors suggested that the tridentate ligand lies in the equatorial plane of the complex along with one *oxido* group while the solvent molecule occupies a labile coordination site in *trans* position to the second *oxido* ligand. The influence of the ligand functionalization was deduced from the observed trends in the UV spectra and in the reduction potentials. The UV spectra of the complexes are dominated by charge transfer transitions.

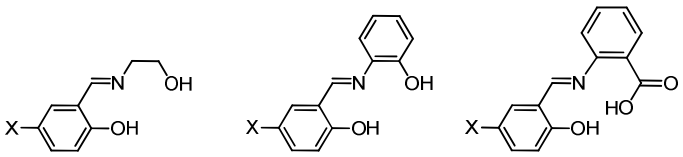

X = H, H_2SAE
NO_2, H_2L^2
Cl, H_2L^3
Br, H_2L^4
OMe, H_2L^5

X = H, H_2SAP
NO_2, H_2L^6
Cl, H_2L^7
Br, H_2L^8
OMe, H_2L^9

X = H, H_2SAN
Cl, H_2L^{10}
Br, H_2L^{11}
OMe, H_2L^{12}

Scheme 1.5

Electron-withdrawing substituents cause an anodic shift in the reduction potential (E_{pc}), the opposite effect being observed for electron-donating substituents. In addition, electronic delocalization and the substitution by a carboxylic acid group of the phenolic oxygen donor atom (*i.e.* on going from *SAP*-type to *SAN*-type ligands) facilitate the molybdenum reduction. The trends observed by electrochemistry can be also observed by UV through the shift of the low-energy ligand-to-metal charge-transfer transition.

In later studies,[15] Topich reported that the oxygen transfer reaction between ethyldiphenylphosphine ($EtPh_2P$) as oxygen acceptor *ONS*-type [MoO_2L] complexes (L = L^{13}-L^{19}) as oxygen donors leads to the phosphine oxide $EtPh_2PO$ with the formation of the corresponding [MoOL] complex (equation 1.1). The *ONS* tridentate Schiff base ligands in these complexes are substituted derivatives based on the SATP and SATE backbones. Kinetics measurements on these reactions showed rates that are 1st order in both reactants (see equation 1.2). The rate constant $\boldsymbol{k_1}$ depends on the ligand X-substituent. A correlation was observed between the cathodic reduction potentials (E_{pc}) and $\boldsymbol{k_1}$ in the case of SATP based complexes.

Equation 1.1 $$MoO_2L + PEtPh_2 \xrightarrow{k_1} MoOL + OPEtPh_2$$

Equation 1.2 $$-\frac{d[MoO_2L]}{dt} = k_1[MoO_2L][PEtPh_2]$$

In 1992, Topich[16] investigated different [MoO_2L] complexes (L = SAP, SATP, SATE, L^2, L^6-L^9 and the new ligands L^{13}-L^{21} in Scheme 1.6 using FT-IR spectroscopy in DMF solution. The starting ligands are based on H_2SAP, H_2SAE, and H_2SAET with different substitutions. For all those complexes, the ν_{as}(Mo=O) stretching frequencies depend on the nature of the Schiff base ligands substituents (delocalization and inductive effects) and on the nature of the donor atoms (*ONS vs*. *ONO*).

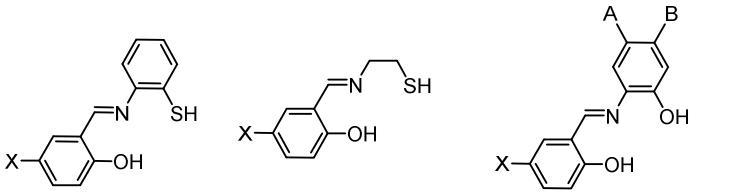

X = Br: H_2L^{13}
X = Cl: H_2L^{14}
X = NO_2: H_2L^{15}
X = OMe: H_2L^{16}

X = Cl: H_2L^{17}
Br: H_2L^{18}
OMe: H_2L^{19}

A,B = NO_2,H; X= NO_2: H_2L^{20}
A,B = H,NO_2; X= NO_2: H_2L^{21}

Scheme 1.6

Correlations were observed between ν_{as}(Mo=O), the Hammett parameter **(σ_p)** for the X substituent on the ligand, and the $\boldsymbol{k_1}$ rate constant for the oxygen atom transfer from [MoO_2L] to $PEtPh_2$. The observed variation in ν_{as}(Mo=O) reflects changes in the relative energy of the Mo=O $\boldsymbol{\pi^*}$ (antibonding) orbital. It has been proposed that this energy change contributes to the activation energy in the oxygen atom transfer reaction with $PEtPh_2$. The results support the proposed reaction mechanism of donation of the phosphorus lone-pair electrons into the Mo=O $\boldsymbol{\pi^*}$ orbital (see Scheme 1.7).

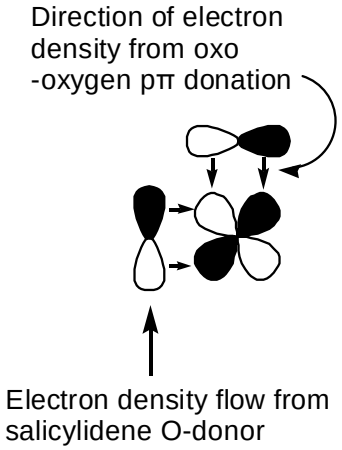

Scheme 1.7. Simplified orbital interaction diagramshowing the atomic orbital overlap between the phosphine P atom p lone pair and the Mo=O π^* orbital.

I.2.3. Structural features

I.2.3.1. ONO coordination

In 2011, Chand and co-workers characterized different chiral Schiff base $[MoO_2L(MeOH)]$ complexes with *H_2SAE*-type ligands (L = L^{22}-L^{27}).[17] The geometry around the Mo is classical in most cases, *i.e.* a molybdenyl moiety surrounded by the tridentate *ONO* Schiff-base ligand and the sixth coordination site is completed by a coordinated labile solvent molecule. This geometry is ubiquitous and will not be further underlined unless there are special points worthy of notice. When a bulky substituent is present in the ligand, however, a monomeric 5-coordinate geometry with an open coordination site was observed, as in the case of ligand H_2L^{26} (see Figure 1.4).

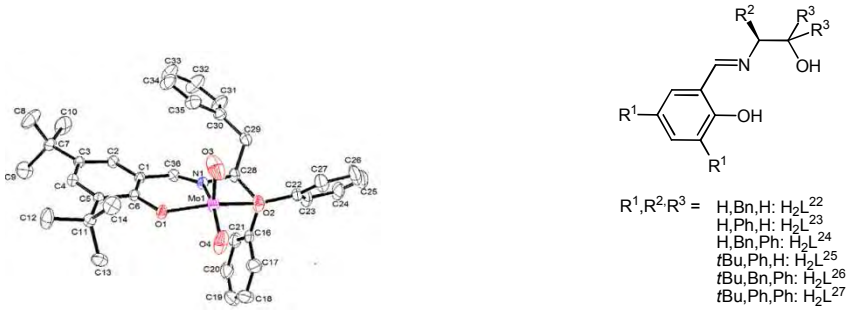

Figure 1.4. ORTEP view of the structure of compound $[MoO_2(L^{31})]$. Reproduced with permission from ref. 17. Copyright 2011 Elsevier Science.

In 2015, Sah and coworker reported the synthesis of the molybdenum (VI) complexes $[MoO_2L(H_2O)]$ from glucopyranosylamine Schiff bases $H_2L^{28\text{-}31}$ in methanol (Scheme 1.8.).[18]

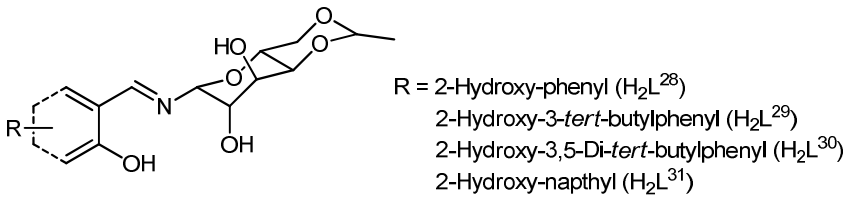

Scheme 1.8.

In 2013, Xue and coworkers reported the synthesis of $[MoO_2L^{32}(MeOH)]$ and $[MoO_2L(EtOH)]$ complexes (see Scheme 1.9). The asymmetric unit of each complex contains two mononuclear dioxomolybdenum(VI) molecules stabilized by alcohols.(see Figure 1.5). [19]

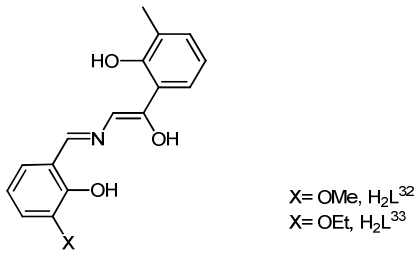

Scheme 1.9

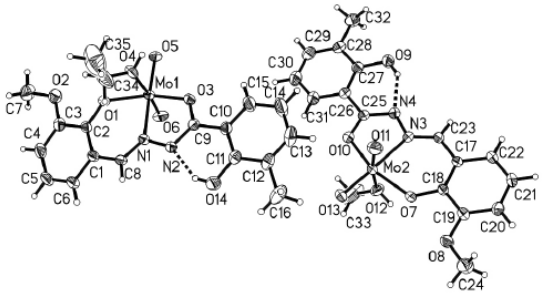

Figure 1.5. Molecular structure of $[MoO_2L^{32}(MeOH)]$ at 30% probability displacement. Reproduced with permission from ref. 19. Copyright 2013.

In 2009, Sheikhshoaie and Rezaeifard reported a new dioxo-molybdenum(VI) complex $[MoO_2L^{34}(CH_3OH)]$, L^{34} = 2-[(2-hydroxy-propylimino)methyl]phenol. A monoclinic space group $P2_1/c$ was determined by X-ray diffraction in Figure 1.6.[20]

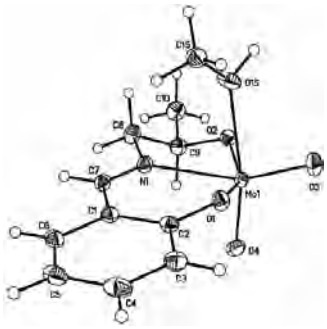

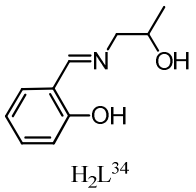

H_2L^{34}

Figure 1.6. ORTEP of complex $[MoO_2(L^{34})(CH_3OH)]$ at 50% probability level with atomic numbering. Reproduced with permission from ref. 20. Copyright 2009 Elsevier.

In 2014, Sergienko and coworkers reported the X-ray structure of $[MoO_2L^{35}(H_2O)]\cdot H_2O$ with a doubly deprotonated 2-[N-(hydroxynaphtylidene)-amino]propane-1,2,3-triol ligand (Figure 1.7). The crystallization water molecule forms two H-bonds through two different O lone pairs with two O-H bonds of the triol function as proton donors.[21]

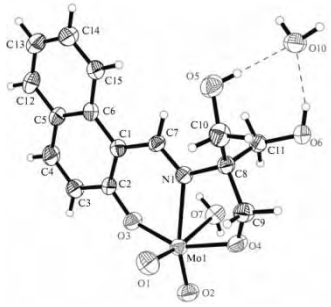

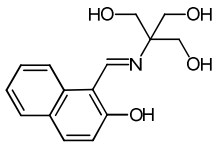

H_2L^{35}

Figure 1.7. ORTEP view of the $[MoO_2L^{35}(H_2O)]\cdot H_2O$ structure. Reproduced with permission from ref. 21. Copyright 2014 Pleiades Publishing, Inc.

In 2010, Bibal, Poli and coworkers presented two anionic Schiff base molybdenum(VI) complexes $[MoO_2L^{36}]^-$ and $[MoO_2L^{37}]^-$ with sulfonated ligands based on the SAE and SAP scaffolds (Scheme 1.10).[22] The relative arrangement of the adjacent molecules in the crystal structure is the same for the two compounds, with a mutual head-tail arrangement of two anions to generate pseudo-dimers in which the position normally occupied by a solvent molecule D is taken by the sulfonate group of the adjacent complex (see Figure 1.8).

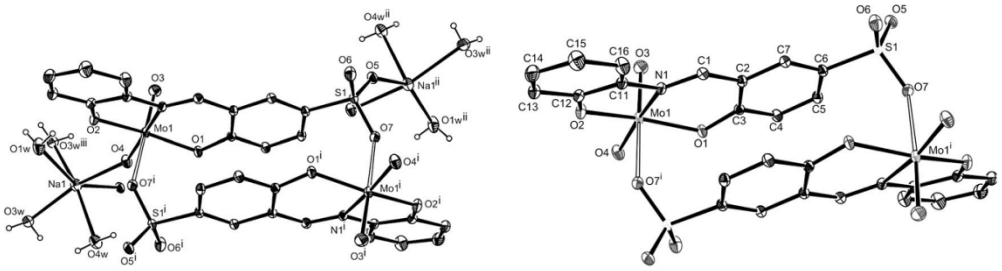

Figure 1.8. ORTEP views of the structures of $Na[MoO_2L^{36}]$ (left) and $Bu_4N[MoO_2L^{37}]$ (right). Reproduced with permission from ref. 22. Copyright 2015 Elsevier B.V.

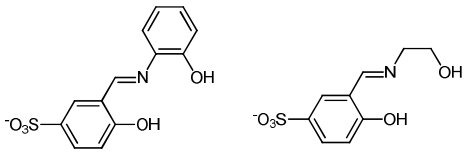

H_2L^{36} H_2L^{37}

Scheme 1.10

In 2014, Umbarkar, Michon, Agbossou-Niedercorn and coworkers synthesized the $[MoO_2L(MeOH)]$ complexes with L = SAP and an *ONO* chiral ligand L^{38} in Scheme 1.11.[23]

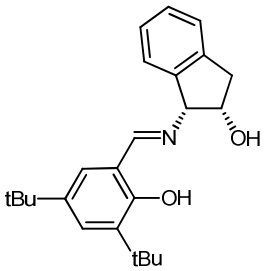

H_2L^{38}

Scheme 1.11

In 2012, Rezaeifard et *al*. synthesized cis-dioxomolybdenum(VI) complexes $[MoO_2L(CH_3OH)]$ (L = L^{39-42}, SAMP as tridentate *ONO* donor Schiff base ligands). $[MoO_2L^{42}(CH_3OH)]$ was crystallized in orthorhombic space (see Figure 1.9).[24]

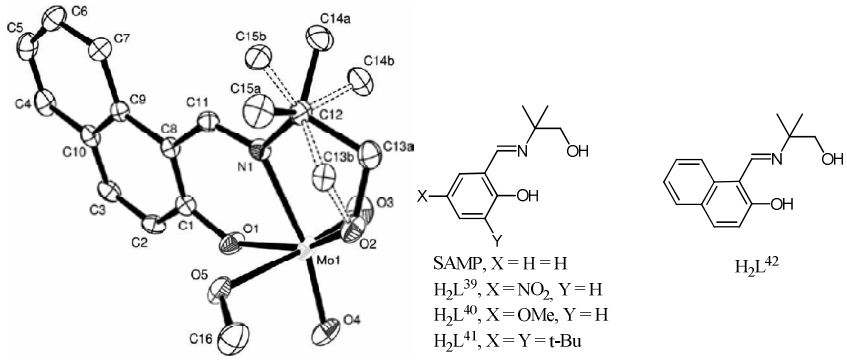

Figure 1.9.A view of the molecular structure of $[MoO_2L^{42}(MeOH)]$, showing the numbering scheme and displacement ellipsoids drawn at the 50% probability level.Reproduced with permission from ref. 24. Copyright 2012 WILEY-VCH Verlag GmbH & Co. KGaA, Weinheim.

In 2011, Bulhac and coworkers published two $[MoO_2L(D)]$ complexes with ligands derived from salicyladehydehydrazones ($L^{43\text{-}44}$, see Scheme 1.12), showing the expected octahedral geometryas verified in the solid state by X-ray crystallography for the $[MoO_2L^{43}(CH_3OH)]$ and $[MoO_2L^{44}(DMSO)]$ complexes.[25]

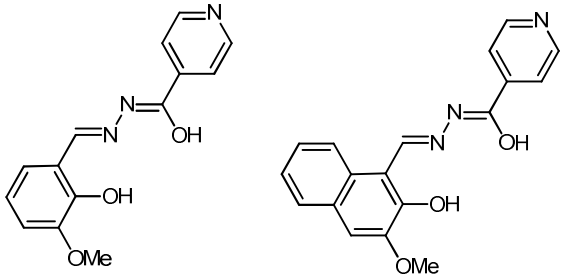

Scheme 1.12

In 2011, Ngan and coworkers reported $[MoO_2L(D)]$ complexes derived from substituted *ONO* salicylaldehydehydrazones (L = L^{45}-L^{48}, see Scheme 1.13) in the presence of donor D molecules (D = DMSO, HMPA, DMF, imidazole or MeOH). Several molecular structures were elucidated by single crystal X-ray diffraction.[26]

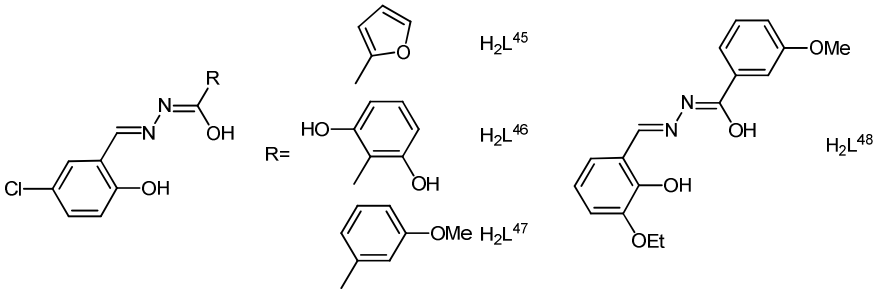

Scheme 1.13

In 2014, Bagherzadeh and co-workers reported a new molybdenum complex $[MoO_2L^{49}(EtOH)]$ (L = N'-[1-(2-hydroxynaphthyl)ethylidene]-2-hydroxybenzohydrazide (see Figure 1.10). The AIM topological analysis of the electron density and a DFT study indicated that the *ONO* ligand coordinates $\{MoO_2\}^{2+}$ in the enol-enamine form rather than in the *keto*-amine tautomeric form.[27]

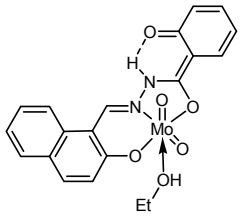

Figure 1.10.

You, Zhu and coworkers reported the synthesis of four mononuclear dioxomolybdenumcomplexes $[MoO_2L(D)]$ with *ONO* tridentate ligands based on benzhydrazonato skeleton (L = $L^{50\text{-}51}$ (D = H_2O); L = $L^{52\text{-}53}$ (D = MeOH), Scheme 1.14).[28]

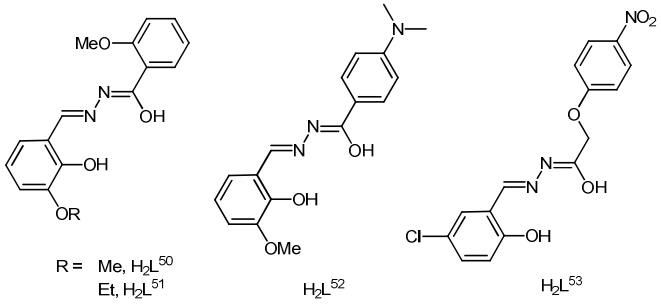

Scheme 1.14

The X-ray structural analysis of the methanol adducts of the L^{52} and L^{53} compounds showed that two adjacent molecules are linked by the methanol ligands through two intermolecular O–H···N hydrogen bonds to form dimers.

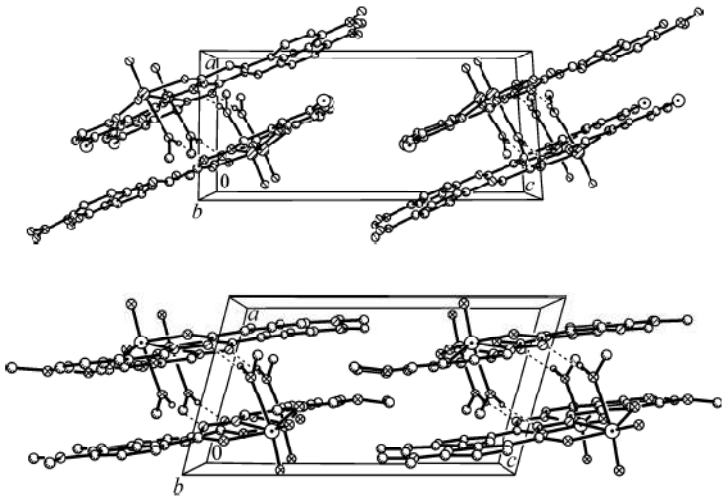

Figure 1.11. Molecular packing arrangements of $[MoO_2L^{52}(MeOH)]$ (above) and $[MoO_2L^{53}(MeOH)]$ (below) displayed in the unit cell. Hydrogen bonds are shown as dashed lines. Reproduced with permission from ref. 28. Copyright 2014 Pleiades Publishing, Ltd.

Pisk et al. reported a series of molybdenum(VI) complexes with novel pyridoxal hydrazonato ligands that can be classified into three categories: mononuclear $[MoO_2(L^{54\text{-}56})(MeOH)]$, polynuclear $[MoO_2(L^{54\text{-}56})]_n$ and hybrid organic–inorganic compounds with a Lindqvist polyoxomolybdate anion, $[MoO_2(L^{54\text{-}56})]_2Mo_6O_{19}$. This last product represents the first reported example of a polycationic dioxomolybdenum complex with a Lindqvist anion (see X-ray structure in Figure 1.12).[29]

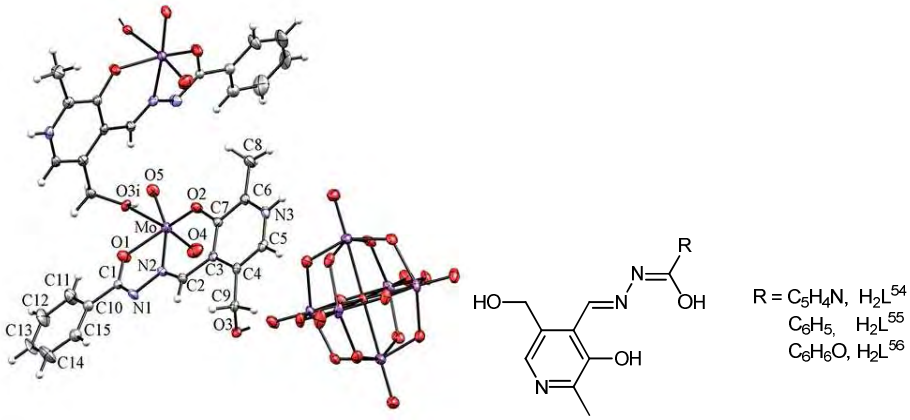

Figure 1.12. Mercury – POV-Ray drawing of compound $[MoO_2(HL^{91})]_2Mo_6O_{19}$. Reproduced with permission from ref. 29. Copyright 2014 Royal Society of Chemistry.

In all these structures, the Mo–O (D molecule, *e.g.* methanol, water, DMSO, *etc.*) bonds are significantly longer than the other Mo–O bonds to the *ONO* ligand, indicating that the neutral donor molecules are weakly bonded to the MoO_2 core. Therefore, this position holds the possibility of functioning as a substrate binding site.

I.2.3.2. ONS coordination

In 2004, Koo and coworkers reported two dioxomolybdenum(VI) complexes with *ONS* tridentate ligands based on substituted salicyldithiocarbazate backbones $[MoO_2L^{57}(OH_2)]$ and $[MoO_2L^{58}(DMSO)]$ (Scheme 1.15). Both were structurally characterized by X-ray diffraction.[30]

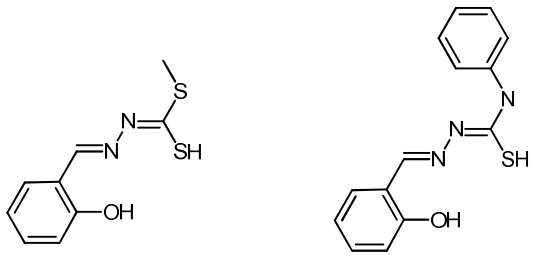

H_2L^{57} H_2L^{58}

Scheme 1.15

In 2009, Vrdoljak and coworkers reported a few dioxomolybdenum(VI) pyridoxal complexes $[MoO_2L]$ with thiosemicarbazonato ligands (L = $L^{59\text{-}61}$, see Scheme 1.16). Crystallization of the L^{59} complex from MeOH afforded a mononuclear solvent adduct which crystallized with an additional MeOH molecule of crystallization, $[MoO_2L^{59}(CH_3OH)]\cdot CH_3OH$, as confirmed by X-ray crystallography.[31]

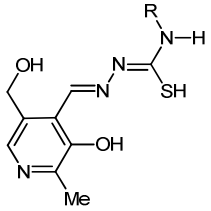

R = H, H_2L^{59}
= Me, H_2L^{60}
= Ph, H_2L^{61}

Scheme 1.16

In 2011, Ngan and coworkers reported three dioxomolybdenum complexes $[MoO_2L]$ based on substituted 5-chloro-salicylthiosemicarbazonato ligands (L = L^{62}-L^{64}, See Scheme 1.17) stabilized by one DMSO molecule as shown by X-ray cristallography.

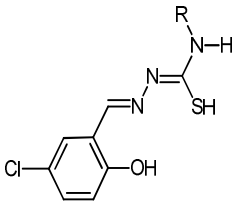

R = H, H_2L^{62}
= Et, H_2L^{63}
= Ph, H_2L^{64}

Scheme 1.17

Intermolecular hydrogen bonds are observed in two of the three cases, yielding networks. In both cases, one N-H bond of the NHR substituent acts as proton donor with a Mo=O moiety of an adjacent molecule as proton acceptor. In addition, when R= H, there is an additional N–H···N intermolecular hydrogen bonding implicating the NH_2 amino substituent as proton donor and an N atom of the adjacent molecule carbazone moiety as proton acceptor yielding a layered structure for R = H and a one-dimentional chain for R = Ph (see Figure 1.13).[32]

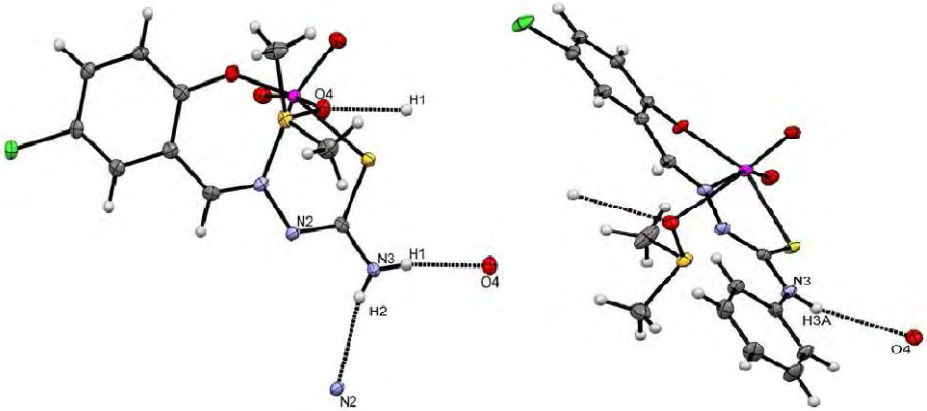

Figure 1.13. Details of the intermolecular H-bonding for the molecules. Left: $[MoO_2L^{62}(DMSO)]$ is linked into a layer by N3–H2···N2 and N3–H1···O4 H-bonds. Right: $[MoO_2L^{64}(DMSO)]$ is joined into a one-dimensional chain by N3–H3···O4 H-bonds. Reproduced with permission from ref. 32. Copyright 2011 Springer.

In 2007, Rao and coworkers synthesized the $[MoO_2L(EtOH)]$ complexes (L = $L^{65\text{-}66}$ being *ONS* ligands based on the dithiocarbazone skeleton in Scheme 1.18).[33]

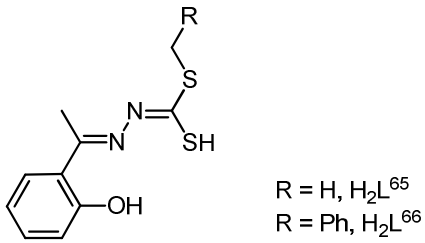

Scheme 1.18. Mo complexes with ligands L^{65-66}.

In 2014, El-Hendawy and coworkers reported new *cis*-dioxomolybdenum complex of the Schiff base derived from S-methyl dithiocarbazate and 2,3-dihydroxybenzaldehyde. The X-ray structure (Figure 1.14) of $[MoO_2L^{67}(EtOH)]$ complex shows distorted octahedral geometry around molybdenum, with *ONS* coordination of the ligand.8

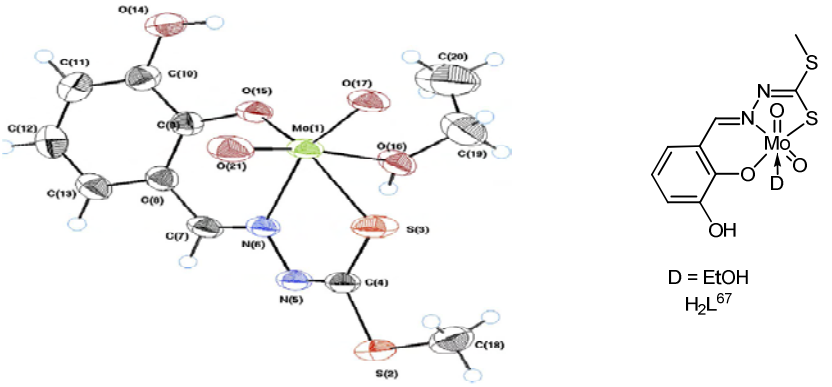

Figure 1.14. ORTEP diagram of the compound $[MoO_2L^{67}(EtOH)]$, with the ellipsoids drawn at the 50% probability level. Hydrogen atoms are shown as smaller spheres of arbitrary radii. Reproduced with permission from ref. 8. Copyright 2014 Elsevier.

In 2013, Boghaei *et al.* synthesized the molybdenum complex $[MoO_2L(CH_3CN)]$ with the *ONS* tridentate semithiocarbazonato ligand L^{68} (Figure 1.15). The complex molecule structure is stabilized by a MeCN molecule.[34]

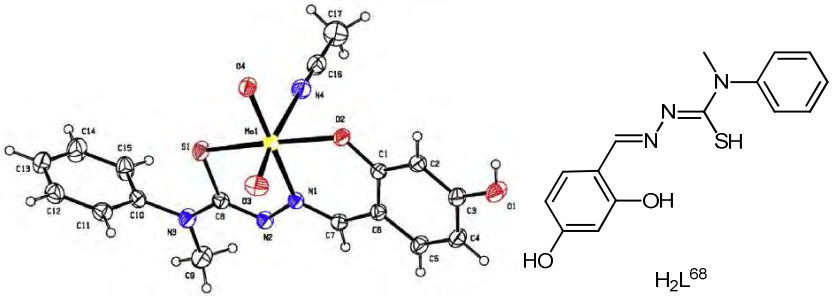

Figure 1.15.The labeled diagram of asymmetric unit of $[MoO_2L^{68}(CH_3CN)]$. Thermal ellipsoids are at 30% probability level. Reproduced with permission from ref. 34. Copyright 2012 Elsevier.

I.2.4. Complexation with donors and coordination polymers

In 2008, Agustin and coworkers reported the X-ray structure of complex $[MoO_2(SAE)(SAEH_2)]$ (Scheme 1.19). In this complex, the additional $SAEH_2$ molecule acts as D ligand to complete the octahedral coordination environment and is bonded to the Mo atom through the anionic phenolato function in the zwitterionic form of the molecule, the OH proton having migrated to the Schiff base imino function. The asymmetric unit contains three $[MoO_2(SAE)(SAEH_2)]$ molecules linked by O-H···O hydrogen bonds which involve the aliphatic OH function of the zwitterionic LH_2 ligand of one molecule as proton donor and an *oxo* O atom attached to the Mo atom of another molecule as proton acceptor. These trimeric units are further linked through O-H···O hydrogen bonds of the same type to form a one-dimensional chain (Figure 1. 16).[35]

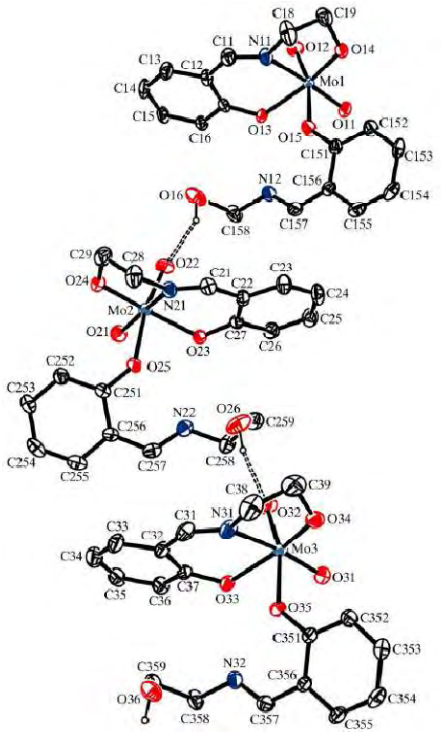

Figure 1. 16.A view of the asymmetric unit of compound $[MoO_2(SAE)(SAEH_2)]$. Reproduced with permission from ref. 35. Copyright 2008 IUCr.

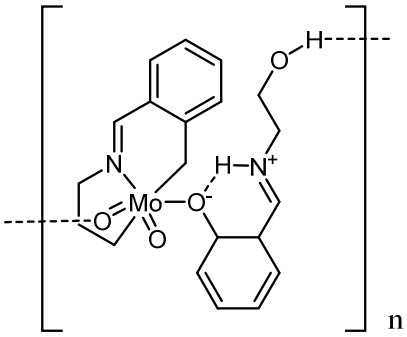

$[MoO_2(SAE)(SAEH_2)]$

Scheme 1.19

In 2009, same authors reported the structure of $[MoO_2(SAP)(EtOH)]$ (Figure 1.17) and associated theoretical calculations to confirm the energy needed to turn a mononuclear hexacoordinated $[MoO_2L(EtOH)]$ complex or the dinuclear $[MoO_2L]_2$ into a pentacoordinate $[MoO_2L]$ complex with a free coordination site on the molybdenum atom.[36]

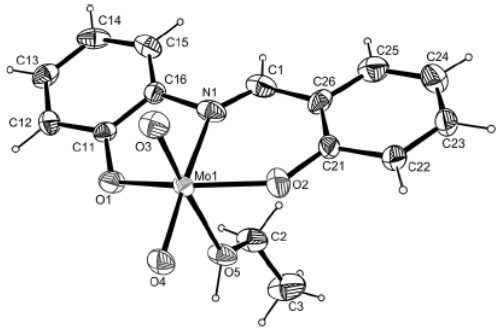

Figure 1.17. Ortep view of [MoO_2(SAP)(EtOH)]. Reproduced with permission from ref. 36. Copyright 2009 Wiley-VCH.

In 2015, Maurya and co-workers synthesised three new *ONO* molybdenum complexes [$MoO_2L^{69\text{-}71}$(MeOH)] (Scheme 1.20).[37] The phenyl groups of the ligands on adjacent complexes interact by π-π interactions (see Figure 1.18). The steric requirements, derived from the coordination sphere around Mo, prevent π-π interactions between the phenol rings.

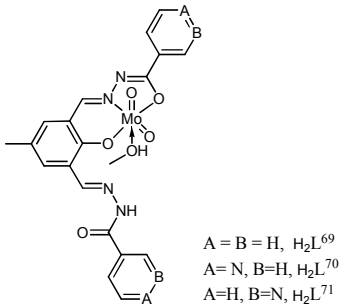

Scheme 1.20

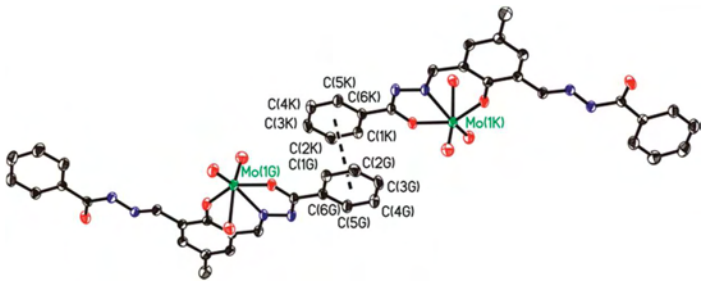

Figure 1.18. Intermolecular π-π interactions in [MoO_2L^{69}]. Dashed lines link the centres of the π clouds involved in each interaction. Reproduced with permission from ref. 37. Copyright with permission from the Royal Society of Chemistry.

In 2014, Dinda and co-workers reported monomeric [$MoO_2L^{72\text{-}73}$(EtOH)], [$MoO_2L^{74\text{-}57}$(MeOH)] or polymeric [$MoO_2L^{72\text{-}75}$]$_n$ depending on the substitution of the *ONO* hydrazone tridentate ligands. X-ray crystallography (Figure 1.19) demonstrated the tridentate behaviour of the ligands and the one dimensional chain arrangement of the Mo complexes via linear Mo=O···Mo bridges.[38]

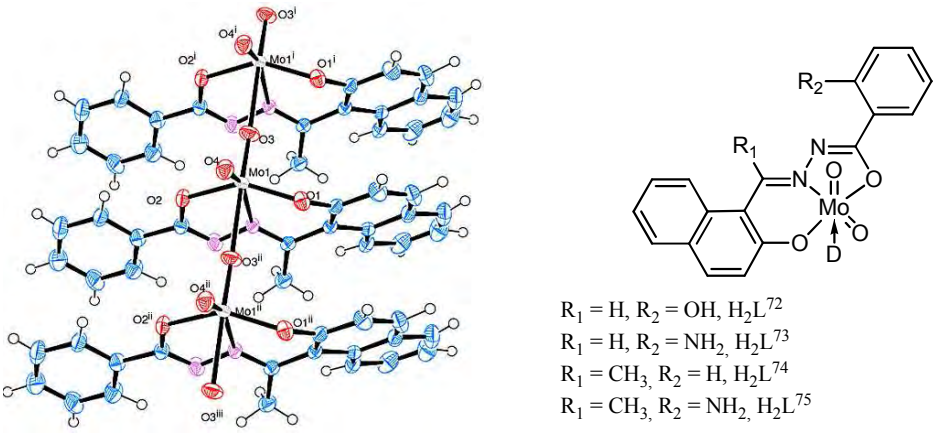

Figure 1.19. A view of the one-dimensional polymeric structure of $[MoO_2L^{74}]_n$. Thermal ellipsoids have been drawn at 50% probability. Reproduced with permission from ref. 38. Copyright 2014 Elsevier Science.

In 2013, Cindrić and coworkers reported mononuclear and polynuclear dioxomolybdenum(VI) complexes with the tridentate *ONO* Schiff base ligand N-4-methoxysalicylidene-2-amino-3-hydroxy-pyridine (H_2L^{76}) in different solvents (Scheme 1.21).[39] The labile sixth coordination site in the $[MoO_2L^{76}(ROH)]$ complexes is responsible for the formation of the polynuclear $[MoO_2L^{76}]_n$ complex upon removal of the ROH ligand or the $\{[MoO_2L^{76}]_2D'\}$ dimer when D' was abidentate ligand. The studies showed that the central molybdenum atom more easily coordinates aromatic *N*-donor than *O*-donor molecules.[40]

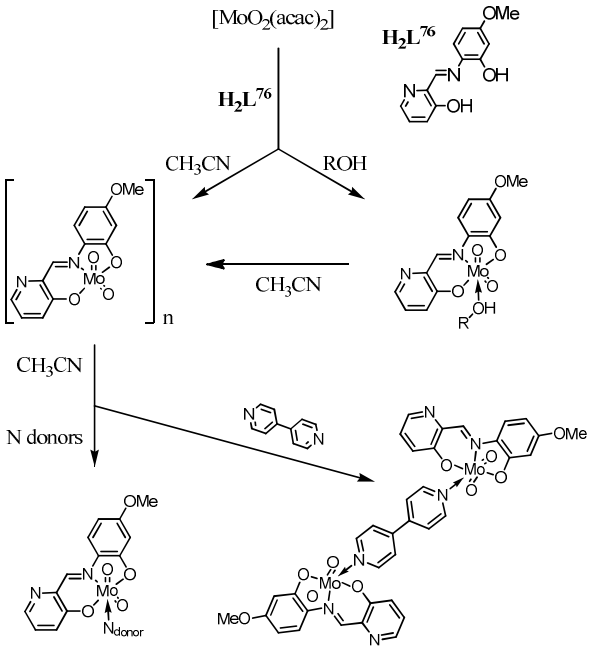

Scheme 1.21. Synthesis of mononuclear and polynuclear $[MoO_2L^{76}]$ complexes

In 2015, Ebrahimipour and coworkers reported the synthesis of monomeric $[MoO_2L^{77}(D)]$ complexes (D = EtOH, py). H-bonds and π-π stacking interaction between dimeric units were observed (see Figure 1.20).[41]

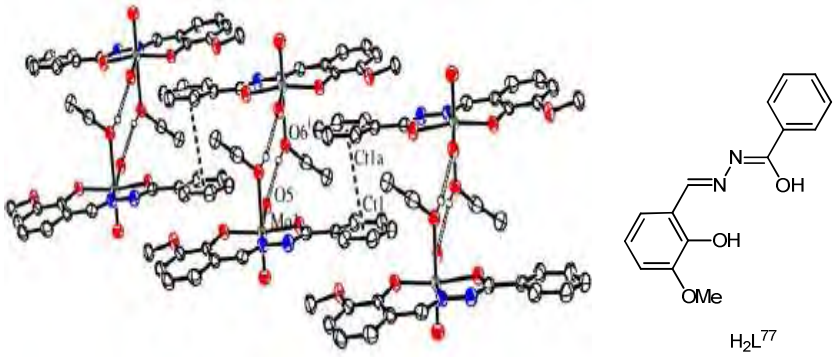

Figure 1.20. H-bonds and π-π stacking interaction between dimeric units in $[MoO_2L^{77}(EtOH)]$. Reproduced with permission from ref. 41. Copyright 2014 Elsevier Science.

I.3. Applications

I.3.1. Biological tests

In 2014 and 2015, Guan and coworkers reported the binding properties of the $[MoO_2L(D)]$ complexes shown in Scheme 1.22 (L = L^{78}-L^{89}, D = MeOH, EtOH, H_2O) with calf thymus DNA. Gel electrophoresis shows that the complexes cleave the pBR322 plasmid DNA.

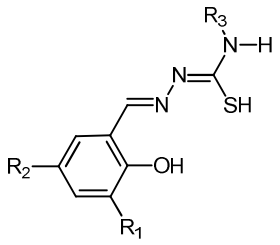

	R_1	R_2	R_3
H_2L^{78}	H	Cl	CH_3
H_2L^{79}	H	CH_3	C_2H_5
H_2L^{80}	$C(CH_3)_3$	H	C_2H_5
H_2L^{81}	OH	H	CH_3
H_2L^{82}	H	Cl	C_2H_5
H_2L^{83}	H	OMe	CH_3
H_2L^{84}	H	CH_3	CH_3
H_2L^{85}	H	$C(CH_3)_3$	CH_3
H_2L^{86}	H	Br	C_2H_5
H_2L^{87}	OCH_3	$CH_2CH{=}CH_2$	C_2H_5
H_2L^{88}	$C(CH_3)_3$	H	CH_3
H_2L^{89}	CH_3	H	C_2H_5

Scheme 1.22

All complexes exhibited cytotoxic properties against human colorectal cell lines showing strong antiproliferative activities with IC_{50} values of 3.2-6.9 µM, smaller than the standard reference drug 5-fluorouracil (IC_{50} = 7.3 μm). It was suggested that the intercalated complex-H_2O_2 mixtures react directly with the DNA strand to cleave it. These studies showed that molybdenum(VI) complexes could be potentially useful in chemotherapy.[42]

I.3.2. Catalytic applications (except olefin epoxidation)

I.3.2.1. Oxidation of sulphides

In 2009, Sheikhshoaie and Rezaeifard reported the catalytic activity of the $[MoO_2L^{34}(CH_3OH)]$ complex (see Figure 1.6) for the oxidation of sulfides using urea hydrogen peroxide (UHP) as oxidant, affording sulfoxides and sulfones (Scheme 1.23).[20] Using a catalytic charge of 5 mol% *vs*. substrate in ethanol as solvent, the substrate conversions were between 75% and 100% for different aliphatic and aromatic substrates (see Table 1.1). An UHP/sulfide ratio of 1 gave optimal yields and selectivities (> 93%) in favor of the sulfoxide intermediate while a ratio of 5 promoted sulfone formation in excellent yields and selectivities (97% for all in less than 30 min).

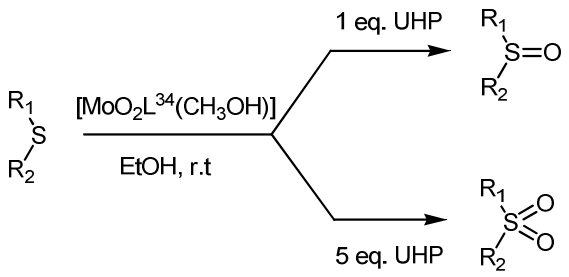

Scheme 1.23. The oxidation of sulfides using urea hydrogen peroxide.

Table 1.1. Oxidation of various sulfides by UHP catalyzed by $[MoO_2L^{34}(CH_3OH)]$ in ethanol.[a]

Entry	Sulfide		UHP/sulfide	Conversion (%)	Selectivity (%)	
	R_1	R_2			sulfoxide	sulfone
1	n-C_4H_9	n-C_4H_9	1	100	100	0
2	n-C_4H_9	n-C_4H_9	5	100	0	100
3	allyl	allyl	1	100	100	0
4	C_6H_5	CH_3	1	92	100	0
5	C_6H_5	CH_3	5	100	2	98
6	C_6H_5	n-C_3H_7	1	90	97	3
7	C_6H_5	i-C_3H_7	1	87	>98	<2
8	C_6H_5	Vinyl	1	93	>99	<1
9	C_6H_5	C_6H_5	1	75	93	7
10	C_6H_5	C_6H_5	5	95	<3	>97
11	C_6H_5	benzyl	1	95	>98	<2
12	C_6H_5	benzyl	1	93	100	0

[a]The reactions were run in air at room temperature and with 5 mol% of $[MoO_2L^{34}(CH_3OH)]$.

[b]The conversion and yield were measured based on the starting sulfides after 10 min for entries 1 and 3, and 30 min for the others.

In 2015, Sah and coworker reported the catalyic oxidation of thioanisole (Scheme 1.24) with the molybdenum(VI) complexes $[MoO_2L^{28\text{-}31}(H_2O)]$ (see Scheme 1.8). A high yield (75-89%) and selective (100%) oxidation to methylphenylsulphoxide at room temperature was achieved in a short time using an equimolar thioanisole/UHP ratio in ethanol with 5% catalyst loading. Using a longer reaction time or excess of UHP led to the formation of the corresponding sulphone, and thioanisole/UHP ratio of 5 gave 94% yield of sulfone without any residual sulphoxide.[18]

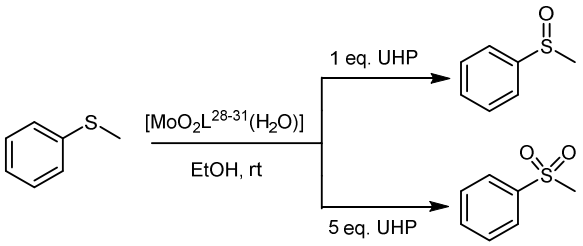

Scheme 1.24. The catalyic oxidation of thioanisole with the molybdenum(VI) complexes.

The $[MoO_2L^{22\text{-}27}(MeOH)]$ complexes (Figure 1.4) were used as catalysts in chlorinated solvents for the enantioselective sulfoxidation of thioanisoles with H_2O_2 as oxidant at 0°C (see Scheme 1.25).[17] With a catalyst/sulfide/H_2O_2 ratio of 5:100:100, the yields were in the 74-90% range after 2 days (see Table 1.2). High selectivities and good to moderate *e.e.*s were found. An ESI-MS study of the catalytic reaction mixture indicatedthe formation of the oxoperoxo complex $[MoO(O_2)L22^{-27}]$. The R^2 substituent at the β position of the amino alcohol influences the enantioselectivity.

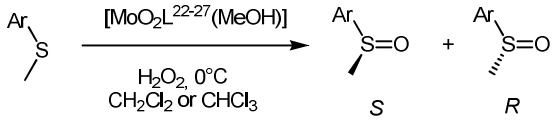

Ar = C_6H_5, p-Me-C_6H_4, p-Cl-C_6H_4, p-MeO-C_6H_4, p-Br-C_6H_4, p-NO_2-C_6H_4

Scheme 1.25. Enantioselective sulfoxidation of thioanisoles.

Table 1.2. Oxidation of thioanisole catalyzed by the $[MoO_2L(MeOH)]$ complexes.[a]

Ligand	Yield (%)	*ee*(%)
L[22]	83	14.6 (*S*)
L[23]	74	33.5 (*S*)
L[24]	82	6.2 (*S*)
L[25]	90	39.6 (*S*)
L[26]	77	5.5 (*S*)
L[27]	78	2.0 (*S*)

[a] Reaction condition: Mo complex (5 mol%), sulphide (1 mmol) and H_2O_2 (1 mmol) in CH_2Cl_2 at 0 °C for 2 days.

A mechanism for the sulfoxidation catalytic cycle was proposed (Scheme 1.26), in which the oxotransfer takes place from the oxoperoxo complex either by direct oxygen atom transfer or by coordination of the sulfide to the metal followed by oxygen transfer.

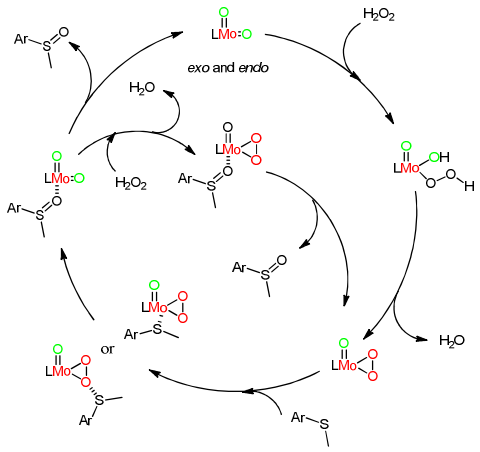

Scheme 1.26. Proposed mechanism of the sulfoxidation catalytic cycle.

In 2013, Xue and coworkers reported the oxidation of sulfides using 1.25 equivalents of H_2O_2 as oxidant with 1 mol% of the catalysts [MoO_2L^{32-33}(D)] (Scheme 1.9) at 10 °C in a CH_2Cl_2/CH_3OH solvent mixture (6:4) (Scheme 1.27). With both complexes, conversions to sulfoxide around 77-79% were observed after 1h, being complete after 2 hours.[19]

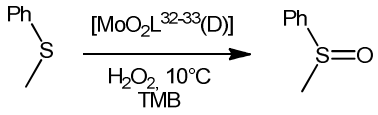

Scheme 1.27. Oxidation of sulfides using H_2O_2 with [MoO_2L^{32-33}(D)]

I.3.2.2. Oxidation of benzoin

Dinda and co-workers tested the catalytic activity of the monomeric [MoO_2L^{72-75}(MeOH)] or polymeric [MoO_2L^{72-75}] complexes (Figure 1.19) in the oxidation of benzoin (see Scheme 1.28) using 3 equivalents aqueous H_2O_2 as an oxidant with 0.02% eq. catalyst in refluxing methanol.[38]

At least four reaction products, *i.e.* benzoic acid, benzaldehyde-dimethylacetal, methyl benzoate and benzil were obtained with 95-99% conversion. Oxidative bromination of salicylaldehyde, a functional mimic of haloperoxidases, in aqueous H_2O_2/KBr in presence of $HClO_4$ was also carried out at room temperature with 0.02% catalyst loading, showing 95-99% conversion of salicylaldehyde to brominated products with high turnover frequencies (1415-1673 h^{-1}).

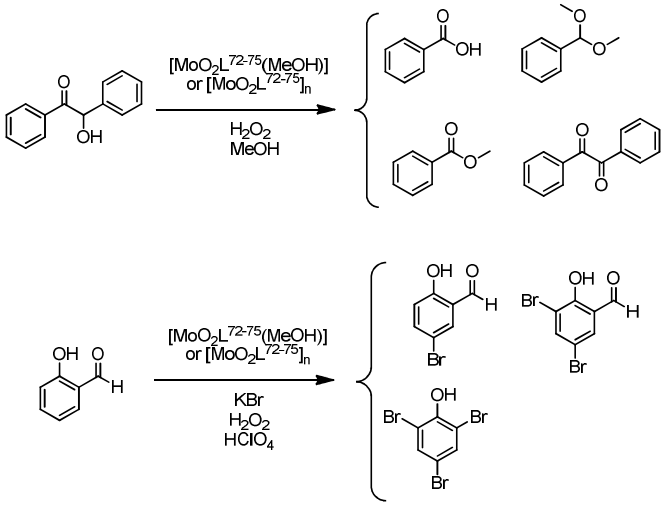

Scheme 1.28. Catalytic action of the [MoO_2L^{72-75}(MeOH)] and [MoO_2L^{72-75}]$_n$ complexes in the oxidation of benzoin and in the oxidative bromination of salicylaldehyde.

I.3.2.3. Oxidative halogenation of olefins

In 2014, Hartung and coworkers reported the catalytic activity of $[MoO_2(SAP)(MeOH)]$ for oxidative chlorination (Scheme 1.29). The reaction was carried out at 40°C in a solution of dry dimethylcarbonate (Me_2CO_3) with 1.5 equivalents of pyridinium hydrochloride (pyHCl) and 1.5 eq. of TBHP (as toluene solution) as oxidant, and 5 mol % of molybdenum *vs.* substrate. After 24h, the reaction yielded 45% of a substituted tetrahydrofuran (*cis*/*trans*-stereoisomers in 45/55 ratio) and 18% of the product of olefin dichlorination.[43]

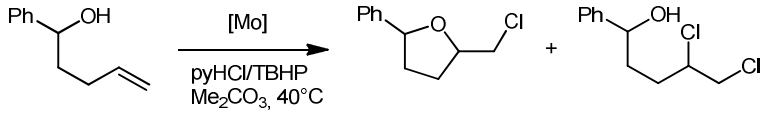

Scheme 1.29. Catalytic of $[MoO_2(SAP)(MeOH)]$ for oxidative chlorination.

I.3.2.4. Oxidation of alcohols

El-Hendawy and coworkers reported the catalytic oxidation of alcohols (Scheme 1.30) under organic solvent free conditions using aqueous H_2O_2 or TBHP as oxidants using complex $[MoO_2L^{67}EtOH)]$ (Figure 1.14) as catalyst. The alcohol (2.5 mmol), the complex (0.01 mmol) and 70% aqueous TBHP (5 mmol) were mixed and stirred at 70°C for 3 h, yielding the corresponding aldehyde or ketone (turnover number between15 and 40, see Table 1.3). When 30% H_2O_2 (5 mmol) was used, aldehydes were produced from the primary alcohols whereas the oxidation of cyclohexanol to cyclohexanone was not effective.8

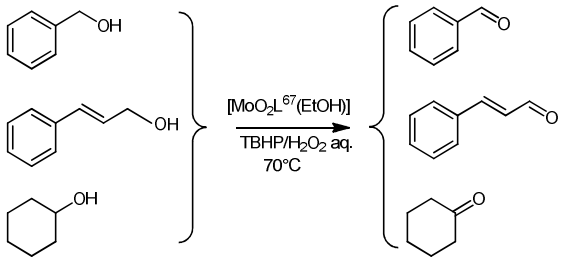

Scheme 1.30. Oxidation of alcohols using H_2O_2 or TBHP with complex $[MoO_2L^{67}(EtOH)]$.

Table 1.3. Oxidation of alcohols by TBHP or H_2O_2 catalyzed by $[MoO_2L^{67}(EtOH)]$ under solvent-free conditions.

Substrate	Product[a]	Time/h	t-BuOOH	H_2O_2
			TON	
Benzyl alcohol	A	3	40	10
Cinnamyl alcohol	A	3	15	35
Cyclohexanol	K	4	20	0

A = corresponding aldehyde, K = corresponding ketone.

Maurya and co-workers used [MoO_2L^{69-71}MeOH)] complexes (Scheme 1.20) as catalysts for the oxidation of secondary alcohols (1-phenyl ethanol, 2-propanol and 2-butanol) using acetonitrile as solvent and 30% H_2O_2 as oxidant with a substrate/H_2O_2/catalyst ratio of 100/300/0.7 at 80°C (Scheme 1.31). The corresponding ketones were obtained in 90-95% yields after 20 h. For [MoO_2L^{69}(MeOH)], 91% of 1-phenyl ethanol was converted into the ketone product with a TOF of 66 h^{-1}. A microwave (MW) assisted method was also used, giving the same conversion in a shorter time. In terms of mechanism, the authors assume that the Mo^{VI} complexes instantly react with H_2O_2 in methanol generating the peroxo species [$Mo^{VI}O(O_2)(L^{69-71})$] in solution, considered to be responsible for the oxygen transfer to the substrates during catalytic oxidation.[37]

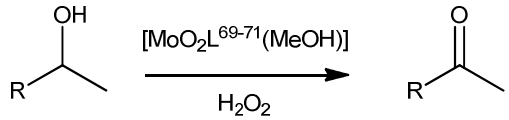

R= Ph, Et, Me

Scheme 1.31. [MoO_2L^{69-71}(MeOH)] catalyzed oxidation of secondary alcohols

I.3.2.5. Synthesis of bis (indolyl)methanes

In 2015, Ebrahimipour and coworkers reported the catalysed synthesis of bis(indolyl)methane derivatives from indole and aldehydes in molten Bu_4NBr, using monomeric [MoO_2L^{77}(D)] (Figure 1.20) complexes as catalysts (Scheme 1.32). The reaction run in the presence of 10 mol% catalyst afforded the products with 83-97% yield after 12-25 min at 110°C.[41]

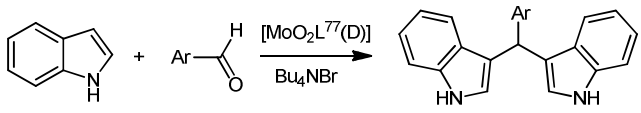

Ar = C_6H_5, 4-X-C_6H_4 (X= Cl, NO_2, MeO, Me)
2-Cl-C_6H_4, 3-NO_2-C_6H_4, 2-4-$Cl_2C_6H_3$

Scheme 1.32. Synthesis of bis(indolyl)methane derivatives in molten Bu_4NBr.

I.3.3. Olefin epoxidation

In 2003, Sobczak and coworkers reported the catalytic activity of [MoO_2(SAP)(EtOH)] complex in the epoxidation of oleic acid using TBHP or cumene hydroperoxide (CHP) as oxidants. The reaction shows 86.8% selectivity to 9,10-epoxystearic acid at 67% conversion. Through kinetic studies, the authors proposed a mechanism involving the intermediate complex [MoO_2(SAP)(t-BuOOH)] where the coordinated oxidant molecule is activated for the oxygen transfer to the olefinic bond (Scheme 1.33).[44]

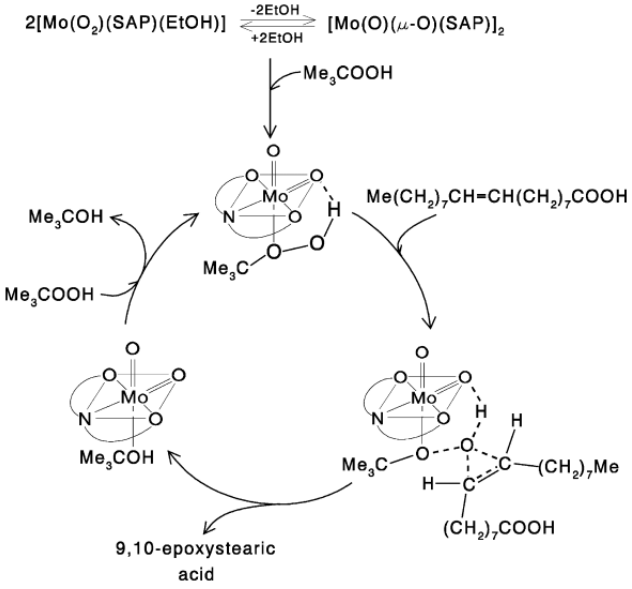

Scheme 1.33. Reaction mechanism of oleic acid epoxidation with *t*-BuOOH catalysed by MoO_2(SAP)(EtOH)].

In 2010, Bagherzadeh and coworkers tested several *ONO* and *ONS* complexes [MoO_2L(EtOH)] and [MoO_2(SAP)(D)] (L= SAE, SATP, $L^{1,6,8}$ and L^{91}, D = EtOH, Im or Py-N-O) for thecatalytic olefin epoxidation with TBHP (80% in water) as oxidant in dichloroethane (DCE) at 80°C (Scheme 1.34) resulting in very high epoxide yields (more than 94% for cyclooctene oxide).

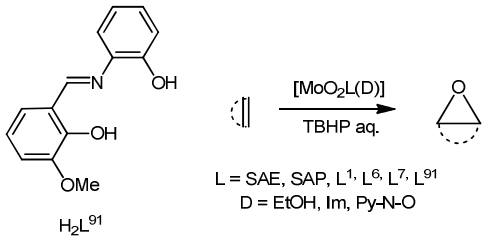

Scheme 1.34. Catalytic olefins epoxidation with TBHP as oxidant.

A selection of the results is shown in Table 1.4. All complexes showed very good conversion (92-99%) and complete selectivity in the cases of cyclooctene and 1-octene after 2 hours, the epoxide yield increasing with the nucleophilicity of the olefin. Under solvent-less conditions and with aqueous TBHP, the conversions of the olefins are similar (ca. 95% at 2 h).[45]

Table 1.4. Epoxidation of different olefins with $[MoO_2(SAP)(EtOH)]$ as catalyst.[a]

Ligand	Substrate	Conversion (%)		Selectivity (%)[c]
		30 min	60 min	
L^1	Cyclooctene	-	98[b]	-
L^6	Cyclooctene	-	94[b]	-
L^8	Cyclooctene	-	99[b]	-
L^{91}	Cyclooctene	-	98 [b]	-
SATP	Cyclooctene	-	98 [b]	-
SAE	Cyclooctene	-	95 [b]	-
SAP	Cyclooctene	95	99	100
SAP	Cyclohexene	79	92	100
SAP	1-Methylcyclohexene	99	99	100
SAP	1-heptene	77	86	100
SAP	1-Octene	45	63	100
SAP	2-Octene	80	91	100
SAP	styrene	42	46	65
SAP	α-Methylstyrene	37	44	63
SAP	4-Methylstyrene	24	26	58
SAP	4-Methoxystyrene	11	20	60
SAP	Indene	29	29	70
SAP	2-cyclohexene-1-one	-	15	74
SAP	2-cyclohexene-1-ol	-	84	95
SAP	α-terpineol	-	43	58

[a] Conditions: The molar ratio for using catalyst: substrate: oxidant are 1:800:800. The reactionswere run at 80°C.[b]yield. [c]Selectivity to epoxide at 60 min.Reproduced from Ref. 45.

In 2010, Rezaeifard and coworkers tested $[MoO_2L^{34,92-94}(MeOH)]$ complexes (with *ONO* tridentate Schiff base ligands based on substituted *SAE*) (Scheme 1.35) for the catalytic epoxidation of various olefins. The reactions were performed at 80 °C in DCE using TBHP as oxidant with olefin/TBHP/catalyst molar ratio of 100:200:1. The conversion after 45 minutes was between 66-100% with a 94 to 100% epoxide selectivity. Electron-poor and bulky groups on the salicylidene ring of ligand promote the effectiveness of the catalysts.[46]

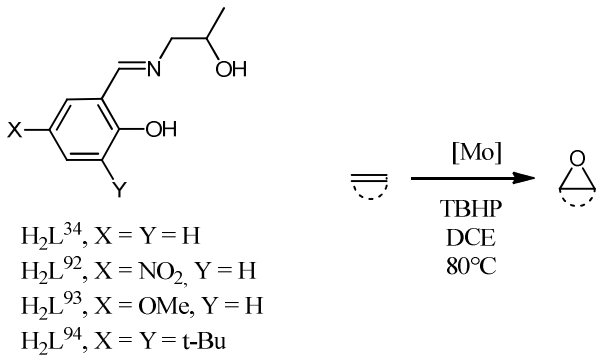

H_2L^{34}, X = Y = H
H_2L^{92}, X = NO_2, Y = H
H_2L^{93}, X = OMe, Y = H
H_2L^{94}, X = Y = t-Bu

Scheme 1.35. Epoxidation of various olefins catalyzed by $[MoO_2(L^{34,92-94})(MeOH)]$.

In 2012, Rezaeifard et *al*. tested $[MoO_2L(CH_3OH)]$ complexes (L = SAMP, L[39-42]) (Figure 1.9) in the epoxidation of different olefins and in thioether oxidation with lower catalyst loading, *i.e.* olefin/TBHP/catalyst molar ratio of 1000:1500:1 (Scheme 1.36). Olefin conversions between 38% to 100% after 25 minutes and selectivities up to 90% were reported. The catalytic activity is influenced by nature of the ligand (rigidity, steric hindrance and electron properties), as investigated by Kühn.[47] The oxidation of thioethers using H_2O_2 gave good/excellent conversions (65-100%) and selectivities higher than 97%. The reactions were conducted in ethanol with a sulfide/H_2O_2/$[MoO_2L(CH_3OH)]$ molar ratio of 100:150:1. For example, the cyclooctene epoxidation by TBHP and the thioanisole oxidation by H_2O_2 gave TOFs of 8800 h^{-1} and 2000 h^{-1} respectively, and TONs after 24h of 10000 and 9000.[24]

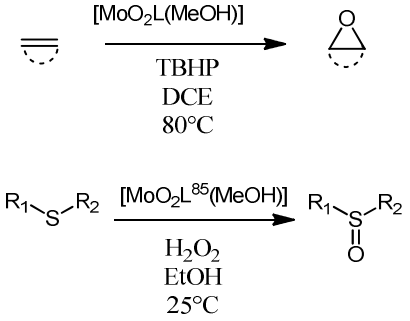

Scheme 1.36. Olefins Epoxidation and thioethers sulfoxidation by $[MoO_2L(CH_3OH)]$ (L = SAMP, L[39-42]).

In 2013, Poli, Agustin and coworkers have shown that $[MoO_2(SAP)]_2$ is an effective pre-catalyst in an organic solvent-free process for cyclooctene epoxidation using aqueous TBHP.[48] In comparison with previous related studies using organic solvents, this system shows high activity and selectivity towards the epoxidation product with an environmentally friendlier process. The epoxidation was carried out at 80°C with Mo/TBHP/cyclooctene = 1:200:100, yielding a cyclooctene conversion of 79% after 5.5 h and 98% epoxide selectivity. Computational investigations on the catalytic cycle using this metal complex validated the mechanistic proposition of Sobczak (Scheme 1.33), which exhibited a lower energy span relative to other mechanisms, including that proposed in ref. 46.

In 2007, Rao and coworkers tested the $[MoO_2L^{65-66}(EtOH)]$ (Figure 1.18) complexes at 60°C during 6 hours using O_2 (1 atm) as oxidant in DMF for the catalytic oxidation of different olefins, obtaining conversion between 86% and 98% (see Scheme 1.37). 1-Hexene was exclusively oxidized to 1-hexanal, while styrene gave styrene epoxide and phenyl acetaldehyde, and cyclohexene gave cyclohexene epoxide and 2-cyclohexen-1-ol. Kinetics study suggested a two-stage first order reaction involving the formation of an intermediate in a first fast step prior to the rate-limiting formation of the final oxidation products.[33]

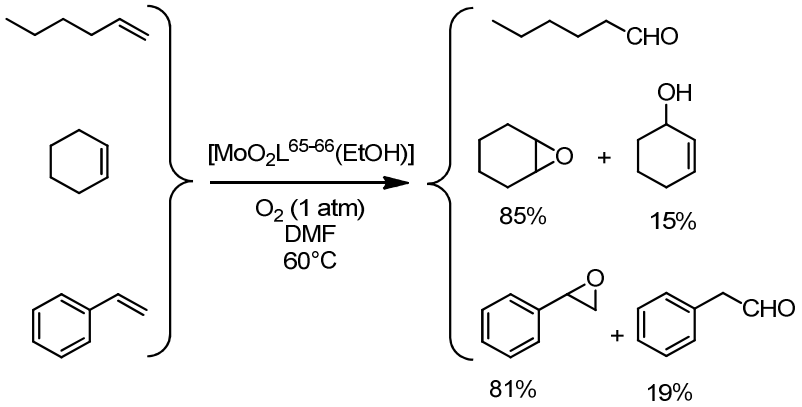

Scheme 1.37. Epoxidation of olefins by O_2 catalyzed by Mo complexes with ligands L^{65-66}.

In 2014, Agustin, Vrdoljak and coworkers[6] reported the organic solvent free cyclooctene epoxidation using dioxomolybdenum and tungsten complexes of type $[MoO_2L]$ with ligands L^{95-97} (Scheme 1.38) and aqueous TBHP as oxidant at 80°C with a [Mo]/cyclooctene/TBHP molar ratio of 0.25/100/200. After 5 h, good conversions (86-89%), moderate selectivities (46-53%) and high TOF_{20min} (344-469/h) were observed.

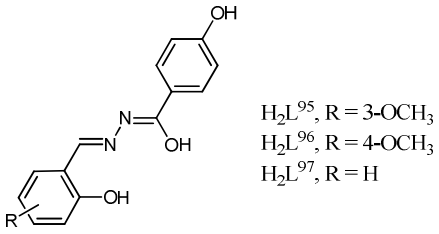

Scheme 1.38.

Agustin et *al*. reported a series of molybdenum(VI) complexes [MoO_2L^{54-56}] used as (pre)catalysts in olefin epoxidation under organic solvent-free conditions at 80°C, with a catalyst/cyclooctene/TBHP molar ratio of 0.05/100/200 for all compounds. The conversions for the different catalysts are in the 23%-72% range, with 53%-87% epoxide selectivity.[29]

In 2010, Bibal, Poli and coworkers used two anionic Schiff base molybdenum(VI) complexes $[MoO_2L^{36-37}]^-$ (Scheme 1.10)[22] as catalysts for the cyclooctene epoxidation in ionic liquid media with TBHP as oxidant and a catalyst/substrate/oxidant ratio of 1:100:200 at 55°C. The epoxide yield varied from 5%-62% depending on conditions. The ionic liquid phase containing the immobilized catalyst could be reused for three runs with a comparable catalytic activity when the ionic liquid was [BMIM][NTf_2].

Vrdoljak, Agustin and coworkers used [MoO_2L] complexes with the pyridoxalthiosemicarbazonato ligands L^{59-61} (Scheme 1.39) as catalysts in the epoxidation of cyclooctene by aqueous TBHP in absence of organic solvent at 80°C. For the first time, it was shown that Mo^{VI} compounds with a pyridoxal moiety are efficient epoxidation (pre)catalysts at a very low catalyst loading of 0.05% *vs*. substrate. [MoO_2L^{59}(MeOH)] was observed to be the best (pre)catalyst (highest TOF (3360 h^{-1}) and TON values). The comparison between the mononuclear MeOH adducts and the polynuclear material and the effect of the MeOH/Mo ratio for the experiments with added MeOH have revealed a new facet of the solvent effect on the catalytic activity of this family of compounds.[49]

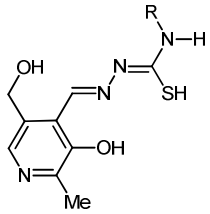

R = H, H_2L^{59}
= Me, H_2L^{60}
= Ph, H_2L^{61}

Scheme 1.39. Ligands used for the organic solvent free cyclooctene epoxidation by TBHP.

In 2013, Boghaei *et al.* tested [MoO_2L^{68}(CH_3CN)] (Figure 1.15) as catalyst for the epoxidation of various olefins at 80°C using TBHP as an oxidant (see Scheme 1.40), with a [Mo]/olefin/TBHP molar ratio of 1:5000:5000. Good to excellent conversions (44-98%) were observed after 1 h. In the case of styrene, several products were obtained, but styrene epoxide was major product.[34]

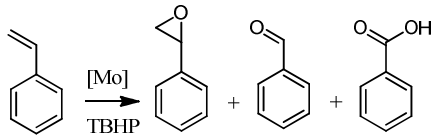

Scheme 1.40. Styrene epoxidation byTBHP catalyzed by complex $[MoO_2L^{68}(CH_3CN)]$.

In 2014, Umbarkar, Michon, Agbossou-Niedercorn and coworkers tested two $[MoO_2L(MeOH)]$ complexes (L = SAP or L^{38}) (Scheme 1.11) as catalysts for allylic alcohol epoxidation (Scheme 1.41) using 0.5-2 equivalents of oxidant per substrate (H_2O_2 35 wt.% in water or TBHP 5.5 M in decane). The reaction was tested at different temperatures and different catalyst/substrate molar ratio between 0.2% and 2.5%. The presence of an electron rich moiety on the substrate allowed selective reactions. Cinnamyl alcohol was selectively oxidized into the corresponding aldehyde. The chiral complex proved efficiency in terms of activity but was not adapted for asymmetric epoxidation.[23]

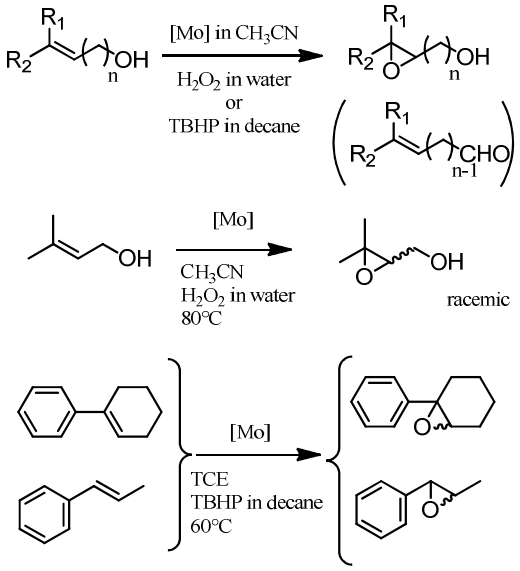

Scheme 1.41. Allylic alcohol epoxidation with $[MoO_2(L)(MeOH)]$ (L = SAP or L^{38}).

In 2014, Bagherzadeh and co-workers tested the molybdenum complex $[MoO_2L^{49}(EtOH)]$ (Scheme 1.10) as a catalyst in the epoxidation of olefins with aqueous TBHP in DCE, with a substrate/TBHP/[Mo] molar ratio of 100/100-200/2. In less than 45 minutes at 80°C, the conversion with different olefins was from 66 to 99%, with complete selectivity except for styrene (60%). Room temperature oxidation of sulphides with sulphide/UHP/[Mo] ratio of 40/45/1, in a 1:1 CH_2Cl_2/MeOH solvent mixture yielded the corresponding oxides.[27]

I.4. Grafted molybdenum complexes

I.4.1. Polystyrene supports

In 2006, Maurya and coworkers reported the heterogeneized complex complex PS-[MoO_2L^{98}(DMF)], which is a heterogenized model of the SAP system, obtained from the PS-anchored ligand L^{98} (Scheme 1.42).[50] The polymer-anchored ligand PS-H_2L^{98} was prepared from H_2L^{98} and chloromethylated polystyrene in DMF at 90°C for 15 h. The separated PS-H_2L^{98} was swollen in DMF and reacted with [$MoO_2(acac)_2$] at 90°C for 10 h to yield the polymer-anchored complex. This complex and the corresponding homogeneous [MoO_2(SAP)(MeOH)] were applied to the oxidation of styrene, ethylbenzene and phenol at 80°C using aqueous 30% H_2O_2 as oxidantin CH_3CN. Three cycles without significant loss of catalytic activity showed that the catalyst is recyclable.

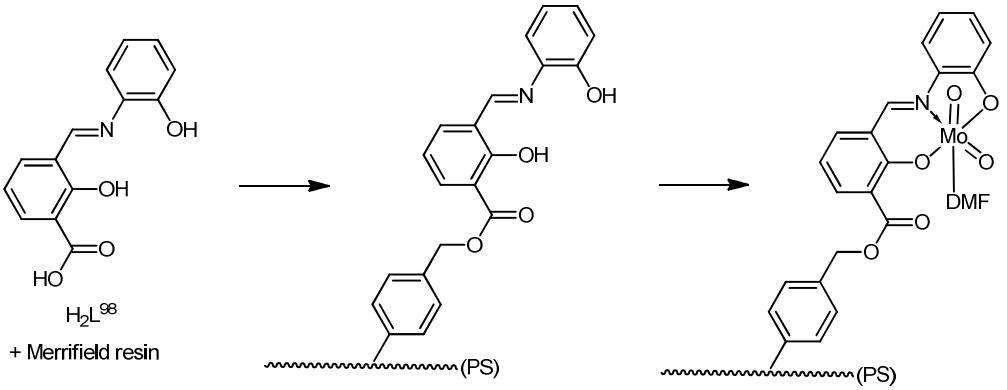

Scheme 1.42. Preparation of the PS-supported *SAP*-type catalyst.

In 2014, Maurya and coworkers reported the PS-grafted *ONO* Schiff base molybdenum complex shown in Scheme 1.43. The [MoO_2L^{99}(MeOH)] complex was reacted with a suspension of chloromethylated polystyrene in DMF followed by addition of triethylamine in ethylacetate at 80°C to obtain the PS-grafted molybdenum complex. Both the PS-[MoO_2L^{99}(MeOH)] and the molecular analogous system [MoO_2L^{99}(MeOH)] were used for the oxidative bromination of styrene and *trans*-stilbene by aqueous H_2O_2 in CH_2Cl_2. Although the non grafted complex gave similar activities, the recyclability and easy separation of the polymer-grafted complex is a clear advantage.[51]

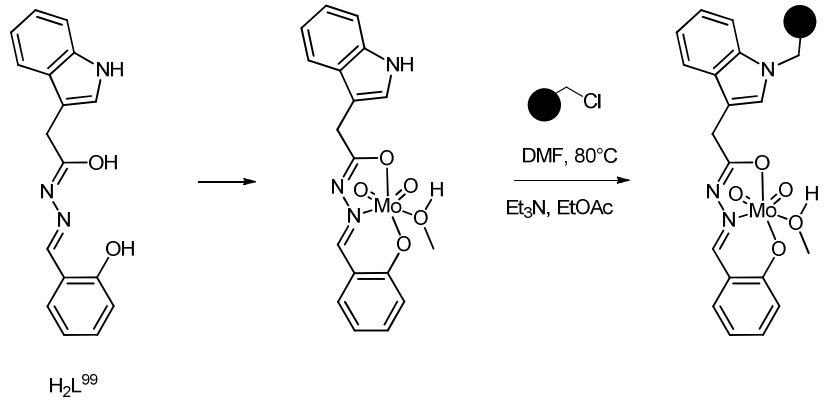

H_2L^{99}

Scheme 1.43. Synthesis of a PS-grafted complex with the Schiff base L^{99}. The black circle represents the backbone of the chloromethylated polystyrene.

I.4.2. Hybrid inorganic-organic support

In 2010, Li *et al.* reported a series of tridentate Schiff base molybdenum(VI) complexes immobilized on chloromethyl-ZPS-PVPA [ZPS= zirconium poly(styrene-phenylvinylphosphonate)-phosphate] through covalent bonds (see Scheme 1.44). ZCMPS-PVPA swollen in toluene reacts with 1,2-diaminocyclohexane or with 1,2-diaminobenzene at 80°C to yield ZAMPS-PVPA.

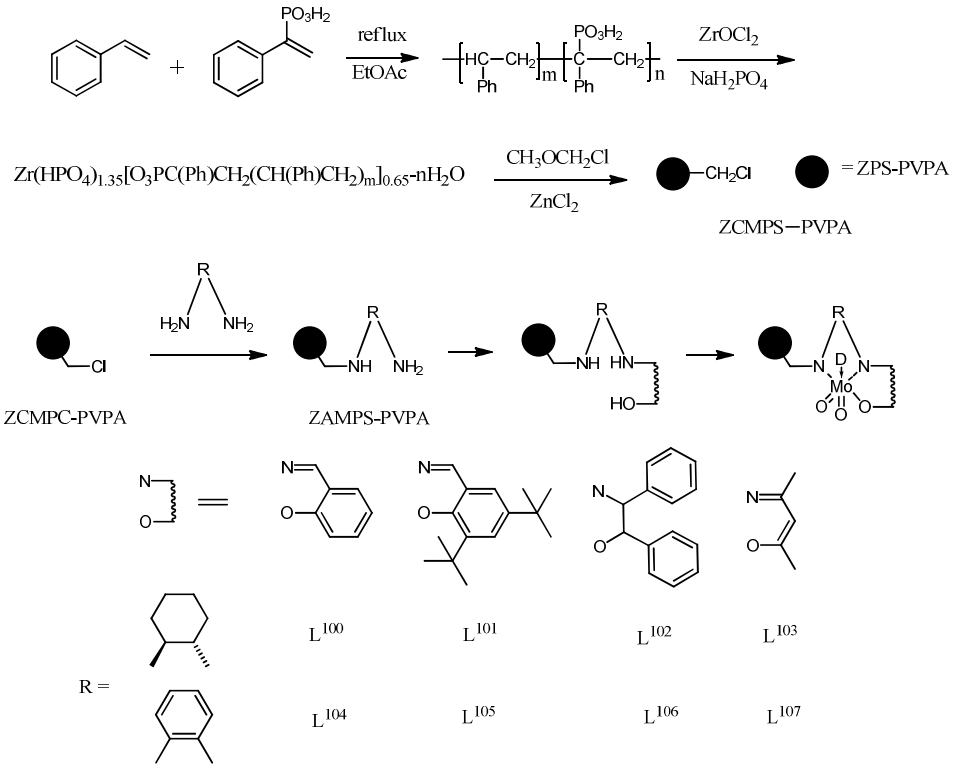

Scheme 1.44. Synthesis of PS-grafted complex with the Schiff base $L^{100\text{-}107}$.

ZAMPS-PVPA was treated with aldehydes or ketones to obtain the immobilized Schiff base ligands, then the ligands react with $[MoO_2(acac)_2]$ at 60 °C to give the immobilized dioxomolybdenum(VI) complexes. The prepared heterogeneous catalysts showed good to excellent catalytic efficiency in epoxidation of unfunctionalized olefins, using 2 eq. of TBHP (in tBuOOtBu) as oxidant in DCE with 2 mmol% of catalyst at 75°C. Up to 99% *ee* values were obtained with α-methylstyrene when the linker R is cyclohexane-1,2-diyl, although the heterogeneous catalysts are achiral. Furthermore, these catalysts are highly stable and could be reused ten times without noticeable loss of activity.[52]

I.4.3. Inorganic supports

I.4.3.1. Zeolite

In 2012, Rao and coworkers anchored complex $[MoO_2L^{108}(H_2O)]$, which contains the hydrazine-N-salicylidene-N'-salicyloyl ligand L^{108}, to zeolite-Y (Scheme 1.45). The anchoring is accomplished through the pending phenol function, encapsulation of $[MoO_2L^{108}(H_2O)]$ through flexible ligand method for entrapping molecular species inside zeolite cavities. This heterogenized catalyst was applied to the epoxidation of 1-hexene in DMF using atmospheric O_2, environmentally friendly oxidant, from 60 to 90°C.[53] While the corresponding homogeneous catalyst $[MoO_2L^{108}(H_2O)]$ produced 1,2-epoxyhexane, 1-hexanal and 2-hexanone in a 1:20:6 ratio after 6 h, the heterogenized catalyst yields only 1-hexanal with a 100% selectivity. The TON is eight times greater with the zeolite encapsulated complex.[54]

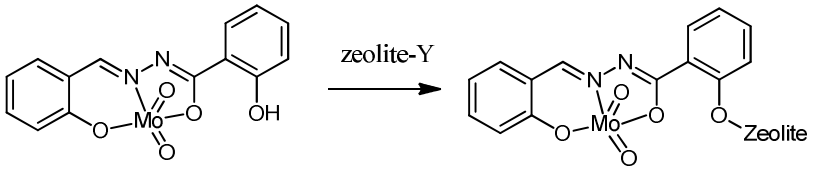

Scheme 1.45. $[MoO_2L^{108}(H_2O)]$ complex and its zeolite-Y composite.

I.4.3.2. Mesoporous silica

In 2006, Farzaneh and coworkers reported various molybdenum complexes supported on MCM-41, obtained by the reaction between $[MoO_2(acac)_2]$ and aminopropyl modified MCM-41 (AmpMCM-41) and bidentate Schiff base ligands derived from pyrrolcarbaldehyde (L^{109}), 2-aminoacetophenone (L^{110}), salicylaldehyde (L^{111}), furfural (L^{112}), 2-acetylpyrrole (L^{113}) and acetylacetone (L^{114}) (Scheme 1.46). These complexes are closely related but not quite identical to those of interest in this thesis, because the Schiff base is only bidentate and one acetylacetonate ligand of the $[MoO_2(acac)_2]$ precursor remains coordinated to saturate the Mo^{VI} coordination

sphere in the heterogenized catalyst. The resulting materials were used as catalysts in chloroform at reflux under a nitrogen atmosphere for the epoxidation of cyclooctene, cyclohexene, 1-hexene and 1-octene with 1.8 eq. of TBHP (in tBuOOtBu) as oxidant. The corresponding epoxides were obtained with good to high conversion and excellent selectivities (98-100%). These heterogeneous molybdenum catalysts show no measurable leaching.[55]

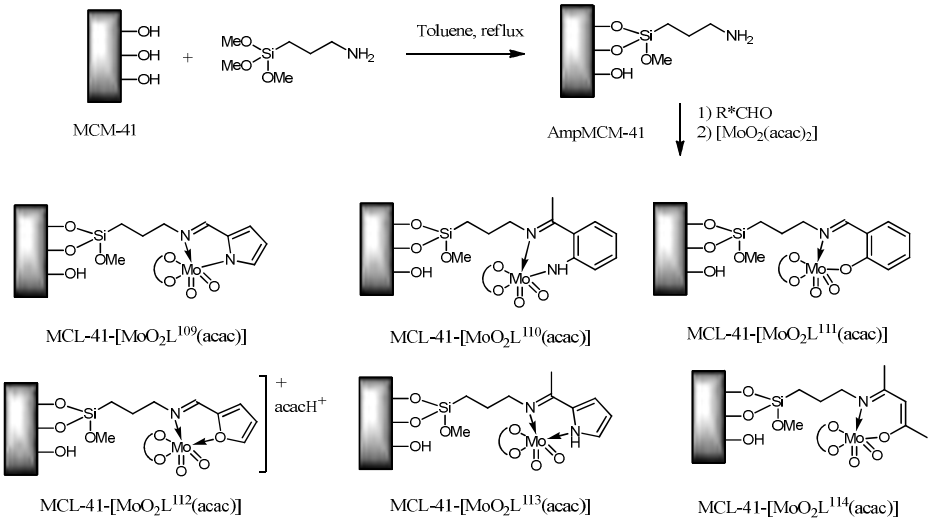

Scheme 1.46. Synthesis of catalysts from AmpMCM-41 and structures of the MCM-41-[MoO_2L(acac)] catalysts with the Schiff bases $L^{109\text{-}114}$.

In 2012, Masteri-Farahani and coworkers reported the covalent grafting of MCM-41 with 3-chloropropyltrimethoxysilane and the subsequent reaction with acacdien and complexation with [$MoO_2(acac)_2$] (Scheme 1.47), affording MoO_2acacdien@MCM-41. The obtained compound was used as heterogeneous catalyst (12.5 mg/mol substrates) for the epoxidation of cyclooctene, 1-hexene and 1-octene with 1.8 eq. TBHP (80% in tBuOOtBu) in refluxing chloroform with relatively good conversion and 97-99% selectivities.[56]

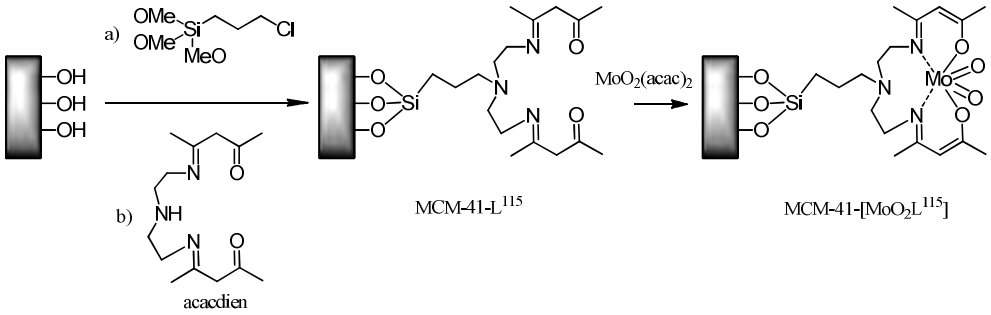

Scheme 1.47. Grafting of MCM-41 with ligand L^{115}.

In 2014, Farzaneh and coworkers described an Al-MCM-41-immobilized [MoO_2L] complex with the N-salicylidene-L-histidine ligand L^{116} (Scheme 1.48). [MoO_2L^{116}] was used as non-grafted or immobilized as sulfoxidation catalyst for a variety of sulfides with H_2O_2 as oxidant at room temperature in acetonitrile. The heterogeneous catalyst exhibited enhanced catalytic activity. The recovered catalyst showed similar catalytic activity without detectable molybdenum leaching, indicating the heterogeneous character of the catalysis system.[7]

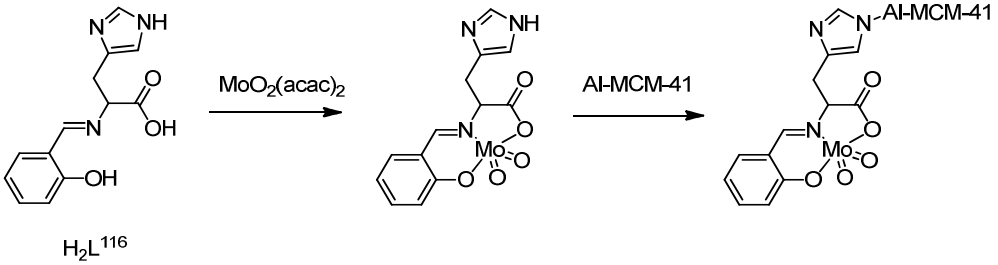

Scheme 1.48. Catalyst [MoO_2L^{116}] immobilized on Al-MCM-41.

In 2014, Bagherzadeh and coworkers reported the immobilization of the molybdenum complex with the salicylidene 2-picoloyl hydrazone ligand L^{117} by linking to the 3-chloropropyl groups inside the pores of mesoporous SBA-15 (Scheme 1.49). The hybrid material was found to be a highly active catalyst in the epoxidation of olefins with t-BuOOH in decane as oxidant. The solid catalytic material exhibits high activity and selectivity in the epoxidation of cyclooctene (almost 100% to epoxycyclooctene), in agreement with the performance of the corresponding homogeneous systems. Leaching tests and metal analyses of the reaction solutions showed that the catalytic activity came from the immobilized species. The heterogeneous catalyst showed good recyclability. Trace amount of *t*-BuOH observed by IR on the recovered solid catalyst could be the reason for the lower initial reaction rates in successive runs, although increasing reaction time showed conversions identical of those of the fresh catalyst.[57]

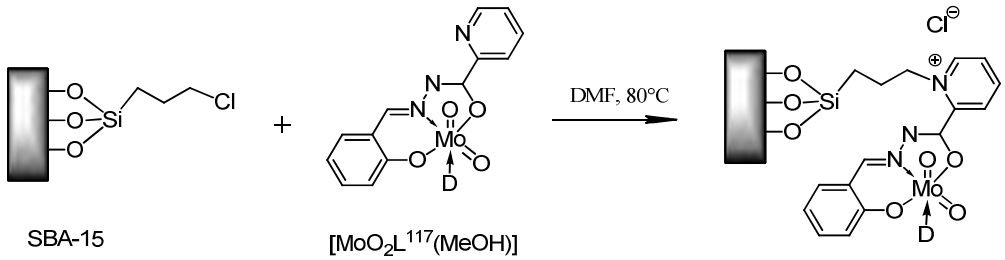

Scheme 1.49. Immobilization of the [$MoO_2(L^{117})$(MeOH)] complex on SBA-15 mesoporous silica.

I.4.4. Multiwall Carbon Nanotubes (MWCNT)

In 2013, Masteri-Farahani and coworkers reported a new well dispersed molybdenum Schiff base complex covalently attached to the surface of MWCNTs (Scheme 1.50). The nanomaterial showed catalytic ability and stability in the catalytic epoxidation of olefins with TBHP or CHP. The conversions are good and the selectivities are high. ICP-AES analyses confirmed no metal leaching. The recovered $[MoO_2L^{118}(acac)]$-MWCNTs maintained a similar activity after 2 cycles.[58] Note that this system, like those shown in Scheme 1.46, contains only a bidentate Schiff base and is therefore saturated by an acac ligand. There are, to the best of our knowledge, no $[MoO_2L]$-type catalysts with tridentate Schiff bases supported on carbon nanotubes yet reported in the literature.

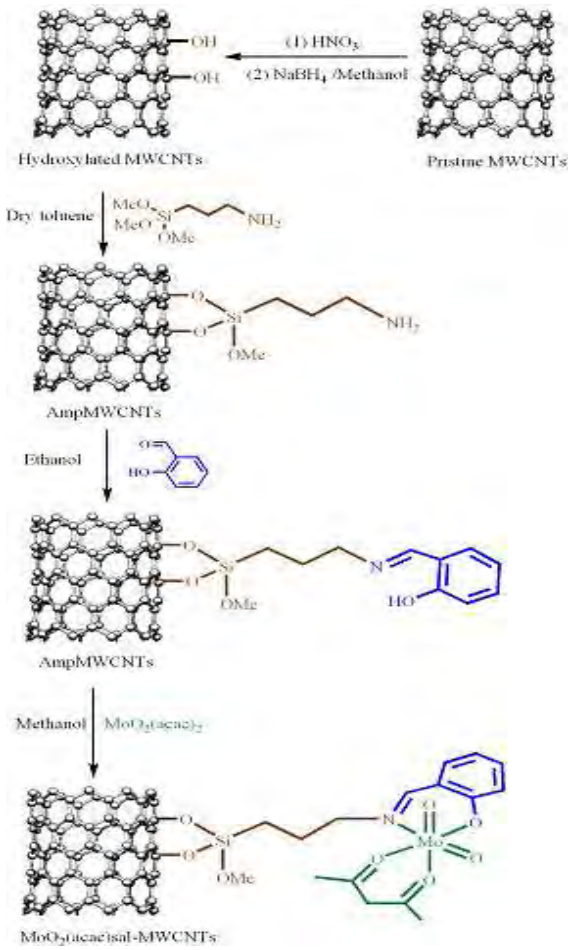

Scheme 1.50. Synthesis of MWCNT-grafted $[MoO_2L^{118}(acac)]$. Reproduced with permission from ref. 58. Copyright 2013 Elsevier.

I.5. Summary and conclusion

From the discovery of tridentate Schiff base molybdenum complexes in the 1970s, these complexes have been widely investigated. In this chapter, we have shortly reviewed their general structure, their properties depending on the nature of the ligands, and some of their applications with particular emphasis on their catalytic activities and on their assumed mechanism of action. Among the presented catalytic applications, we have focused particularly this bibliographic survey on the oxidation of olefins, more precisely epoxidation which will be the studied reaction of the thesis. We have also highlighted the previous efforts at anchoring these complexes on various solid supports, both organic and inorganic, and the subsequent use of the products in heterogenized catalytic applications. The catalyst recovery and recycling has been explored by several groups.

It has been emphasized that most of the presented catalytic procedures were performed in the presence of organic solvent, implying an increased cost in terms of treatment and a poor performance with respect to the green chemistry rules.

The next chapters will present the procedures that we have developed all along this thesis work, *i.e.* the synthesis and the characterization of different molybdenum complexes (chapter II), as well as their use as catalysts under organic solvent-free conditions (chapter III, IV and V), pointing out finally the strategy for the grafting of the active complex on PS resins for the catalytic use and in view of their recovery and recycling.

Since we are mostly concerned with the green chemistry guidelines, we have developed new strategies of research keeping in mind two main aspects. The first one is to avoid volatile organic solvents and thus develop an organic solvent-free oxidation process and the second one aims at the catalyst recovery and recycling. The ideal situation would be to combine both aspects, which will be the ultimate goal of this work.

II. Chapter II

Synthesis and characterization of monomeric and dimeric molybdenum complexes

II.1. Introduction

As shown in previous chapter, the number of possible structures of ligands is huge, and several authors pointed out the effect of the substitution on ligands on different effect, as *OAT* reactions or electrochemical behaviors. In order to study deeper those effects on catalyzed epoxidation reactions (in Chapter III and IV), we have synthesized in this chapter different types of molybdenum complexes with tridentate *ONO* and *ONS* Schiff base ligands. Their characterization by infrared, NMR, TGA and X-ray diffraction are described. Several modified ligands were used, adding free OH in certain positions or NEt_2 and NO_2 fragments.

II.2. Results and discussion

II.2.1. ONO Tridentate Ligands

II.2.1.1. Synthesis

The *ONO* Schiff base tridentate ligands H_2SAP and $H_2L^{a\text{-}f}$ were prepared by standard condensation of the corresponding substituted salicylaldehyde and substituted 2-aminophenol (Scheme 2.1) in alcoholic solution at reflux or at room temperature working in air until the product was formed as a red precipitate and the solution remained colourless. The compounds prepared are listed in Scheme 2.1. All compounds were analyzed by IR, NMR, and spectroscopic data were found in agreement with those from literature.[3, 59]

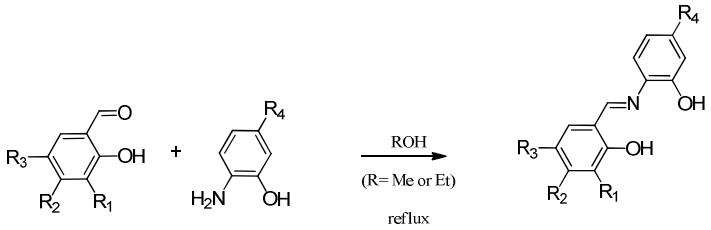

H_2SAP
$H_2L^{a\text{-}g}$

	Substituents			
	R_1	**R_2**	**R_3**	**R_4**
H_2SAP	H	H	H	H
H_2L^a	OH	H	H	H
H_2L^b	H	OH	H	H
H_2L^c	H	H	OH	H
H_2L^d	H	H	H	NO_2
H_2L^e	H	NEt_2	H	H
H_2L^f	H	NEt_2	H	NO_2

Scheme 2.1. Synthesis of *ONO* Tridentate Ligands.

II.2.1.2. Characterization

II.2.1.2.1. IR

The most important feature for the *ONO* H_2L ligands in the infrared spectrum are the C=N vibration bands around 1600-1630 cm^{-1}, indicating the formation of the Schiff base ligand (see Table 2.1) and the complete disappearance of the vibration bands corresponding to the aromatic aldehyde.

Table 2.1.Selected IR data (in cm^{-1}) for ligands.

Formula	ν (cm^{-1})
	C=N
H_2SAP	1633
H_2L^a	1618
H_2L^b	1603
H_2L^c	1600
H_2L^d	1603
H_2L^e	1606
H_2L^f	1608

II.2.1.2.2. ^{1}H NMR

The formation of the Schiff base is also verified by the appearance of one resonance corresponding to the CH=N proton at 6.20-7.70 ppm in the ^{1}H NMR spectrum, depending on the aromatic ring substituents. The disappearance of the corresponding aldehydic NMR resonance is also observed. All OH groups are visible in the case of the ligands H_2L^{a-f} (see Table 2.2).

Table 2.2. Selected ^{1}H NMR data for ligands.

Formula	^{1}H NMR (δ in ppm) in d_6-DMSO				
	ArH	CH=N	OH	CH_2	CH_3
H_2SAP	6.86-7.66	8.99	9.79, 13.78	-	-
H_2L^a	6.69-7.42	8.93	9.05, 9.83, 14.21	-	-
H_2L^b	6.24-7.38	8.78	9.66, 10.17, 14.24	-	-
H_2L^c	6.75-7.34	8.84	9.04, 9.64, 12.88	-	-
H_2L^d	6.97-7.80	8.99	10.72, 13.02	-	-
H_2L^e	5.96-7.22	8.61	14.26, 9.57	3.35	1.09
H_2L^f	6.00-7.77	8.74	10.57, 13.83	3.42	1.13

II.2.2. Molybdenum complexes

II.2.2.1. Molybdenum complexes with ONO ligands

The molybdenum complexes with *ONO* ligands were obtained classically mixing the H_2L ligand and freshly prepared $[MoO_2(acac)_2]$ in alcoholic solution. (Scheme 2.2). The mixture was stirred under reflux or at room temperature for 4 hours. The resulting orange precipitate was separated by filtration, characterized as $[MoO_2L(D)]$ in the case of L^a and L^b. Methanol and ethanol were elected as solvents in case of L^a and L^b, leading to the isolation of the corresponding monomeric complexes $[MoO_2L^a(MeOH)]$ and $[MoO_2L^b(EtOH)]$ in optimal way. With the other ligands, we obtained a mixture of monomeric and dimeric species. In order to obtain one unique dimeric compound type $[MoO_2L]_2$, and for better comparison of the catalytic activities of the complexes (in chapter III and IV), in all the cases, all the powders were dried by heating under reduced pressure for 12 hours and were characterized as $[MoO_2L]_2$.

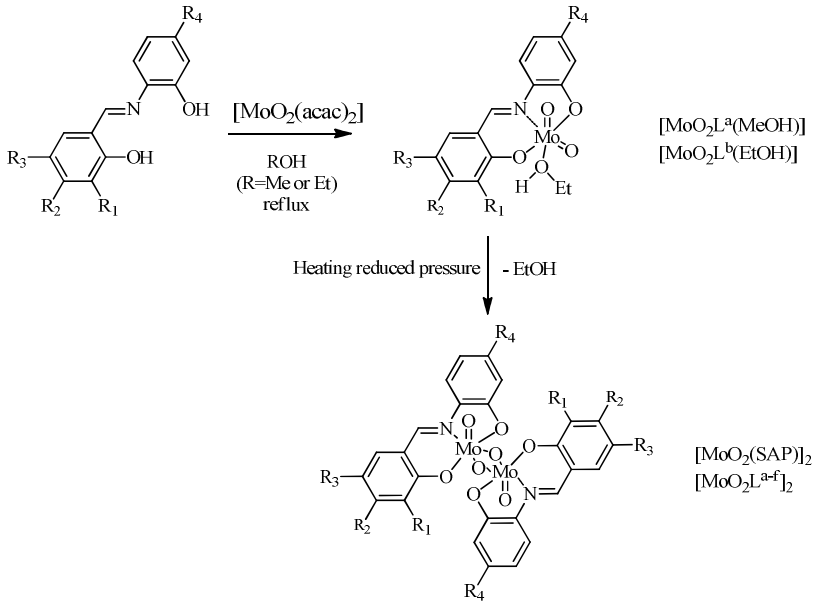

Scheme 2.2. Synthesis of *ONO* Molybdenum complexes.

II.2.2.2. Molybdenum complexes with ONS ligands

The typical procedure applied for the *ONO* ligands and complexes could not be followed for the *ONS* compounds. The isolation of the corresponding *ONS* ligands could not be achieved under our experimental condition since disulfides were obtained.[60] For this reason, all *ONS* molybdenum complexes were isolated in a one pot procedure with addition of the molybdenum precursor to the solution where the ligand is formed, without isolation of the ligand (see Scheme 2.3). In this way, four complexes were isolated and characterized as $[MoO_2(SATP)]_2$ and $[MoO_2L^{g-i}]_2$.

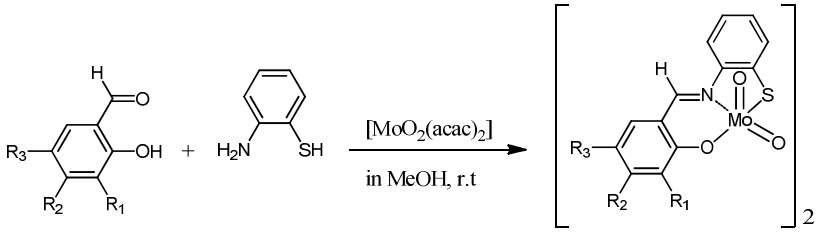

$[MoO_2(SATP)]_2$
$[MoO_2L^{g-i}]_2$

Complex	**R_1**	**R_2**	**R_3**
$[MoO_2(SATP)]_2$	H	H	H
$[MoO_2L^g]_2$	OH	H	H
$[MoO_2L^h]_2$	H	OH	H
$[MoO_2L^i]_2$	H	H	OH

Scheme 2.3. Synthesis of *ONS* Molybdenum complexes.

II.2.2.3. Characterization

II.2.2.3.1. Infrared Spectroscopy

The most relevant IR spectroscopic properties of the complexes are collected in Table 2.3. The complexation of the L^{2-} ligand to the $\{MoO_2^{2+}\}$ fragment is suggested by a weak shift of the *CH=N* vibration in the 1600-1620 cm^{-1} region. The vibration pattern observed between 750 and 1100 cm^{-1} corresponding to the $\{MoO_2^{2+}\}$ fragment gives additional information about the form of the isolated complex. The most diagnostic Mo-O vibration bands are those appearing between 850 and 940 cm^{-1}. In the case of the monomeric species stabilized by one solvent molecule, $[MoO_2L^a(MeOH)]$ and $[MoO_2L^b(EtOH)]$, two narrow absorbtion bands corresponding to Mo=O bonds are observed between 908 and 945 cm^{-1}. In the case of dimeric and polymeric compounds, one Mo=O vibration is visible in same region, and another band corresponding to Mo-O-Mo is observed around 800-820 cm^{-1}.

Table 2.3. Selected IR data for molybdenum complexes (in cm^{-1}).

Type	Formula	ν (cm^{-1})		
		C=N	*Mo=O*	*Mo-O-Mo*
ONO	$[MoO_2(SAP)]_2$	1608	935	808
	$[MoO_2L^a(MeOH)]$	1612	908, 933	-
	$[MoO_2L^a]_2$	1612	919	780
	$[MoO_2L^b(EtOH)]$	1600	908, 945	-
	$[MoO_2L^b]_2$	1598	904	821
	$[MoO_2L^c]_2$	1613	912	804
	$[MoO_2L^d]_2$	1603	922	798
	$[MoO_2L^e]_2$	1615	927	844
	$[MoO_2L^f]_2$	1614	934	809
ONS	$[MoO_2(SATP)]_2$	1602	920	781
	$[MoO_2L^g]_2$	1605	935	770
	$[MoO_2L^h]_2$	1600	871	760
	$[MoO_2L^i]_2$	1603	901	772

The formation of monomer or oligomers strongly depends on the nature of the ligand L surrounding the metal atom, the choice of the solvent, the presence of other donor molecules D, and the product isolation conditions. For example, Rajan and Chakravorty[11] reported the thermal conversion of the complex $[MoO_2L(D)]$ (L = SAE, SAP, and their peripheral-substituted analogues) to $[MoO_2L]_2$ (see Scheme 1.3 in Chapter **I**). The authors stated that, in order to isolate the complex $[MoO_2(SAP)(EtOH)]$, $[MoO_2(acac)_2]$ needed to be refluxed with H_2SAP in ethanol. In fact, reflux is not obliged. All the ligands and complexes can be obtained ar room temperature. In our case, by this method, no formation of dimeric species was observed.[11,61] In our case, under alcoholic conditions, ligands L^c and L^{g-i} led directly to the isolation of the oligomeric molybdenum species $[MoO_2L]_2$. However, a dimeric species with stoichiometry $[MoO_2(SAP)]_2$ was obtained by heating solid $[MoO_2(SAP)(EtOH)]$ at 110 °C under vacuum.[11,62] The formation of $[Mo(O)(\mu\text{-}O)(SAP)]_2$ was evidenced by IR spectroscopy with the appearance of an intense band between 800 and 850 cm^{-1}.[12]

II.2.2.3.2. ^1H NMR

The ligand complexation is evidenced by the disappearance of two OH resonances in each case and by a weak downfield shift of the imine resonance, because of the nitrogen coordination to the molybdenum center. (Table 2.4) In the case of the molybdenum complexes with *ONS* based ligands, the one-pot formation of the desired complex is suggested by the imine resonance in the 8.83 to 9.06 ppm range. It has to be pointed out that, since the measurements were performed in d_6-DMSO, the spectra observed for each complex correspond formally to the mononuclear $[MoO_2L(DMSO)]$ stoichiometry.

Table 2.4. Selected ^{1}H NMR data for complexes.

Type	Formula	^{1}H NMR (δ in ppm) in d_6-DMSO		
		ArH	CH=N	OH
ONO	$[MoO_2(SAP)]_2$	6.83-7.81	9.23	-
	$[MoO_2L^a(MeOH)]$	6.82-7.82	9.20	9.36
	$[MoO_2L^a]_2$	6.82-7.82	9.20	9.36
	$[MoO_2L^b(EtOH)]$	6.32-7.82	9.03	10.6
	$[MoO_2L^b]_2$	6.32-7.82	9.03	10.6
	$[MoO_2L^c]_2$	6.76-7.83	9.16	9.43
	$[MoO_2L^d]_2$	6.97-8.07	9.43	-
	$[MoO_2L^e]_2$	6.15-7.69	8.89	-
	$[MoO_2L^f]_2$	6.16-7.83	9.01	-
ONS	$[MoO_2(SATP)]_2$	6.89-7.81	9.06	-
	$[MoO_2L^h]_2$	6.25-7.70	8.83	10.7
	$[MoO_2L^i]_2$	6.68-7.72	8.91	9.41

II.2.2.3.3. Thermal measurements (TGA)

The thermogravimetric analyses of the isolated complexes, shown in Table 2.5, confirm the stoichiometry of the metallic complex, *i.e.* monomeric stabilized through a solvent molecule, $[MoO_2L(D)]$, or oligomeric, $[MoO_2L]_n$, by the presence of a mass change in the case of $[MoO_2L^b(D)]$ (Equation 2.1 and Figure 2.1) below 150°C corresponding to the loss of the coordinated solvent molecule D (EtOH). The second mass loss that occurs at much higher temperatures (> 250°C) corresponds to the degradation and loss of the ligand as observed earlier with similar ligand.[36]

$$[MoO_2L(D)] \xrightarrow{\Delta m_1\,(-D)} [MoO_2L] \xrightarrow{\Delta m_2\,(-L+O)} MoO_3$$

Equation 2.1

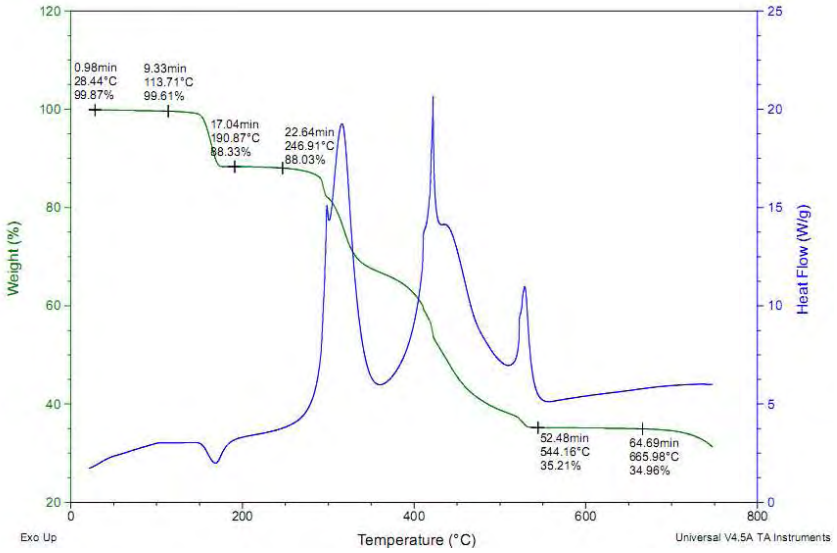

Figure 2.1. Thermogravimmetric diagram of $[MoO_2L^b(EtOH)]$.

Complex $[MoO_2L^a(MeOH)]$ loses the coordinated solvent MeOH very easily (at ca. 100°C in the TGA (Table 2.5) experiment and even at room temperature by slight depressurization). The alcohol can also be removed by washing with solvents such as Et_2O or DCM. Complex $[MoO_2L^b(EtOH)]$, on the other hand, loses EtOH at ca. 110°C. The alcohol in $[MoO_2L^b(EtOH)]$ cannot be removed only by washing with solvents, certainly indicating stronger coordination. On the contrary, the two oligomeric forms are transformed readily into the corresponding monomeric states once alcohol is added.

Table 2.5. TGA data for complexes.

Type	Formula	Δm_1 (< 250°C)		Δm_2(250°C ~ 700°C)	
		Exp	Theo	Exp	Theo
ONO	$[MoO_2(SAP)]_2$	-	-	58.5	57.6
	$[MoO_2L^a(MeOH)]$	8.3	9.8	62.8	63.4
	$[MoO_2L^a]_2$	-	-	59.1	59.5
	$[MoO_2L^b(EtOH)]$	11.6	11.5	65.0	64.1
	$[MoO_2L^b]_2$	-	-	59.2	59.5
	$[MoO_2L^c]_2$	-	-	58.7	59.5
	$[MoO_2L^d]_2$	-	-	62.6	62.9
	$[MoO_2L^e]_2$	-	-	64.9	64.4
	$[MoO_2L^f]_2$	-	-	68.4	69.2
ONS	$[MoO_2(SATP)]_2$	-	-	58.5	59.5
	$[MoO_2L^g]_2$	-	-	61.1	61.2
	$[MoO_2L^h]_2$	-	-	60.1	61.2
	$[MoO_2L^i]_2$	-	-	61.8	61.2

II.2.2.3.4. X-ray structures analyses.

Several complexes stabilized by a solvent molecule have given crystals suitable

for a structural determination by X-ray diffraction (see Tables 2.7 and 2.8). The structures determined have been presented briefly in this chapter.

The common feature of all those complexes is the pseudo-octahedral geometry around the molybdenum complex as depicted in chapter I, *i.e.* the *cis*-$\{MoO_2\}^{2+}$ fragment is surrounded by an *ONO* tridentate ligand and by a sixth donor molecule D.

With complexes $[MoO_2L^n]$ (L^n = SAP, L^a, L^c, L^e and L^f), crystals were obtained in DMSO as DMSO adducts of general formula $[MoO_2L^n(DMSO)]$ In the case of ligand L^b, the crystal has been isolated using a mixture acetonitrile water as an adduct with water, with the general formula $[MoO_2L^b(H_2O)]$.

The structures of all cited complexes were determined by single crystal X-ray crystallography, confirming the expected molecular connectivity. The two Mo=O bonds are located in a *cis* conformation, the L ligand occupies three positions in a *mer* arrangement and one solvent molecule (DMSO or water) coordinates the sixth coordination position *trans* to an oxido ligand in a pseudo-octahedral geometry, in accordance with similar structures.

All relevant bond lengths around the molybdenum have been compiled in Table 2.6.

Table 2.6. Relevant bond lengths around the molybdenum.

$[MoO_2L^n(D)]$	SAP	L^a	L^b	L^c	L^e	L^f
Bonds						
Mo=O	1.696(4)	1.714(2)	1.731(3)	1.708(2)	1.687(4)	1.701(3)
	1.686(4)	1.698(2)	1.696(3)	1.704(2)	1.698(3)	1.707(2)
Mo–O	1.929(4)	1.957(2)	1.948(3)	1.967 (1)	1.926(3)	1.941(3)
	1.943(4)	1.943(2)	1.944(3)	1.930 (1)	1.973(3)	1.980(3)
Mo–O (from donor)	2.267(6)	2.285(2)	2.325(3)	2.289(3)	2.23(1)	2.318(3)
Mo–N	2.281(8)	2.277(2)	2.252(3)	2.275 (2)	2.266(3)	2.245(3)

Table 2.7. Crystal data and structure refinement parameters.

Formula	$[MoO_2L^a(DMSO)]$	$[MoO_2L^b(H_2O)](CH_3CN)$	$[MoO_2L^c(DMSO)]$, 2DMSO
Empirical formula	$C_{15}H_{15}MoNO_6S$	$C_{15}H_{14}MoN_2O_6$	$C_{15}H_{15}MoNO_6S$, $2C_2H_6SO$
Formula weight	436.30	414.22	589.54
Temperature, K	173(2)	180(2)	180(2)
Wavelength, Å	0.71073	0.71073	0.71073
Crystal system	Monoclinic	Monoclinic	Monoclinic
Space group	$P\,2_1/c$	$I\,2/a$	$P\,2_1/n$
a, Å	7.4084(4)	21.202(5)	15.1752(4)
b, Å	20.8805(12)	6.599(5)	7.5571(2)
c, Å	10.8957(6)	24.110(5)	22.2331(6)
α, °	90.0	90.0	90.0
B, °	99.961(2)	106.582(5)	105.963(2)
γ, °	90.0	90.0	90.0
Volume, $Å^3$	1660.06(16)	3233(3)	2451.39(11)
Z	4	8	4
Density (calc), Mg/m^3	1.746	1.702	1.597
Abs. coefficient, mm^{-1}	0.947	0.845	0.834
F(000)	884	1664	1208
Crystal size, mm^3	0.500 x 0.200 x 0.040	0.625 x 0.075 x 0.05	0.37 x 0.35 x 0.20
θ range, °	2.134 to 28.281	3.210 to 29.520	1.457 to 30.031
Reflections collected	27592	15189	96079
Indpt reflections (R_{int})	4114 (0.0360)	10994 (0.040)	7181 (0.0291)
Completeness, %	99.6	99.9	100.0
Absorption correction	Multi-scan	Multi-scan	Multi-scan
Max. /min. transmission	0.7461 and 0.6777	1.0 and 0.948	0.7474 / 0.6860
Refinement method	F^2	F^2	F^2
Data /restraints/parameters	4114 / 6 / 234	10994 / 3 / 220	7181 / 8 / 322
Goodness-of-fit on F^2	1.164	1.042	1.224
R1, wR2 [$I>2\sigma(I)$]	0.0360, 0.0923	0.0315, 0.0819	0.0305, 0.0792
R1, wR2 (all data)	0.0464, 0.1004	0.0424, 0.0840	0.0343, 0.0815
Residual density, $e.Å^{-3}$	1.068 / -1.019	0.570 / -0.466	0.989 / -0.915

Table 2.8. Crystal data and structure refinement parameters.

Formula	$[MoO_2(SAP)(DMSO)](DMSO)$	$[MoO_2L^e(DMSO)]$	$[MoO_2L^t(DMSO)](H_2O)_{0.5}$
Empirical formula	$C_{17}H_{21}MoNO_6S_2$	$C_{19}H_{24}MoN_2O_5S$	$C_{19}H_{24}MoN_3O_{7.5}S$
Formula weight	495.41	488.40	542.41
Temperature	293(2)	293(2)	293(2)
Wavelength	0.71073	0.71073	0.71073
Crystal system	Monoclinic	Monoclinic	Triclinic
Space group	$P2_1/c$	$P2_1$	P-1
a (Å)	12.5387(5)	9.210	7.7016(11)
b (Å)	6.8015(2)	7.947	12.3088(16)
c (Å)	24.0157(10)	14.503	12.8230(19)
α,°	90	90	117.249(5)
β,°	93.460(2)	102.46	91.073(6)
γ,°	90	90	92.406(6)
Volume ($Å^3$)	2044.37(13)	1036.5	1078.7(3)
Z	4	2	2
Density (calc), Mg/m^3	1.610	1.565	1.670
Abs. coefficient, mm^{-1}	0.878	0.766	0.754
F(000)	1008	500	554
Crystal size (mm^3)	0.25 x 0.1 x 0.05	0.25 x 0.125 x 0.05	0.45 x 0.025 x 0.013
θ range (°)	2.91-27.48	2.91-27.48	2.65-26.43
Reflections collected	12136	10413	29410
Indpt reflections (R_{int})	4053 (0.0498)	3770 (0.0275)	4574 (0.0736)
Completeness to θ_{max} (%)	96.7	99.3	97.0
Absorption correction	Multi-scan	Multi-scan	Multi-scan
Max./min. transmission	0.9591/0.8953	0.9496 / 0.8971	0.7454 /0.5136
Refinement method	F^2	F^2	F^2
Data / restraints / parameters	4053 / 9/ 304	3770 / 8 / 295	4574 / 2 / 299
Goodness-of-fit on F^2	1.049	1.045	1.047
R1, wR2 [I>2σ(I)]	0.0520, 0.1144	0.0267, 0.0622	0.0638, 0.1616
R1, wR2 (all data)	0.0741, 0.1279	0.0301, 0.0636	0.0727, 0.1710
Residual density, $e.Å^{-3}$	1.022 / -0.768	0.304 /-0.415	2.860 / -2.130

Views of the six molecules are shown respectively in Figure 2.2 in case of SAP ligand and Figure 2.3 for the two DMSO adducts with L^a and L^c. The water adduct with L^b is in Figure 2.5, while the two other compounds with L^e and L^f are in Figure 2.7.

All six complexes have the similar classical structure with the *cis*-$\{MoO_2\}^{2+}$ fragment surrounded by an *ONO* tridentate ligand and by a sixth donor molecule D. The structures are briefly commented here.

$[MoO_2(SAP)(DMSO)]$

$[MoO_2(SAP)(DMSO)]$ crystallized with one additional disordered DMSO molecule. This may be related to the disorder of the imine function linking the two aromatic rings. Indeed, as seen in the Figure 2.2, The Mo(1)-O(1) and Mo(1)-O(2) bonds are identical and the aromatic rings of the two forms are superimposed. The two different ligand positions around the molybdenum atom, particularly the different orientations of the Mo-N bond in the two possible arrangements, possibly induce the DMSO positional disorder.

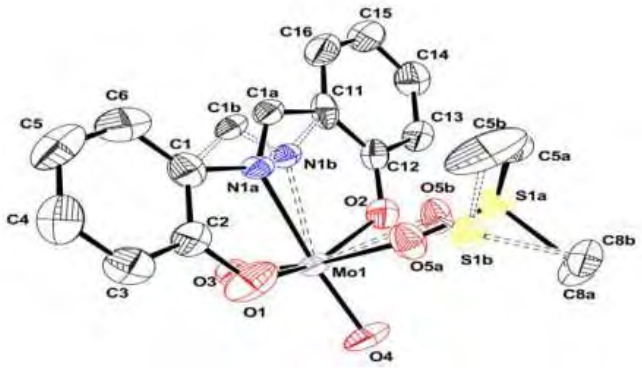

Figure 2.2. ORTEP view of $[MoO_2(SAP)(DMSO)]$. The ellipsoids are drawn at the 30% probability level. The second form is represented by dotted lines.

$[MoO_2L^a(DMSO)]$ and $[MoO_2L^c(DMSO)]$

$[MoO_2L^a(DMSO)]$ and $[MoO_2L^c(DMSO)]$ (Fig. 2.3) crystallize in a very similar manner. No disorder has been observed in this case within the crystal lattice that the position of the OH in the ligand breaks the symmetry. Related interatomic distances around the metal center are essentially identical in the two complexes The L ligands deviate slightly from coplanarity, with very similar dihedral angles of 10.61° for the L^b complex and 10.41° for the L^d complex.

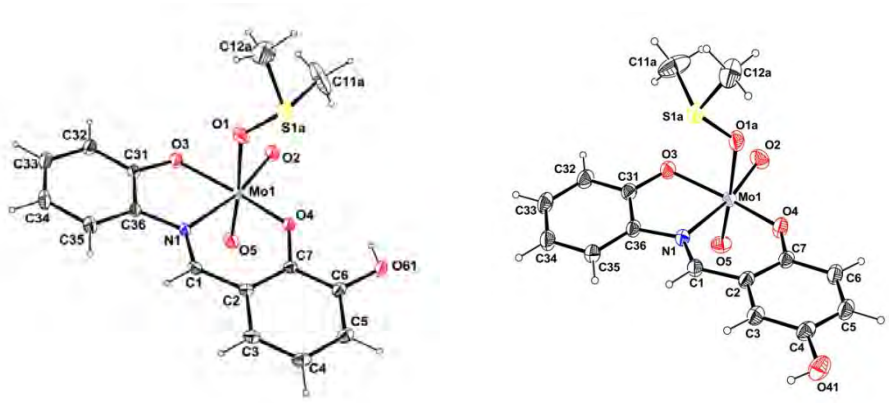

Figure 2.3. Molecular view of compound [MoO_2L^a(DMSO)] (left) and [MoO_2L^c(DMSO)] (right) with the atom labelling scheme. Displacement ellipsoids are drawn at the 50% probability level. For the sake of clarity, only one component of the disordered DMSO is represented.

In the case of the complex [MoO_2L^a(DMSO)], intermolecular O-H···O hydrogen bonds are observed between an oxo of one molecule and the OH of a second molecule, resulting in the formation of a dimer (Figure 2.4).

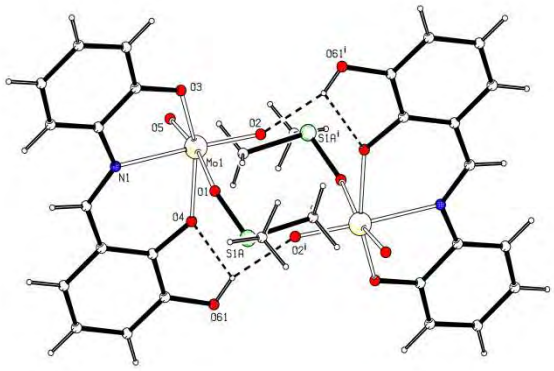

Figure 2.4. View of the dinuclear unit formed by intermolecular hydrogen bonds between two [MoO_2L^a(DMSO)] molecules.

On the other hand, the L^c complex does not show any intermolecular H-bonding but crystallizes with two additional DMSO molecules per complex in the crystal lattice.

[$MoO_2L^b(H_2O)$]

The complex [MoO_2L^b(DMSO)] was crystallized and the same problem as in the case of [MoO_2(SAP)(DMSO)] was observed, not giving the possibility to solve its structure. However, by changing the crystallization solvent, the structure could be solved. It is observed the stabilization of the sixth position of the molybdenum by one molecule of water (Figure 2.5). One H-N coordination between the water and one molecule of acetonitrile was observed.

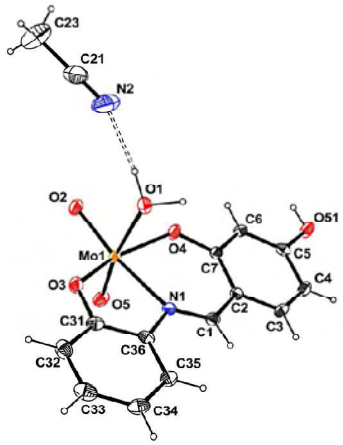

Figure 2.5. Molecular view of compound $[MoO_2L^b(H_2O)]\cdot CH_3CN$ with the atom labelling scheme. Displacement ellipsoids are drawn at the 50% probability level.

As for the compound $[MoO_2L^a(DMSO)]$, some hydrogen bonds were oserved between molecules, giving the formation of dimer between the pending OH (O51) of one complex and the oxido moiety (O2) in the plane of the ligand of the second molecule. A second coordination is observed between the water molecule (O1) of one complex and the OH of the second complex (Figure 2.6).

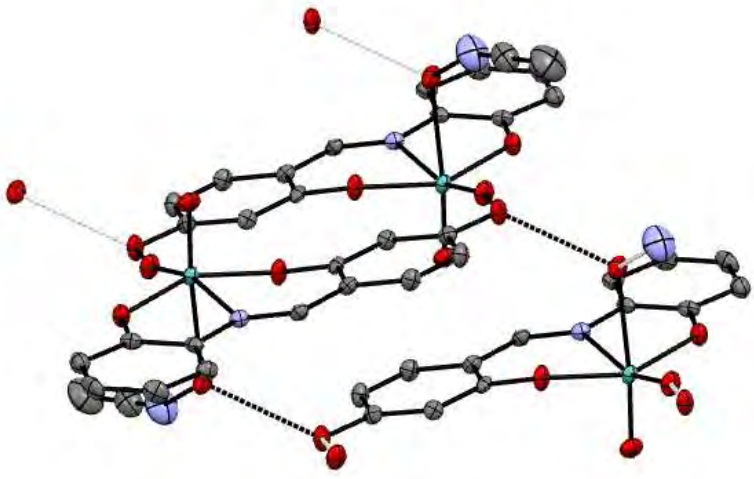

Figure 2.6. Molecular view of compound $[MoO_2L^b(H_2O)]\cdot CH_3CN$ with the hydrogen bonds between the different complexes.

$[MoO_2L^e(DMSO)]$ and $[MoO_2L^f(DMSO)]$

The $[MoO_2L^e(DMSO)]$ complex does not show any intermolecular H-bonding but crystallizes with two additional DMSO molecules per complex in the crystal lattice (Figure 2.7).

While compound [MoO_2L^f(DMSO)] crystallized with one water molecule per two molecules of complex, the structure of compound [MoO_2L^e(DMSO)] did not contain any solvent of crystallization.

In the case of [MoO_2L^e(DMSO)], as for [MoO_2(SAP)(DMSO)], the DMSO ligand shows disorder but this disorder cannot be attributed to the same phenomena as for L^a since the Schiff base is not disordered.

The diethylamino group is quasi-coplanar with the aromatic group in the structures of [MoO_2L^e(DMSO)] and [MoO_2L^f(DMSO)] (dihedral angles between the phenyl C6 ring and the NC2 fragment of 11.2(4)° and 4.8(5)°, respectively), showing π conjugation (sp^2 hybridization for the N atom), which is confirmed by the N atom trigonal planarity with a sum of the three bond angles of 360.0(4)° and 359.8(4)°, respectively). Finally, the NO_2 group in the structure of [MoO_2L^f(DMSO)] is also quasi coplanar with the aromatic ring, with a dihedral angle of 5.0(6)° for O11-N11-C14-C13.

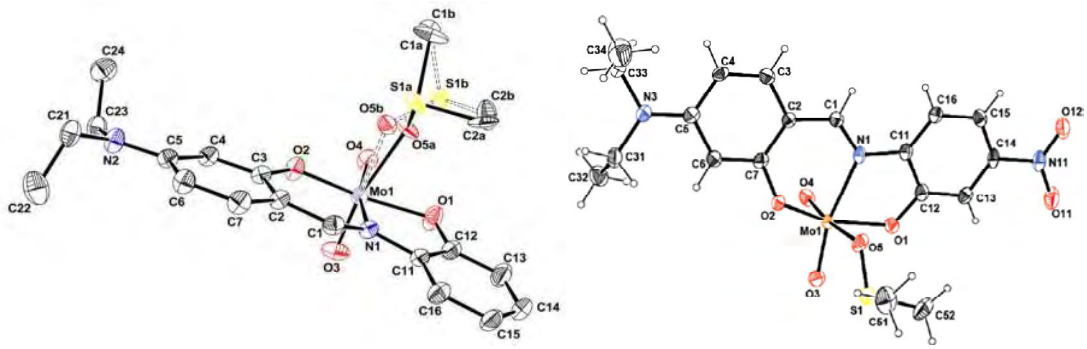

Figure 2.7. ORTEP view of [MoO_2L^e(DMSO)] (left) and [MoO_2L^f(DMSO)] (right). The ellipsoids are drawn at the 30% probability level. The second position of DMSO is represented by dotted lines.

II.3. Conclusion

In this chapter, several tridentate molybdenum complexes with *ONO* and *ONS* coordination spheres around molybdenum have been synthesized and characterized by IR, NMR and TGA. Compounds with different substituents, *i.e.* OH or donor and/or acceptor groups, at various positions of the aromatic ring could be generated. We could characterize by X-ray diffraction 6 new complexes, especially all *ONO* ones with OH in different position on the aromatic ring and two compounds with donor (NEt_2) and acceptor (NO_2) substituents.

Most of the previously published work reviewed in chapter **I** deals with catalytic procedures in the presence of an organic solvent. Since one of the interests for the development of greener processes is the use of organic solvent-free procedures, all the complexes described in the present chapter will be used as catalysts for the organic solvent-free epoxidation of cyclooctene (chapter **III**) and for the limonene and cyclohexene oxidation (chapter **IV**).

II.4. Experimental part

II.4.1. Materials and methods

All preparations were carried out in air. Water was deionised twice before use. Organic solvents (ethanol, methanol, diethylether) and 2-aminophenol (99%, Aldrich), 2,5-dihydroxybenzaldehyde (98%, Aldrich), 2,3-dihydroxybenzaldehyde (97%, Aldrich), 2,4-dihydroxybenzaldehyde (98%, Aldrich), salicylaldehyde (98%, Aldrich) and 2-aminothiophenol (97%, Merck) 4-(*N*,*N*-diethylamino) salicylaldehyde were used as received without any purification. $[MoO_2(acac)_2]$ was synthesized as previously described and used freshly prepared.[63] The thermogravimetric analyses (TGA) were performed on a SETARAM TGA 92-16.18 thermal analyzer. The sample was placed into a nickel/platinum alloy crucible and heated at 0.83 $K \cdot s^{-1}$ in a reconstituted air flow from 15°C to 700°C. An empty crucible was used as a reference. Infrared (IR) spectra were recorded in KBr matrices at room temperature with a Mattson Genesis II FTIR spectrometer. ^{1}H NMR spectra were recorded at 200.1 MHz on a Bruker Avance DPX-200 spectrometer. The elemental analyses were obtained from the analytical services of the Laboratoire de Chimie de Coordination (LCC). The data collection and structural determination for all X-ray diffraction experiments were carried out by Dr. Jean-Claude Daran at LCC. High resolution mass spectra were recorded in an Agilent G1969A mass spectrometer.

II.4.2. Syntheses of the ligand precursors

II.4.2.1. Synthesis of H_2SAP.

In a 100 mL Erlenmeyer flask, 1.22 g (10 mmol) of 2-hydroxybenzaldehyde were added to 30 mL of ethanol. 2-aminophenol (1.09 g 10 mmol) was added. The mixture was stirred under reflux for 4 hours until the product formed as a red precipitate and the solution remained colorless. The precipitate was filtered, recrystallized from boiling ethanol and filtered again, then washed with diethylether and dried under vacuum at room temperature to give a red microcrystalline powder. Yield: 1.96 g (92 %). IR (KBr, ν(cm^{-1})): 1633 (C=N). ^{1}H NMR (300 MHz, DMSO-d_6, δ(ppm)): 6.86-7.66 (m, 8H, Ar-*H*), 8.99 (s, 1H, C*H*=N), 9.79 (s, 1H, Ar-O*H*), 13.78 (s, 1H, ArO*H*).

II.4.2.2. Synthesis of H_2L^a.

In a 100 mL Erlenmeyer flask, 1.00 g (7.24 mmol) of 2,3-dihydroxybenzaldehyde was added to 30 mL of ethanol. 2-aminophenol (0.79 g, 7.24 mmol) was then added. The mixture was stirred under reflux for 4 hours until the product formed as a red solution, the methanol was removed by vacuum evaporation. The resulting red solid was washed with methanol, recrystallized from boiling ethanol and filtered, then washed with diethylether and dried under vacuum at room temperature to give a red microcrystalline powder.

Yield: 1.34 g (81 %). IR (KBr, ν(cm^{-1})): 1618 (C=N). ^{1}H NMR (300 MHz, DMSO-d_6, δ(ppm)): 6.69-7.42 (m, 7 H, Ar-*H*), 8.93 (s, 1 H, C*H*=N), 9.05 (s, 1 H, Ar-O*H*), 9.82 (s, 1 H, Ar-O*H*), 14.21 (s, 1 H, Ar-O*H*). ^{13}C{^{1}H} NMR (300 MHz, DMSO-d_6) δ: 161.6 (C_H-N), 152.2 (C_q-O), 151.3 (C_q-O), 146.5 (C_q-O), 134.3 (C_q-N), 128.6 (C_H-Ar), 122.8 (C_H-Ar), 120.2 (C_H-Ar), 119.6 (C_H-Ar), 119.4 (C_q), 118.6 (C_H-Ar), 118.4 (C_H-Ar), 116.9 (C_H-Ar).

II.4.2.3. Synthesis of H_2L^b.

In a 100 mL Erlenmeyer flask, 1.0 g (7.24 mmol) of 2,4-hydroxybenzaldehyde were added to 30 mL of ethanol. 2-aminophenol (0.79 g, 7.24 mmol) was added. The mixture was stirred under reflux for 4 hours producing a red solution, then the solvent was removed by vacuum evaporation. The solid was filtered, recrystallized from boiling ethanol and filtered again, then washed with diethylether and dried under vacuum at room temperature to give an orange powder. The characterization results are consistent with the literature. 3

Yield: 0.9 g (54 %). IR (KBr, ν(cm^{-1})): 1603 (C=N). ^{1}H NMR (300 MHz, DMSO-d_6, δ(ppm)): 6.24-7.38 (m, 7H, Ar-*H*), 8.78 (s, 1H, C*H*=N), 9.66 (s, 1H, Ar-O*H*), 10.17 (s, 1H, ArO*H*) , 14.24 (s, 1H, ArO*H*). ^{13}C{^{1}H} NMR (300 MHz, DMSO-d_6) δ: 165.4 (C_q-O), 162.8 (C_q-O), 160.8 (C_H-N), 150.9 (C_q-O), 135.1 (C_q-N), 134.6 (C_H-Ar), 127.6 (C_H-Ar), 120.1 (C_H-Ar), 119.6 (C_H-Ar), 116.8 (C_H-Ar), 112.8 (C_q), 108.0 (C_H-Ar), 103.1 (C_H-Ar).

II.4.2.4. Synthesis of H_2L^c.

In a 100 mL Erlenmeyer flask, 2,5-dihydroxybenzaldehyde (1.03 g, 7.45 mmol) was added to 30 mL of ethanol. 2-aminophenol (0.79 g, 7.24 mmol) was added. The mixture was stirred under reflux for 4 hours until the product formed as a red precipitate. The precipitate was filtered, recrystallized from boiling ethanol and

filtered again, then washed with diethylether and dried under vacuum at room temperature to give a red microcrystalline powder.

Yield: 1.51 g (91 %). IR (KBr, ν(cm^{-1})): 1612 (C=N). ^{1}H NMR (300 MHz, DMSO-d_6, δ(ppm)): 6.75-7.34 (m, 7 H, Ar-*H*), 8.84 (s, 1 H, C*H*=N), 9.04 (s, 1 H, Ar-O*H*), 9.64 (s, 1 H, Ar-O*H*), 12.88 (s, 1 H, Ar-O*H*). ^{13}C{^{1}H} NMR (300 MHz, DMSO-d_6) δ: 161.9 (C_H-N), 153.9 (C_q-O), 151.5 (C_q-O), 149.8 (C_q-O), 135.8 (C_q-N), 128.4 (C_H-Ar), 121.2 (C_H-Ar), 120.2 (C_H-Ar), 120.0 (C_H-Ar), 119.9 (C_q), 117.6 (C_H-Ar), 117.4 (C_H-Ar), 116.9 (C_H-Ar).

II.4.2.5. Synthesis of H_2L^{d-f}.

The Schiff base ligands H_2L^{e-g} were prepared according to the literature procedures.

General procedure

In a round bottom flask equipped with a magnetic bar, 41 mmol of the desired 2-hydroxybenzaldehyde and 41 mmol of the corresponding 2-aminophenol were suspended in 30 mL of ethanol. The resulting suspension was stirred at reflux temperature for two hours; the solution was evaporated to two thirds the volume and cooled in an ice bath. The solid obtained was filtered and washed with cold ethanol. The Schiff bases H_2L^{e-g} that were already reported were characterized by ^{1}H and ^{13}C NMR and the data were compared with the literature.

(H_2L^d) [64]

Red solid, mp: 220-222 °C, yield: 72%. IR (KBr, ν(cm^{-1})):1603(C=N). ^{1}H NMR (400 MHz, DMSO-d_6, δ(ppm)): 6.97 (m, 2H), 7.43 (ddd, 1H, *J* = 8.4, 8.0, 1.6 Hz), 7.51 (dd, 1H, *J* = 6.8, 2.0 Hz), 7.66 (dd, 1H, *J* = 7.7, 1.5 Hz), 7.77-7.75 (m, 2H), 8.99 (s, 1H), 10.69 (s, 1H), 13.00 (s, 1H). ^{13}C{^{1}H} NMR (100 MHz, DMSO-d_6) δ: 165.3, 161.1, 151.6, 146.3, 142.5, 134.4, 133.1, 121.0, 119.8, 119.6, 117.3, 115.5, 111.2.

(H_2L^e) [65]

Yellow solid, mp: 202-204 °C, yield: 80%. IR (KBr, ν(cm^{-1})): 1606(C=N). ^{1}H NMR (400 MHz, DMSO-d_6, δ(ppm)): 1.09 (t, 6H, *J* = 7 Hz), 3.35 (q, 4H, *J* = 7 Hz), 5.96 (d, 1H, *J* = 2.4 Hz), 6.24 (dd, 1H, *J* = 8.6, 2.4 Hz), 6.81 (ddd, 1H, *J* = 7.6, 7.6, 1.2 Hz), 6.89 (dd, 1H, *J* = 8.0, 1.6 Hz), 6.99 (ddd, 1H, *J* = 7.8, 7.4, 1.6 Hz), 7.26-7.22 (m, 2H), 8.61 (s, 1H), 9.57 (s, 1H), 14.26 (s, 1H). ^{13}C{^{1}H} NMR (100 MHz, DMSO-d_6) δ: 166.1, 159.1, 152.1, 150.5, 135.1, 134.4, 126.6, 120.0, 119.0, 116.6, 109.5, 104.1, 97.7, 44.3, 13.1.

(H_2L^f) [66]

Orange solid, yield: 67%. IR (KBr, ν(cm^{-1})): 1608(C=N). ^{1}H NMR (400 MHz, DMSO-d_6, δ(ppm)): 1.12 (t, 6H, *J* = 7 Hz), 3.39 (q, 4H, *J* = 14, 7 Hz), 5.94 (d, 1H, *J* = 2.2 Hz), 6.32 (dd, 1H, *J* = 8.8, 2.2 Hz), 7.27 (d, 1H, *J* = 8.8 Hz), 7.46 (d, 1H, *J* = 8.4 Hz), 7.64-7.62 (m, 2H), 8.77 (s, 1H). ^{13}C{^{1}H} NMR (75 MHz, DMSO-d_6) δ: 168.9, 159.1, 156.8, 153.2, 145.8, 141.6, 135.2, 119.2, 111.9, 111.2, 110.3, 104.8, 98.4, 44.7, 12.7.

II.4.3. Synthesis of molybdenum complexes

II.4.3.1. Synthesis of $[MoO_2(SAP)]_2$.

In a 100 mL Erlenmeyer flask, 2.29 g (10 mmol) of H_2SAP was dissolved in 50 mL of ethanol and 3.26 g (10 mmol) of [$MoO_2(acac)_2$] was added. The mixture was stirred under reflux for 4 hours. The resulting orange precipitate was separated by filtration. The precipitate was dried (120°C) under reduced pressure for 4 hours.The orange compound is $[MoO_2(SAP)(EtOH)]_2$ which is comfirmed by IR, NMR and TGA. After heated at reduced pressure at 80°C, the color changed to brown with the leaving of coordinated EtOH and yield the form of $[MoO_2(SAP)]_2$. Yield: 86%. TGA: exp(theo) Δm over 200-600 °C = 58.5 (57.6) %. IR (KBr, ν(cm^{-1})): 1608 (C=N), 937, 906 (Mo=O), 794 (Mo-O-Mo). ^{1}H NMR (300 MHz, DMSO-d_6, δ(ppm)): 6.83-7.81 (m, 8H, Ar-*H*), 9.23 (s, 1H, C*H*=N). ^{13}C{^{1}H} NMR (300 MHz, DMSO-d_6) δ: 161.5 (C_q-O), 160.5 (C_q-O), 157.1 (C_H-N), 136.1 (C_H-Ar), 136.0 (C_q-N), 135.6 (C_H-Ar), 130.6 (C_H-Ar), 122.3 (C_q), 121.4 (C_H-Ar), 120.9 (C_H-Ar), 119.3 (C_H-Ar), 117.7 (C_H-Ar), 116.8 (C_H-Ar).

II.4.3.2. Synthesis of $[MoO_2L^a(MeOH)]$ and $[MoO_2L^a]_2$.

In a 100 mL Erlenmeyer flask, 0.35 g (1.53 mmol) of H_2L^a was dissolved in 20 mL of methanol and 0.50 g (1.53 mmol) of [$MoO_2(acac)_2$] was added. The mixture was refluxed under magnetic stirring for 4 hours. The resulting red solution was left overnight. The orange needlesformed were separated by filtration and divided into two fractions: the first was characterized as $[MoO_2L^a(MeOH)]$ and the second one was dried (80°C) under reduced pressure for 12 hours and characterized as $[MoO_2L^a]_2$. Addition of MeOH led a color change and yielded $[MoO_2L^a(MeOH)]$.

$[MoO_2L^a(MeOH)]$:

TGA: exp(theo) Δm_1 over 20-120 °C = 8.3 (9.8) %, Δm_2 over 250-600 °C = 62.8 (63.4) %. IR (KBr,ν(cm^{-1})): 1612 cm^{-1} (C=N), 919 (Mo=O), 780 (Mo-O-Mo).

$[MoO_2L^a]_2$:

Anal. Calcd. for $C_{13}H_9MoNO_5$ (Mr = 355.15): C, 43.96; H, 2.55; N, 3.9 %. Found: C, 43.01; H, 1.97; N, 3.90 %. TGA: exp(theo) Δm over 200-600 °C = 59.4 (59.5) %. IR (KBr, ν(cm^{-1})): 1612 cm^{-1} (C=N), 933 (Mo=O), 908 (Mo-O-Mo). The NMR spectra in DMSO-d_6 are the same as that for compound $[MoO_2L^b(MeOH)]$ and $[MoO_2L^b]_2$, since in DMSO, all compounds go to $[MoO_2L^2(DMSO)]$.

^{1}H NMR (300 MHz, DMSO-d_6, δ(ppm)): 6.82-7.82 (m, 7 H, Ar-*H*), 9.20 (s, 1 H, C*H*=N), 9.36 (s, 1 H, Ar-O*H*). $^{13}C\{^1H\}$ NMR (300 MHz, DMSO-d_6) δ: 160.3 (C_q-O), 157.3 (C_H-N), 150.3 (C_q-O), 147.0 (C_q-O), 135.9 (C_q-N), 130.5 (C_H-Ar), 125.7 (C_H-Ar), 122.9 (C_q), 121.5 (C_H-Ar), 121.4 (C_H-Ar), 120.7 (C_H-Ar), 117.7 (C_H-Ar), 116.8 (C_H-Ar).

II.4.3.3. Synthesis of $[MoO_2L^b(EtOH)]$ and $[MoO_2L^b]_2$

In a 100 mL Erlenmeyer flask, 0.70 g of H_2L^b (3.05 mmol) was dissolved in 25 mL of ethanol and 1.00 g of $[MoO_2(acac)_2]$ (3.06 mmol) were added. The mixture was refluxed under magnetic stirring overnight. The precipitate was separated by filtration. The resulting orange needles were divided into two fractions: the first was characterized as $[MoO_2L^b(EtOH)]$ and the second was dried (120 °C) under reduced pressure for 12 hours and characterized as $[MoO_2L^b]_2$. The loss of EtOH from $[MoO_2L^b]_2$ led a color change to brown and yielded $[MoO_2L^b]_2$.

$[MoO_2L^b(EtOH)]$:

TGA: exp(theo) Δm_1 over 20-200 °C = 11.6 (11.5) %, Δm_2 over 200-600 °C = 62.8 (63.4) %. IR (KBr, ν(cm^{-1})): 1600 cm^{-1} (C=N), 933 (Mo=O), 877 (Mo-O-Mo).

$[MoO_2L^b]_2$:

Anal. Calc. for $C_{13}H_9MoNO_5$ (Mr = 355.15): C, 43.96; H, 2.55; N, 3.9 %. Found: C, 43.93; H, 2.10; N, 3.92 %. TGA: exp(theo) Δm over 200-600 °C = 59.2 (59.5) %. IR (KBr, ν(cm^{-1})): 1598 cm^{-1} (C=N), 821 (Mo=O), 904 (Mo-O-Mo). The NMR spectra in DMSO-d_6 are the same as that for compound $[MoO_2L^b(EtOH)]$ and $[MoO_2L^b]_2$, since in DMSO, all compounds go to $[MoO_2L^b$ (DMSO)]

^{1}H NMR (300 MHz, DMSO-d_6, δ(ppm)): 6.32-7.82 (m, 7 H, Ar-*H*), 9.03 (s, 1 H, C*H*=N), 10.65 (s, 1 H, Ar-O*H*). $^{13}C\{^1H\}$ NMR (300 MHz, DMSO-d_6) δ: 165.4 (C_H-N), 163.6 (C_q-O), 159.9 (C_q-O), 156.3 (C_H-Ar), 137.4 (C_H-Ar), 136.7 (C_q-N), 129.4 (C_H-Ar), 120.8 (C_H-Ar), 117.4 (C_H-Ar), 116.1 (C_H-Ar), 115.2 (C_q), 110.6 (C_H-Ar), 105.1 (C_H-Ar).

II.4.3.4. Synthesis of $[MoO_2L^c]_2$.

In a 100 mL Erlenmeyer flask, 0.45 g of H_2L^c (1.96 mmol) was dissolved in 30 mL of methanol and 0.64 g of $[MoO_2(acac)_2]$ (1.96 mmol) was added. The mixture was refluxed under magnetic stirring for 4 hours. The resulting brown precipitate was separated by filtration. The precipitate was dried (80 °C) under reduced pressure for 24 hours.
Yield: 87%. Anal. Calc. for $C_{13}H_9MoNO_5$ (Mr = 355.15): C, 43.96; H, 2.55; N, 3.9 %. Found: C, 43.84; H, 1.83; N, 3.84 %. TGA: exp(theo) Δm over 200-600 °C = 58.7 (59.5) %. IR (KBr, ν(cm^{-1})): 1613 (C=N), 912 (Mo=O), 804 (Mo-O-Mo). ^{1}H NMR (300 MHz, DMSO-d_6, δ(ppm)): 6.27-7.74 (m, 7 H, Ar-*H*), 9.09 (s, 1 H, C*H*=N), 10.65 (s, 1 H, Ar-O*H*). $^{13}C\{^1H\}$ NMR (300 MHz, DMSO-d_6) δ: 160.6 (C_q-O), 156.9 (C_H-N), 155.0 (C_q-O), 151.4 (C_q-O), 136.0 (C_q-N), 130.6 (C_H-Ar), 123.8 (C_H-Ar), 122.5 (Cq), 120.6 (C_H-Ar), 119.7 (C_H-Ar), 119.4 (C_H-Ar), 117.8 (C_H-Ar), 116.9 (C_H-Ar).

II.4.3.5. Synthesis of $[MoO_2L^{d\text{-}f}]_2$.

General procedure for the synthesis of molybdenum complexes $[MoO_2L^{d\text{-}f}]_2$.

In a round bottom flask equipped with a magnetic stirrer bar, 9.1 mmol of the selected Schiff base $H_2L^{d\text{-}f}$ and 10 mmol of $[MoO_2(acac)_2]$ were suspended in 50 mL of ethanol. The resulting suspension was stirred at reflux temperature for two hours. After that time, two thirds of the solvent were evaporated and the solution was cooled in an ice bath. The solid obtained was filtered and washed with cold ethanol and diethyl ether. The compounds were then dried under vacuum at 50°C for several days.

$[MoO_2L^d]_2$.
Yellow solid, yield: 38%. Anal. Calc. for $C_{13}H_8MoN_2O_6$ (Mr = 384.15): C, 40.6; H, 2.1; N, 7.3%. Found: C, 40.5; H, 1.5; N, 7.1%. TGA: exp(theo) Δm over 200-600 °C = 62.9 (62.6) %. IR (KBr, ν(cm^{-1})): 1603 (C=N), 1511 (NO_2), 1342 (NO_2), 922 (Mo=O), 798 (Mo-O-Mo). ^{1}H NMR (500 MHz, DMSO-d_6, δ(ppm)): 6.95 (d, 1H, *J* = 6.5 Hz), 7.09 (ddd, 1H, *J* = 7.5, 6.5, 1.0 Hz), 7.62-7.58 (m, 2H), 7.82-7.79 (m, 2H), 8.02 (d, 1H, *J* = 9.5 Hz) , 9.43 (s, 1H). $^{13}C\{^1H\}$ NMR (125 MHz, DMSO-d_6) δ: 162.0 (C_q-O), 161.5 (C_H-N), (C_q-O), 148.3 (C_q-N), 141.8 (C_q-N), 137.5 (C_H-Ar), 136.6 (C_H-Ar), 122.3 (C_q), 121.9 (C_H-Ar), 119.6 (C_H-Ar), 117.7 (C_H-Ar), 115.8 (C_H-Ar), 112.6 (C_H-Ar). HRMS (ESI) calc. for $C_{13}H_9N_2O_6Mo$, [M^++1] 386.9509, found 386.9511 [M^++1].

$[MoO_2L^e]_2$.

Brown solid, yield: 44%, mp >300 °C. Anal. Calc. for $C_{17}H_{18}MoN_2O_4$ (Mr = 410.28): C, 49.8; H, 4.4; N, 6.8%. Found: C, 49.6; H, 3.8; N, 6.7%. TGA: exp(theo) Δm over 200-600 °C = 64.4 (64.9) %. IR (ATR, ν(cm^{-1})): 1615(C=N), 927 (Mo=O), 844 (Mo-O-Mo). ^{1}H NMR (500 MHz, DMSO-d_6, δ(ppm)): 1.09 (t, 6H, *J* = 7 Hz, CH_3), 3.39 (q, 4H, *J* = 7 Hz, NCH_2), 6.07 (d, 1H, *J* = 2.5 Hz), 6.41 (dd, 1H, *J* = 9.0, 2.5 Hz), 6.72 (dd, 1H, *J* = 8, 1.5 Hz), 6.82 (ddd, 1H, *J* = 7.8. 7.5, 1.5 Hz), 7.04 (ddd, 1H, *J* = 7.8, 7.5, 1.5 Hz), 7.44 (d, 1H, *J* = 9.0 Hz), 7.59 (dd, 1H, *J* = 8.0, 1.0 Hz), 8.89 (s, 1H). ^{13}C{^{1}H} NMR (125 MHz, DMSO-d_6) δ: 163.5 (C_q-O), 159.7 (C_q-N), 154.8 (C_H-N), 154.2 (C_q-O), 137.6 (C_q-N), 137.1 (C_H-Ar), 128.0 (C_H-Ar), 120.5 (C_H-Ar), 117.0 (C_H-Ar), 115.6 (C_H-Ar), 111.6 (C_q), 106.4 (C_H-Ar), 99.5 (C_H-Ar), 44.7 (NCH_2), 13.1 (CH_3). HRMS (ESI), calc. for $C_{17}H_{19}N_2O_4Mo$ [M^++1] 413.0393, found: 413.0400 [M^++1].

$[MoO_2L^f]_2$.

Brown solid, yield: 42%, mp >300 °C. TGA: exp(theo) Δm over 200-600 °C = 69.2 (68.4) %. IR (ATR, ν(cm^{-1})): 1614 (C=N), 1503 (NO_2), 1325 (NO_2), 934 (Mo=O), 809 (Mo-O-Mo). Anal. Calc. for $C_{17}H_{17}MoN_3O_6$ (Mr = 455.27): C, 44.8; H, 3.8; N, 9.2%. Found: C, 44.7; H, 3.2; N, 9.1%. ^{1}H NMR (500 MHz, DMSO-d_6, δ(ppm)): 1.11 (t, 6H, *J* = 7 Hz, CH_3), 3.44 (q, 4H, *J* = 7 Hz, NCH_2), 6.12 (d, 1H, *J* = 2.5 Hz), 6.50 (dd, 1H, *J* = 9.0, 2.5 Hz), 7.48 (d, 1H, *J* = 2.3 Hz), 7.49 (d, 1H, *J* = 5.5 Hz), 7.74 (dd, 1H, *J* = 8.9, 2.3 Hz), 7.75 (d, 1H, *J* = 9 Hz), 9.01 (s, 1H). ^{13}C{^{1}H} NMR (125 MHz, DMSO-d_6) δ: 164.1 (C_q-O), 159.3 (C_q-O), 157.4 (C_H-N), 155.5 (C_q-N), 146.0 (C_q-N), 144.3 (C_q-N), 138.3 (C_H-Ar), 116.1 (C_H-Ar), 115.5 (C_H-Ar), 111.9 (C_q), 111.5 (C_H-Ar), 107.5 (C_H-Ar), 99.4 (C_H-Ar), 44.9 (NCH_2), 13.2 (CH_3). HRMS (ESI) calc. for $C_{17}H_{18}N_3O_6Mo$, [M^++1] 458.0244, found: 458.0250 [M^++1].

II.4.3.6. Synthesis of $[MoO_2(SATP)]_2$.

In a 100 mL Erlenmeyer flask, 0.50 g of salicylaldehyde (4.09 mmol) was dissolved in 50 mL of methanol and 0.50 g of 2-aminothiophenol (3.99 mmol) was added. Half an hour later, 1.34 g of [$MoO_2(acac)_2$] (4.11 mmol) was added. The mixture was stirred under reflux for 4 hours at room temperature. The resulting brown precipitate was separated by filtration, washed with CH_2Cl_2 and dried under reduced pressure for 24 hours.

Yield: 52%. TGA: exp(theo) Δm over 200-600 °C = 58.5 (59.5) %. IR (KBr, ν(cm^{-1})): 1602 (C=N), 920 (Mo=O), 781 (Mo-O-Mo). ^{1}H NMR (300 MHz, DMSO-d_6, δ(ppm)): 6.89-7.81 (m, 7 H, Ar-*H*), 9.06 (s, 1 H, C*H*=N). ^{13}C{^{1}H} NMR (300 MHz, DMSO-d_6)

δ: 163.0 (C_H-N), 161.3 (C_q-O), 148.1 (C_q-S), 138.6 (C_H-N), 137.0 (C_H-Ar), 136.8 (C_H-Ar), 129.8 (C_H-Ar), 129.1 (C_H-Ar), 125.8 (C_H-Ar), 123.1 (C_q), 120.9 (C_H-Ar), 119.6 (C_H-Ar), 119.1 (C_H-Ar). The ^{1}H and ^{13}C NMR spectra in DMSO-d_6 correspond to compound [MoO_2(SATP)(DMSO)].

II.4.3.7. Synthesis of [MoO_2L^g]$_2$.

In a 100 mL Erlenmeyer flask, 0.50 g of 2,3-dihydroxybenzaldehyde (4.09 mmol) was dissolved in 50 mL of methanol and 0.50 g of 2-aminothiophenol (3.99 mmol) was added, 0.5 hour later, 1.34 g of [$MoO_2(acac)_2$] (4.11 mmol) was added. The mixture was stirred for 4 hours at room temperature. The resulting brown precipitate was separated by filtration, washed with CH_2Cl_2 and dried under reduced pressure for 24 hours.

Yield: 69.9%. Anal. Calc. for $C_{13}H_9MoNO_4S$ (Mr = 371.225): C, 42.06; H, 2.44; N, 3.77%. Found: C, 43.37; H, 2.02; N, 3.64%. TGA: exp(theo) Δm over 200-600 °C = 61.1 (61.2) %. IR (KBr, ν(cm^{-1})): 1609 (C=N), 932, 901 (Mo=O), 770 (Mo-O-Mo).

II.4.3.8. Synthesis of [MoO_2L^h]$_2$

In a 100 mL Erlenmeyer flask, 0.50 g of 2,4-dihydroxybenzaldehyde (4.09 mmol) was dissolved in 50 mL of methanol and 0.50 g of 2-aminothiophenol (3.99 mmol) was added, 0.5 hour later, 1.34 g of [$MoO_2(acac)_2$] (4.11 mmol) was added. The mixture was stirred for 4 hours at room temperature. The resulting brown precipitate was separated by filtration, washed with CH_2Cl_2 and dried under reduced pressure for 24 hours.

Yield: 79%. Anal. Calc. for $C_{13}H_9MoNO_4S$ (Mr = 371.225): C, 42.06; H, 2.44; N, 3.77%. Found: C, 37.25; H, 2.37; N, 3.13%. TGA: exp(theo) Δm over 200-600 °C = 60.1(61.2) %. IR (KBr, ν(cm^{-1})): 1600 (C=N), 871 (Mo=O), 760 (Mo-O-Mo). ^{1}H NMR (300 MHz, DMSO-d_6, δ(ppm)): 6.26-7.66 (m, 7 H, Ar-*H*), 8.88 (s, 1 H, C*H*=N), 10.75 (s, 1 H, Ar-O*H*).

II.4.3.9. Synthesis of [MoO_2L^i]$_2$.

In a 100 mL Erlenmeyer flask, 0.25 g of 2,5-dihydroxybenzaldehyde (1.81 mmol) was dissolved in 40 mL of methanol and 0.25 g of 2-aminothiophenol (2.01 mmol) was added.Half an hour later, 0.70 g of [$MoO_2(acac)_2$] (2.14 mmol) was added. The mixture was stirred for 4 hours at room temperature. The resulting brown precipitate

was separated by filtration, washed with CH_2Cl_2 and dried under reduced pressure for 24 hours.

Yield: 88%. Anal. Calc. for $C_{13}H_9MoNO_4S$ (Mr = 371.225): C, 42.06; H, 2.44; N, 3.77%. Found: C, 42.04; H, 2.25; N, 3.77%. TGA: exp(theo) Δm over 200-600 °C = 61.8 (61.2) %. IR (KBr, ν(cm^{-1})): 1603 (C=N), 901 (Mo=O), 772 (Mo-O-Mo). ^{1}H NMR (300 MHz, DMSO-d_6, δ(ppm)): 6.68-7.72 (m, 7 H, Ar-*H*), 8.91 (s, 1 H, C*H*=N), 9.41 (s, 1 H, Ar-O*H*). ^{13}C{^{1}H} NMR (300 MHz, DMSO-d_6): 162.7 (C_H-N), 154.9 (C_q-O), 151.1 (C_q-O), 148.3 (C_q-S), 139.1 (C_H-Ar), 129.9 (C_H-Ar), 129.1 (C_H-Ar), 125.6 (C_H-Ar), 125.0, 122.9 (C_q), 120.4 (C_H-Ar), 120.0 (C_H-Ar), 119.2 (C_H-Ar).

III. Chapter III

Epoxidation of cyclooctene with molybdenum catalysts under organic solvent-free conditions

III.1. Introduction

Epoxides are important and widely used starting materials for value added products such as pharmaceuticals, flavor and fragrance molecules.[67] A broad variety of catalysts for olefin epoxidation has been described over the years with organometallic complexes being very efficient as catalysts for the synthesis for fine chemicals and for sophisticated organic substrates.[68]

Molybdenum Schiff base *ONO* and *ONS* Schiff base tridentate complexes have been tested in epoxidation of olefins by several authors in organic solvents.[69] In order to develop a cleaner process, we are exploring organic solvent-free oxidation condition,[70] *i.e.* using aqueous TBHP as oxidant and no added organic solvent. It has to be pointed out that water (that could be considered as a solvent in general way) is only working in the studied process as the oxidant carrier and not as a solvent for the catalytic reaction. It was therefore of interest to study these complexes under organic solvent-free conditions.

We have synthesized several (see chapter II) new molybdenum complexes containing *ONO* or *ONS* Schiff base donor ligands. All these complexes have been tested as catalysts in the epoxidation of cyclooctene. Different parameters have been compared, such as the effect of the substitution within the ligand, the catalyst loadings, the oxidant loading, the temperature, and the effect of water.

A general feature in all the experiments is that the complexes are slightly soluble at room temperature in cyclooctene and become soluble after addition of TBHP at the reaction temperature. The complexes are then confined in the organic phase at 80°C as shown by the color of the two phases during the entire reaction procedure. The water phase remains colorless or only slightly colored.

III.2. Results and discussion

III.2.1. Influence of the coordination sphere ONO vs. ONS

Nakamura *et al.*[71] have shown that a variation in the ligand donor atom has an effect on the reduction potential of octahedral mononuclear *cis*-dioxomolybdenum(VI) complexes. It was shown to be easier for a molybdenum complex to accept additional electrons due to the electron delocalization in the presence of sulfur. Topich found that the higher the energy of the first electronic transition the easier the complex was reduced (-0.97 Volts versus Ag/AgCl [13a]). In parallel to the qualitative results of Nakamura concerning the oxidation of hydrazines,

organophosphines, and alcohols using Mo^{VI} complexes, Topich studied the oxygen atom transfer (*OAT*) reactivity of Mo^{VI} complexes toward organophosphines, which was found in the order: *ONS* > *ONO*. [13b]

We thought that such coordination difference around the molybdenum metal could also have an influence on its activity within a catalytic process, especially for oxygen transfer. Thus, we have decided to compare the difference of catalytic activity of molybdenum precatalysts surrounded with a tridentate *ONS* ligand salicylideneaminothiophenolato (SATP) and *ONO* salicylideneaminophenolato (SAP). The activities have been tested within the organic solvent-free epoxidation of cyclooctene with aqueous TBHP (See Scheme 3.1).

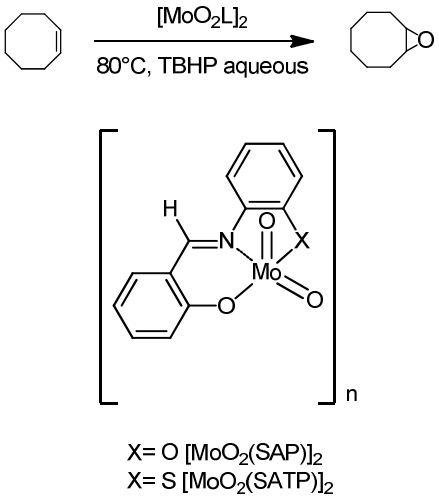

Scheme 3.1. Organic organic solvent-free epoxidation of cyclooctene with aqueous TBHP

The epoxidation of cyclooctene catalyzed by 0.5 mol% of $[MoO_2(acac)_2]$, $[MoO_2(SAP)]_2$ and $[MoO_2(SATP)]_2$ (Scheme 3.1) were carried out using 2 equivalents of TBHP as oxidant at 80°C. Among the three complexes, the most active catalyst is $[MoO_2(acac)_2]$ (96% conversion after 4 h, initial TOF = 270 h^{-1}). Complex $[MoO_2(SATP)]_2$, however, shows only slightly lower activity (90% of conversion after 4 hours, $TOF_{init.}$ = 253 h^{-1}), but much greater than $[MoO_2(SAP)]_2$ (76% of conversion, $TOF_{init.}$ = 70 h^{-1}).

The epoxide selectivity is high and similar for all three complexes (91, 93 and 94% for $[MoO_2(acac)_2]$, $[MoO_2(SAP)]_2$ and $[MoO_2(SATP)]_2$, respectively) (Table 3.1). In spite of its higher activity, however, complex $[MoO_2(acac)_2]$ is of less interest because of its decomposition under the catalytic conditions as pointed out before.

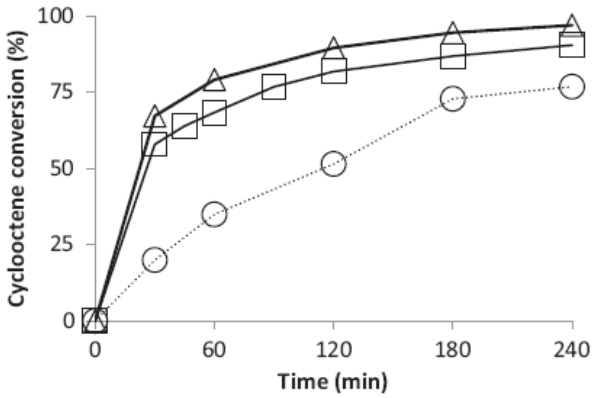

Fig. 3.1. Cyclooctene conversion *vs*. time catalyzed by $[MoO_2(acac)_2]$ (Δ), $[MoO_2(SAP)]_2$ (○) and $[MoO_2(SATP)]_2$ (□). Experimental conditions: Mo/TBHP/cyclooctene= 0.5/200/100; T = 80 ℃.

It was interesting to pursue the studies of those processes by evaluating the consequences of modifying different parameters.

III.2.2.Influence of the OH substitution on the aromatic ring

Since it was previously shown that a Mo/substrate ratio of 1% leads to efficient conversion, we have carried out new investigations with a reduced catalyst loading. Furthermore, the effect of introducing a free OH group on one aromatic ring, as well as the replacement of one oxygen atom by a sulfur one in the coordination sphere, has been studied using less than 0.5% Mo/substrate ratio and two equivalents of aqueous TBHP without addition of organic solvent.

III.2.2.1. Case of the ONO ligands: effect of the OH substitution

The introduction of an OH group at different positions on the organic ligand (Scheme 3.2) has resulted in an increase of the cyclooctene conversion after 4 h (See table 3.1). Indeed, while the reference catalyst $[MoO_2(SAP)]_2$ led to a 76% conversion after 4 h under these conditions, the introduction of an OH group in any of the aromatic ring positions accelerated the reaction for the dinuclear $[MoO_2L]_2$ catalysts and also for one ethanol-stabilized mononuclear $[MoO_2L(EtOH)]$ catalyst.

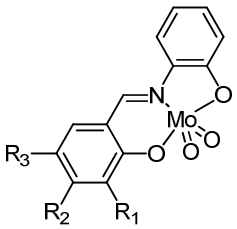

$[MoO_2L^{a-c}]$, $[MoO_2(SAP)]$

SAP, $R_1=R_2=R_3=H$
L^a, $R_1=OH$, $R_2=R_3=H$
L^b, $R_1=R_3=H$, $R_2=OH$
L^c, $R_1=R_2=H$, $R_3=OH$

Scheme 3.2.The pentacoordinated “active species” with *ONO* ligands substituted by an OH group on the salicylaromatic ring.

The cyclooctene conversion was higher with the OH-containing dimeric compounds in the order $[MoO_2L^a]_2$ (92%) > $[MoO_2L^c]_2$ (81%) > $[MoO_2(SAP)]_2$ (74%) ≈ $[MoO_2L^b]_2$ (73%) (Fig. 3.2, Table 3.1). The selectivity towards cyclooctene oxide is very good, higher than 90% for all the complexes. The absolute yield of cyclooctene oxide being around 85% with $[MoO_2L^a]_2$, it is possible to elect it as the best catalyst of the series. It has to be noticed that complex $[MoO_2L^b(EtOH)]$ gave a lower conversion (73%) than the dinuclear complexes $[MoO_2L^a]_2$ and $[MoO_2L^c]_2$, similar to $[MoO_2(SAP)]_2$. The lower reactivity of $[MoO_2L^b(EtOH)]$ relatively to $[MoO_2L^a]_2$ and $[MoO_2L^c]_2$ might be attributed to the ability to form the coordination ethanol molecule (hard to remove from the coordination sphere from the synthetic process), while the dimer $[MoO_2L^b]_2$ (74%) has the similar activity. It has to be noticed that the color of $[MoO_2L^b]_2$ changed to orange immediately once TBHP was added to the mixture of $[MoO_2L^b]_2$ and cyclooctene. This could indicate that, due to its strong coordination ability, $[MoO_2L^b]_2$ might form a monomer with some donor present in solution. This coordination could explain why the catalytic activity is slower than the other ones.

In order to try to explain the difference between all these complexes, several factors could be invoked. A noticeable acceleration can be observed in the case of $[MoO_2L^a]_2$ (TOF is around 250 h^{-1}) in which the free OH group lies in the 2 position. The second catalyst in order of activity is $[MoO_2L^c]_2$ in which the free OH group is in 5 position relative to the oxygen atom linked to the molybdenum atom, indicating the favorable contribution of electronic delocalization on the catalytic cycle energy span.

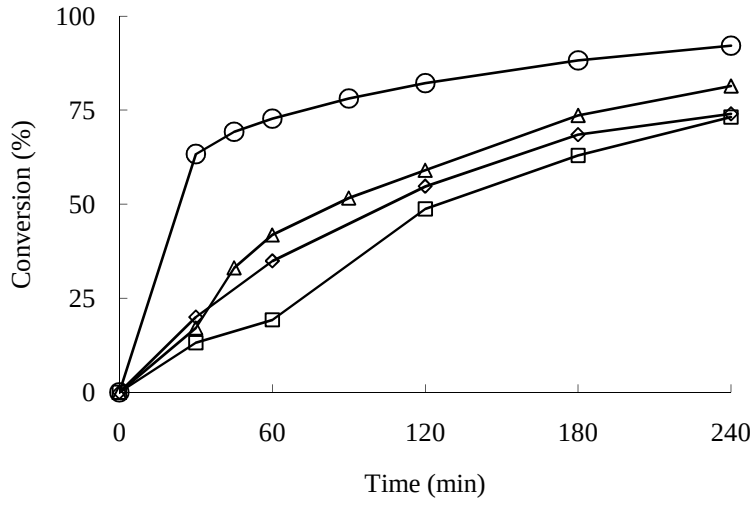

Fig. 3.2. Cyclooctene conversion *vs*. time with different *ONO* based (pre)catalysts $[MoO_2(SAP)]_2$ (◇), $[MoO_2L^a]_2$ (○), $[MoO_2L^b(EtOH)]$ (□) and $[MoO_2L^c]_2$ (Δ) at 80℃. Experimental conditions are given in Table 3.1.

III.2.2.2. Case of the ONS ligands: effect of the OH substitution

The influence of the ring substitution by an OH group at the same three positions has been also investigated for the *ONS*-type ligands (Scheme 3.3) using the same experimental conditions.

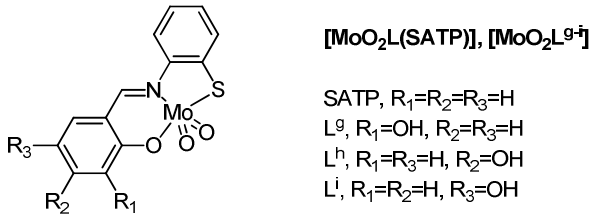

Scheme 3.3. The pentacoordinated "active species" with *ONS* ligands substituted by an OH group on the salicylaromatic ring.

The activation of the catalyst seems very fast (See Table 3.1 and Fig. 3.3), since very high activity relatively to the oxygen containing complexes has been observed with TOF up to 250 h^{-1} for all compounds. In this case, like for the relative *ONO* complexes, the $[MoO_2(SATP)]$ complex (bearing no OH on the aromatic ring) gives the lowest conversion in comparison to the OH substituted analogues (90% for $[MoO_2(SATP)]$, up to 95% for the other ones) but also the highest selectivity towards oxide (94%, relative to 82-88% for the other complexes). It seems that the presence of the OH group favors a faster transformation of the cyclooctene oxide into its corresponding diol through ring opening.

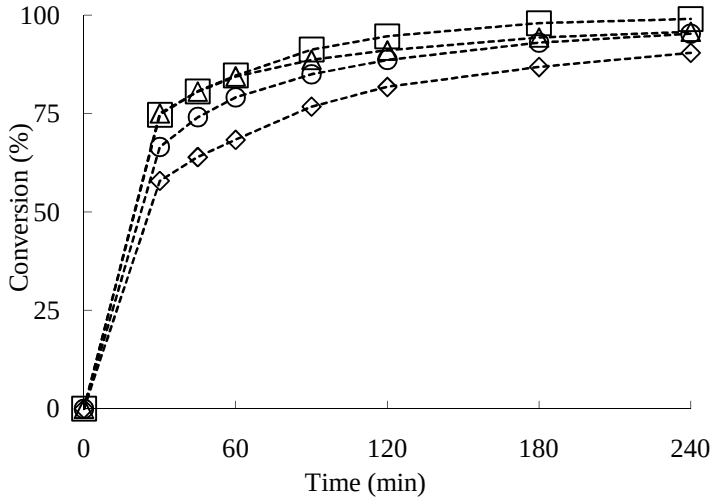

Fig. 3.3. Cyclooctene conversion *vs*. time with different ONS based (pre)catalysts $[MoO_2(SATP)]_2$ (◇), $[MoO_2L^g]_2$ (○), $[MoO_2L^h]$ (□) and $[MoO_2L^i]_2$ (Δ) at 80℃. Experimental conditions are given in Table.

Table 3.1– Organic solvent-free epoxidation of cyclooctene with different molybdenum complexes.

Catalyst	Conversion [%]	Selectivity [%]	TOF [h^{-1}]	TON
$[MoO_2(SAP)]_2$	74	93	70	153
$[MoO_2L^a]_2$	92	93	251	184
$[MoO_2L^b]_2$	73	85	71	146
$[MoO_2L^b(EtOH)]$	74	90	68	148
$[MoO_2L^c]_2$	81	91	127	163
$[MoO_2(SATP)]_2$	90	94	253	180
$[MoO_2L^g]_2$	95	88	267	195
$[MoO_2L^h]_2$	98	82	298	196
$[MoO_2L^i]_2$	96	87	303	193

Conditions : Mo/TBHP/cyclooctene = 0.5/200/100; T = 80°C; t = 4 h. TOF is calculated on the time interval with maximum slope for the conversion plot.

III.2.3.Influence of the substitution with electron donor (NEt_2) and/or electron acceptors (NO_2)

$[MoO_2(SAP)]_2$ and $[MoO_2L^{d-f}]_2$ complexes have been tested under the same organic solvent-free conditions and using the same substrate (cyclooctene) and oxidant (TBHP) as described in the previous sections[48] for the derivatives with the OH-substituted SAP-type and SATP-type ligands in order to further evaluate the role of the substituents on the ligand backbone on the catalytic activity.

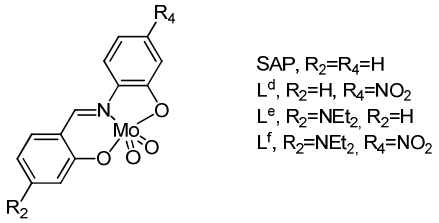

SAP, R_2=R_4=H
L^d, R_2=H, R_4=NO_2
L^e, R_2=NEt_2, R_2=H
L^f, R_2=NEt_2, R_4=NO_2

Scheme 3.4.

The catalysts (very low catalyst/substrate ratio (0.25/100)) become fully soluble in the organic phase upon warming after addition of the aqueous TBHP reagent, which is also transferred together to the organic phase. The small amount of water originating from the oxidant solution remains as a separate colorless phase. The results have been compiled in Table 3.2 and the kinetic results are shown in Fig. 3.4.

The cyclooctene conversion after 4 h was found to decrease in the following order $[MoO_2L^d]_2$ > $[MoO_2L^f]_2$ ≈ $[MoO_2(SAP)]_2$ > $[MoO_2L^e]_2$. The selectivity, however, is always high (always greater than 90%).

The presence of the electron withdrawing NO_2 group (ligand L^d) has a small positive effect on the activity, while the NEt_2 donor group (ligand L^e) shows a weak negative effect. When both groups are present within the structure (ligand L^f), the two effects overlay which gives an activity very close to that of the parent SAP backbone.

Table 3.2 Epoxidation of cyclooctene with catalysts with electron withdrawing and donor group.

Catalyst	Conversion (%)[a]	Selectivity (%)[a]	TON	TOF/h^{-1}
$[MoO_2\ (SAP)]_2$	71	94	286	195
$[MoO_2L^e]_2$	62	93	252	167
$[MoO_2L^d]_2$	86	96	346	344
$[MoO_2L^f]_2$	73	91	293	192

[a] values were taken after 4 h.

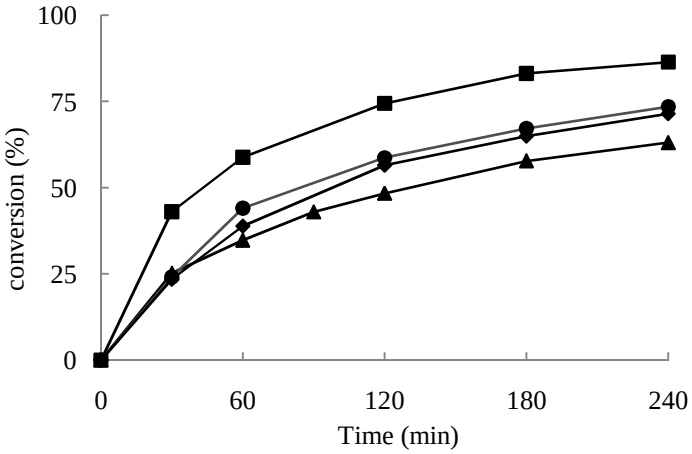

Fig. 3.4. Kinetic profile of converted cyclooctene *vs*. time with dioxidomolybdenum(VI) catalysts: $MoO_2(SAP)]_2$ (♦), $[MoO_2L^d]_2$ (■), $[MoO_2L^e]_2$ (▲), $[MoO_2L^f]_2$(●). Conditions: TBHP/substrate/[Mo] = 800:400:1; T = 80℃.

III.2.4. Influence of the catalyst loading

The first experiments were performed with 1% catalyst *vs*. substrate. The influence of catalyst loading has been investigated by carrying out additional catalytic experiments following the same procedures but with decreased amounts of catalyst.

Decreasing the catalyst loading down to 0.025% (250 ppm) while maintaining the same substrate amount and TBHP/substrate ratio still allowed attainment of high conversions after 4 h for the $[MoO_2(SATP)]_2$ catalyst, higher than with a greater loading of the $[MoO_2(SAP)]_2$ catalyst, see Table 3.3, Fig 3.5. The selectivity remains high for the $[MoO_2(SATP)]_2$ catalyst while it is slightly eroded at the lowest loadings of $[MoO_2(SAP)]_2$, see Table 3.3. The increase of initial TOF as the catalyst loading is decreased (up to 2697 h^{-1} with 0.025% of the $[MoO_2(SATP)]_2$ complex) suggests that at high concentrations, the catalyst is not entirely in its active form, although optical evidence was in favor of complete dissolution and confinement of the complex in the organic phase at the high temperature of the catalytic runs. A possible interpretation is equilibrium dissociation of the stable dimer into catalytically active monomer.

Table 3.3 Influence of catalyst loading on epoxidation of cyclooctene with $[MoO_2(SAP)]_2$, and $[MoO_2(SATP)]_2$.

Catalyst	x / Mo	Conversion (%)	Selectivity (%)	$TOF_{init.}[h^{-1}]$	TON
$[MoO_2(SAP)]_2$	1.00	64	93	44	64
	0.60	66	90	42	100
	0.33	65	82	104	240
	0.24	63	79	123	252
	0.15	59	74	203	393
	0.10	50	73	131	500
$[MoO_2(SATP)]_2$	1.00	95	89	203	95
	0.60	94	98	273	156
	0.11	86	94	920	760
	0.05	82	94	1270	1639
	0.025	68	93	1204	2697

[a]Conditions: Mo/TBHP/cyclooctene = x/200/100, T = 80°C, t = 4 h. The initial TOF is calculated from the conversion after the first 30 min.

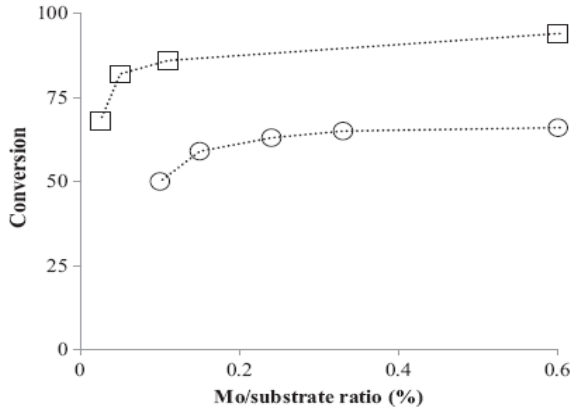

Fig. 3.5. Cyclooctene conversion after 4 h as a function of the catalyst loading for $[MoO_2(SAP)]_2$ (○) and $[MoO_2(SATP)]_2$ (□). Conditions: T = 80 ℃, [Mo]/cyclooctene/TBHP = x/100/200.

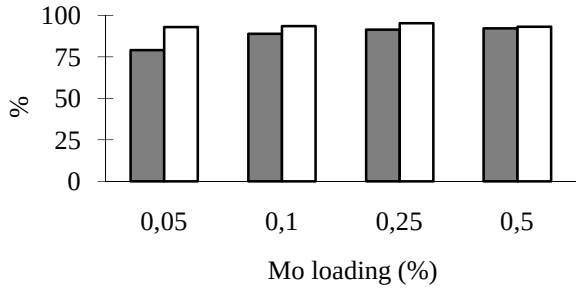

Fig. 3.6. Effect of catalyst ($[MoO_2L^a]$) loading for epoxidation of cyclooctene conversion (■), selectivity (□). Conditions: substrate/TBHP = 100:200; T = 80℃.

Different catalyst loadings have also been tested with the most active *ONO* complex $[MoO_2L^a]_2$ (Fig. 3.6 and Table 3.4) in order to see the effect of the Mo/substrate ratio for fixed substrate and TBHP amounts. The conversion increases slightly with the catalyst loading and selectivity remains constant (in the range 92-95%). Nevertheless, the activity of the catalyst is very high with relatively low Mo loading since the TOF goes up to a value of 1074 h^{-1} when using only 0.05% catalyst. This trend is identical to that shown above for the $[MoO_2(SAP)]_2$ and $[MoO_2(SATP)]_2$ catalysts. The activity is not proportional to the catalyst concentration, indicating that other factors should be taken into account along the process. One assumption is that the decrease of catalyst loading increases the water/Mo ratio and might be one factor in order to activate efficiently the catalyst. At the same time, the TBHP/Mo ratio increases linearly with the water/Mo ratio. These concomitant factors may counterbalance the putative negative effect brought by water. Other experiments with fixed TBHP/Mo ratio and variable water/Mo ratio have been carried out as shown below, using the $[MoO_2(SATP)]_2$, in order to assess the possible negative effect of water.

Table 3.4 Influence of catalyst loading on epoxidation of cyclooctene with $[MoO_2(SAP)]$ and $[MoO_2L^a]$ complexes at 80℃: [Mo]/cyclooctene/TBHP = x/100/ 200 TBHP. Reaction time is 4 h.

Complex	x / Mo	Conversion (%)	Selectivity (%)	$TOF_{init.}[h^{-1}]$	TON
$[MoO_2L^a]_2$	0.05	79	92	1074	1596
	0.10	88	93	1124	895
	0.25	91	95	517	365
	0.50	92	93	251	184
$[MoO_2(SAP)]_2$	1.00	64	93	44	64
	0.60	66	90	42	100
	0.33	65	82	104	240
	0.24	63	79	123	252
	0.15	59	74	203	393
	0.10	50	73	131	500

III.2.5.Influence of water

The oxidant is carried into the mixture in aqueous solution. Since a decrease of catalyst loading entails an increase of the water/catalyst ratio, the effect of water was independently investigated while keeping the catalyst loading and TBHP/substrate ratio constant.

Additional experiments were carried out for catalysts $[MoO_2(SAP)]_2$, $[MoO_2L^a]_2$ and $[MoO_2(SATP)]_2$ with constant amounts of catalyst, substrate and TBHP at the fixed 0.5/100/200 ratio in the presence of increasing amounts of additional water (see Table 3.5). These catalytic runs yield only slightly lower TOF values at higher water/[Mo] ratios, showing only a slightly negative effect of water on the catalysis. Therefore, the dramatic TOF increase observed at lower catalyst loading (greater water/[Mo] ratios) in Figures 3.7 and 3.8 cannot be attributed to a chemical activation of the catalyst by water. Increasing amounts of water have only a slightly negative effect on the conversion, which could simply be related to a decreasing TBHP concentration in the olefin phase. The selectivity does not appear to be significantly affected by the water amount.

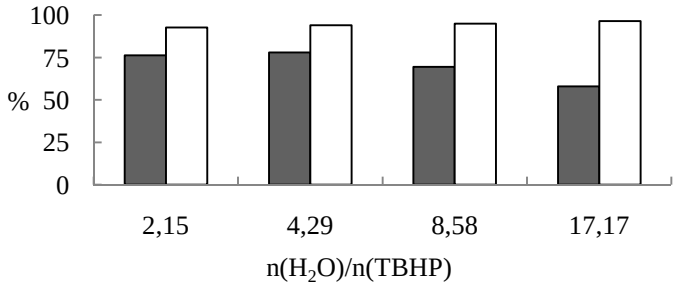

Fig. 3.7. Water influence of epoxidation of Cyclooctene with catalyst ($[MoO_2(SAP)]_2$), conversion (■), selectivity (□). Conditions: substrate/TBHP = 100:200; T = 80℃.

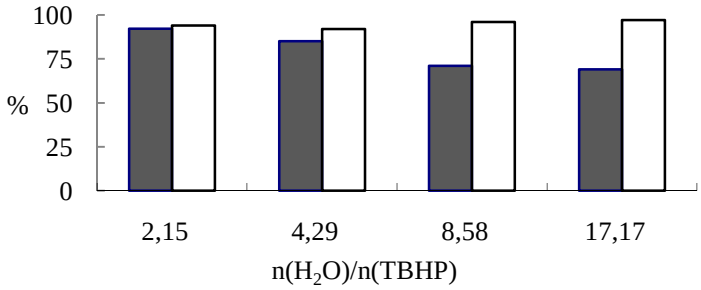

Fig. 3.8. Water influence of epoxidation of Cyclooctene with catalyst ([MoO_2L^a]$_2$), conversion (■), selectivity (□). Conditions: substrate/TBHP = 100:200; T = 80℃.

Table 3.5. Influence of water on cyclooctene epoxidation catalyzed by [MoO_2(SAP)]$_2$, [MoO_2L^a]$_2$ and [MoO_2(SATP)]$_2$.[a]

Complex	n(H_2O)/n(TBHP)	Conversion/%			Oxide selectivity%			$TOF_{init}/[h^{-1}]$	TON
		2h	3h	4h	2h	3h	4h		
[MoO_2(SAP)]$_2$	2.15	51	72	76	89	93	92	70	153
	4.29	63	-	78	-	93	94	111	157
	8.58	47	-	69	-	94	95	67	139
	17.17	37	-	58	-	98	96	52	117
[MoO_2L^a]$_2$	2.15	82	88	92	95	94	94	256	184
	4.29	83	-	85	96	-	92	206	170
	8.58	73	-	71	94	-	96	82	143
	17.17	54	-	69	98	-	97	68	152
[MoO_2(SATP)]$_2$	2.15	97	99	99	90	84	79	308	199
	3.22	96	98	99	89	87	83	293	199
	4.29	91	96	98	92	90	87	244	198
	8.58	87	94	97	91	90	88	237	194
	17.17	75	86	92	95	89	88	175	185

[a] Conditions: [Mo]/cyclooctene/TBHP = 0.5/100/200; T = 80°C, t = 4 h. The initial TOF is calculated from the conversion after the first 30 min.

The influence of water was also tested with [MoO_2(SATP)]$_2$ (Table 3.5 and figure 3.9). Increase of the water amount as an effect on several parameters. The starting water/TBHP ratio of 2.15 corresponds to the reaction without added water, *i.e.* considering only water brought by the commercial aqueous TBHP. The cyclooctene conversion slightly decreases with the increase of the water content, indicating that water does certainly affect the catalytic cycle, whether interacting with the catalyst to generate an inactive form or interfering with the mass transfer process (diminishing the quantity of TBHP in the organic phase). The TOF is also lower when more water is added. The selectivity is also affected by the water amount. Surprisingly, the increase of the water amount seems to increase the selectivity towards oxide (which at first glance seems counterintuitive). Another noteworthy fact is that, in each reaction, the selectivity towards oxide decreases slightly at longer reaction times, being slightly lower after 4 h than after 3 h.

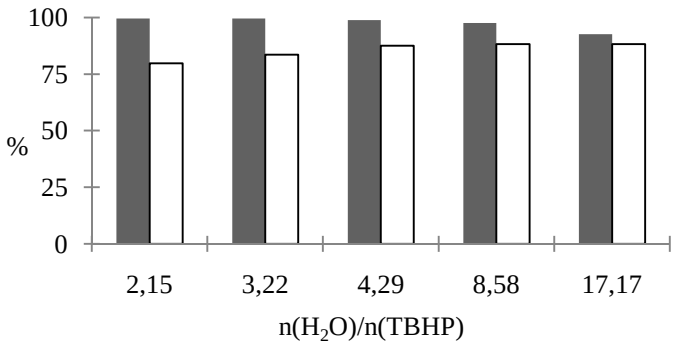

conversion (■), selectivity (□).

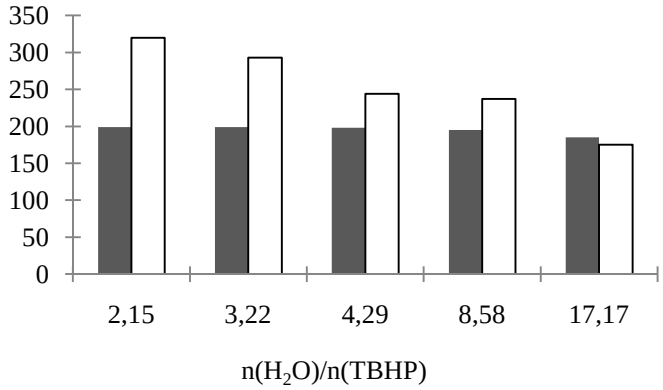

TON (■), TOF (□).

Fig. 3.9. Water influence of epoxidation of Cyclooctene with catalyst ([MoO_2(SATP)]), Conditions: substrate/TBHP/catalyst = 100:200:0.5, T = 80℃, after 4 h.

III.2.6.Influence of TBHP ratio

In addition to the above trends, the effect of other experimental parameters on catalysis has been investigated for selected systems. For the $[MoO_2L^c]_2$ and $[MoO_2L^i]_2$ catalysts, the reaction was run at various THBP/substrate ratios between 1.1 and 2.5.

These two complexes were selected in order to study the influence of *O vs. S* as a donor atom. The results are summarized in Table 3.6. It is shown as expected that higher TBHP/substrate ratios give higher conversions after 4h, with relatively high TOFs.

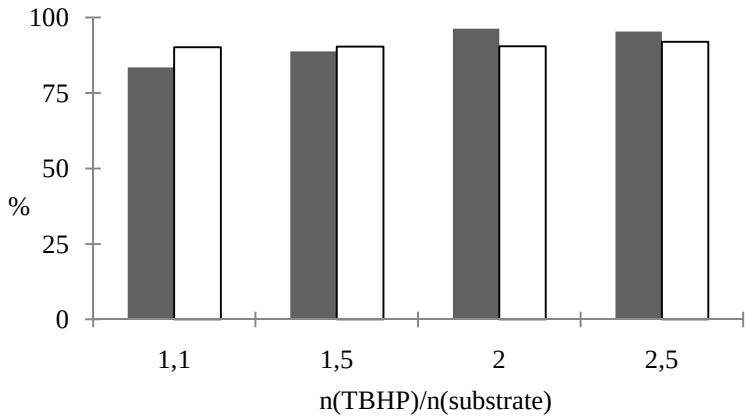

Fig. 3.10. TBHP influence of $[MoO_2L^c]_2$, conversion (■), selectivity (□). Conditions: substrate/TBHP/catalyst = 100:x*100:0.5, T = 80℃, after 4 h.

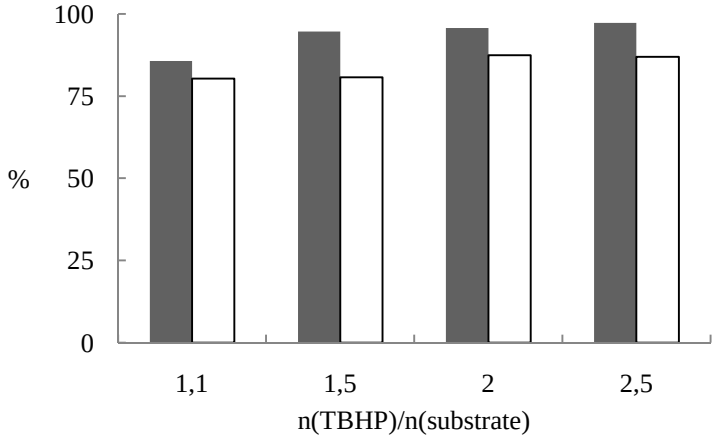

Fig. 3.11. TBHP influence of $[MoO_2L^i]_2$, conversion (■), selectivity (□). Conditions: substrate/TBHP/catalyst = 100:x*100:0.5, T = 80℃, after 4 h.

For both catalysts, the TOF increased when the THBP/substrate molar ratio is less than 2. The TOF started to decrease while the THBP/substrate ratio is beyond 2, the highest TOF was observed at a THBP/substrate ratio of 2 for both catalysts.

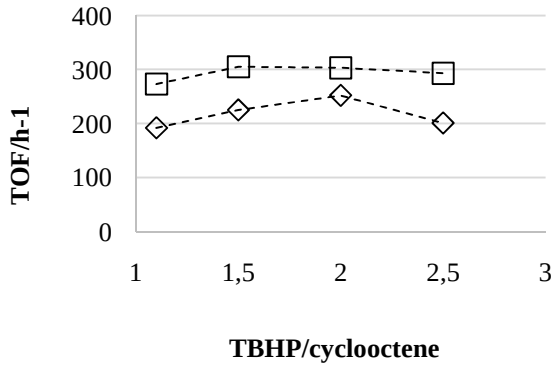

Fig. 3.12 Variation of the initial TOF as a function of TBHP/cyclooctene ratio for the processes catalyzed by $[MoO_2L^c]_2$ (◊) and $[MoO_2L^i]_2$ (□), conditions: substrate/TBHP/catalyst = 100:x*100:0.5, T = 80℃, after 4 h..

Table 3.6 Influence of TBHP quantity for epoxidation of cyclooctene with $[MoO_2L^c]_2$ and $[MoO_2L^i]_2$: [Mo]/cyclooctene/TBHP ratio = 0.5/100/x. Reaction time = 4 h, T = 80℃.

Complex	x TBHP	Conversion [%]	Selectivity [%]	TOF [h^{-1}]	TON
$[MoO_2L^c]_2$	110	83	90	192	167
	150	88	90	225	178
	200	96	90	252	193
	250	95	92	201	191
$[MoO_2L^i]_2$	110	85	80	273	171
	150	94	76	305	189
	200	96	87	303	193
	250	97	86	293	194

Conditions : Mo/TBHP/cyclooctene = 0.5/x/100; T = 80°C; t = 4h. TOF is calculated on the time interval with maximum slope for the conversion plot.

III.2.7.Recovery and Reuse of catalyst $[MoO_2(SATP)]_2$

The catalyst recovery and recycling was investigated for catalyst $[MoO_2(SATP)]_2$ for 6 consecutive runs. The complex was left in the reactor, all the volatiles being removed though high vacuum and reused directly in the reactor by adding new subtstarte and oxidant. The conversion remains over 90%, and the selectivity does not decrease. This shows that there is no significant loss of catalytic activity (Fig. 3.14) of the catalyst present in the reactor.

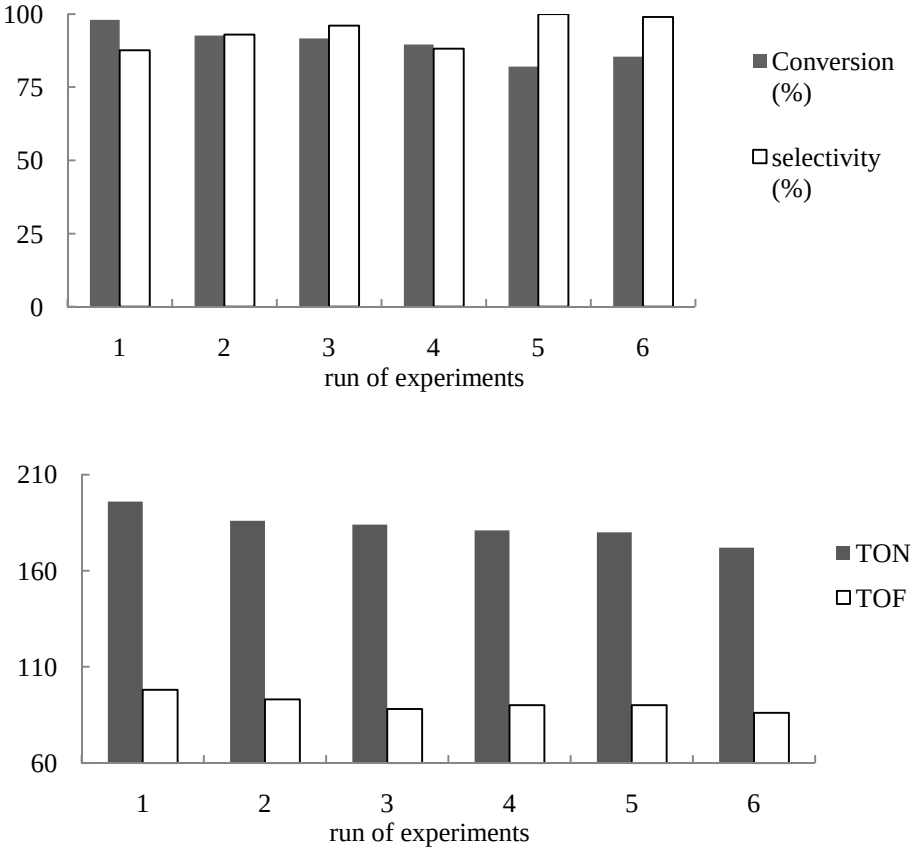

Fig. 3.13. [Mo]/cyclooctene/TBHP ratio = 0.5/100/x. Each experiment was done during 2 h.

This experiment showed that it is possible to recover a catalyst from reactor and the catalyst is stable in the reaction condition. However, the procedure being time and energy consuming, this method is not the right one to obtain recoverable catalysts. Based on this fact, it is possible to develop another way for the recovery and reuse of the molybdenum catalysts, grafting being a possible method.

III.3. Conclusion

In this chapter, the catalysts prepared in chapter **II** have been applied to the epoxidation of cyclooctene under organic solvent-free conditions. The influence of ligand substituents at different positions has been studied.

The cyclooctene conversion was higher with the OH-containing dimeric compounds in the order $[MoO_2L^a]_2$ (92%) > $[MoO_2L^c]_2$ (81%) > $[MoO_2(SAP)]_2$ (76%) ≈ $[MoO_2L^b]_2$ (73%). The cycloctene oxide selectivity is very high, more than 90% for all the complexes. The $[MoO_2L^a]$ catalyst shows the highest catalytic activity (conversion: 92%, selectivity: 93% after 4 h) among the *ONO*-type complexes.

In another aspect, the replacement of the aminophenolato oxygen donor atom by a sulfur atom leads to higher conversions but the selectivity is slightly decreased compared to that of the corresponding *ONO* catalyst.

In order to optimize the reaction conditions, various parameters have been studied, such as catalyst loading using different Mo/substrate ratio at a 80°C, oxidant loading, as well as different added amount of water. The catalyst recovery and recycling have been investigated, indicating the stability and recyclability of these complexes. This result suggests the possibility to graft these complexes to inert solid supports.

III.4. Experimental section

III.4.1. Materials and methods

All preparations were carried out in air. Cyclooctene (98% Aldrich), cyclooctene oxide and TBHP (70% in water, ACROS), were used as received without any purification. Catalytic reactions were followed by gas chromatography on an Agilent 6890A chromatograph equipped with FID detector, a HP5-MS capillary column (0.30 m x 0.25 mm x 0.25 m) and automatic sampling, or on a Fisons GC 8000 chromatograph equipped with FID detector and with a SPB-5 capillary column (30 m x 0.32 mm x 0.25 m). The GC parameters were quantified with authentic samples of the reactants and products. The conversion of *cis*-cyclooctene and the formation of cyclooctene oxide were calculated from calibration curves (r^2= 0.999) relatively to an internal standard.

III.4.2. Catalytic Procedures.

In a typical experiment, cyclooctene (1 equiv) and catalyst (x equiv, see tables) were mixed together then stirred in air in a round bottom flask. Acetophenone was added as internal standard. The reaction temperature was fixed at 80°C and then THBP aqueous (70% in water, y equiv see tables) was added to the mixture, starting the reaction. Samples of the organic phase were periodically withdrawn. The reaction was quenched by addition of MnO_2, followed by the addition of diethylether and removal of the manganese oxide and residual water by filtration through silica before GC analysis.

Recovery procedure for $[MoO_2(SATP)]_2$

The procedure of catalysis is the same as above. After two hours of reaction, one sample of the organic phase was taken for the analysis. The complex was maintained in the reactor, removing all the volatiles removed though high vacuum for more than 12 hours. The same amount of substrate and oxidant was added as in the first run, and the next run was started. Each experiment was left at 80°C under stirring during 2 h.

IV. Chapter IV

Oxidation with aqueous TBHP of cyclohexene and limonene under organic solvent-free conditions with molybdenum catalysts

IV.1. Introduction

Monoterpenic compounds are widely distributed in nature as constituents of the essential oil of many plants and fruits. These natural substances play an important role for the flavor and fragrance industries, essentially based on the chemistry of terpenes.[72] Monoterpene epoxides often serve as starting materials for the synthesis of several fragrances, flavors, food additives, herbicides, fungicides and biologicallyactive and therapeutically useful compounds.[73] Enantiopure epoxy-terpenes are valuable building blocks in the asymmetric synthesis of natural products.[74]

The compound studied in this chapter, limonene, is an inexpensive compound obtained commercially from citrus fruits, especially as a sub-product of the orange juice industry. (+)-Limonene is the monocyclic terpene spread worldwide.[75] The corresponding endocyclic epoxide, also called 1,2-epoxy-p-menth-8-ene (LO will be used as abbreviation), is the product of the endocyclic double bond epoxidation (see Scheme 4.1). LO is found naturally in the essential oil of *Cymbopogon densiflorus*, is a typical representative of a substituted cyclohexene epoxide.[76] LO is useful in several applications including metal coatings, varnishes, printing inks, and can copolymerize with CO_2 to form biodegradable polycarbonates.[77]

Using innocuous oxidants and non-hazardous catalysts for environmentally friendly processes are important requirements within the concept of green chemistry.

So far, using non-catalytic transformations of limonene to more valuable oxygenated derivatives by oxidation processes is the most common method.

As shown in the literature, it is possible to epoxidize regioselectively (+)-limonene via a Prilezhaev reaction to generate LO as an enantiomeric mixture.[78] Limonene is considered[79] as a suitable model terpene to evaluate the activity and selectivity properties of an epoxidation catalyst.

IV.2. Results and discussion

IV.2.1. General considerations about the oxidation of limonene catalyzed by molybdenum catalysts

The complexes synthesized in chapter **II** have also been used as catalysts in the oxidation of limonene. The effect of the substitution of one aromatic ring by OH-functional groups, as well as the replacement of one oxygen atom by a sulfur one have been studied using different Mo/substrate ratio at different reaction temperatures and different equivalents of aqueous TBHP.

The epoxidation of limonene is challenging since the molecule contains two different alkene moieties, one internal and one terminal. The oxidation products obtained strongly depend on the nature of catalyst, oxidant and reaction conditions. For instance, aqueous media facilitate the epoxide ring opening reaction. It has been shown that O_2 in the air can affect the products yield and selectivity catalyzed by biomimetic Ru-(terpy)(bpy) complex on silica surface.[80]

In literature, high stereoselectivities have been achieved in favor of LOs with different metal-based catalysts, such as $[\gamma\text{-}1,2\text{-}H_2SiV_2W_{10}O_{40}]^{4-}$ (exo-LO: 99% of all LOs),[81] $Fe(bpmen)(OTf)_2$ (LOs/exo-LO = 10:1),[82] or Ti/SiO_2-DI catalysts (LOs/exo-LO = 98:2).[83]

In our case, the main products of limonene oxidation are LOs (*cis* & *trans*), diaxial & diequatorial limonene diols (called *ax*-LD and *eq*-LD) and traces of other compounds, as carvone, carveol or other diols (scheme 4.1).

The *ax*-LD is (1S, 2S, 4R)-(+)-limonene-1,2-diol. Besides LOs and LDs, the diepoxide[84] can also be produced. The ring opening of the two oxiranes of the diepoxide gives the 1,2,8,9-diol product.[85] As expected, *cis* and *trans*-LOs are more abundant than limonene 8,9-epoxide over all the catalysis experiments, the preferential oxidation of the endocyclic C=C bonds being due to its higher electronic density.

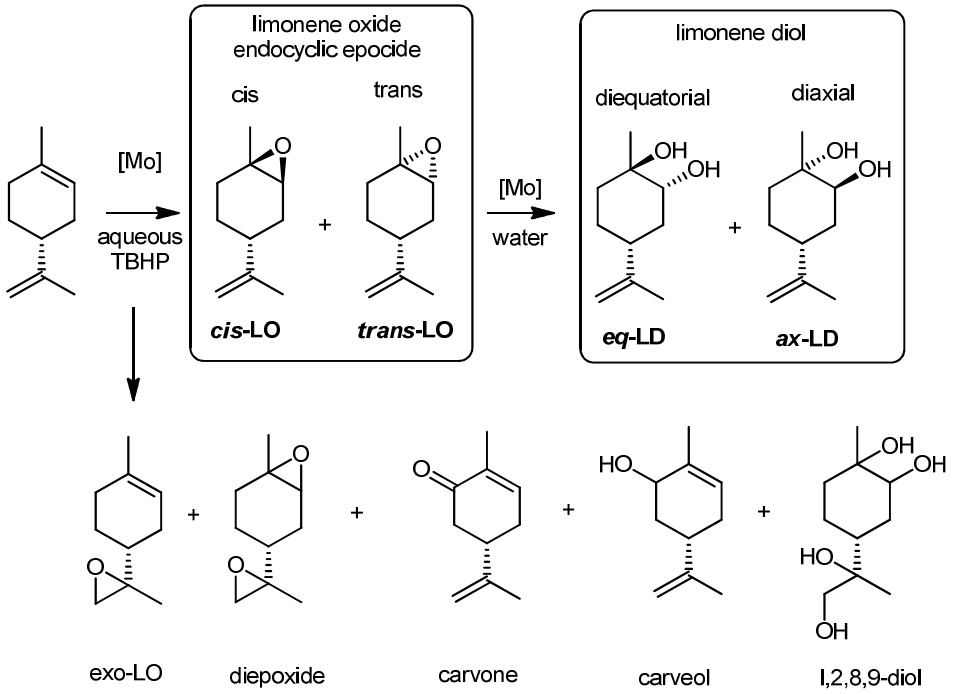

Scheme 4. 1. oxidation of limonene by molybdenum complex and potential products.

IV.2.2. Influence of coordination sphere: ONO vs. ONS

The influence of the coordination sphere around the molybdenum (*ONO vs. ONS*) has been investigated at 80°C with 2 equivalents of TBHP and limonene (Scheme 4.2). With 0.5% catalyst loading (see Table 4.1 and Figure 4.1), very high activity was observed in presence of $[MoO_2(SAP)]_2$ and $[MoO_2(SATP)]_2$, higher for the latter, the conversion of limonene being 79% (after 4 hours) and 93% (after 30 minutes) for the both catalysts, respectively, A blank experiment, with oxidant but without catalyst at 80°C, showed that only 7.6% of limonene was converted after 6 hours, proving the catalytic activity of both complexes.

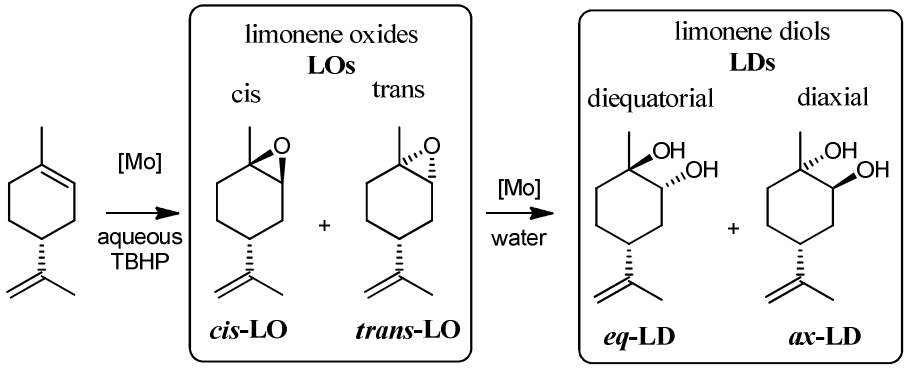

Scheme 4. 2. Epoxidation of limonene and the ring opening of its products.

Table 4. 1. Influence of O *vs*. S for oxidation of limonene: [Mo]/limonene/TBHP = 0.5/100/200, T = 80℃.

catalyst	Conversion (%)	Selectivity LO (%)	Yield (%)				TON	TOF (h^{-1})
			LO		LD			
			cis	trans	eq	ax		
No cat.[a]	7.6	18.5	0.4	1.1	0.03	0.5	-	-
$[MoO_2(SAP)]_2$[a]	79	28.5	2.6	19.8	1.8	26.5	158	130
$[MoO_2(SATP)]_2$[b]	93	0	0	0	11.5	37.8	185	371

[a]4h,[b]0.5 h

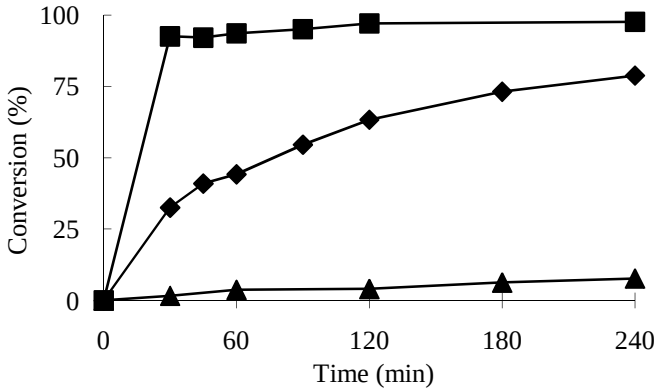

Figure 4. 1. Kinetic profile of *ONO vs*. *ONS* to oxidation of limonene: without catalyst (▲), $[MoO_2(SAP)]_2$ (♦), $[MoO_2(SATP)]_2$ (■). [Mo]/limonene/TBHP = 0.5/100/200, T = 80℃.

Without catalyst, only 7.6% of the limonene was converted after 4 hours reaction. Traces of *cis*-LO, *trans*-LO and *eq*-LD, *ax*-LD were detected.

With the $[MoO_2(SAP)]_2$ catalyst, the quantity of *cis*-LO detected from 30 minutes of the reaction decreases slowly, while the quantity of *trans*-LO keeps constant. Both diols are observed, ax-LD being more present than *eq*-LD. The proportions of LOs and LDs were studied more deeply between 60 minutes and 240 minutes. During this time period, the limonene conversion increased from 44 to 78% (see Figure 4.1) with $[MoO_2(SAP)]_2$. The quantity of *cis*-LO decreased from 13.8% to 2.6% while the *trans*-LO increased slightly (15.3%-19.8%) (Fig. 4.2). After 60 min, the rate of ring *cis*-LO opening exceeds its generation by epoxidation of limonene, where the *trans*-LO opening is slower than its generation. The continued epoxidation of residual starting material further increases its concentration. At the same time, the *ax*-LD increased from 4.7% to 26.5%, and traces of *eq*-LD were detected, certainly indicating that *cis*-LO is preferentially converted into *ax*-LD.

With the $[MoO_2(SATP)]_2$ complex, the conversion is 95% at 30 minutes, no LOs were observed. More *ax*-LD than *eq*-LD was observed at 30 minutes but the observed quantity of *ax*-LD decreased faster than the *eq*-LD, certainly due to the transfer into the water phase or further reaction.

For both catalysts, traces of other compounds were observed. Carvone and carveol were identified but not quantified, taking into account their high water solubility. In the presence of water, with the help of the $[MoO_2(SATP)]_2$ catalyst, the hydrolysis of the LOs occurred very fast and was complete in 30 min. In conclusion, $[MoO_2(SATP)]_2$ is not only a better catalyst for limonene epoxidation but also for the hydrolytic ring opening of the epoxide product.

IV.2.2.1. Considerations on the mass balance.

For the reaction performed without catalyst at 80°C, after 4 h, the number of moles of limonene, LOs and LDs identified in the organic phase represented 94% of the starting number of moles of limonene (after 4 h, 7.6% conversion only in Table 4.1). The *cis/trans* LOs and the *ax/eq*-LDs are present as traces in the organic phase, the missing 6% might result from products transferred to the water phase.

For the reaction in presence of the $[MoO_2(SAP)]_2$ catalyst, the mass balance was 80% after 2 h and 70% after 4 h for the sum of starting material and the main products in Table 4.1.

With the $[MoO_2(SATP)]_2$ catalyst, the total number of moles of LOs and LDs quantified is quite low (56% after 0.5 h, 39% after 4 h). The loss appears to be due to the transformation of those products by the water present in the reaction brought by the oxidant, since at the end of the reaction, no water phase could be observed. Several other products were identified but not quantified such as carvone and carveol. Additional products were visible in very low quantity in the chromatogram, but they could not be clearly identified.

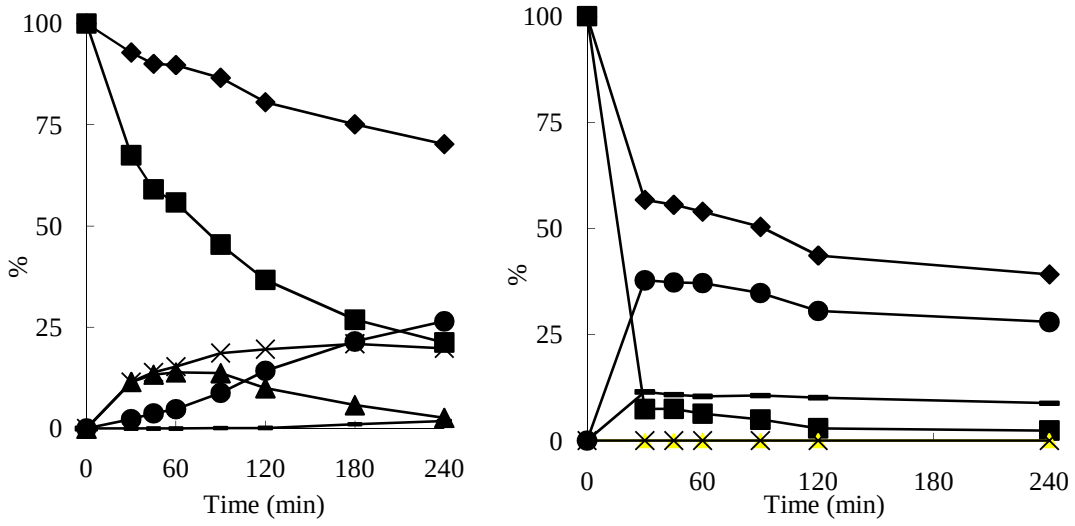

Figure 4. 2. Kinetic profile of Mass balance for the limonene oxidation catalyzed by $[MoO_2(SAP)]_2$ (left), $[MoO_2(SATP)]_2$ (right): [Mo]/limonene/TBHP = 0.5/100/200, T = 80℃. Mass balance (♦), limonene (■), n(cis-LO)/n(Lim0) (▲), n(trans-LO)/n(Lim0)(×), n(eq-LD)/n(Lim0) (–), n(ax-LD)/n(Lim0) (●). Lim0 = limonene introduced initially introduced.

IV.2.3. Influence of the OH substitution

IV.2.3.1. Oxidation of limonene catalyzed by the ONO Molybdenum catalysts $[MoO_2(SAP)]_2$ and $[MoO_2L^{a-c}]_2$

The organic solvent-free catalyzed oxidation of limonene was also investigated with the *ONO* molybdenum complexes containing OH substituent, *i.e.* $[MoO_2(SAP)]_2$ and $[MoO_2L^{a-c}]_2$. With 0.5% mol of catalyst/substrate, the conversion was very good for each catalyst (see Table 4.2 and Figure 4.3), in the order:

$[MoO_2L^a]_2$ (90%) > $[MoO_2(SAP)]_2$ (79%) ~ $[MoO_2L^c]_2$ (77%) > $[MoO_2L^b]_2$ (68%)

The $[MoO_2L^a]_2$ complex reacted much faster than other catalysts. The selectivity towards LOs follows the reverse order:

$[MoO_2L^a]_2$ (4.2%) < $[MoO_2(SAP)]_2$ (14.2%) ~ $[MoO_2L^c]_2$ (24.0%) < $[MoO_2L^b]_2$ (36.5%)

Meanwhile, the yield of LDs follows the same trend as the conversion. This seems to indicate that the $[MoO_2L^a]_2$ is a better catalyst for epoxidation and for ring opening. Indeed, the faster LO is produced, the faster it is consumed to yield the LD. Here, the ring opening products are mainly LDs with preferential formation of *ax*-DL (*ax*-LD/*eq*-LD ratio of 10).

Table 4. 2. Oxidation of limonene catalyzed by *ONO* Molybdenum catalysts: [Mo]/limonene/TBHP = 0.5/100/200, reaction time = 4 h, T = 80℃.

catalyst	Conversion (%)	Selectivity (%)	Yield/%				TON	TOF (h^{-1})
			LO		LD			
		LO	*cis*	*trans*	*eq*	*ax*		
No cat.	7.6	18.5	0.4	1.1	0.03	0.5	-	-
$[MoO_2(SAP)]_2$	79	28.5	11.5	19.8	1.8	26.5	158	130
$[MoO_2L^a]_2$	90	4.2	1.9	3.8	3.7	39.9	180	308
$[MoO_2L^b]_2$	68	36.5	12.9	19.7	0.9	20.6	136	77
$[MoO_2L^c]_2$	77	24.0	8.4	16.0	2.8	27.5	144	110

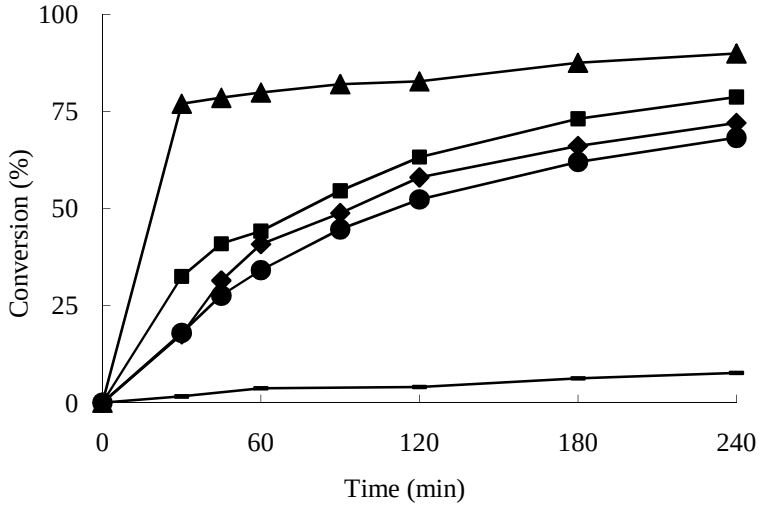

Figure 4. 3. Kinetic profile of oxidation of limonene catalyzed by *ONO* cayalysts: [Mo]/limonene/TBHP = 0.5/100/200, reaction time = 4 h, T = 80℃. Without catalyst (–), $[MoO_2(SAP)]_2$ (■), $[MoO_2L^a]_2$(▲), $[MoO_2L^b]_2$ (●), $[MoO_2L^c]_2$(♦).

IV.2.3.2. Oxidation of limonene catalyzed by ONS Molybdenum catalysts

Additional limonene epoxidation experiments under organic solvent-free conditions were also carried out with the $[MoO_2(SATP)]_2$ and $[MoO_2L^{h\text{-}i}]_2$ complexes, where OH substituent is present at different positions one the SATP ligand. With the same loading as for the *ONO* complexes, *i.e.* 0.5% mol of catalyst/substrate, the conversion of limonene was excellent with each catalyst (see Table 4.3 and Figure 4.4), being greater than 92% after 30 minutes. No LOs were observed whereas the LDs were found in large amounts. The *ax*-LD yield was around 3.5 times greater than that of *eq*-LD, *i.e.* in average 38% *vs.*11%. One interesting thing is the *ax*-LD/*eq*-LD ratio is different with different catalysts. All these values are lower than in the literature, which mean that more *eq*-LD were observed. For $[MoO_2(SATP)]_2$, the *ax*-LD/*eq*-LD ratio is the smallest.

This result confirms that a good catalyst for epoxidation is also a good catalyst for ring opening, the hydrolysis of the formed epoxides being already complete by the time of the first measurement in this case.

Table 4. 3. Oxidation of limonene catalyzed by *ONS* Molybdenum catalysts: [Mo]/limonene/TBHP = 0.5/100/200, reaction time = 0.5 h, T = 80℃.

catalyst	Conversion (%)	Selectivity (%)			Yield (%)				*ax/eq-LD ratio*	TON	TOF (h^{-1})
		LO	LD		LO		LD				
			eq	ax	cis	trans	eq	ax			
No catalyst[a]	7.6	18.5	0.5	6.7	0.4	1.1	0.03	0.5	16.7	-	-
$[MoO_2(SATP)]_2$[b]	93	0	12.4	40.8	0	0	11.5	37.8	3.3	185	371
$[MoO_2L^h]_2$[b]	92	0	12.0	41.6	0	0	11.0	38.1	3.5	184	367
$[MoO_2L^i]_2$[b]	92	0	11.3	42.4	0	0	10.3	38.8	3.7	181	361

[a]4h,[b]0.5 h

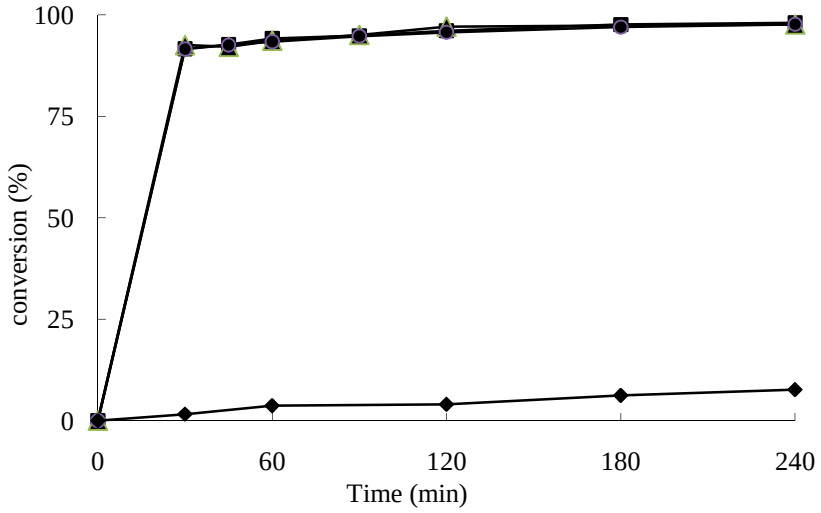

Figure 4. 4. Kinetic profile of oxidation of limonene catalyzed by $[MoO_2(SATP)]_2$ and $[MoO_2L^{h-i}]_2$: [Mo]/limonene/TBHP = 0.5/100/200, reaction time = 4 h, T = 80℃. Without catalyst (♦), $[MoO_2(SATP)]_2$ (▲), $[MoO_2L^h]_2$ (■), $[MoO_2L^i]_2$ (●).

IV.2.4. Influence of different parameters.

The $[MoO_2(SATP)]_2$ catalyst was chosen as example to investigate the influence of different parameters on the oxidation of limonene.

IV.2.4.1. Influence of the temperature

Without catalyst

The experiments without catalyst have been done at different temperatures (see Table 4.4 and Figure 4.5). Although the conversion was very slow, a temperature increase slightly promotes the conversion.

Table 4.4. Temperature influence on the oxidation of limonene without catalyst, [Mo]/limonene/TBHP = 0/100/200.

T/°C	Conversion (%)	Yield (%)			
		cis-LO	*trans*-LO	*eq*-LD	*ax*-LD
30[a]	3.2	0.3	0.3	0.06	0.2
50[a]	4.8	0.55	0.03	0.03	0.3
80[b]	7.6	0.4	1.1	0.03	0.5

[a] 5 h, [b] 4 h.

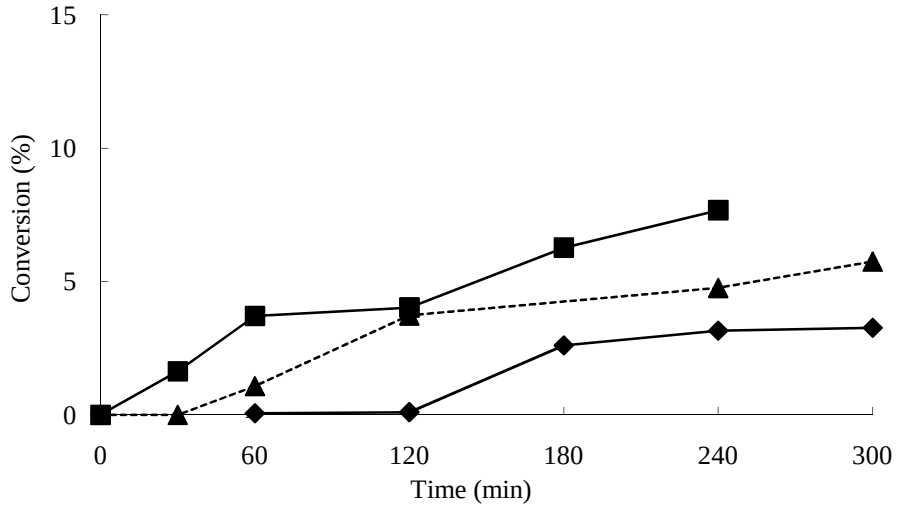

Figure 4. 5. Kinetic profile of limonene epoxidation by aqueous TBHP without catalyst: 30℃ (♦), 50℃ (▲), 80℃ (■). Conditions: limonene/TBHP = 100/200.

In the presence of $[MoO_2(SATP)]_2$

The influence of temperature on limonene epoxidation catalyzed by $[MoO_2(SATP)]_2$ was studied at four different temperatures in the 30-80°C range (Table 4.5 and Figure 4.6). The limonene conversion after 4 h increased with temperature, from 30°C (38%) to 50°C (83%), 60°C (88%) and 80°C (93%).

The *ax*-LD/*eq*-LD ratio is different at different temperature, at 30°C, the *ax*-LD/*eq*-LD ratio is the highest, higher than at 80°C (19.2 *vs.* 3.3).

At 30 and 50°C, the *trans*/*cis*-LO ratio present in solution is always in favor to the *trans*-LO. That has to be linked to the preferential hydrolysis of *cis*-LO, as showed by other authors under different experimental conditions. The ring opening is even faster at 60°C and 80°C, since the LOs are not observed, the only visible products from the chromatograms being the LDs.

Table 4. 5. Temperature influence on the oxidation of limonene catalyzed by $[MoO_2(SATP)]_2$, [Mo]/limonene/TBHP = 0.5/100/200.

T/°C	Conversion (%)	Selectivity (%)/LO	Yield/%				*ax/eq-LD ratio*	TON	TOF (h^{-1})
			cis-LO	*trans*-LO	*eq*-LD	*ax*-LD			
30[a]	38	33.4	1.1	11.5	0.7	13.5	19.2	76	26
50[a]	83	0.2	0.1	8.6	8.6	43.1	5.0	166	161
60[b]	88	0	0	0	4.8	41.5	8.6	176	235
80[c]	93	0	0	0	11.5	37.8	3.3	185	371

[a]5 h, [b]4 h, [c]0.5 h.

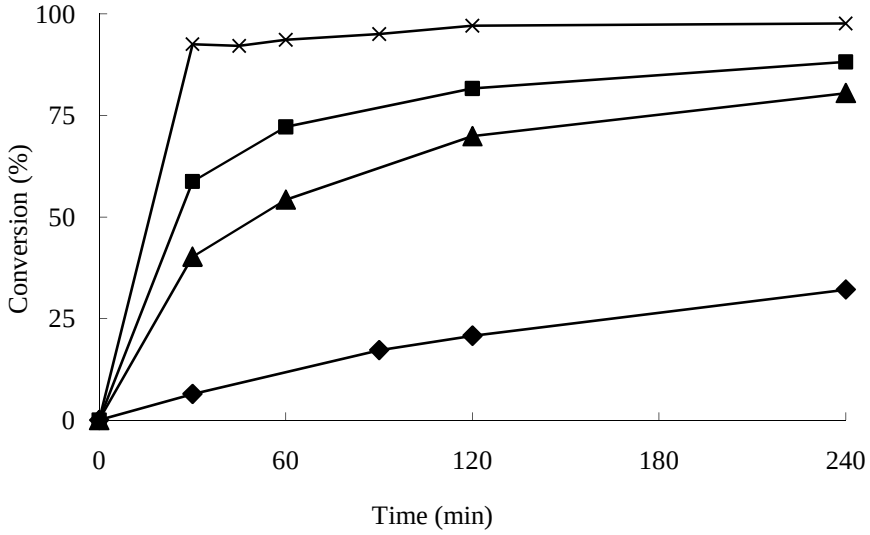

Figure 4. 6. Temperature influence to oxidation of limonene catalyzed by $[MoO_2(SATP)]_2$: 30℃ (♦), 50℃ (▲) , 60℃ (■), 80℃ (×). Conditions: [Mo]/limonene/TBHP = 0.5/1 00/200.

IV.2.4.2. Influence of catalyst loading and temperature in the presence of $[MoO_2(SATP)]_2$

The influence of catalyst loading on limonene epoxidation catalyzed by $[MoO_2(SATP)]_2$ was studied at different concentrations and three different temperatures: 30, 50 and 80°C (see Table 4.6 and Figure 4.7).

At 50°C, the limonene conversion after 5 h increased from 60 to 80% by increasing the catalyst amount by a factor of 10 from 0.05 to 0.5%. Interestingly, whereas the *trans*-LO/*cis*-LO ratio was in favor to the *cis*-LO in the absence of catalyst, it reverted in favor of the *trans*-LO in the presence of catalyst, for all catalyst concentrations. The ax-LD/eq-LD ratio also changed, being highest with the lowest catalyst charge.

Table 4. 6. Influence of the catalyst loading for epoxidation of limonene catalyzed by $[MoO_2(SATP)]_2$ at 50℃: [Mo]/limonene/TBHP = x/100/200, reaction time = 5 h.

x	Conversion (%)	Selectivity (%)/LO	Yield (%)				TON	TOF (h^{-1})
			cis-LO	*trans*-LO	*eq*-LD	*ax*-LD		
0[a]	5.7	10.6	0.59	0.03	0.034	0.29	-	-
0.05[a]	60.0	22.6	0.4	13.2	1.9	23.2	1188	759
0.1[a]	62.5	20.6	0.2	12.7	2.9	26.4	627	312
0.5[a]	83.2	0.2	0	0.1	8.6	43.1	166	161

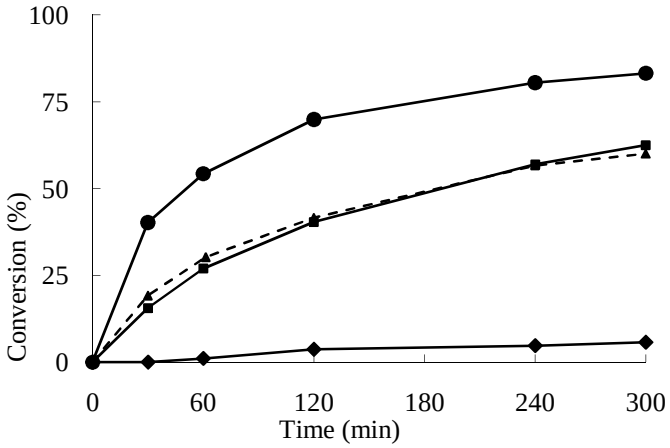

Figure 4. 7. Influence of the catalyst loading for the epoxidation of limonene catalyzed by $[MoO_2(SATP)]_2$ at 50℃: [Mo]/limonene/TBHP = x/100/200, x = 0 (♦), 0.05 (▲), 0.1 (■), 0.5 (●).

At 80°C in the presence of catalyst $[MoO_2(SATP)]_2$ in Table 4.7, limonene is transformed selectively into LDs as at 50°C (Table 4.6) and as previously described in literature with molybdenum acetylide complex $CpMo(CO)_3(C{\equiv}CPh)$.[86] Comparison between Tables 4.6 and 4.7 indicate that the result is independent on temperature from 50°C. The best *ax*-LD/*eq*-LD ratio is again observed with the lower catalyst charge.

Table 4. 7. Influence of catalyst loading for epoxidation of limonene with $[MoO_2(SATP)]_2$ complex at 80℃ with [Mo]/limonene/TBHP = x/100/200 .

x Mo	Conversion (%)	Selectivity (%)/LO	Yield (%)				TON	TOF (h^{-1})
			LO		LD			
			cis	*trans*	*eq*	*ax*		
0	7.7	18.5	0.4	1.1	0.03	0.5	-	-
0.1[a]	85	0	0	0	6.7	62	683	1042
0.25[b]	87	0	0	0	9.9	40.3	910	1743
0.5[b]	93	0	0	0	11.5	37.8	185	371

[a]2 h, [b]0.5 h

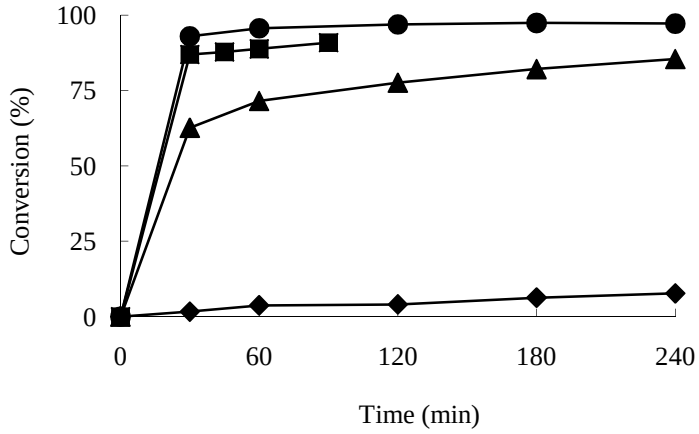

Figure 4. 8. Influence of the catalyst loading for epoxidation of limonene catalyzed by $[MoO_2(SATP)]_2$ at 80℃. [Mo]/limonene/TBHP = x/100/200, x = 0 (♦), 0.1 (▲), 0.25 (■), 0.5 (●).

At 30°C, the presence of catalyst transforms limonene into LOs and especially LOs into LD smore slowly, showing clearly the effect of the temperature. Indeed, at this temperature the LOs are still present in the mixture after 4 h (see Table 4.8 and Figure 4.9).

Table 4. 8. Influence of catalyst loading for epoxidation of limonene with $[MoO_2(SATP)]_2$ complex at 30℃: [Mo]/limonene/TBHP = x/100/200, re action time = 4 h.

x Mo	Conversion (%)	Selectivity (%)/LO	Yield (%)				TON	TOF (h^{-1})
			cis-LO	*trans*-LO	*eq*-LD	*ax*-LD		
0	3.2	20	0.3	0.3	0.04	0.16	-	-
0.5	32	38	1.4	10.9	0.5	11.2	64	26

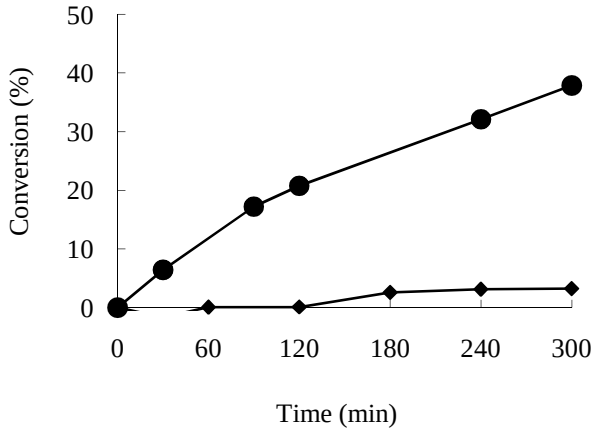

Figure 4. 9. Kinetic profile of catalyst loading for epoxidation of limonene with $[MoO_2(SATP)]_2$ complex at 30℃: [Mo]/limonene/TBHP = x/100/200, x = 0 (♦), 0.5 (●).

IV.2.4.3. Influence of the TBHP/substrate ratio in the case of [MoO₂(SATP)]₂

The effect of TBHP quantity used in the organic solvent-free epoxidation of limonene catalyzed by $[MoO_2(SATP)]_2$ has been investigated at 50°C and 80°C with a 0.5% catalyst loading.

Table 4. 9. Influence of TBHP quantity for epoxidation of limonene with $[MoO_2(SATP)]_2$ complexe at 50℃: [Mo]/limonene/TBHP = 0.5/100/y. R eaction time = 4 h.

y	Conversion (%)	Selectivity (%)/LO	Yield (%)				TON	TOF (h^{-1})
			cis-LO	*trans*-LO	*eq*-DL	*ax*-DL		
110	61	1.4	0	0.3	5.8	35.7	123	109
200	80	0.3	0	0.2	8.4	42	161	161

Previously published work has reported results with 1.1 equivalents,[87] 1.5 equivalents[88] and 2.0 equivalents[86] of TBHP. Therefore, we carried out our experiments using those ratios. At 50°C, using two equivalents of TBHP speeds up the reaction significantly relative to 1.1 eq (Table 4.9 and Figure 4.10), (conversion: 80% *vs*. 61%, TOF: 161 *vs*. 109), and affords LDs in higher yields. Trace amounts of *trans*-LO only were detected after 4 h in each case. At 80°C, only a slight rate increase is observed on going from 1.5 to 2 equiv. of TBHP (see Figure 4.11). No LOs were observed in this case (Table 4.10).

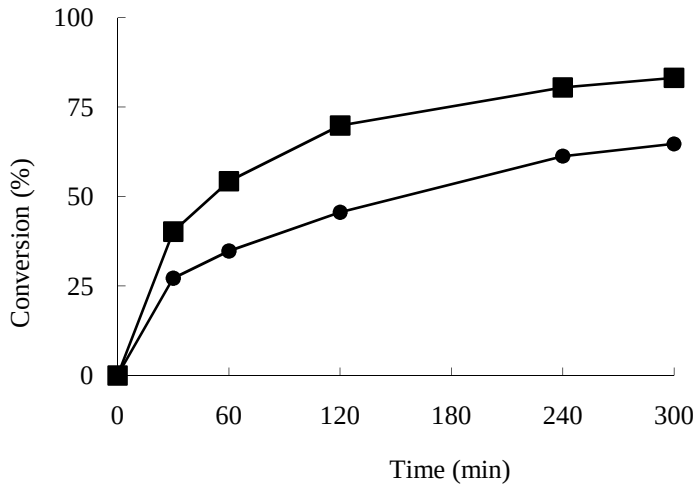

Figure 4. 10. Influence of TBHP quantity for Organic solvent-free epoxidation of limonene with $[MoO_2(SATP)]_2$ complex at 50℃: [Mo]/limonene/TBHP = 0.5/100/y. Re action time = 4 h, y = 110 (●), 200 (■).

Table 4. 10. Influence of TBHP quantity for epoxidation of limonene with $[MoO_2(SATP)]_2$ complex at 80℃: [Mo]/limonene/TBHP = 0.5/100/y. Re action time = 0.5 h.

y	Conversion (%)	Selectivity (%)/LO	Yield (%)				TON	TOF (h^{-1})
			cis-LO	*trans*-LO	*eq*-LD	*ax*-LD		
150	89	0	0	0	10.7	42.2	178	357
200	93	0	0	0	11.5	37.8	185	371

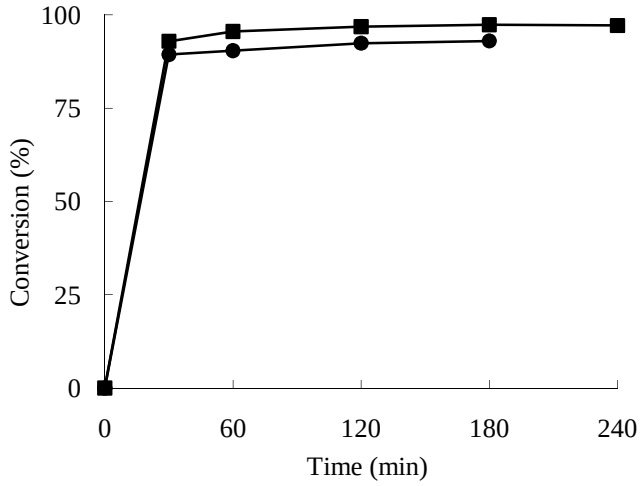

Figure 4. 11. Influence of TBHP quantity for epoxidation of limonene with $[MoO_2(SATP)]_2$ complex at 80℃: [Mo]/limonene/TBHP = 0.5/100/y. Re action time 4 h, y = 150 (●), 200 (■).

IV.2.5. Ring opening tests

As shown in the above sections, the epoxidation of limonene produced not only LOs but also LDs, especially in the presence of *ONS* catalysts. The observed evolution of the concentrations as a function of catalyst amount suggested that the ring opening process is metal catalyzed. At high temperatures, only LDs were observed. It seems obvious that the LDs are obtained from the LOs by ring opening rather than by direct dihydroxylation to yield *p*-Menthanetetrol-1,2,8,9.[89] It was therefore of interest to investigate the ring opening process independently and in detail, in order to better assess the role of the catalyst in this process and its mechanism.

The mechanism of the selectivity to ring opening of LD has been studied in the literature.[90] Under acidic conditions, the hydrolysis of *trans*- and *cis*-LOs is reported in several articles[91] to lead to the same *ax*-LD product, although with different reaction rates. The selective axial nucleophilic attack to *cis* LO is faster due to lower

steric hindrance and to electronic effects that can be rationalized by the Fürst-Plattner rule.[92]

In the absence of catalyst, the *trans*/*cis* LO mixture (around 50:50) gave rise to ring opening slowly at 80°C, with a total conversion of 36% after 4 h. (Table 4.11 and Figure 4.12) Small amounts of the *trans*-LO were transformed, whereas 60% the *cis*-LO was consumed. The reaction yielded mostly *ax*-LD (yield: 21.2%) and trace amounts of *eq*-LD (total yield: 0.43%) were detected. The total mass balance was 86% after 4 h (90% after 3 h), indicating low percent transfer of these compounds to the water phase.

In the presence of the $[MoO_2(SAP)]_2$ catalyst (Table 4.11), the limonene oxide conversion was substantially higher (60%) than without catalyst and yielded *ax*-LD as the major product (yield: 34.9%). The *trans*-LO reacted slowly, only 27% being converted, whereas the conversion of *cis*-LO was nearly complete. Only a trace of *eq*-LD (total yield: 1.6%) was formed.The total mass balance was 77% after 4 h (82% after 3 h).

When 0.5% $[MoO_2(SATP)]_2$ was used, on the other hand, the ring opening reaction was even faster, being complete in less than 30 minutes and yielding 45% of *ax*-LD and 12.1% of *eq*-LD. (Table 4.11 and Figure 4.12) After four hours, the measured yield of diequatorial diol in the organic phase had decreased to 9.7% and that of *ax*-LD to 26.9%. The mass balance had correspondingly decreased from 57.1% (0.5 h) to 36.6% (4 h), which indicates that the LDs were converted to others compounds.

A comparison of these three experiments confirms the catalytic role of the Mo compounds, particularly the compound with SATP as ligand, in the ring opening process and also indicates that this catalytic role is particularly effective for the production of the *eq*-LD product, whereas only traces of this compound are produced by the non-catalyzed process.

Table 4. 11. Ring opening of mixture of LOs (*cis* and *trans*) under organic solvent-free condition at 80℃: [Mo]/limonene/TBHP = 0.5/100/200 .

catalyst	Conversion (%)	Selectivity (%)		Yield (%)		TON	TOF (h^{-1})
		LD		LD			
		eq	*ax*	*eq*	*ax*		
No catalyst[a]	36	1.2	58.7	0.43	21.2	-	-
$[MoO_2(SAP)]_2$[a]	60	2.6	58.5	1.6	34.9	119	45
$[MoO_2(SATP)]_2$[b]	100	12.1	45	12.1	45	200	400

[a]4h,[b]0.5 h.

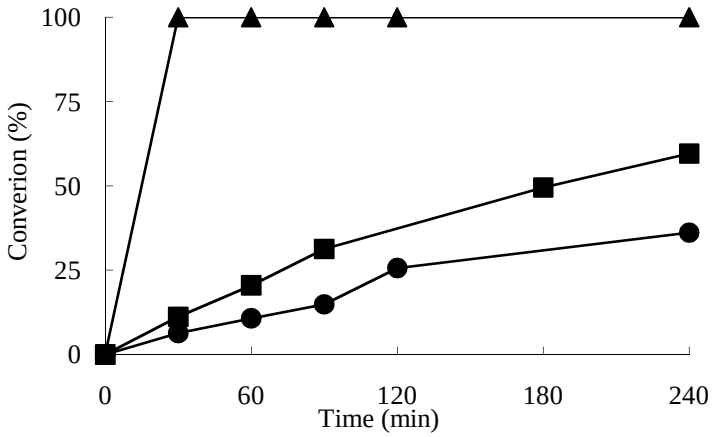

Figure 4. 12. The conversion of oxidation of mixture of cis/trans LO: [Mo]/limonene/TBHP = 0.5/100/200, reaction time = 4 h, T = 80℃. Without catalyst (●), $[MoO_2(SAP)]_2$ (■), $[MoO_2(SATP)]_2$ (▲).

Furthermore, it seems that the presence of catalysts affects the ratio of *ax*-LD/*eq*-LD, *i.e.* 3.71 (45/12.1) < 21.8 (34.9/1.6) for $[MoO_2(SAP)]_2$ and $[MoO_2(SATP)]_2$ respectively in reverse order of the reaction rate. This gave us the guess that the opeing of the two LOs may not react at the same rate. Very few reports deal about the eq-DL.[91] In order to solve this problem, we tried to perform the ring opening with pure *cis*-LO and pure *trans*-LO. Different experiments were performed. Experimental conditions and results are listed in Table 4.12.

Table 4. 12 – Oxidation of limonene oxides (pure cis, pure trans or cis-trans mixture) catalyzed by $[MoO_2(SATP)]_2$[c] under organic solvent-free condition at 80℃: [Mo]/limonene/TBHP = 0.5/100/200.

substrate	catalyst	Conversion (%)	Selectivity (%)		Yield (%)		TON	TOF (h^{-1})
			DL		DL			
			eq	ax	eq	ax		
mix	No catalyst[a]	36	1.2	58.7	0.43	21.2	-	-
	$[MoO_2(SAP)]_2$[a]	60	2.6	58.5	1.6	34.9	119	45
	$[MoO_2(SATP)]_2$[b]	100	12.1	45	12.1	45	200	400
cis	No catalyst[a]	13.5	0	6.4	0	0.87	-	-
	$[MoO_2(SAP)]_2$[a]	27	0	28.4	0	7.7	52	27
	$[MoO_2(SATP)]_2$[b]	100	0	25.3	0	25.3	200	400
trans	$[MoO_2(SATP)]_2$[c]	100	15.8	20.8	15.8	20.8	200	130
axial diol	$[MoO_2(SATP)]_2$[d]	93	0	-	0	-	516	161

[a]4 h, [b]0.5 h, [c]1.5 h, [d]cat 0.2%, 3h .

Without catalyst, the *cis*-LO reacts very slowly with a conversion of 13.5 % after 4 h

When the ring opening of cis-LO is carried out with $[MoO_2(SAP)]_2$ (see Figure 4.13), the conversion is double with 27% after 4 h reaction.

Both cis-LO and trans-LO react very fast in the presence of 0.5% of catalyst $[MoO_2(SATP)]_2$ (Table 1.12 and Figure 4.13 for cis-LO) with complete conversion in less than 0.5 h. Those results indicate that the complexes catalyse the ring opening.

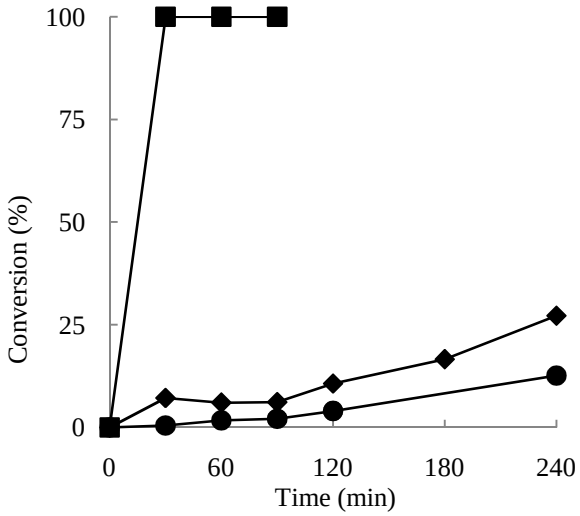

Figure 4. 13. Kinetic profile (conversion *vs*. time) of ring opening of limonene oxide catalyzed by $[MoO_2(SATP)]_2$: [Mo]/limonene/TBHP = 0.5/100/200, T = 80℃. *Cis*-LO without catalyst (●), *cis*-LO with $[MoO_2(SAP)]_2$ (◆), *cis*-LO $[MoO_2(SATP)]_2$ (■)

IV.3. Oxidation of cyclohexene catalyzed by $[MoO_2(SAP)]_2$ and $[MoO_2L^{a-c}]_2$ catalysts

Since limonene can be considered as a substituted cyclohexene, in order to understand better how the two different double bonds work and the possible mechanism of the reaction, cyclohexene was also investigated as a simplified model of limonene.

The catalysts $[MoO_2(SAP)]_2$ and $[MoO_2L^{a-c}]_2$ were used in classical organic solvent-free conditions.

The catalytic procedure was carried out at 80°C with 2 equivalent of aqueous TBHP and 0.1% mol of catalyst loading. For higher catalyst loadings (*e.g.* 0.5%), the catalysts are hard to dissolve in the mixture.

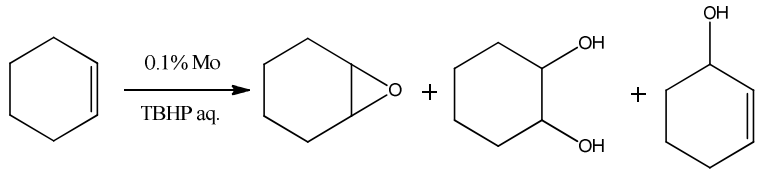

Scheme 4.4. Oxidation of cyclohexene

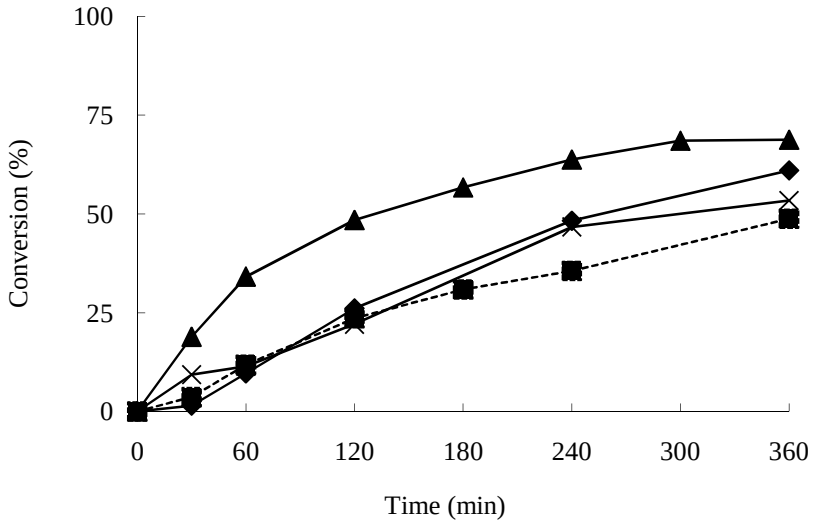

Figure 4. 14. Kinetic profile of converted cyclohexene *vs*. time with dioxidomolybdenum (VI) catalysts: $[MoO_2(SAP)]_2$ (■), $[MoO_2L^a]_2$ (▲), $[MoO_2L^b]_2$ (×), $[MoO_2L^c]_2$(◆). Conditions: substrate/[Mo] = 400:1; T = 80℃.

Table 4. 13. Results of cyclohexene oxidation by $[MoO_2(SAP)]_2$ and $[MoO_2L^{a-c}]_2$.

catalyst	Conversion (%)	Selectivity (%)/ oxide	Yield (%)			TON	TOF (h^{-1})
			oxide	diol	2-cyclohexen-1-ol		
$[MoO_2(SAP)]_2$	48.8	41.6	20.3	8.7	1.1	447	150[a]
$[MoO_2L^a]_2$	68.8	22.8	15.7	21.8	2.1	687	377[b]
$[MoO_2L^b]_2$	53.4	35.8	19.1	8.1	1.0	535	187[b]
$[MoO_2L^c]_2$	61.0	22.7	13.9	21.2	1.8	612	165[a]

[a]1 h, [b]0.5 h

In the case of the reactions catalyzed by $[MoO_2(SAP)]_2$ and $[MoO_2L^a]_2$, the catalyst is totally dissolved in the system, giving similar bright orange solutions. The $[MoO_2L^c]_2$ catalyst dissolves quite slowly and get eventually fully dissolved. The trend of the dissolution rate is $[MoO_2L^a]_2 > [MoO_2(SAP)]_2 > [MoO_2L^b]_2 > [MoO_2L^c]_2$.

The highest activity is exhibited by $[MoO_2L^a]_2$ (see Figure 4.14).The slower conversion observed with the other catalysts, especially at the beginning of the reaction, may be due to the slow catalyst dissolution in organic phase.

The cyclohexene conversion decreases in the order $[MoO_2L^a]_2 > [MoO_2L^c]_2 > [MoO_2L^b]_2 > [MoO_2(SAP)]_2$, consistent with a positive effect of the introduction of the OH substituent on the catalytic activity.

There are three main products for the oxidation of cyclohexene, *i.e.* cyclohexene epoxide, trans-1,2-cyclohexanediol and a trace of 2-cyclohexen-1-ol (1-2.1%). The table shows that the two catalysts affording the highest cyclohexene conversion (with ligands L^a and L^c) also lead to a greater extent of ring opening. $[MoO_2L^a]_2$ and $[MoO_2L^c]_2$ give less epoxide than diol, while $[MoO_2L^b]_2$ and $[MoO_2(SAP)]_2$ give more epoxide than diol.

IV.4. Conclusion

In this chapter, the catalysts prepared in chapter II have been used as catalysts in the oxidation of limonene and cyclohexene under organic solvent-free conditions. The influence of ligand substituents at different positions and several parameters have been studied.

The limonene conversion was higher with the OH-containing dimeric compounds in the order $[MoO_2L^a]_2$ > $[MoO_2(SAP)]_2$ > $[MoO_2L^c]_2$ > $[MoO_2L^b]_2$ at 80°C with 0.5% catalysts loading. The *ONS*-type catalysts always have higher reaction rate than the *ONO*-type under the same condition. The main products are LOs and LDs. The $[MoO_2L^a]$ catalyst shows the highest catalytic activity (conversion: 90%) among the *ONO*-type complexes.

Furthermore, In order to study mechanism of the limonene epoxydation and LOs ring opening, few parameters have been studied, such as catalyst loading, oxidant loading, using different Mo/substrate ratio at a 80°C and using mixture or pure LO.

The oxidation of cyclohexene follows similar trend showing the formation of the epoxide and the formation of diol through ring opening.

IV.5. Experimental part

IV.5.1. Materials and methods

All preparations were carried out in air. Water was deionised twice before use. Organic solvents (ethanol, methanol, diethylether) were employed as received without any purification. All molybdenum complexes were synthesized as previously described in chapter **II** and used freshly prepared. Limonene (98% Aldrich), limonene oxides, limonene diol and TBHP (70% in water, ACROS) were used as received. Infrared spectra were recorded in KBr matrices at room temperature with a Mattson Genesis II FTIR spectrometer. ^{1}H spectra were recorded at 200.1 MHz on a Bruker Avance DPX-200 spectrometer. Catalytic reactions were followed by gas chromatography on an Agilent 6890A chromatograph equipped with FID detector, a HP5-MS capillary column (0.30 m x 0.25 mm x 0.25 m) and automatic sampling, or on a Fisons GC 8000 chromatograph equipped with FID detector and with a SPB-5 capillary column (30 m x 0.32 mm x 0.25 m). The GC parameters were quantified with authentic samples of the reactants and products. The conversion of limonene and the formation of limonene oxides and corresponding diol oxide were calculated from calibration curves ($r^2 = 0.999$) relatively to an internal standard.

IV.5.2. Preparation of trans- and cis-LO

These compounds were prepared following previously published methods, as described in the next two paragraphs.[93] The preparation of pure *trans*-LO is based on the hydrolysis reaction of the *trans*/*cis* LO mixture, which involves the much faster and total hydrolysis of the *cis*-LO isomer and recovery of the unreacted isomerically pure *trans*-LO.

General procedure for preparation of trans-(R)-(+)-limonene oxide

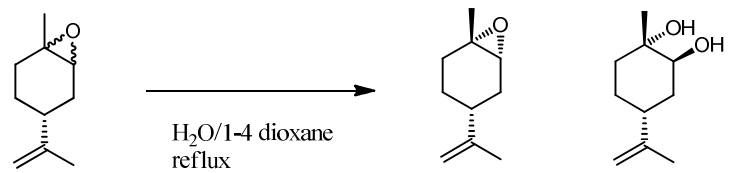

LOs ***trans*-LO** ***ax*-LD**

The *trans*/*cis*-(R)-(+)-LO mixture (2.96 g, with 50:50, 0.02 mmol), distilled water (15 mL) and 1,4-dioxane (15 mL) were added to a 100 mL round-bottom flask equipped with a magnetic stir bar and a reflux condenser. The reaction mixture was heated to reflux until total consumption of the *cis*-LO occurred as detected by GC

analysis (1.5 h). The unreacted *trans*-LO was extracted with diethyl ether, then the ether phase was washed with brine and dried over anhydrous Na_2SO_4. Column chromatography (hexane:diethyl ether = 95:5, Rf = 0.5) gave *trans*-LO as a colorless oil (1.1 g, 74% yield). The recovered yield was calculated on the basis of the initial amount of *trans*-LO in the *trans*/*cis*-LO mixture with a ratio of 50:50.

Trans-LO: colorless oil. ^{1}H NMR (300 MHz, $CDCl_3$-*d*, δ(ppm)): 4.67 (s, 2H), 2.99 (d, *J*= 5.2 Hz, 1H), 2.05-2.00 (m, 2H), 1.88-1.85 (m, 1H), 1.74-1.62 (m, 2 H), 1.67 (s, 3 H), 1.39-1.36 (m, 2H), 1.33 (s, 3H). ^{13}C{^{1}H} NMR (300 MHz, DMSO-d_6) δ: 149.15, 109.03, 59.20, 57.44, 40.67, 30.68, 29.81, 24.27, 23.04, 20.16.

General procedure for preparation of cis-(+)-limonene oxide

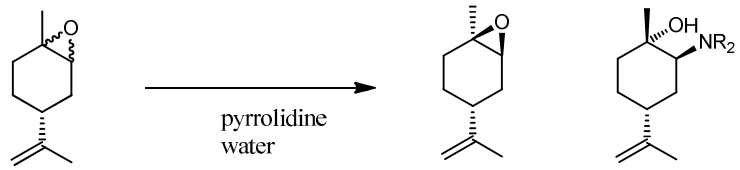

LOs ***cis*-LO** **β-amino alcohol**

Pyrrolidine (0.36 mL, 0.005 mol), (R)-(+)-limonene oxide (0.76 g, 0.005 mol), and deionized water (0.75 mL, 0.004 mol) were added to a 50 mL round-bottom flask equipped with a magnetic stir bar and a reflux condenser. The reaction mixture was heated to reflux at 100°C, and stirred under reflux for 24 h. The contents of the round-bottom flask were transferred to a separatory funnel with pentane (3 mL). The organic solution was extracted with deionized water (2×3 mL). The pentanelayer was dried with anhydrous magnesium sulfate and then filtered. The pentane was removed in *vacuo* (with rotary evaporator). The *cis*-LO was then distilled under reduced pressure, giving the product (0.27 g).

Cis-LO: ^{1}H NMR (300 MHz, $CDCl_3$-*d*, δ(ppm)): 1.26 (s, 3H), 1.55 (m, 2H), 1.71 (s, 3H), 1.74 (m, 2H), 1.82 (m, 2H), 2.12 (m, 1H), 3.00 (t, 1H), 4.65 (d, 2H). ^{13}C{^{1}H} NMR (300 MHz, DMSO-d_6) δ: 21.1, 24.3, 25.9, 28.6, 30.7, 36.2, 57.2, 60.5, 109.0, 148.9. These values are quite similar with those reported in the literature.[93b]

IV.5.3.*Catalytic procedure*

- Routine experiments

In a typical experiment, limonene or cyclohexene (1 equiv) and catalyst (x equiv, see tables) were mixed together then stirred in air in a round-bottom flask. Acetophenone was added as internal standard in some experiments (see tables). The reaction temperature was regulated at the desired value and then wet THBP (70% in water, y equiv, (see tables) was added to the mixture, starting the reaction. Samples of the organic phase were periodically withdrawn. The reaction was quenched by addition of MnO_2, followed by the addition of diethylether and removal of the manganese oxide and the residual water by filtration through silica before GC analysis.

V. Chapter V

Grafting of molybdenum complexes on Merrifield resin for organic solvent-free epoxidation of cyclooctene

V.1. Introduction

Soluble molybdenum complexes catalyzing the epoxidation of olefins have been well investigated.[94] They have been shown to be efficient under different conditions, with or without organic solvent, but the main problem of those studies lays in the fact that the catalysts could not be easily separated and recovered from the reaction mixture. Since a few of the drawbacks of homogeneous catalysts are the cost of the catalysts and the possible contamination of the environment by the metal, the development of efficient methods for recovery and reuse of the catalysts is a very important aspect from an economical and environmental point of view. One strategy to solve this problem briefly presented on chapter **I** is to anchor the active site to a solid surface which brings the easy separation of the catalyst from the reaction medium by filtration while ideally maintaining the activity of the recovered catalyst during reuse.

As presented in chapter **I**, heterogenisation of molecular molybdenum catalysts has been the subject of several efforts using several supports such as organic polymers based on polystyrene,[50,51] hybrid inorganic-organic support,[52] inorganic supports (Zeolite, Mesoporous silica[55-57]) and multiwall carbon nanotubes.[58] The heterogenized catalysts can be summarized as shown Scheme 5.1. On any support, the metal complex is anchored covalently through a linker.

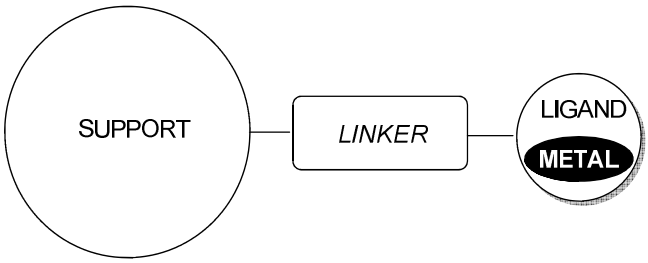

Scheme 5.1 General scheme of the supported metal-complexes

Polystyrene resins (PS) are interesting supports because of their compatibility with organic media, commercial availability and low price. Know-how in polymer functionalization has provided a large variety of resins on which grafting is possible, electing those polymers as an interesting choice within the quest of cleaner processes. Indeed, the ideal support for anchoring a catalyst for the epoxidation of olefins should be inexpensive and stable toward thermal and oxidative stress.

The main advantages of the PS supports are their high surface area, easy separation and recyclability and good stability under the reaction conditions. Herein, we report on the preparation and characterization of molybdenum complexes supported on Merrifield resins and the investigation of their catalytic activity in the epoxidation of cyclooctene with aqueous TBHP under organic solvent-free conditions.

V.2. Results and discussion

V.2.1. Molecular models

V.2.1.1. Synthesis

As is shown in chapter **III**, the molybdenum complexes with an *ONO* backbone ligand $[MoO_2L^{a-f}]_2$ are sufficiently stable for the epoxidation conditions, *i.e.* at 80°C in the substrate as solvent in the presence of water and TBHP. Furthermore, those molecular complexes could be recovered from the reaction mixture and successfully reused but the workup required several steps and the use of organic solvents.

5-Chloromethyl-2-hydroxybenzaldehyde **1** was chosen as the starting precursor of the ligand. Indeed, the chloromethyl pending function can be easily substituted.[95] Using this substituted aldehyde, the *ONO* ligand can be linked to solid supports through suitable linkers.

First of all, $[MoO_2L^j]_2$ has been synthesized as a molecular model of the grafted catalyst. Because the Schiff base H_2L^j is not so easy to isolate, the $[MoO_2L^j]_2$ complex was directly accessed by a one-pot reaction adding directly $[MoO_2(acac)_2]$ to the intermediate Schiff base solution. We have avoided to graft $[MoO_2L^j]_2$ directly on a modified resin, because we have observed that the CH_2Cl of **1** can react with amine (from 2-aminophenol) group - competing with aldehyde group - and the Schiff base was not stable during the grafting conditions. Thus, an alternative to graft the compound on the pending CH_2Cl functions of the Merrifield resin was needed.

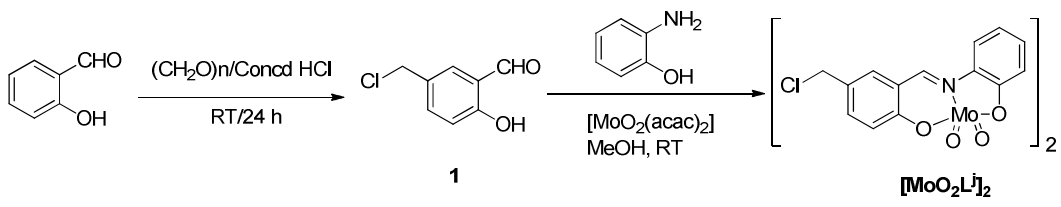

Scheme 5.2. Synthesis of molecular model $[MoO_2L^j]_2$.

To this end purpose, a piperazine was introduced as linker between the resin and the complex. This molecule possesses two amine functions that can be substituted. This strategy gives the possibility to develop an “a priori” simple synthetic methodology.

The reactivity of the hydroxybenzaldehyde **1** with piperazine has been studied. A first test was done using unprotected piperazine. Unfortunately, this simpler strategy was not successful, since the main isolated product was the disubstituted piperazine **2** (see Scheme 5.3). From compound **2**, the bis(Schiff base) compound **3 (H_2L-pip-LH_2)** was obtainedby the condensation reaction with two equivalents of 2-aminophenol. Compound **3** was subsequently treated with [$MoO_2(acac)_2$], leading to the isolation of the [(MeOH)MoO_2(L-pip-L)MoO_2(MeOH)] complex **4**. Compound **4** was dried to give [MoO_2(L-pip-L)MoO_2]$_n$ (**4’**). Complex **4’** is an interesting molecular model in order to compare the catalytic activity with molecular equivalents [MoO_2L]$_2$ and with molybdenum grafted resins.

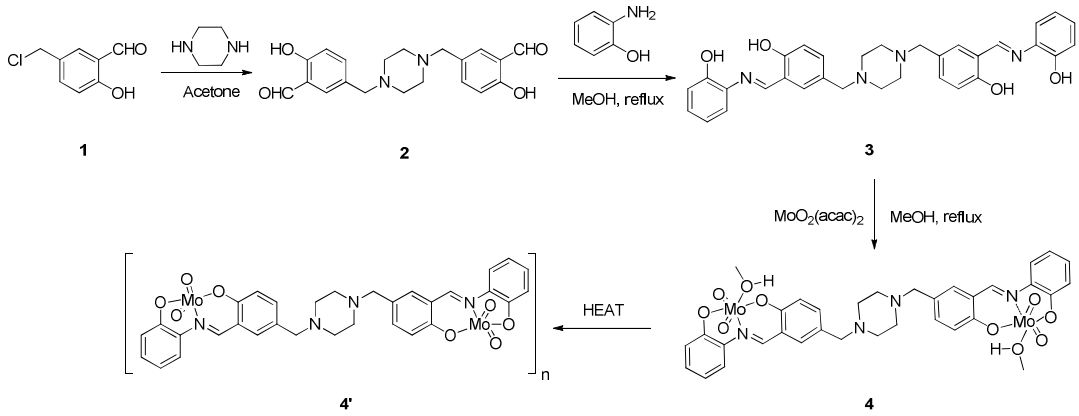

Scheme 5.3. Synthesis of bis(*ONO* molybdenum complex).

Another molecular model was designed as shown in Scheme 5.4. Benzylchloride reacts with piperazine (used as large excess) to yield the monosubstituted piperazine **5**, which then reacts with **1** to give the corresponding aldehyde **6**. Then, reflux with 2-aminophenol forms a Schiff base **7** (H_2L-pip-Bz). Compound **7** was treated in methanol with [$MoO_2(acac)_2$], yielding complex [(MeOH)MoO_2L-pip-Bz] (**8**). This synthesis route parallels the possible strategy of grafting the molybdenum complex to the Merrifield resin, by simple replacement of the benzyl chloride with the resin.

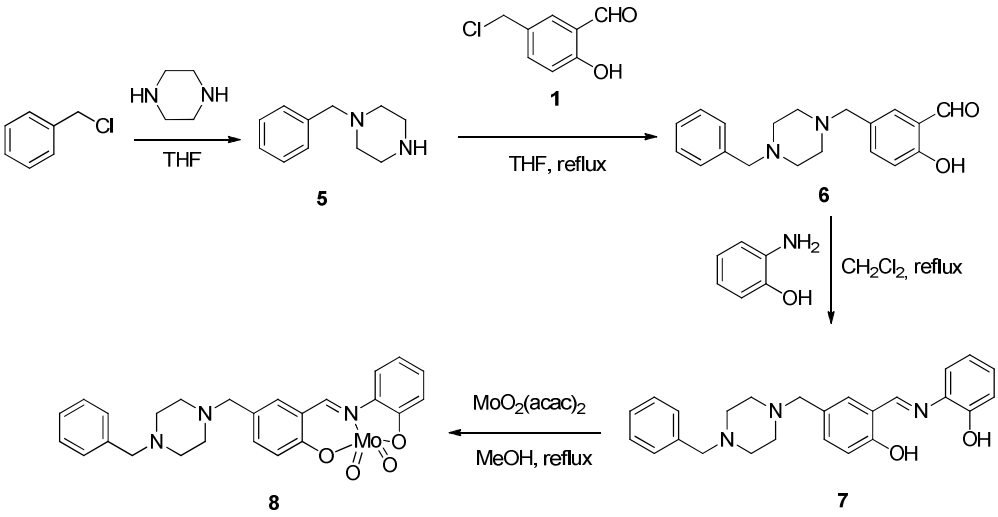

Scheme 5.4. Synthesis of [MoO_2L-pip-Bz].

V.2.1.2. Characterization

V.2.1.2.1. Infrared Spectroscopy

The most relevant IR spectroscopic properties of the starting compounds, ligands and complexes are collected in Table 5.1. The formation of the Schiff base (CH=N), brings a typical new vibration at around 1600-1620 cm^{-1}, at the same time the CH=O (1650 cm^{-1}) signal derived from salicylaldehyde disappears.

Table 5.1. IR of molecular compounds **1-8** and $[MoO_2L^j]_2$.

compound	OH	υ(CH_2)	CHO	C=N	Mo=O	Mo-O-Mo
1	3219	2876	1648	-	-	-
$[MoO_2L^j]_2$	-	2876	-	1610	931	884
2	3113	2939, 2810, 2771	1651	-	-	-
3		2928, 2805, 2757	-	1620	-	-
4	-	2919, 2811	-	1610	924, 903	-
4'	-	2919, 2811	-	1610	890	834
5	-	2938, 2804	-	-	-	-
6		2937, 2805, 2759	1657	-	-	-
7		2937, 2805, 2759	-	1621	-	-
8	-	2933, 2801, 2754	-	1611	895	838

The complexation of the L^{2-} ligand to the $\{MoO_2\}^{2+}$ fragment is suggested by a weak shift of the *CH=N* vibration in the 1600-1620 cm^{-1} region. For the complexes $[MoO_2L^j]_2$, **4** and **8**, the C=N vibration is red-shifted relative to the corresponding ligand.

The vibration pattern observed between 750 and 1100 cm^{-1} corresponding to the $\{MoO_2\}^{2+}$ fragment give additional information about the form of the isolated

complex. The most diagnostic Mo-O vibration bands are those appearing between 850 and 940 cm^{-1}. In the case of the monomeric species stabilized by one solvent molecule, (complexes **4**), two narrow absorption bands corresponding to Mo=O bonds are observed between 903 and 924 cm^{-1}. In the case of dimeric and polymeric compounds, one Mo=O vibration is visible in same region, and another band corresponding to Mo-O-Mo is observed around 800-885 cm^{-1}, which is 884, 834, 838 cm^{-1} for complexes $[MoO_2L^j]_2$, **4** and **8** respectively.

The formation of monomer or oligomers strongly depends on the nature of the ligand ***L*** surrounding the metal atom, in alcoholic solvent (EtOH, MeOH) the complex **4** is isolated in monomeric form, while $[MoO_2L^j]_2$, **8** are separated as oligomers.

V.2.1.2.2. NMR Spectroscopy

The ligand complexation is evidenced by the disappearance of two OH resonances in each case and by a weak downfield shift of the imine resonance (**4**, **8**) because of the nitrogen coordination to the molybdenum center (Table 5.2). In the case of the molybdenum complexes $[MoO_2L^j]_2$, the one-pot formation of the desired complex is suggested by the CHO (9.92) to imine resonance (9.30) ppm. It has to be pointed out that, since the measurements were performed in d_6-DMSO, the spectra observed for each complex correspond formally to the mononuclear $[MoO_2L(DMSO)]$ stoichiometry.

Table 5.2. ^{1}H NMR shifts of the molecular compounds 1-8 and $[MoO_2L^j]_2$

compound	OH	CHO	CH=N	Ar-H	(CH_2)	CH_2 in piperazine
1	11.08	9.92	-	7.00-7.75	4.58	-
$[MoO_2L^j]_2$	-	-	9.30	6.84-7.84	4.40	-
2	10.94	9.90	-	6.94-7.52	3.52	2.50
3	13.67, 9.70	-	8.95	6.85-7.53	3.42	2.39
4	-	-	9.29	6.83-7.84	3.47	2.43
4'	-	-	9.29	6.83-7.84	3.47	2.43
5	-		-	7.23-7.34	3.49	2.87, 2.39
6	10.88	9.90	-	6.95-7.51	3.49, 3.54	2.50
7	12.24	-	8.68	6.95-7.39	3.50, 3.54	2.51
8	-	-	9.28	6.83-7.84	3.39, 3.47	2.42

V.2.2. Grafting of molybdenum complexes on Merrifield resin

The molybdenum complex has been grafted on the Merrifield resin by two different synthetic routes. The analysis and catalytic activities of the two different resins will be presented and discussed. All relevant data (IR, elemental analysis and TGA) will be presented in Tables 5.3 and 5.6.

V.2.2.1. Direct Stepwise divergent approach – Route A

Based on the synthetic route of complex **8** (Scheme 5.4), the grafting starts from the Merrifield resin by stepwise addition of each required reagent (see Scheme 5.5).

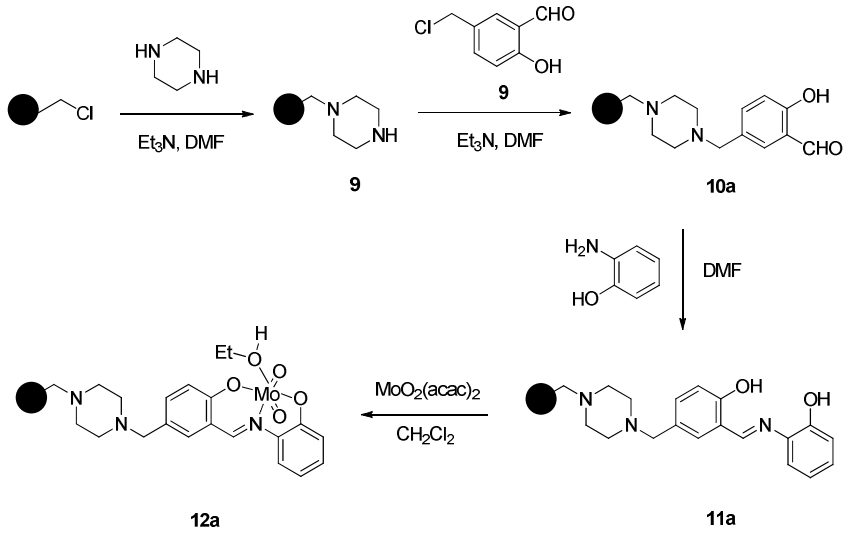

Scheme 5. 5 Route A: grafting of the molybdenum on Merrifield resin

The first step was the grafting in DMF of one function of piperazine on chloromethyl pending functions of the Merrifield resin (leading to **9**) in the presence of a base (Et_3N turned out to be the best choice). The colour of the resin changed from pale beige to pale yellow.The second step was the grafting of the aldehyde **1** to the free function of the piperazine through the chloromethyl function of **1** using the same synthetic method as for the first step, leading to a salicyladehyde grafted on a resin (**10a**). At this step, the resin color changed from pale yellow to yellow. The next step was the creation of the Schiff base **11a** by reaction between aminophenol and **10a** in DMF. The Schiff base formation was proved by the change of colour of the resin from yellow for **10a** to dark red for **11a** The last step, *i.e.* the generation of the grafted complex on the resin (**12a**), was accomplished by the simple reaction of **11a** with $[MoO_2(acac)_2]$. At this step, a colour change was also observed going to deep red. All those optical observations have been completed by some characterizations compiled in Table 5.3.

Characterizations

Table 5.3 Characterization of compounds for route A.

	Elemental analyses			TGA	IR	Color
	C	H	N	MoO_3 Residue (%)		
MR	79.13	6.36	0	0	3024, 2921, 1263 (C-Cl)	beige
Route A						
9	80.62	8.10	7.33	0	3023, 2921, 2084, 1675	Pale yellow
10a	79.12	7.54	6.18		1658 (CHO)	yellow
11a	76.23	6.96	6.55		1609 (C=N)	Dark red
12a	52.31	4.76	4.42	31.9	1612 (C=N) 938, 905 (Mo-O)	Yellow orange

Starting Merrifield resin

The starting Merrifield resin is a copolymer of styrene and divinylbenzene with some pending chloromethyl functions. Its formula is $C_xH_yCl_w$. Using elemental analysis data, the chlorine content (%Cl = 14.51) was obtained by difference from the experimental C and H % values.

$$\frac{n_{Cl}}{m_{polymer}} = \frac{\frac{\%Cl}{M_{Cl}} * 1}{100} = \frac{\frac{14.51g}{35.45g/mol}}{100g} = 4.09\ mmol\ Cl/g$$

The value is in agreement with the supplier specifications.

Compound 9

Compound **9** was characterized by IR and elemental analyses, the data were collected in Table 5.3. The elemental analysis is a good tool for the quantification in the case of compound **9**, since from the MR to **9**, the only N source isthe piperazine. Hence, the degree of piperazine grafting can be calculated from the N content as mmol pip/g polymer. From the experimentally determined nitrogen percentage of compound **9** (7.33%), the piperazine content can be calculated as

$$\frac{n_{pip}}{m_{polymer}} = \frac{\frac{\%N}{M_N} * 0.5}{100} = \frac{\frac{7.33g}{14.0067g/mol} * 0.5}{100g} = 2.62\ mmol/g$$

Compound 9

New vibrations are observed in compound **9**, such as 3374 [υ_s(N–H)], 1677 υ(N-H). The signal at 1263 cm^{-1} present in the strating Merrifield resin disappeared, which shows the -CH_2-Cl was replaced by -CH_2-N.

Compound 10a

The compound **10a** was characterized by IR with a vibration at 1658 corresponding to aldehyde. At this step, calculations done from elemental analysis with N gave a value of 2.21 mmol N_2 ligand/g polymer.

Compound 11a

The formation of the Schiff base in **11a** was indicated by the change of color of the resin (from yellow for **10a** to dark red for **11a**). The IR spectrum of **11a** showed a vibration band in the IR spectrum at 1609 cm^{-1} attributed to the imine function. The N content form elemental analysis, according to the equation,

$$\frac{n_{11a}}{m_{polymer}} = \frac{\frac{\%N}{M_N} * 0.33}{100} = \frac{\frac{6.55g}{14.0067g/mol} * 0.33}{100g} = 1.55\ mmol\ ligand\ /g$$

Compound 12a

Compound **12a** was formed with a slight color change. The IR showed signals at 942 and 903 cm^{-1} proving the presence of the MoO_2 moiety. The TG analysis of the polymer showed a residue of 32 % corresponding to MoO_3. The elemental analysis showed a decrease of the C, H and N content, in agreement with the introduction of the MoO_2 fragment.

The measured percent value of the residue from the TGA experiment leads to the estimation of a number of mole of molybdenum per gram of polymer of

$$\frac{n_{Mo}}{m_{polymer}} = \frac{\frac{residue}{M_{MoO3}}}{100} = \frac{\frac{31.9g}{143.94\ g/mol}}{100g} = 2.22\ mmol\ MoO3\ per\ g\ of\ polymer$$

This direct step-by-step approach is interesting but has some drawbacks. Indeed, as is typical for the grafting methods, each reaction step is incomplete. It is to be considered that the piperazine functions in compound **9** could remain protonated (even in presence of Et_3N) of could react with up to two chloromethyl functions within the polymer. While the first problem can be attenuated by increasing the

quantity of added base, the second is not easy to control. Those two phenomena decrease the amount of functions available for subsequent grafting. In addition, the step from **9** to **10a**, although simple in the case of the molecular species, is not so straightforward when one of them is anchored on the polymer, especially because of solubility problems. In order to solve this problem, an alternative step by step procedure was developed as presented below.

V.2.2.2. Modified stepwise divergent approach (route B)

This procedure needs in the first step the synthesis of molecular precursors, presented herein.

Molecular precursors

In order to achieve efficient grafting of the ligands on the support, the strategy employed here started with the BOC protection (see Scheme 5.6) of one piperazine function (compound **13).** This allows the selective addition of only one aldehyde function to **13** leading to compound **14**. After deprotection, the free amine function of the compound was regenerated in the isolated compound **15**.

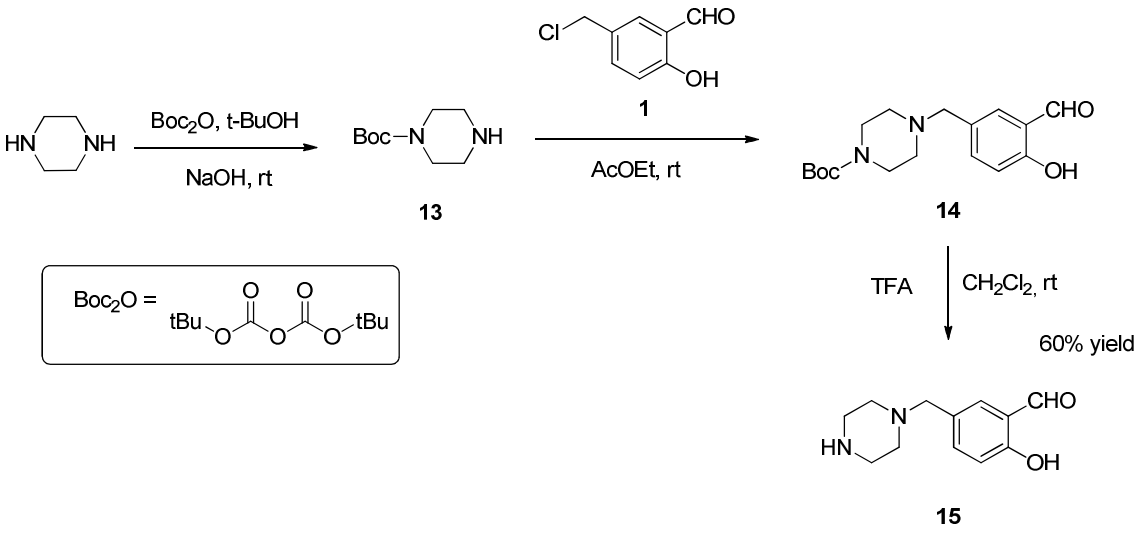

Scheme 5. 6 Synthesis of Molecular precursors

The ^{1}H NMR spectra of the molecular precursors are collected in Table 5.4. The grafting was proved by the signal corresponding to the aldehyde of **14** and **15** around 10 ppm. The deprotection of BOC brings a weak lowfield shift of the (CH_2) and a shift of the signal of the aldehyde for compound **15**.

The IR spectroscopic data of the molecular precursors are collected in Table 5.5. The (C=O) is observed at 1682 cm^{-1} derived from BOC in **13**. CHO is observed in **14** after the reaction between **13** and **1**.

Table 5.4. ^{1}H NMR shifts of the molecular compounds **13-15**.

compound	OH	CHO	Ar-H	(CH_2)	CH_2 in piperazine	CH_3
13	-	-	-	-	2.81,3.3	1.47
14	10.97	9.9	6.96-7.5	3.48	2.38, 3.43	1.46
15		10.06	6.9-7.68	3.61	2.72, 3.23	-

Table 5.5. IR of molecular compounds **13-15**.

compound	υ(N-H)	C=O	CHO	υ(CH_2)
13	3330	1682	-	2974, 2805
14	-	-	1652	2974, 2809
15		-	1652	2805

Grafting reactions

The precursor **15** was reacted directly with the Merrifield resin to obtain the modified resin **10b**. This then reacts with aminophenol to obtain formally the *ONO* ligand grafted on resin, called here **11b**. Relative to route A, the reaction appeared to produce a greater degree of surface functionalization as visually indicated by the resin colour (red-blood). The synthesis was then completed as already described in route A with the metal complexation step to obtain the molybdenum grafted resin **12b**. A very strong colour change was observed during this step, from red to brown.

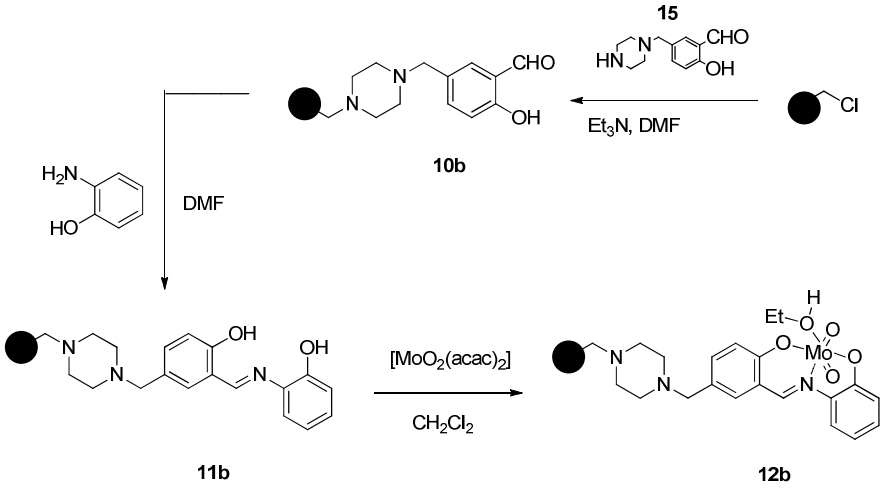

Scheme 5. 7 Route B: grafting of the molybdenum on Merrifield resin

Characterization of the resins

Table 5.6 –Spectroscopic data of resins for route B

	Elemental analyses			TGA	IR	Color
	C	H	N	MoO_3 Residue (%)		
MR	79.13	6.36	0			beige
Route B						
10b	75.92	7.33	5.70		1653 (CHO)	Red-orange
11b	74.02	7.16	6.00		1609 (C=N)	Red-blood
12b	44.25	4.25	3.44	32.0	943, 903 (Mo-O)	brown

Compound 10b

It is possible to evaluate the percentage of compound **15** grafted per gram of polymer from the elemental analysis data, since the starting resin does not contain nitrogen. As already shown above for compound **9**, the value is

$$\frac{n_{\mathbf{10b}}}{m_{polymer}} = \frac{\frac{\%N}{M_N} * 0.5}{100} = \frac{\frac{6.55g}{14.0067g/mol} * 0.5}{100g} = 2.03\ mmol/g$$

The amount in this case is lower than in compound **9**, which can be rationalized by the greater size of the grafting molecule.

Compound 11b

The formation of the Schiff base in **11b** could not be proven by the change of the resin color (from red for **10b** to dark red for **11b**) but a vibration peak at 1610 cm^{-1} appears in the IR spectrum, proving the generation of the CH=N function. Using the N content form the elemental analysis, the degree of functionalization is calculated as

$$\frac{n_{11b}}{m_{polymer}} = \frac{\frac{\%N}{M_N} * 0.33}{100} = \frac{\frac{6.0g}{14.0067g/mol} * 0.33}{100g} = 1.43\ mmol\ /g$$

Compound 12b

The IR spectrum of **12b** showed signals at 942 and 903 cm^{-1} proving the presence of the MoO_2 moiety. The TG analysis of the polymer showed a residue of 32 % corresponding to MoO_3. As for route A, the elemental analysis showed a decrease of the C, H and N content, in agreement with the introduction of the $\{MoO_2\}^{2+}$ fragment. The TGA analysis gave the same value as for **12a**, corresponding to 2.22 mmol Mo/g polymer.

V.2.3. Catalytic tests

V.2.3.1. Epoxidation of cyclooctene catalyzed by the grafted molybdenum catalysts (12a and 12b).

The molecular complexes $[MoO_2(SAP)]_2$ and $[MoO_2L^j]_2$, (Scheme 5.2) and the grafted complexes **12a** and **12b** were compared as catalysts in the epoxidation of cyclooctene at 80 °C under the same organic solvent-free condition described above in chapter **III**.

The first observation of interest is the different activity between the two molecular molybdenum complexes. Complex $[MoO_2L^j]_2$ is more active than $[MoO_2(SAP)]_2$ (see Scheme 5.7). After 4 h, the conversion is 88% *vs*. 76%, and the initial TOF value is nearly three times higher (193 *vs.* 70 h^{-1}). The selectivity was not affected by the functionalization.The catalytic reactions in the presence of the grafted complexes are slower. This is certainly due to the insoluble nature of the resins and consequently the greater impact of mass transport limitations. Catalyst **12a** was slightly less active than **12b** in the first run.

Table 5. 7– Influence of catalyst for organic solvent-free epoxidation of cyclooctene[a].

complex	Conversion/%	Selectivity/%	TOF_{init} [h^{-1}]	TON
$[MoO_2(SAP)]_2$[a]	74	93	70	153
$[MoO_2L^j]_2$[a]	88	93	193	175
12a[b]	51	72	28	102
12a'[b]	70	72	18	142
12a"[b]	79	68	93	159
12b[b]	63	64	15	127
12b'[b]	64	78	15	129
12b"[b]	54	59	18	107

[a]Conditions: Mo/TBHP/cyclooctene = 0.5/200/100; T = 80°C; t = 4 h. The initial TOF is calculated from the conversion after the first 30 min.

[b]Mo/TBHP/cyclooctene = 0.5 /200/100, T = 80°C, t = 8 h.

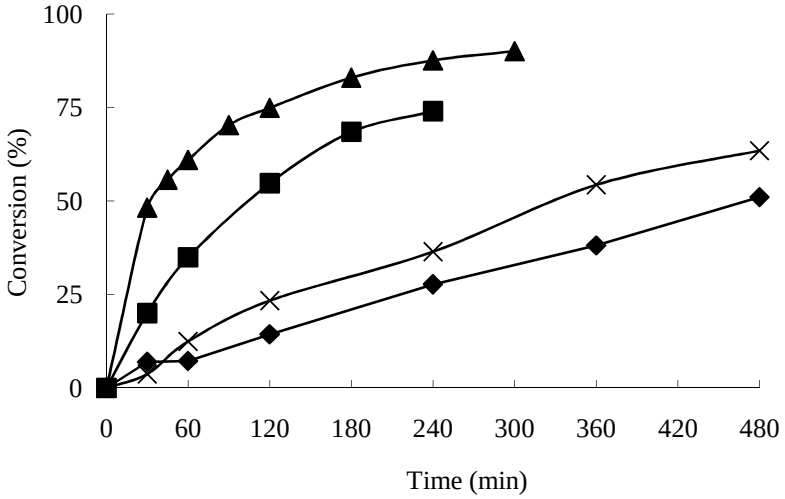

Figure 5.1 Kinetic profile of converted cyclooctene *vs*. time, conditions: Mo/TBHP/cyclooctene = 0.5/200/100; T = 80℃, $[MoO_2(SAP)]_2$ (■), $[MoO_2L^j]_2$ (▲), 12b (×), 12a (◆).

V.2.3.2. Recycling and reuse of catalysts for organic solvent-free epoxidation of cyclooctene with grafted molybdenum catalysts 12a and 12b.

The two grafted compounds were recycled and reused 3 times each. Catalyst **12a** is the less active one in the first run (51% conversion after 8 h), but the activity increases each time (70% in the second run and 79% in the third run). Catalyst **12b**, on the other hand, gives a nearly identical conversion (63%), as well as TOF and TON, in the first and second run. In the third run, the conversion and selectivity slightly decreased (Table 5.8).

Table 5. 8– Recycle and reuse of catalysts for organic solvent-free epoxidation of cyclooctene with grafted Molybdenum catalysts12a and 12b [a].

Catalyst	Runs	Conversion/%	Selectivity/%	TOF_{init} [h^{-1}]	TON
12a	1	51	72	28	102
	2	70	72	18 (53)	141
	3	79	68	93 (36)	159
12b	1	63	64	15 (34)	127
	2	64	78	15 (25)	129
	3	54	59	19 (21)	107

[a]Conditions: Mo/TBHP/cyclooctene = 0.5/200/100; T = 80°C, t = 8 h. The initial TOF is calculated from the conversion after the first 30 min, in parenthses is after 60 min.

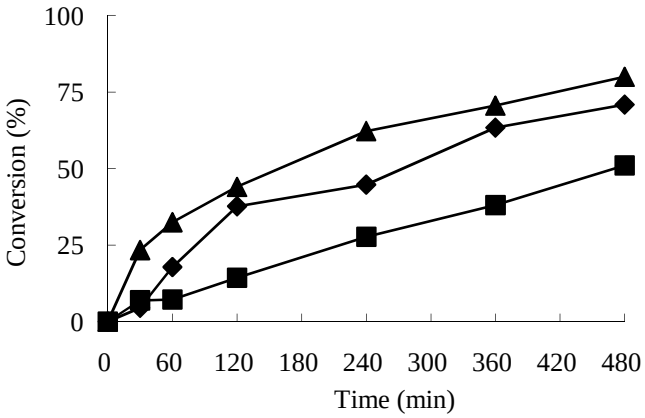

Figure 5. 2 Recycle and reuse of catalysts for organic solvent-free epoxidation of cyclooctene with grafted Molybdenum catalyst **12a**, conditions: Mo/TBHP/cyclooctene = 0.5/200/100, T = 80℃, t = 8 h, 1 st run (■), 2nd run(◆),3rd run (▲).

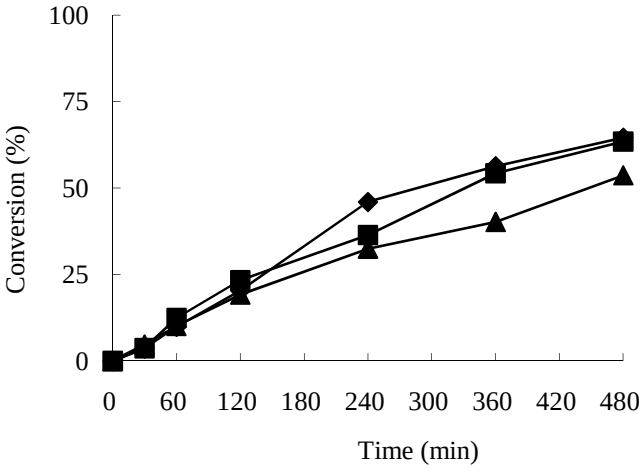

Figure 5. 3 Recycle and reuse of catalysts for solvent-free epoxidation of cyclooctene with grafted Molybdenum catalyst **12b**, conditions: Mo/TBHP/cyclooctene = 0.5/200/100, T = 80℃, t = 8 h, 1st run (■), 2nd run(◆),3rd run (▲).

The colour of **12a** gradually changed from orange to yellow, possible caused by alcohol coordination to the Mo center. Catalyst **12b**, on the other hand, did not show any color change. There was no significant change of the IR spectrum after each step, suggesting catalyst stability (Fig. 5.4 and Fig. 5.5). The vibrations corresponding to Mo=O vibrations were observed at 937 and 899 cm^{-1} for all steps before and after the catalysis. A value at 800 cm^{-1} could be attributable to Mo-O-Mo vibrations. This vibration is constantly present in case of **12b** after each run and appears in case of **12a** after the first run.

Furthermore, TGA of both resins (Table 5.9) after the third run indicate no obvious mass loss (< 6%), indicating that there is no significant catalyst leaching.

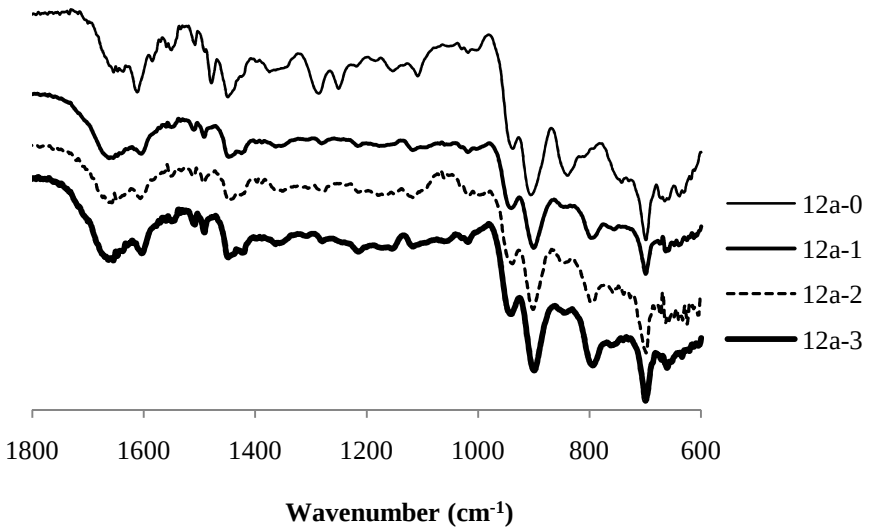

Figure 5. 4 IR before and after recycle of catalysts **12a**.

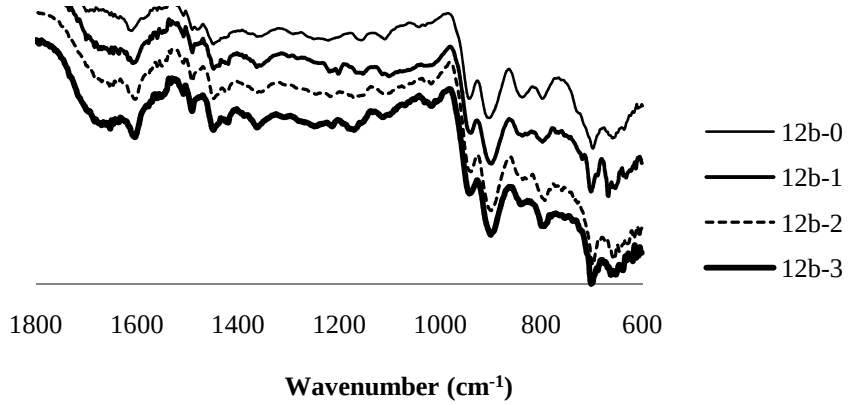

Figure 5. 5 IR before and after recycle of catalysts **12b**.

Table 5. 9 TGA (residue) of catalysts used before and after catalysis.

	12a		**12b**	
runs	TGA (residue)	nMo/g resin	TGA (residue)	nMo/g resin
0	31.9	2.22	32.0	2.22
3	30.8	2.14	30.1	2.09

V.3. Conclusion

In this chapter, a molybdenum complex with *ONO* tridentate ligand has been grafted to Merrifield resin by piperazine linkers through several successive reactions steps and *via* two different routes.

These compounds have been characterized by IR, TGA and elemental analysis. The two grafted compounds have been tested the catalytic activity in the epoxidation of cyclooctene. Since, the complexes are insoluble, they can work as heterogeneous catalysts and can be recovered and reused 3 times for the epoxidation of cyclooctene with no significant activity loss.

V.4. Experimental part

V.4.1. Materials and methods

All preparations were carried out in air.

Merrifield resin (1% cross-linked, 3.5-4.5 mmol/g Cl, Aldrich), salicylyladehyde (98% Aldrich), paraformaldehyde (96%, ACROS), 37% hydrochloric acid (Aldrich), 2-aminophenol, piperazine anhydrous (98%, TCI), triethylamine (99% Aldrich), Boc_2O (98% Aldrich), benzylchloride (99% Aldrich), trifluoroacetic acid (99% Aldrich) were used as received. $[MoO_2(acac)_2]$ was freshly prepared as descried in literature.[63] Cyclooctene (98% Aldrich), cyclooctene oxide and TBHP (70wt% in water, ACROS) were used as received.

The thermogravimetric analyses were performed on a SETARAM TGA 92-16.18 thermal analyzer. The sample was placed into a nickel/platinum alloy crucible and heated at 0.83 $K \cdot s^{-1}$ in a reconstituted air flow from 15°C to 700°C. An empty crucible was used as a reference. Infrared spectra were recorded in KBr matrices at room temperature with a Mattson Genesis II FTIR spectrometer. ^1H spectra were recorded at 200.1 MHz on a Bruker Avance DPX-200 spectrometer. The elemental analyses were obtained from the analytical services of the Laboratoire de Chimie de Coordination (LCC).

Catalytic reactions were followed by gas chromatography on an Agilent 6890A chromatograph equipped with FID detector, a HP5-MS capillary column (0.30 m x 0.25 mm x 0.25 m) and automatic sampling, or on a Fisons GC 8000 chromatograph equipped with FID detector and with a SPB-5 capillary column (30 m x 0.32 mm x 0.25 m). The GC parameters were quantified with authentic samples of the reactants and products. The conversion of *cis*-cyclooctene and the formation of cyclooctene oxide were calculated from calibration curves (r^2= 0.999) relatively to an internal

standard (acetophenone).
The procedure of recovery was done in the similar condition.The grafted catalysts were first used for the recovery/recycle, after the cycle finished, the mixture were filtered and washed with H_2O, acetone, CH_2Cl_2 and Et_2O, then dried under reduced pressure at 30°C for overnight before the next cycle.

V.4.2. Synthetic part

V.4.2.1. 5-Chloromethyl-2-hydroxybenzaldehyde (1).

This compound was prepared by a modification of the already described procedure.[95] Salicylaldehyde (13.3 mL, 0.125 mol), paraformaldehyde (6.75 g, 0.225 mol), and 70 mL of concentrated hydrochloric acid (37%) were mixed and stirred at room temperature for 24 h. The pink solid that formed was separated from the reaction mixture by filtration, dissolved in diethyl ether, and the solution was dried over sodium sulphate. The solvents were evaporated and the pink slurry residue was recrystallized from n-hexane affording 9.91 g of white needles (yield: 50%).

IR (KBr, ν(cm^{-1})): 1648 (CH=O).
^{1}H NMR (300 MHz, $CDCl_3$, δ(ppm)): 4.58 (s, 2H) , 7.03-7.00 (d, 1H, J = 8.49 Hz), 7.61-7.55 (m, 2H), 9.92 (s, 1H), 11.08 (s, 1H).

V.4.2.2. Synthesis of the Mo complex $[MoO_2Li]_2$

In a 100 mL Erlenmeyer flask, 0.30 g of 5-chloromethyl-2-hydroxybenzaldehyde (**1**) (1.89 mmol) was dissolved in 2 mL of methanol and 0.21 g of 2-aminophenol (1.92 mmol) was added. Thirty minutes later, 0.61 g of [MoO_2(acac) $_2$] (1.89 mmol) was added. The mixture was stirred for 4 hours at room temperature. The resulting red solution was evaporated at room temperature, washed with Et_2O and dried under reduced pressure for 24 hours to afford 0.52 g product.

Yield: 71%.Anal. Calc. for $C_{14}H_{10}ClMoNO_4$ (Mr = 387.633): C, 43.38; H, 2.60; N, 3.61%. Found: C, 46.14; H, 2.98; N, 3.51%. TGA Δm= exp(theo) 62.3 (62.8) %.IR (KBr, ν(cm^{-1})): 1610 (C=N), 931 (Mo=O), 884 (Mo-O-Mo). ^{1}H NMR (DMSO-d_6, 300 MHz, δ(ppm)): 4.40 (s, 2 H, CH_2Cl), 6.84-7.84 (m, 7 H, Ar-*H*), 9.30 (s, 1 H, C*H*=N). ^{13}C{^{1}H} NMR (300 MHz, DMSO-d_6) δ: 162.7 (C_H-N), 154.9 (C_q-O), 151.1 (C_q-O), 148.3 (C_q-S), 139.1 (C_H-Ar), 129.9 (C_H-Ar), 129.1 (C_H-Ar), 125.6 (C_H-Ar), 125.0, 122.9 (C_q), 120.4 (C_H-Ar), 120.0 (C_H-Ar), 119.2 (C_H-Ar).

V.4.2.3. Synthesis of compound 2.

The procedure modified from the reported method.[96] A solution of 0.24 g of **9** (1.44 mmol) in 6 mL acetone was added dropwise to a stirred solution of 0.06 g of piperazine (0.72 mmol) in 4 mL acetone. The resulting yellow solution was allowed to reflux with stirring for 6 h to give a yellow precipitate of dialdehyde chlorhydrate. The precipitate was washed with solvent THF (3×1 mL) and water (3×1 mL) to remove unreacted starting materials. The resulting solid was treated with saturated sodium bicarbonate solution (8 mL) and the desired dialdehyde **2** was extracted with CH_2Cl_2 (4×5 mL). The organic layer was washed with water (2×1 mL) and brine (2×1 mL), and dried over anhydrous Na_2SO_4. The removal of the organic solvent gave yellow solid dialdehyde **2** 0.20 g (yield: 78%), which was used as such without further purification for the next step.

IR (KBr, cm^{-1}): 3113 (OH); 2939, 2810, 2771(C-H); 1651(CH=O); 1592, 1483 (C=C).^{1}H NMR ($CDCl_3$, 300 MHz, δ (ppm)): 2.50 (br, s, 8H, CH_2 in piperazine), 3.51 (s, 4H, CH_2), 6.94-7.52 (6H; Ar-H), 9.90 (s, 2H, CHO), 10.94 (s, 2H, OH).^{13}C{^{1}H} NMR (300 MHz, DMSO-d_6) δ: 196.5 (C_H-N), 160.8 (C_q-O), 138.0 (C_H-Ar), 133.9 (C_H-Ar), (C_q), 130.0 (C_q), 120.4 (C_H-Ar), 61.8 (C_{H2}-CH_2), 62.9 (C_{H2}-CH_2-CH_2).

V.4.2.4. Synthesis of schiff base 3

In a 100 mL Erlenmeyer flask, 0.166 gof **2** (0.469 mmol) was added to 8 mL of methanol. Then, 0.102 g of 2-aminophenol (0.937 mmol) in 2 mL of methanol was added. The mixture was stirred at the reflux temperature for 6 hours until the product formed as a red precipitate. The precipitate was filtered, washed with methanol, CH_2Cl_2, diethylether and dried under vacuum at room temperature to give an orange powder.

Yield: 0.227 g (90%). IR (KBr, cm^{-1}): 2928 (m, νC-H), 2757, 2805, 1620 (C=N). ^{1}H NMR (300 MHz, DMSO-d_6, δ(ppm)): 2.39 ((br s, 8H, CH_2 in piperazine), 3.42 (s, 4 H, CH_2). 6.85-7.53 (m, 14 H, Ar-*H*), 8.95 (s, 2 H, C*H*=N), 9.70 (s, 2 H, Ar-O*H*), 13.67 (s, 2 H, Ar-O*H*). ^{13}C{^{1}H} NMR (300 MHz, DMSO-d_6) δ: 162.0 (C_H-N), 160.2 (C_q-O), 151.5 (C_q-O), 135.4 (C_q-N), 134.0 (C_H-Ar), 132.9 (C_H-Ar), 129.7 (C_H-Ar), 128.8 (C_q), 120.1 (C_H-Ar), 120.0 (C_H-Ar), 119.5 (C_q), 116.9 (C_H-Ar), 61.6 (C_{H2}-CH_2), 53.4 (C_{H2}-CH_2-CH_2).

V.4.2.5. Synthesis of complex 4 and 4'.

In a 100 mL Erlenmeyer flask, 0.20 g of **3** (0.373 mmol) was dissolved in 8 mL of methanol and 0.249 g of $[MoO_2(acac)_2]$ (0.763mmol) was added. The mixture was refluxed with magnetic stirring for 4 hours. The resulting orange precipitate was separated by filtration and washed with methanol, CH_2Cl_2, Et_2O, to yield 0.31 g of **4** as an orange powder. The solid was dried at 80 °C under reduced pressure for 12 h yielding **4'** as a brown compound.

4': Anal. Calc. for $C_{32}H_{28}Mo_2N_4O_8$ (Mr = 788.47): C, 48.75; H, 3.58; N, 7.11%. Found: C, 44.64; H, 3.41; N, 6.45%.
TGA Δm= exp(theo) 63.7 (63.5) %. IR (KBr, ν(cm^{-1})) 1610 (C=N), 890 (Mo=O), 834 (Mo-O-Mo). ^{1}H NMR (300 MHz, DMSO-d_6, δ(ppm)): 2.43 ((br, s, 8H, CH_2 in piperazine), 3.47 (s, 4 H, CH_2). 6.83-7.84 (m, 14H, Ar-*H*), 9.29 (s, 2H, C*H*=N).

V.4.2.6. General Procedure for 1-Benzylpiperazine 5.

Similar to the reported method,[97] 1.81 g of anhydrous piperazine (21.0 mmol, 6 equiv.) was added to 25 mL THF and heated to the reflux temperature until the piperazine was fully dissolved. To the resulting solution, 0.445 g of benzyl chloride (3.51 mmol, 1 equiv.) was added dropwise.[98] A white precipitate formed immediately. The reaction mixture was refluxed for 3 hours. The resulting mixture was evaporated, then washed with a basic aqueous solution with 5% brine and KOH (pH >12). The aqueous layer was extracted with CH_2Cl_2 (3 x 10mL) and EtOAc (10 mL) at pH > 12, washed with H_2O (2 x 2 mL) and brine (2 x 2 mL). The organic layers were combined, dried over Na_2SO_4 and concentrated *in vacuo* to dryness to leave a colorless oil (yield: 0.57 g, 3.3 mmol, 91%).

IR (KBr, ν(cm^{-1})): 2938, 2804 υ(CH_2). ^{1}H NMR (300 MHz, $CDCl_3$-*d*, δ(ppm)) δ: 1.95 (br s, 1H, NH), 2.87 (t, J = 4.86, 4H CH_2), 2.39 (t, 4H, CH_2), 3.49 (s, 2H, CH_2Ph), 7.23-7.34 (m, 5H, Ph). ^{13}C{^{1}H} NMR (300 MHz, DMSO-d_6) δ: 138.0 (C_q), 129.2 (C_H-Ar), 128.2 (C_H-Ar), 127.0 (C_H-Ar), 63.70 (C_{H2}-CH_2), 54.4 (C_{H2}-CH_2-CH_2), 46.1 (C_{H2}-CH_2-CH_2).

V.4.2.7. General Procedure for 6.

To a solution of 0.54 g of benzylpiperazine **5** (3.08 mmol) in 5 mL THF was added dropwise a solution of 0.526 g of 5-chloromethyl-2-hydroxybenzaldehyde (**1**) (3.08 mmol) in 5 mL THF. A yellow precipitate formed immediately. The reaction mixture was refluxed for 6 hourswith TLC monitoring. The mixture was evaporated, then washed with a basic aqueous solution with 5% brine and KOH (pH >12). The

aqueous layer was extracted with CH_2Cl_2 (3 x 10 mL) and EtOAc (10 mL) at pH > 12, washed with H_2O (2 x 2 mL) and brine (2 x 2 mL). The organic layers were combined, dried over Na_2SO_4 and concentrated to dryness under reduced pressure leaving a colorless oil which was dried in vacuo (yield: 0.87 g, 2.81 mmol, 91%).

IR (KBr, ν(cm^{-1})): 1657 (CHO). ^{1}H NMR (300 MHz, $CDCl_3$-*d*, δ (ppm)): 2.50 (br, s, 8H, CH_2 in piperazine), 3.49 (s,2H, CH_2), 3.54 (s, 2H, CH_2), 6.954-7.51 (m, 8H, Ar-H), 9.90 (s, 1H, CHO), 10.88 (s, 1H, Ar-OH). $^{13}C\{^1H\}$ NMR (300 MHz, DMSO-d_6) δ: 196.6 (CHO), 160.7 (C_q-O), 138.0 (C_H-Ar), 137.8 (C_H-Ar), 130.3 (C_q), 129.9 (C_q), 129.2 (C_H-Ar), 128.2 (C_H-Ar), 127.0 (C_H-Ar), 120.3 (C_q), 117.4 (C_H-Ar), 63.0 (C_H-CH_2), 62.1 (C_H-CH_2), 52.9 (C_H-CH_2).

V.4.2.8. General procedure for Schiff base 7.

In a 100 mL Erlenmeyer flask, to a solution 0.499 g of **6** (1.61 mmol) dissolved in 10 mL of CH_2Cl_2 was added a solution of 0.176 g of 2-aminophenol (1.61 mmol) in 5 mL of CH_2Cl_2. The mixture was refluxed with magnetic stirring for 6 hours until the solution became red. The solution was evaporated, washed with pentane and dried under vacuum at room temperature to give an orange powder. Yield 0.586 g (90 %). Anal. Calc. for $C_{25}H_{27}N_3O_2$ (Mr = 401.5): C, 74.79; H, 6.78; N, 10.47%. Found: C, 73.79; H, 6.41; N, 10.13%.IR (KBr, ν(cm^{-1})): 2937, 2805, 2759 (CH_2), 1621 (C=N). ^{1}H NMR (300 MHz, $CDCl_3$-*d*, δ(ppm)): 2.51 (br, s, 8H, CH_2 in piperazine), 3.50 (s, 2H, CH_2), 3.54 (s, 2H, CH_2), 6.95-7.39 (m, 12H, Ar-*H*), 8.68 (s, 1H, C*H*=N), 12.24 (s, 1H, Ar-O*H*). $^{13}C\{^1H\}$ NMR (300 MHz, DMSO-d_6) δ: 163.6 (C_H-N), 160.1 (C_q-O), 150.1 (C_q-O), 137.8 (C_q-N), 135.9 (C_q-O), 134.8 (C_H-Ar), 133.2 (C_H-Ar), 129.3 (C_H-Ar), 128.6 (C_H-Ar), 128.2 (C_H-Ar), 127.1 (C_H-Ar), 120.9 (C_H-Ar), 119.0 (C_q), 118.5 (C_H-Ar), 117.0 (C_H-Ar), 116.1 (C_H-Ar), 63.0 (C_H-CH_2), 62.1 (C_H-CH_2), 52.9 (C_H-CH_2).

V.4.2.9. Synthesis of complex 8.

In a 100 mL Erlenmeyer flask, to 0.28 g of **7** (0.699 mmol) dissolved in 10 mL of methanol was added 0.223 g of [$MoO_2(acac)_2$] (0.74 mmol). The mixture was stirred under reflux for 6 hours. The resulting orange solution was evaporated under vacuum and washed with Et_2O, pentane, dried (50 °C) under reduced pressure for 12 hours to give **8** (0.356 g, 96%).

Anal. Calc. for $C_{25}H_{25}MoN_3O_4$ (Mr = 527.42): C, 56.93; H, 4.78; N, 7.97%. Found: C, 52.97; H, 4.37; N, 6.95%. TGA Δm= exp(theo) 72.7 (72.7) %. IR (KBr, ν(cm^{-1})) 2933, 2801, 2754 [m, ν(C-H)], 1611 (C=N), 895 (Mo=O), 838 (Mo-

O-Mo). ^{1}H NMR (300 MHz, DMSO-d6, δ (ppm)): 2.42 (br, s, 8H, CH_2 in piperazine), 3.39 (s, 2H, CH_2), 3.47 (s, 2H, CH_2), 6.83-7.84 (m, 12H, Ar-*H*), 9.28 (s, 1H, C*H*=N). ^{13}C{^{1}H} NMR (300 MHz, DMSO-d_6) δ: 160.7 (C_q-O), 160.5 (C_q-O), 157.1 (C_H-N), 136.6 (C_H-Ar), 136.1 (C_q-N), 135.5 (C_H-Ar), 130.5 (C_H-Ar), 129.7 (C_q), 129.3 (C_H-Ar), 128.6 (C_H-Ar), 127.4 (C_H-Ar), 122.1 (C_q), 120.8 (C_H-Ar), 120.1 (C_q), 119.0 (C_H-Ar), 118.0 (C_q), 117.7 (C_H-Ar), 116.9 (C_H-Ar), 62.3 (C_H-CH_2), 61.1 (C_H-CH_2), 52.9 (C_H-CH_2).

V.4.2.10. Procedure for the preparation of piperazine resin (8)

In a 250 ml three-necked round bottom with a magnetic stirrer, 1.98 g (23.0 mmol) of piperazine were suspended in 10 ml of DMF and dissolved at 60 °C. Then, 0.96 ml of triethylamine (6.9 mmol) and 0.56 g of Merrifield resin (2.3 mmol Cl, approx. 4.1 mmol Cl/g) were added. The mixture was stirred for three days at 70 °C. The hot resin was filtered off and washed with different solvents in the following order (DMF, water, ethanol, acetone, dichloromethane and diethylether) and dried under high vacuum to give 0.67 g pale yellow solid.

Anal. found: C, 79.12; H, 7.54; N, 6.18%. IR (neat): υ = 3374 [m, υ_s(N–H)], 2913, 2809 [s, υ(CH_2)], 1677 υ(N-H), 1140 (m), 1006 (m), 815 (m).

V.4.2.11. Procedure for the preparation of aldehyde piperazine resin (10a) and (10b)

10a:

In a 250 ml three-necked round bottom with magnetic stirrer, 0.335 g (1.96 mmol) of 5-chloromethyl-2-hydroxybenzaldehyde (**1**) were dissolved in 10 ml of DMF and stirred. Then, and $NaHCO_3$ (0.193 g, 2.29 mmol) were added, and 0.5 g of piperazine resin **(9)** (approx. 3.5-4.5 mmol/g) were added. The mixture was stirred for 3 days at 70 °C. The hot resin was filtered off, washed with different solvents in the following order (DMF, water, ethanol, acetone, dichloromethane and diethylether) dried under high vacuum to obtain 0.307 g of a yellow solid.

Anal. found: C, 79.12; H,7.54; N, 6.18%.
IR (neat): 2913, 2802 [s, υ(CH_2)], 1658 [s, υ(CHO)].

10b:
In a 250 ml three-necked round bottom with magnetic stirrer, 0.15 g (0.68 mmol) of

2-hydroxy-5-(piperazin-1-ylmethyl)benzaldehyde (**15**) were dissolved in 10 ml of DMF and stirred. Then, and triethyamine (0.2 ml, 2.04 mmol) were added, and 0.107 g of Merrifieldresin (approx. 4.1 mmol/g) were added. The mixture was stirred for 3 days at 70 °C. The hot resin was filtered off and washed with different solvents in the following order (DMF, water, ethanol, acetone, dichloromethane and diethylether) and dried under high vacuum affording 0.154 g of a red-orange solid.

Anal. found: C, 75.92; H, 7.33; N, 5.70.
IR (neat): 2922, 2806 [s, υ(CH_2)], 1653 [s, υ(CHO)].

V.4.2.12. Procedure for the preparation of aldehyde piperazine resin (11a) and (11b)

In a 250 ml three-necked round bottom with a magnetic rotor, 2-aminophenol was dissolved in DMF. Then, the piperazine resin **(10a, b)** (approx. 3.5-4.5 mmol/g) was added. The mixture was stirred for 24 h at 60 °C. The hot resin was filtered off and washed with different solvents in the following order (DMF, water, ethanol, acetone, dichloromethane and diethylether) and dried under high vacuum yielding a dark red solid.

11a:
Anal. found: C, 76.23; H, 6.96; N, 6.55%.
IR (neat): 3023, 2916, 2807 υ(CH_2), 1618 (C=N), 1006 (m).

11b:
Anal. found: C, 74.02; H, 7.16; N, 6.00%.
IR (neat): 3023, 2923, 2807 υ(CH_2), 1609 (C=N), 1007 (m).

V.4.2.13. N-Boc-piperazine (4)

Boc_2O (6.72 g, 30.8 mmol) was added dropwise over 30 minutes to a solution of piperazine (6.685 g, 77.6 mmol) in *t*-BuOH (90 mL) and NaOH (12 mL of a 2.5 N aqueous solution). The reaction mixture was stirred at room temperature for 1h. t-BuOH was evaporated under reduced pressure. The aqueous layer was extracted with CH_2Cl_2 (3 x 50 mL), the organic fractions were dried over Na_2SO_4 and evaporated under vacuum to give the product as a light yellow oil (4.807 g, 84%).

IR (KBr, cm^{-1}): 3330 υ(N-H), 2974 (CH_3), 2805 (CH_2), 1682 [s, (C=O)]. ^1H NMR (300 MHz, $CDCl_3$-*d*, δ(ppm)): 1.47 (s, 9H, CH_3), 1.63 (br, N-H), 2.81 (t, *J* = 4.7, 4H, CH_2 in piperazine), 3.3 (t, *J* = 4.6, 4H, CH_2 in piperazine). $^{13}C\{^1H\}$ NMR (300 MHz, DMSO-d_6) δ: 45.9 (C_H-CH_2), 28.4 (C_H-CH_3).

V.4.2.14. 2-hydroxy-5-(4-Boc-piperazin-1-ylmethyl)benzaldehyde (14).

1-Boc-piperazine (**13**) (1.643g, 8.82 mmol) was added dropwise to a solution of **1** (1.000 g, 4.41 mmol) in EtOAc (15 mL) at room temperature. The reaction mixture was stirred for 1 h, diluted with EtOAc (20 mL), rinsed with $NaHCO_3$ (2 x 30 mL of a saturated aqueous solution), dried over $NaSO_4$ and concentrated under vacuum to afford a light thick yellow oil (1.323 g, 80%) which was deprotected in the next step without further purification.

IR (KBr, cm^{-1}): 2974 (CH_3), 2809 (CH_2), 1684 [s, (C=O)], 1652 (CHO). ^1H NMR (300 MHz, $CDCl_3$-*d*, δ(ppm)): 1.46 (s, 9H, CH_3), 2.38 (t, *J* = 4.8, 4H, CH_2 in piperazine), 3.43 (t, *J* = 5.1, 4H, CH_2 in piperazine), 3.48 ((s, 2H, CH_2 in piperazine), 3.42 (s, 4 H, CH_2). $^{13}C\{^1H\}$ NMR (300 MHz, DMSO-d_6) δ: 196.5 (C_H-CHO), 160.9 (C_q-O), 154.8 (C_q-O), 137.9 (C_H-Ar), 133.8 (C_H-Ar), 129.6 (C_q-O), 120.3 (C_q), 117.6 (C_H-Ar), 62.0 (C_H-CH_2), 53.1 (C_H-CH_2-CH_2), 28.4 (C_H-CH_3).

V.4.2.15. 2-hydroxy-5-(piperazin-1-ylmethyl)benzaldehyde (15)

To the product obtained above **(14)** (376.5 mg, 1 mmol) in dry CH_2Cl_2 (15 mL) was added trifluoroacetic acid (2 mL) dropwise at 0°C. The reaction mixture was stirred at room temperature for 2 h and was evaporated, quenched by addition of $NaHCO_3$ (5 mL of a saturated aqueous solution). The crude material was extracted with EtOAc (2 x 50 mL), dried over Na_2SO_4, concentrated under vacuum, purified over a short plug of silica gel (100% EtOAc) to afford **15** as a light yellow solid (212.3 mg, 77%).

IR (KBr, cm^{-1}): 2805 (CH_2), 1652 (CHO). ^1H NMR (300 MHz, $CDCl_3$-*d*, δ(ppm)): 1.63 (br, N-H), 2.38 (t, *J* = 4.8, 4H, CH_2 in piperazine), 3.43 (t, *J* = 5.1, 4H, CH_2 in piperazine), 3.48 (s, 2H, CH_2), 3.42 (s, 4 H, CH_2). $^{13}C\{^1H\}$ NMR (300 MHz, DMSO-d_6) δ: 196.5 (C_H-CHO), 160.9 (C_q-O), 154.8 (C_q-O), 137.9 (C_H-Ar), 133.8 (C_H-Ar), 129.6 (C_q-O), 120.3 (C_q), 117.6 (C_H-Ar), 62.0(C_H-CH_2), 53.1 (C_H-CH_2-CH_2).

V.4.2.16. Procedure for the preparation of aldehyde piperazine resin (12a) and 12b)

In a 250 ml three-necked round bottom with a magnetic stirrer, 0.48 g (1.46 mmol) of $[MoO_2(acac)_2]$ were dissolved in 15 ml of DCM and EtOH at 60 °C. Then, 0.18 g of piperazine resin **(11a)** or **(11b)** was added. The mixture was stirred at 60°C for 24 h. The hot resin was filtered off and washed with different solvents in the following order (ethanol, acetone, dichloromethane and diethylether) and dried under high

vacuum.

12a:

Yellow orange powder, Anal. found: C, 52.31; H, 4.76; N, 4.42%. TGA: Δm= 68.1 %. IR (neat): 3023, 2919 [s, n(CH_2)], 1612 (C=N)], 938 (Mo=O), 905 (Mo-O-Mo).

12b:

Light black powder, Anal. found: C, 44.25; H, 4.25; N, 3.44%. TGA: Δm= 68.0 %. IR (neat): 3023, 2919 [s, n(CH_2)], 1610 (C=N)], 942 (Mo=O), 903 (Mo-O-Mo). TGA: Δm= 68.0 %.

V.4.3. *Catalytic procedure*

- Routine experiments

In a typical experiment, cyclooctene (1 equiv) and catalyst (x equiv, see tables) were mixed together then stirred in air in a round bottom flask. Acetophenone was added as internal standard (see tables). The reaction temperature was regulated to the desired value and then wet THBP (70% in water, y equiv see tables) was added to the mixture to start the reaction. Samples of the organic phase were periodically withdrawn. The reaction of the withdrawn sample was quenched by addition of manganese oxide, followed by the addition of diethylether and removal of the MnO_2 and residual water by filtration through silica before GC analysis.

- Recovery procedures

After a catalystic experiment, the resin was filtered and washed with acetone, CH_2Cl_2 and Et_2O, then dried under reduced pressure at 30°C overnight before using the recovered solid in the next cycle.

Conclusions and Perspectives

This thesis showed following results.

- Several molybdenum complexes $[MoO_2L]_2$ and $[MoO_2L(D)]$ (D= EtOH or MeOH) were synthesized from $[MoO_2(acac)_2]$ and H_2L tridentate Schiff base ligands. The interest of the work was in the possible ligand variations that can influence catalytic results. Ligands could coordinate the molybdenum center through *ONO* and *ONS* donors. Peripheral functions of the ligand backbone (OH, NEt_2 and NO_2) could be achieved. All complexes were characterized by analytical methods (IR, NMR, TGA). Six molecular structures of stabilized monomer species $[MoO_2L(D)]$ (D= DMSO or H_2O) were determined by X-ray crystallography.

- The synthesized $[MoO_2L]_2$ complexes have been used for the organic solvent-free epoxidation of cyclooctene using aqueous TBHP as oxidant. A noticeable effect of the nature of the ligand was observed. Molybdenum complexes with *ONS* based ligands exhibited higher activity than with *ONO* ones. The effect of the peripheral substitution on ligand (OH, NEt_2 and NO_2) was also observed. The highest conversions were achieved with *ONO* based complex in the case of L^a (with OH in *ortho* position in the ligand) and L^d (with NO_2 on the ligand).

- A similar effect was also observed for the organic solvent-free epoxidation of limonene and cyclohexene using the same $[MoO_2L]_2$ complexes and the same oxidant (aquous TBHP). With these two substrates, the reaction gives the expected epoxides but also the correponding diols, obtained through the epoxide ring opening with water. The nature of the ligand influences strongly the reactivity. The molybdenum complexes with *ONO* based ligands transform the substrates into epoxides and diols, and the molybdenum complexes with *ONS* based ligand lead mainly to the corresponding diols in very short reaction time. By this method, it was also exhibited that one limonene diol (the diaxial limonene diol), non favoured in several reported works, was obtained until 20% in the limonene diols mixture. As for cyclooctene, an effect on the conversion was observed with the OH containing *ONO* complexes.

- Finally, it has been possible to graft a molybdenum complex with an *ONO* Schiff base ligand on a commercial Merrifield resin. Piperazine was used as linker between the resin and the molybdenum complex. The multistep grafting was presented using two different routes and the compounds were characterized by IR, TGA and elemental analysis. Those heterogeneous catalysts were used for the epoxidation of cyclooctene under organic solvent-free conditions. Although the process was slower than for homogeneous analogues, good conversion was

observed after 8h and catalysts could be reused four times without dramatic activity loss. The IR analyses of the resins did not point out strong modifications of metal surrounding, but TGA showed few metal leaching.

All the catalytic reactions have been performed under organic solvent-free conditions. It was the main challenge of this work, and one interesting step towards greener chemical processes.

The perspectives of this work concern different challenges in agreement with the frame of Green Chemistry. It is planned to continue to study the oxidation of different model substrates from fossil resources in order to validate the oxidations on very simple functions. The next step is to study more complex molecules issued from biomass. As an example, some terpenes, available in Europe, are highly interesting by the diversity of oxidation compounds that can be found.

Finally, optimization studies for the grafting of those molybdenum complexes on other types of supports, being grafted silica, other organic polymers or monodisperse macromolecules as dendrimers seem to be another challenging work. Indeed, the variety of existing supports can lead to catalytic objects more stable (low metal leaching) than those presented in this work. It would be a step towards the development of organic solvent-free reaction under continuous flow mode.

Bibliographic References

[1] H. Schiff, *Justus Liebigs Ann Chem.*, 131(1864) 118-119.
[2] (a) C. M. da Silva, D. L. da Silva, L. V. Modolo, R. B. Alves, M. A. de Resende, C. V. B. Martins, A. de Fátima, *J. Adv. Res.*, 2 (2001) 1-8.
(b) I. Kim, G. B. Mercelle, D. D. Waller, G. A. Cordell, H. H. S. Fong, *Contraception*, 35 (1987) 289-297.
[3] A. D. Mulazimoglu, I. E. Mulazimoglu, B. Mercimek, *E-Journal of Chemistry*, 6 (2009) 965-974.
[4] M. A. Vázquez, F. Muñoz, J. Donoso, F. García-Blanco, *Helv. Chim. Acta*, 75 (1992) 1029-1038.
[5] (a) R. H. Holm, Jr G. W. Everett, A. Chakravorty, *Prog. Inorg. Chem.*, 7 (1966) 83-214.
(b) M. Calligaris, L. Randaccio, G. Wilkinson, R. D. Gillard, J. A. McCleverty, (Eds.) *Comprehensive Coordination Chemistry, Pergamon Press, Oxford,* 2 (1987).
(c) A. D. Garnovski, I. S. Vasilchenko, *Russ. Chem. Rev.,* 71 (2002) 943-968.
[6] V. Vrdoljak, J. Pisk, D. Agustin, P. Novak, J. P. Vuković, D. Matković-Čalogović, *New J. Chem.*, 38 (2014) 6176-6185.
[7] E. Zamanifar, F. Farzaneh, J. Simpson, M. Maghami, *Inorg. Chim. Acta*, 414 (2014) 63-70.
[8] A. M. Fayed, S. A. Elsayed, A. M. El-Hendawy, M. R. Mostafa, *Spectrochim. Acta Part A*, 129 (2014) 293-302.
[9] K. Chjo, *J. Korean Chem. Soc*., 17(1973) 169-173.
[10] L. S. Liebeskind, K. B. Sharpless, R. D. Wilson, J. A. Ibers, *J. Am. Chem. Soc*., 100 (1978) 7061-7063.
[11] O. A. Rajan, A. Chakravorty, *Inorg. Chem.*, 20 (1981) 660-664.
[12] J. M. Sobczak, T. Głowiak, J. J. Ziókowski, *Trans. Met. Chem.*, 15 (1990) 208-211.
[13] (a) J. Topich, *Inorg. Chim. Acta*, 46 (1980) L37-L39.
(b) J. Topich, J. T. Lyon III, *Inorg. Chem.*, 23(1984) 3202-3206.
(c) J. Topich, *Inorg. Chem.,* 20 (1981) 3704-3707.
[14] L. B. Jerzykiewicz, J. M. Sobczak, J. J. Ziółkowski, *J. Chem. Res.*, (2000) 423-425.
[15] (a) J. Topich, J. T. Lyon, III, *Inorg. Chim. Acta*, 80 (1983) L41-L43.
(b) J. Topich, J.T. Lyon, III, *Polyhedron*, 3 (1984) 61-65.
[16] J. Topich, J. O. Bachert, III, *Inorg. Chem.*, 31 (1992) 511-515.
[17] R. D. Chakravarthy, K. Suresh, V. Ramkumar, D. K. Chand, *Inorg. Chim. Acta*, 376 (2011) 57-63.
[18] A. K. Sah, N. Baig, *Catal. Lett.*, 145 (2015) 905-909.
[19] G.-P. Cheng, L.-W. Xue, W.-C. Yang, G.-Q. Zhao, *J. Chil. Chem. Soc.*, 58 (2013) 1632-1636.

[20] I. Sheikhshoaie, A. Rezaeifard, N. Monadi, S. Kaafi, *Polyhedron,* 28 (2009) 733-738.

[21] V. S. Sergienko, V. L. Abramenko, A. V. Churakov, Yu. N. Mikhailov, M. D. Surazhskaya, *Cryst. Reports,* 59(2014) 523-526.

[22] C. Bibal, J.- C. Daran, S. Deroover, R. Poli, *Polyhedron,* 29 (2010) 639-647.

[23] S. L. Pandhare, R. R. Jadhao, V. G. Puranik, P. V. Joshi, F. Capet, M. K. Dongare, S. B. Umbarkar, C. Michon, F. Agbossou-Niedercorn, *J. Organomet. Chem.,* 772-773 (2014) 271-279.

[24] A. Rezaeifard, M. Jafarpour, H. Raissi, M. Alipour, H. Stoeckli-Evans, *Z. Anorg. Allg. Chem.,* 638 (2012) 1023-1030.

[25] L. Gusina, I. Bulhac, D. Dragancea, Y.A. Simonov, S. Shova, *Rev. Roum. Chim.,* 56(2011) 981-985.

[26] N. K. Ngan, K. M. Lo, C. S. R. Wong, *Polyhedron,* 30 (2011) 2922-2932.

[27] M. Bagherzadeh, M. M. Haghdoost, A. Ghanbarpour, M. Amini, H. R. Khavasi, E. Payab, A. Ellern, L. K. Woo, *Inorg. Chim. Acta,* 411 (2014) 61-66.

[28] (a) S.-S. Qian, M.-M. Zhen, Y. Zhao, N. Zhang, Z.-L. You, H.-L. Zhu, *J. Chil. Chem. Soc.*, 58 (2013) 1647-1650.
(b) S.-S. Qian, H.-H. Li, Y.-N. Li, Z.-L. You, H.-L. Zhu, *J. Struct. Chem*., 55 (2014) 332-336.

[29] J. Pisk, B. Prugovečki, D. Matković-Čalogović, T. Jednačak, P. Novak, D. Agustin, V. Vrdoljak, *RSC Adv*., 4 (2014) 39000-39010.

[30] D.-W. Kim, U. Lee, B.-K. Koo, *Bull. Korean Chem. Soc*., 25(2004) 1071-1074.

[31] V. Vrdoljak, J. Pisk, B. Prugovečki, D. Matković-Čalogović, *Inorg. Chim. Acta*, 362 (2009) 4059-4064.

[32] N. K. Ngan, C. S. Wong, K. M. Lo, *J. Chem. Crystallogr*., 41(2011) 1700-1706.

[33] S. N. Rao, N. Kathale, N. N. Rao, K. N. Munshi, *Inorg. Chim. Acta*, 360 (2007) 4010-4016.

[34] Z. Moradi-Shoeili, D. M. Boghaei, M. Amini, M. Bagherzadeh, B. Notash, *Inorg. Chem. Commun.,* 27 (2013) 26-30.

[35] D. Agustin, J.-C. Daran, R. Poli, *Acta Cryst,* C64 (2008) m101-m104.

[36] D. Agustin, C. Bibal, B. Neveux, J.-C. Daran, R. Poli, *Z. Anorg. Allg. Chem*., 635 (2009) 2120-2125.

[37] M. R. Maurya, S. Dhaka, F. Avecilla, *New J. Chem.,* 39 (2015) 2130-2139.

[38] S. Pasayat, S. P. Dash, S. Roy, R. Dinda, S. Dhaka, M. R. Maurya, W. Kaminsky, Y. P. Patil, M. Nethaji, *Polyhedron,* 67 (2014) 1-10.

[39] M. Cindrić, G. Galin, D. Matković-Čalogović, P. Novak, T. Hrenar, I. Ljubić, T. Kajfež, *Polyhedron,* 28 (2009) 562-568.

[40] K. Užarević, G. Pavlović, M. Cindrić, *Polyhedron,* 52 (2013) 294-300.

[41] S. Y. Ebrahimipour, H. Khabazadeh, J. Castro, I. Sheikhshoaie, A. Crochet, K. M. Fromm, *Inorg. Chim. Acta*, 427 (2015) 52-61.

[42] (a) M. A. Hussein, T. S. Guan, R. A. Haque, M. B. Khadeer Ahamed, A. M. S. Abdul Majid, *Inorg. Chim. Acta*, 421 (2014) 270-283.
(b) M. A. Hussein, T. S. Guan, R. A. Haque, M. B. Khadeer Ahamed, A.M.S. Abdul Majid, *Spectrochim. Acta Part A*, 136 (2015) 1335-1348.

(c) M. A. Hussein, T. S. Guan, R. A. Haque, M. B. Khadeer Ahamed, A.M.S. Abdul Majid, *Polyhedron*, 85 (2015) 93-103.

[43] O. Brücher, J. Hartung, *Tetrahedron*, 70 (2014) 7950-7961.

[44] J. M. Sobczak, J. J. Ziółkowski, *Appl. Catal. A: General*, 248 (2003) 261-268.

[45] M. Bagherzadeh, S. Ghazali Esfahani, *Scientia Iranica C*, 17 (2010) 131-138.

[46] A. Rezaeifard, I. Sheikhshoaie, N. Monadi, M. Alipour, *Polyhedron*, 29 (2010) 2703-2709.

[47] (a) F. E. Kühn, A. M. Santos, A. D. Lopes, I. S. Gonçalves, E. Herdtweck, C. C. Romão, *J. Mol. Catal. A*, 164 (2000) 25-38.
(b) F. E. Kühn, M. Groarke, É. Bencze, E. Herdtweck, A. Prazeres, A. M. Santos, M. J. Calhorda, C. C. Romão, I. S. Gonçalves, A. D. Lopes, M. Pillinger, *Chem. Eur. J.*, 8 (2002) 2370-2383.

[48] J. Morlot, N. Uyttebroeck, D. Agustin, R. Poli, *ChemCatChem*, 5 (2013) 601-611.

[49] J. Pisk, D. Agustin, V. Vrdoljak, R. Poli, *Adv. Synth. Catal.*, 353 (2011) 2910-2914.

[50] M. R. Maurya, U. Kumara, P. Manikandan, *Dalton Trans*., 2006, 3561-3575.

[51] M. R. Maurya, N. Kumar, F. Avecilla, *J. Mol. Catal. A: Chem.*, 392 (2014) 50-60.

[52] Y. Li, X. Fu, B. Gong, X. Zou, X. Tu, J. Chen, *J. Mol. Catal. A: Chem*., 322 (2010) 55-62.

[53] S. N. Rao, K. N. Munshi, N. N. Rao, *J. Mol. Catal. A: Chem.*, 145 (1999) 203-210.

[54] M. A. Katkar, S. N. Rao, H. D. Juneja, *RSC Adv.*, 2 (2012), 8071-8078.

[55] M. Masteri-Farahani, F. Farzaneh, M. Ghandi, *J. Mol. Catal. A: Chem*., 248 (2006) 53-60.

[56] M. Masteri-Farahani, P. Eghbali, F. Salimi, *J. Nanostructures*, 1 (2012) 14-20.

[57] M. Bagherzadeh, M. Zare, T. Salemnoush, S. Özkar, S. Akbayrak, *Appl. Catal., A: General*, 475 (2014) 55-62.

[58] M. Masteri-Farahani, S. Abednatanzi, *Inorg. Chem. Commun.*, 37 (2013) 39-42.

[59] (a) L. E. Clougherty, J. A. Sousa, G. M. Wyman, *J. Org. Chem*., 22 (1957) 462-464.
(b) N. E. Eltayeb, S. G. Teoh, H.-K. Fun, S. Chantrapromma, *Acta Cryst. E*, 66 (2010) o1536-o1537.
(c) R. J. Argaueri, C. E. White, *Anal. Chem.*, 36 (1964), 2141-2144.

[60] (a) S. Das, S. Samanta, S. K. Maji, P. K. Samanta, A. K. Dutta, D. N. Srivastava, B. Adhikary, P. Biswas, *Tetrahedron Lett.*, 54 (2013) 1090-1096.
(b) K. M. Khan, F. Rahim, S. A. Halim, M. Taha, M. Khan, S. Perveen, Zaheer-ul-Haq, M. A. Mesaik, M. I. Choudhary, *Bioorg. Med. Chem.*, 19 (2011) 4286-4294.

[61] P. K. Nath, K. C. Dash, *Trans. Met. Chem*., 10 (1985) 262-264.

[62] J. U. Mondal, F. A. Schultz, T. D. Brennan, W. R. Scheidt, *Inorg. Chem*., 27 (1988) 3950-3956.

[63] G. J. J. Chen, J. W. McDonald, W. E. Newton , *Inorg. Chem*., 15 (1976) 2612-2615.

[64] M. Rodríguez, M. E. Ochoa, R. Santillán, N. Farfán, V. Barba, *J. Organomet. Chem.,* 690 (2005) 2975-2988.

[65] K. A. Neeraj, V. Kumar, R. Prajapati, S. K. Asthana, K. K. Upadhyay, J. Zhao, *Dalton Trans.,* (2014) 5831-5839.

[66] B. M. Muñoz, R. Santillán, M. Rodríguez, J. M. Méndez, M. Romero, N. Farfán, P. Lacroix, K. Nakatani, G. Ramos-Ortíz, J. L. Maldonado, *J. Organomet. Chem.,* 693 (2008) 1321-1334.

[67] (a) R. E. Parker, N.S. Isaacs, *Chem. Rev.,* 59 (1959) 737-799.
(b) N. Gharah, S. Chakraborty, A. K. Mukherjee, R. Bhattacharyya, *Chem. Commun.,* (2004) 2630-2632
(c) M. Herbert, E. Álvarez, D. J. Cole-Hamilton, F. Montilla, A. Galindo, *Chem. Commun*., 546 (2010) 5933-5935
(d) C. J. Thibodeaux, W. C. Chang, H. W. Liu, *Chem. Rev.,* 112 (2012) 1681-1709.

[68] (a) N. Grover, F. E. Kühn, *Curr. Org. Chem*., 16 (2012) 16-32
(b) M. Wu, C. Miao, S. Wang, X. Hu, C. Xia, F. E. Kühn, W. Sun, *Adv. Synth. Catal.,* 353 (2011) 3014-3022.
(c) D. Betz, P. Altmann, M. Cokoja, W.A. Herrmann, F. E. Kühn, *Coord. Chem. Rev.,* 255 (2011) 1518-1540.
(d) D. Betz, A. Raith, M. Cokoja, F. E. Kühn, *ChemSusChem,* 3 (2010) 559-562.
(e) K. R. Jain, F. E. Kühn, *Dalton Trans.,* (2008) 2221-2227.
(f) F. E. Kühn, A. M. Santos, M. Abrantes, *Chem. Rev.*, 106 (2006) 2455-2475.
(g) Q. H. Xia, H. Q. Ge, C. P. Ye, Z. M. Liu, K. X. Su, *Chem. Rev.,* 105 (2005) 1603-1662.

[69] (a) D. D. Agarwal, S. Shrivastava, *Polyhedron*, 7 (1988) 2569-2573.
(b) D. D. Agarwal, *J. Mol. Catal*., 44 (1988) 65-72.
(c) Z. Dawoodi, R.L. Kelly, *Polyhedron*, 5 (1986) 271-275.
(d) A. Rezaeifard, I. Sheikhshoaie, N. Monadi, H. Stoeckli-Evans, *Eur. J. Inorg. Chem.,* (2010) 799-806.
(e) Y Sui, X. Zeng, X. Fang, X. Fu, Y. Xiao, L. Chen, M. Li, S. Cheng, *J. Mol. Catal. A: chem.,* 270 (2007) 61-67.
(f) X. Zhou, J. Zhao, A. M. Santos, F. E. Kuehn, *Z. Naturforsch. B,* 59 (2004) 1223-1228.
(g) J. Zhao, X. Zhou, A. M. Santos, E. Herdtweck, C. C. Romao, F. E. Kuehn, *Dalton Trans*., (2003) 3736-3742.
(h) L Casella, M. Gullotti, A. Pintar, S. Colonna, A. Manfredi, *Inorg. Chim. Acta*, 144 (1988) 89-97.

[70] (a) J. Pisk, B. Prugovecki, D. Matkovic-Calogovic, R. Poli, D. Agustin, V. Vrdoljak, *Polyhedron*, 33 (2012) 441-449.

(b) M. Loubidi, D. Agustin, A. Benharref, R. Poli, *C. R. Chimie*, 17 (2014) 549-556.
(c) C. Cordelle, D. Agustin, J.-C. Daran, R. Poli, *Inorg. Chim. Acta*, 364 (2010) 144-149.
(d) B. Guérin, D. Mesquita Fernandes, J.-C. Daran, D. Agustin, R. Poli, *New J. Chem.*, 37 (2013) 3466-3475.
71 A. Nakamura, M. Nakayama, K. Suxihashi, S. Otsuka, *Inorg. Chem*., 18 (1979) 394-400.
72 (a) K. A. D. Swift, *Top. Catal.*, 27 (2004) 143-155.
(b) J. L. F. Monteiro, C. O. Veloso, *Top. Catal.*, 27 (2004) 169-180.
73 (a) J. M. Derfer, M. M. Derfer, *Encyclopedia of Chemical Technology* Kirk-Othmer, vol. 22, third ed., Wiley, New York,1978, p. 709.
(b) E. Herrero, S. Casuscelli, J. Fernandez, C. Poncio, M. Rueda, O. Oyola, *Molecules*, 5 (2000) 336-337.
(c) K. Bauer, D. Garbe, H. Surburg, *Common Fragrance and Flavor Materials, Preparation, Properties and Uses*, Wiley VCH, New York, 1997.
74 (a) D. Comins, L. Guerra-Weltzien, J. M. Salvador, *Synlett.*, (1994) 972-974.
(b) W. Chrisman, J. N. Camara, K. Marcellini, B. Singaram, C. T. Goralski, D. L. Hasha, P. R. Rudolf, L. W. Nicholson, K. K. Borodychuk, *Tetrahedron Lett*., 42 (2001) 5805-5807.
(c) H. Lebel, E. N. Jacobsen, *J. Org. Chem*., 62 (1998) 9624-9625.
75 G. A. Burdock, 1995. *Fenaroli's handbook of flavor ingredients, 3rd ed., p.107. CRC Press, Boca Raton*.
76 E. E. Royals, J. C. Leffingwell, *J. Org. Chem*. 31 (1966) 1937-1944.
77 (a) C. M. Byrne, S.D. Allen, E. B. Lobkovsky, G. W. Coates, *J. Am. Chem. Soc*., 126 (2004) 11404-11405.
(b) A. Corma, S. Iborra, A. Velty, *Chem. Rev.*, 107 (2007) 2411-2502.
78 W. Knöll, C.Tamm, *Helv. Chim. Acta*, 58 (1975) 1162-1171.
79 (a) R. A. Sheldon, in: F. E. Harkes (Ed.) *Catalysis of Organic Reaction*, USA, 1998.
(b) R. A. Sheldon, in: G. Centi, F. Trifiro (Eds.) *New Developments in Selective Oxidation*, Elsevier, Amsterdam, 1990.
80 F. Papafotiou, K. Karidi, A. Garoufis, M. Louloudi, *Polyhedron*, 52 (2013) 634-638.
81 N. Mizuno, S. Hikichi, K. Yamaguchi, S. Uchida, Y. Nakagawa, K. Uehara, K. Kamata, *Catalysis Today*, 117 (2006) 32-36.
82 D. Clemente-Tejeda, A. López-Moreno, F. A. Bermejo, *Tetrahedron*, 69 (2013) 2977-2986.
83 A. Gallo, C. Tiozzo, R. Psaro, F. Carniato, M. Guidotti, *J. Catal.*, 298 (2013) 77-83.
84 C. M. Granadeiro, A. D. S. Barbosa, P. Silva, F. A. Almeida Paz, V. K. Saini, J. Pires, B. de Castro, S. S. Balula, L. Cunha-Silva, *Appl. Catal. A,* 453 (2013) 316-326.
85 (a) J. Kitajima, Y. Aoki, T. Ishikava, Y. Tanaka, *Chem. Pharm. Bull.*, 46 (1998)

1580-1582.
(b) T. Matsumura, T. Ishikawa, J. Kitajima, *Chem. Pharm. Bull.*, 50 (2002) 66-72.

86 A. V. Biradar, B. R. Sathe, S. B. Umbarkar, M. K. Dongare, J. *Mol. Catal. A: Chem.*, (2008) 111-119.

87 C. Pirovano, M. Guidotti, V. Dal Santo, R. Psaro, O. A. Kholdeeva, I. D. Ivanchikova, *Catal. Today*, 197 (2012) 170-177.

88 S. Figueiredo, A. C. Gomes, J. A. Fernandes, F. A. Almeida Paz, A. D. Lopes, J. P. Lourenço, M. Pillinger, I. S. Gonçalves, *J. Organomet. Chem.*, 723 (2013) 56-64.

89 N. A. Milas, S. Sussman, *J. Am. Chem. Soc.*, 59 (1937) 2345-2347.

90 L. Salles, A.F. Nixon, N. C. Russell, R. Clarke, P. Pogorzelec, D. J. Cole-Hamilton, *Tetrahedron: Asym.*, 10 (1999) 1471-1476.

91 (a) M. Blair, P. C. Andrews, B. H. Fraser, C. M. Forsyth, P. C. Junk, M. Massi, K. L. Tuck, *Synthesis*, (2007) 1523-1527.
(b) T. R. Amarante, P. Neves, A. A. Valente, F. A. Almeida Paz, A. N. Fitch, M. Pillinger, I. S. Gonçalves, *Inorg. Chem*., 52 (2013) 4618-4628.

92 A. Fürst, P. A. Plattner, *Helv. Chim. Acta*, 32 (1949) 275-283.

93 (a) Z.-B. Xu, J. Qu, *Chin. J. Chem*., 30 (2012) 1133-1136.
(b) D. Steiner, L. Ivison, C. T. Goralski, R. B. Appell, J. R. Gojkovic, B. Singaram, *Tetrahedron: Asymmetry*, 13 (2002) 2359-2363.

94 W. Wang, T. Vanderbeeken, D. Agustin, R. Poli, *Catal. Commun*., 63 (2015) 26-30.

95 (a) C.-X. Miao, J.-Q. Wang, Y. Wu, Y. Du, L.-N. He, *ChemSusChem*, 1 (2008) 236-241.
(b) A. D. Cort, L. Mandolini, C. Pasquini, L. Schiaffino, *Org. Biomol. Chem*., 4 (2006) 4543-4546.

96 M. Bagherzadeh, M. Zare, *J. Coord. Chem*., 66 (2013) 2885-2900.

97 M.-J. Lim, C. A. Murray, T. A. Tronic, K. E. Krafft, A. N. Ley, J. C. Butts, R. D. Pike, H. Lu, H. H. Patterson, *Inorg. Chem.*, 47 (2008) 6931-6947.

98 Q. P. Peterson, D. C. Hsu, D. R. Goode, C. J. Novotny, R. K. Totten, P. J. Hergenrother, *J. Med. Chem.*, 52(2009) 5721-5731.

Abstract in English

The work of this PhD thesis deals with the study of molybdenum complexes of general formula $[MoO_2L]_n$ (L being a tridentate Schiff base ligand with an ONO or ONS coordination sphere around the molybdenum) as catalysts for the organic solvent-free epoxidation of olefins. Within the spirit of Green Chemistry, the work has focused on four of the twelve Green Chemistry principles: the use of catalysis rather than stoichiometric transformations, the use of organic solvent-free procedures rather than operating in solution of organic solvents, the use of renewable substrates and the grafting of catalysts for their recovery.

The first part of the manuscript presents a concise state of the art on the chemistry of molybdenum complexes with ligands similar to those used within the thesis. Specific aspects such as the effect of ligand substituents and the different activities – mainly catalytic – observed in organic media are reviewed. A section of this chapter is dedicated to the different strategies employed for the grafting of molybdenum complexes to solid supports as well as to the use of the resulting supported complexes in heterogenized homogeneous catalysis.

The next chapter details the synthesis and characterization of all the molecular complexes used as catalysts. This chapter shows the different substitutions operated on the ligands, i.e. changing the *ONO* coordination sphere to *ONS* and adding different substituents on the ligands, i.e. OH free functions or additional donor (diethylamino) and/or withdrawing (nitro) substituents at different positions on the tridentate ligand in order to modify the catalytic activity. Six of the synthesized complexes could be characterized by X-ray crystallography.

The third chapter reports the results obtained for the catalyzed organic solvent-free epoxidation of cyclooctene as a model substrate using all the molybdenum complexes presented in the previous chapter. It is shown that the nature of the coordination sphere around the molybdenum (ONO vs ONS) is in favour of the latter in terms of catalytic activity towards the formation of the desired epoxide. The catalyzed reactions with complexes containing an OH substituent at different positions on the aromatic ring have shown more significant effects in the case of the ONO coordination sphere than in the corresponding ONS case. The epoxidation performed in the presence of a dimethylamino and/or a nitro substituent on the ONO ligand revealed that the catalytic activity is enhanced by the electron withdrawing group.

The catalytic investigations were pursued by the epoxidation of cyclohexene and of one natural substrate, limonene. This study has shown that limonene oxides and/or limonene diols are generated, depending on the nature of the catalyst. The ONS complexes are very reactive and quickly lead to the limonene diols. The effect of different parameters has been studied with particular attention to the reaction temperature.

Finally, one stable molybdenum complex with an ONO coordination sphere has been grafted onto a commercial Merrifield resin. Different grafting strategies are presented. The isolated objects have been tested as catalysts under organic solvent-free conditions for the epoxidation of cyclooctene. The catalytic results are promising in terms of activity and the recovery/recycling tests have shown that the catalysts could be used three times without significant decrease of conversion and selectivity, but some metal leaching was observed.

Résumé en français

Le sujet de cette thèse concerne l'étude de complexes du molybdène de formule $[MoO_2L]_n$ (L étant un ligand base de Schiff tridente ayant une coordination ONO ou ONS autour du molybdène) en tant que catalyseurs d'époxydation d'oléfines sans solvant organique ajouté.

Le travail s'est concentré sur quatre des douze principes de la chimie verte: l'utilisation de la catalyse plutôt que des transformations stœchiométriques, l'utilisation de procédures sans solvant organique ajouté plutôt que des procédures opérant dans des solvants organiques, l'utilisation de substrats renouvelables et le greffage de catalyseurs pour leur récupération.

La première partie du manuscrit présente un état de l'art concis de la chimie des complexes du molybdène à ligands similaires de ceux utilisés dans cette thèse. Des aspects spécifiques comme l'effet des substituants sur les ligands et les différentes activités – essentiellement catalytiques – observées en milieu organique ont été recensées. Un partie de ce chapitre est aussi dédiée aux différentes stratégies employées pour le greffage de complexes du molybdène sur des supports solides ainsi que l'utilisation des complexes supportés résultants en catalyse homogène hétérogénéisée.

Cette partie bibliographique est suivie d'un chapitre détaillant la synthèse et la caractérisation de tous les complexes moléculaires utilisés comme catalyseurs. Ce chapitre montre les différentes substitutions opérées sur les ligands, c.-à-d. remplaçant la sphère de coordination ONO par ONS et ajoutant différents substituants sur les ligands, telles des fonctions OH libres ou des substituants donneurs (diéthylamino) et/ou attracteurs (nitro) à différentes positions sur le ligand tridente afin de modifier l'activité catalytique. Six des complexes ont pu être caractérisés par diffraction des rayons X.

Le troisième chapitre reporte les résultats obtenus pour l'époxydation catalysée sans solvant organique ajouté du cyclooctène (substrat modèle) utilisant tous les complexes du molybdène présentés dans le chapitre précédent. Il est montré que la nature de la sphère de coordination autour le molybdène (ONO vs ONS) est en faveur de la deuxième en terme d'activité catalytique en faveur de l'époxyde désiré.

Les réactions catalysées par les complexes contenant des OH libres ont montré des effets plus significatifs dans le cas de la sphère de coordination ONO que dans le cas des ONS correspondants. L'époxydation en présence de substituants diéthylamino et/ou nitro sur le ligand ONO ont révélé que l'activité catalytique était améliorée par le groupement attracteur d'électrons.

Les recherches catalytiques ont été poursuivies par l'époxydation du cyclohexène et d'un substrat naturel, le limonène. Cette étude a montré que des oxydes de limonène et/ou des limonènes diols étaient générés, en fonction de la nature du catalyseur. Les complexes ONS sont très réactifs et conduisent rapidement aux limonènes diols. L'effet de différents paramètres a été étudié avec une attention particulière à la température de réaction.

Enfin, un complexe stable ONO du molybdène a été greffé sur une résine de Merrifield commerciale. De différentes stratégies de greffage sont présentées. Les objets isolés ont été testés comme catalyseurs en condition sans solvant organique ajouté pour l'époxydation du cyclooctène. Les résultats catalytiques sont prometteurs en termes d'activité et des tests de récupération/recyclage ont montré que les catalyseurs pouvaient être utilisés trois fois sans perte significative de conversion et de sélectivité. Toutefois, un peu de relargage du métal a été observé.